Université de Montréal

Ionic, Cellular and Molecular Mechanisms underlying the QT Prolongation and Arrhythmias in Diabetic Cardiocomplications

par

Yiqiang Zhang

Programme des Sciences biomédicales
Département de Médecine
Faculté de Médecine

Thèse présentée à la Faculté des études supérieures
en vue de l'obtention du grade de
Doctorat philosophie (Ph. D.)
en Sciences biomédicales

Octobre 2005

© Yiqiang Zhang, 2005

W
4
U58
2006
V016

Université de Montréal

Direction des bibliothèques

AVIS

L'auteur a autorisé l'Université de Montréal à reproduire et diffuser, en totalité ou en partie, par quelque moyen que ce soit et sur quelque support que ce soit, et exclusivement à des fins non lucratives d'enseignement et de recherche, des copies de ce mémoire ou de cette thèse.

L'auteur et les coauteurs le cas échéant conservent la propriété du droit d'auteur et des droits moraux qui protègent ce document. Ni la thèse ou le mémoire, ni des extraits substantiels de ce document, ne doivent être imprimés ou autrement reproduits sans l'autorisation de l'auteur.

Afin de se conformer à la Loi canadienne sur la protection des renseignements personnels, quelques formulaires secondaires, coordonnées ou signatures intégrées au texte ont pu être enlevés de ce document. Bien que cela ait pu affecter la pagination, il n'y a aucun contenu manquant.

NOTICE

The author of this thesis or dissertation has granted a nonexclusive license allowing Université de Montréal to reproduce and publish the document, in part or in whole, and in any format, solely for noncommercial educational and research purposes.

The author and co-authors if applicable retain copyright ownership and moral rights in this document. Neither the whole thesis or dissertation, nor substantial extracts from it, may be printed or otherwise reproduced without the author's permission.

In compliance with the Canadian Privacy Act some supporting forms, contact information or signatures may have been removed from the document. While this may affect the document page count, it does not represent any loss of content from the document.

Université de Montréal

Faculté des études supérieures

Cette thèse intitulée:

Ionic, Cellular and Molecular Mechanisms Underlying the QT Prolongation in Diabetic Cardiocomplications

présentée par:

Yiqiang Zhang

a été évaluée par un jury composé des personnes suivantes:

Dr. Stanley Nattel

président-rapporteur

Dr. Zhiguo Wang

directeur de recherche

Dr. Jacques Billette

membre du jury

Dr. Alvin Shrier

examinateur externe

Dr. Rémy Sauvé

représentant du doyen de la FES

RÉSUMÉ

Le diabète est une maladie grave qui est associée le plus souvent à des complications sévères dont les plus fréquentes sont les pathologies cardiovasculaires. Cinquante pour cent des patients diabétiques meurent suite à des cardiopathies parmis lesquels plus d'un quart des patients présentent un prolongement de l'intervalle QT, qui constitue un facteur de prédiction de la mortalité chez les patients diabétiques. Les études chez les modèles diabétiques des rats et des souris prouvent que la diminution des canaux I_{to} et I_{ss} est le majeur facteur. Ce pendant, plusieurs des problèmes importants ne sont pas expliqués. D'abord, les rôles de canaux I_{Kr} et I_{Ks} qui n'existent pas chez les rats et les souris adultes, ne sont pas clair, mais ils jouent un rôle important determinant l'APD chez l'homme. De plus, les profils des changements des courants ioniques trouvés chez les rats et les souris ne peuvent pas expliquer complètement la survenue de troubles de l'intervalle QT chez les patients diabétiques. Enfin, le diabète est principalement un trouble métabolique pour lequel les niveaux de glucose, de ROS (Reactive Oxygen Species), de TNF-α (tumor necrosis factos-α) et de ceramide sont élevés. A contrario, le niveau de l'insuline est réduit et la voie de signalisation de l'insuline est diminuée. Cependant, ces perturbations métaboliques comme les mécanismes potentiels pour les désordres électriques diabétiques ont été négligé dans le passé.

Cette thèse a pour objectif d'apporter de nouveaux éléments permettant d'approcher plus en détail les mécanismes cellulaires et moléculaires responsables des troubles des rythmes et de la prolongation de l'intervalle QT, chez les individus présentant un diabète. L'hypothèse principale est que le courant I_{Kr} transporté par les canaux HERG chez l'homme joue un rôle majeur dans la survenue des troubles du rythme associés au diabète , et que la réduction du courant I_{Kr}/HERG est le résultat, d'une part d'une diminution de l'expression du canal HERG, mais aussi d'autre part, d'une régulation fonctionnelle négative liée au stress métabolique ainsi qu'aux protéines de signalisation.

Nous avons tout d'abord vérifié l'altération de l'APD et de l'intervalle QT dans les myocytes ventriculaires isolés provenant d'un modèle de lapin présentant un diabète de type-1 induit par l'alloxan. Dans ce modèle, nous avons montré que parmi les principaux courants ioniques, la réduction d'I_{Kr} était un facteur majeur dans l'altération de l'APD et de l'intervalle QT. Nous avons également démontré que chez les animaux diabétiques, les perturbations métaboliques associées au diabète entraînaient d'importantes dysfonctions des canaux I_{Kr}/HERG à cause de la réduction de l'expression de la protéine HERG, ainsi que en raison de la régulation dysfonctionnelle par les ROS,

par l'oxydation protéique, par la peroxydation lipidique qui sont augmentées, et par la réserve endogène d'antioxydants qui est réduite. Ces effets sont contrés par un traitement à l'insuline qui normalise le niveau de glucose ou par l'antioxydante vitamine E, permettant de récupérer le courant I_{Kr}/HERG ainsi que l'APD et l'intervalle QT. Ces résultats sont confirmés par le fait que les lapins diabétiques traités à l'insuline ou à la vitamine E ne présentent aucuns signes d'arythmies.

Au cours d'études plus détaillées, nous avons montré que la fonction du canal HERG était a son maximum dans un contexte de normoglycémie, et que cette fonction était altérée en hypo- ou hyper-glycémie suite à la sous-production d'ATP ou la surproduction de ROS, respectivement.

Nous montrons aussi que l'activité basale de la protéine kinase B (PKB), directement corrélée à l'action d'insuline, est essentielle à la fonction normale du canal HERG. De plus, deux autres facteurs de signalisation impliqués dans le diabète, le TNF-α et le céramide affectent la fonction des canaux I_{Kr}/HERG via un même mécanisme de l'augmentation de ROS.

L'ensemble de ces travaux nous permet de conclure que la modulation fonctionnelle du courant I_{Kr}/HERG joue un rôle central dans la prolongation de l'intervalle QT et l'apparition de troubles du rythme associés au diabète. Le dysfonctionnement du courant I_{Kr}/HERG est le résultat d'un équilibre net entre les facteurs d'activation du courant, tel que l'insuline et la PKB, et les facteurs inhibant le courant tels que l'hyperglycémie, les ROS, le TNF-α et le céramide. Ainsi, l'augmentation du courant I_{Kr}/HERG par manipulation de l'expression ou par modulation fonctionnelle pourrais retarder voir même renverser les désordres électriques du myocarde associés a la pathologie diabétique.

Mots-clés: Cardiomyopathie diabétique, intervalle QT, arythmies, I_{Kr}/HERG, insuline, hyperglycémie, protéine kinase B, TNF-α, céramide, ROS.

ABSTRACT

Heart diseases account for half of all deaths among people with diabetes. Up to one fourth of diabetic patients have prolonged QT interval. QT prolongation, primarily reflecting the lengthening of ventricular action potential duration (APD), can cause sudden cardiac death due to the occurrence of lethal ventricular arrhythmias, and has been considered as a predictor of mortality in both type I and type II diabetic patients. Previous studies found reduction of several ion currents (e.g. reduced I_{to} and I_{ss}) in experimental models of diabetes. These studies contribute significantly to our current understanding of the ionic mechanisms for diabetic QT prolongation, but several important issues remained unresolved. First, previous studies were conducted nearly exclusively in rats and mice, the species in their adulthood not expressing phenotypic and physiologically significant I_{Kr} and I_{Ks} that are otherwise the major repolarizing currents determining the plateau phase and total APD in humans. Second, the profiles of changes of ion currents found in rats and mice could hardly fully explain the clinical diabetic QT prolongation. Finally, diabetes is primarily a metabolic disturbance with elevated levels of glucose, reactive oxygen species (ROS), tumor necrosis factor-α (TNF-α) and ceramide, and reduced insulin and impaired insulin signaling transduction. However, these metabolic perturbations as the potential mechanisms for the diabetic electrical disorders have been overlooked in the past.

In this thesis, we aimed at delineating the underlying ionic, cellular, molecular and signaling mechanisms for diabetic QT prolongation and the associated arrhythmias, and shedding the light on developing novel and rational therapies. We hypothesized that I_{Kr} and its pore-forming α-subunit HERG (human *ether-a-go-go* related gene) is the major contributor to the diabetic QT prolongation and the impairment of I_{Kr}/HERG in diabetic heart is a combined effect of the down-regulation of I_{Kr} channel protein and of the negative functional modulation of I_{Kr}/I_{HERG} by metabolic stresses and signaling molecules.

We reproduced the prolongation of APD and heart-rate corrected QT (QTc) interval in alloxan-induced type 1 diabetic rabbits, and identified the significantly impaired I_{Kr} as the major ionic mechanism for diabetic APD prolongation, while other ion currents as the minor contributors to this abnormality. We demonstrated that diabetic metabolic perturbations cause the dysfunction of I_{Kr}/HERG in diabetic hearts by significant down-regulation of HERG protein and by impairing I_{Kr}/HERG function due to increased levels of ROS, oxidations of lipids and

proteins in diabetic myocardium and simultaneously decreased endogenous antioxidant reserve (total antioxidant status), which can be prevented by insulin or vitamin E therapy to decrease the glucose level and/or to reduce the oxidative stress, rendering normalized I_{Kr}/HERG function and APD and QTc interval, and preventing the associated arrhythmias.

Our studies further revealed that the maximum HERG function operates under normoglycemia, and depression of HERG function occurs with either hypoglycemia or hyperglycemia, due to underproduction of ATP in the former, and overproduction of ROS via oxidative phosphorylation in the latter.

We found that the activity of protein kinase B (PKB), a down-stream component of insulin signaling pathway, is essential for proper function of I_{Kr}/HERG. Moreover, TNF-α and ceramide, which are known to be deleterious factors critical to the progression of diabetes, both impaired I_{Kr}/HERG function via the common pathway, the increases in ROS.

Based on these data, we conclude that I_{Kr}/HERG K^+ channelopathy serves as the ionic basis for diabetic QT prolongation and accompanying arrhythmias, and oxidative stress caused by hyperglycemia as the major metabolic mechanism for diabetic I_{Kr}/HERG K^+ channelopathy. The dysfunction of I_{Kr}/HERG is a combined effect of decrease in the enhancing factors (e.g. insulin, PKB) and increases in the suppressing factors (e.g. hyperglycemia, elevated ROS, TNF-α and ceramide). Thus, increasing I_{Kr}/I_{HERG} by manipulating HERG expression and by functional modulation on related cellular signaling molecules such as antioxidants could retard and even reverse, at least partially, the electrical disorders in diabetic hearts.

Key words: Diabetic cardiomyopathy, QT interval, Arrhythmia, I_{Kr}/HERG, Insulin, Hyperglycemia, Protein kinase B, Tumor necrosis factor-α, Ceramide, Reactive oxygen species.

TABLE OF CONTENT

LIST OF TABLE

Chapter 1

LIST OF FIGURES

Chapter 1

Chapter 3

Chapter 4

Chapter 5

Chapter 6

Chapter 7

Chapter 8

Chapter 9

LIST OF SIGNS AND ABBREVIATIONS

$[Ca^{2+}]_i$	Intracellular calcium concentration
ATP	Adenosine triphosphate
AF	Atrial fibrillation
AP(s)	Action potential(s)
APD	Action potential duration
APD_{50}	50% depolarization of AP
APD_{90}	90% depolarization of AP
AT-II	Angiotensin II
AV node	Atrioventricular node
Bis	Bisindolylmaleimide
Ca^{2+}	Calcium (ion)
CaM	Calmodulin
CHF	Congestive heart failure
CHO	Chinese hamster ovary
CM-H_2DFDA	5-(and-6)-chloromethyl-2', 7 -dichlorodihydrofluorescein diacetate
CNS	Central nerve system
DAD	Delayed early afterdepolarizations
DM	Diabetes mellitus
ECG	Electrocardiogram
EAD	Early afterdepolarizations
GAPDH	Glyseraldehyde-3-phosphate dehydrogenase
GluT4	Glucose transporterase
H_2O_2	Hydrogen peroxide
HEK	Human embryonic kidney
HERG	Human ether-à-go-go-related gene
HF	Heart failure
IDDM	Insulin-dependent diabetes mellitus
I_{CaL} (or I_{CaL})	L-type Ca^{2+} current/channel

I_{CaT} (or I_{CaT})	T-type Ca^{2+} current/channel
I_{HERG} (or I_{HERG})	HERG K^+ currents/channel
I_K (or I_K)	Delayed rectifier K^+ current/channel
I_{K1} (or I_{K1})	inward rectifier K^+ current/channel
I_{KATP} (or I_{KATP})	ATP-sensitive K^+ current/channel
I_{Kr} (or I_{Kr})	Rapidly-activated delayed rectifier K^+ current/channel
I_{Ks} (or I_{Ks})	Slowly-activated delayed rectifier K^+ current/channel
I_{NCX} (or I_{NCX})	Na^+-Ca^{2+} exchanger current /channel
I_{to} (or I_{to})	Transient outward K^+ current/channel
I_{ss}	Quasi-steady-state outward K^+ current
IVF	Idiopathic ventricular fibrillation
I-V	Current-Voltage
JLN syndrome	Jervell and Lang-Nielsen syndrome
K^+	Potassium (ion)
KChIP	K^+-channel interacting protein
K_V	Voltage-gated potassium channel
LPC	Lysophosphatidylcholine
LQTS	Long QT syndrome
MAPK	Mitogen-activated protein kinase
minK	Minimal potassium channel
MiRP1	MinK related peptide 1
MI	Myocardial ischemia
MIS	Myocardial ischemia syndrome
MnTBAP	Mn (III) tetrakis (4-benzoic acid) porphyrin chloride;
Na^+	Sodium (ion)
NIDDM	Non-insulin-dependent diabetes mellitus
$O_2^{\cdot -}$	Superoxide anion
OH^-	Hydroxyl group
PBS	Phosphate-buffered saline
PIP2	Phosphatidyl 4,5-biphosphate
PI3K	Phosphoinositide 3-kinase

PKA	Protein kinase A
PKB	Protein kinase B
PKC	Protein kinase C
QT-↑	Lengthening of QT interval
RMP	Resting membrane potential
ROS	Reactive oxygen species
RW syndrome	Romano-Ward syndrome
SMase	Sphingomyelinase
SOD	Superoxide dismutase
SR	Sarcoplasmic reticulum
STZ	Streptozotocin
TdP	Torsade de pointes
TNF-α	Tumor necrosis factor-α
TNFR	TNF receptor
VF	Ventricular fibrillation
VGKCs	Voltage-gated potassium channels
VitE	Vitamin E
VT	Ventricular tachycardia
WMN	Wortmannin
X/XO	Xanthine/Xanthine oxidase (a system to generate ROS)

ACKNOWLEDGMENTS

This thesis is really the work of more than the person named on the title page.

I want to express my deepest gratitude to my supervisor Dr. Zhiguo Wang for his expert support and guidance throughout these years. I thank Dr. Wang for his accepting me as a student after my coming to Montreal as a science visitor, and for sharing with me his rich scientific and personal experience which I will continue to learn in my future life. Without his essential advises, his encouragement and inspiration, my study would never have been succeeded.

Dr. Stanley Nattel is gratefully acknowledged for his constructive scientific counsel and review in our collaborative projects and his nice recommendation in my applications for a studentship and a postdoctoral fellowship.

Thanks also for creating an outstanding research environment with honesty and friendship which extends from the workplace in the Dr. Wang laboratory, in the Institut de Cardiologie de Montreal (ICM), and in the Université de Montréal. I highly appreciate the expertise at any 'time-point', which I needed from any of the staff at the ICM where the work for this thesis was carried out.

I would like to thank all my collaborators from China: Dr. Baofeng Yang and his teams, for significant contribution to our experimental and writing processes. I express my sincere gratitude to my supervisors, Professors Jiancheng Huang and Shibo Xu during my undergraduate and graduate studies, and my first employer Professor Chuangguang Zhong, for their sustained fascinating me with the passion to science, their great help in my development of scientific and personal quality and their maximum sympathy to me under any circumstance.

I want to sincerely thank the colleagues I worked with, whose company has been very inspiring and whose friendship will always stay in my heart: Dr. Jingxiong Wang, Dr. Huizhen Wang, Dr. Hong Han, Dr. Huixian Lin, Xiaofan Yang, Marc-Antoine Gillis, Louis R. Villeneuve, Dr. Jiening Xiao, Ling Xiao, Dr. Liming Zhang, Hong Long, Dr. Stephen Zicha, Dr. Huanhuan Gao, Xiaobin Luo, Dr. Marc Pourrier, Dr. Gernot Schram, Daniel Herrera, Denis Chartier, Dr. Yukiomi Tsuji, Chantal Maltais, Natalie L'Heureux, Evenlyn Landry, and people in the laboratories of Dr. Nattel, Dr. Terence E. Hébert, Dr. Céline Fiset, and Dr. Bruce G. Allen, and many others, with whom I have been interacted and helped for various needs.

My special thanks go to classmate Jingxiong Wang for his in-time help in work and in life and for his friendship, to Huizhen Wang for her first-hand help to initiate my learning in Dr. Wang's lab, to Xiaofang Yang for her ready-for-help daily assistance, to Louis R. Villeneuve for his sophisticated assistance in confocal experiments, and to Marc-Antoine Gillis for his professional aids in telemetry ECG recordings, and to Dr Ange Maguy for his kind help in working out the French version of the thesis summary.

I address my warmest thanks to Karine Bouthillier, Emilie Nadeau, Stephenie Blanchet, Nathalie Degrasse, Benoit Chambarron and Kristine Perez for their professional assistance in animal care, making the animal studies undergo smoothly; and to Jacqueline Loiselle, Luce Bégin, and other secretaries for their excellent secretarial and other helps. Special recognition is due as well to the administrative office and audio-vision section staff at the Centre de Recherche de l'ICM. I want to say "Merci!" to Madame Denise Varennes and the stuff in the Faculté de médecine and the Faculté de études supérieurs of the Université de Montréal, for their helps in my PhD studies and preparing for this thesis.

I would like to extend my gratitude to Dr. Terence E. Hébert, Dr. Céline Fiset, Dr. Bruce G. Allen, Dr. Jacques Billette, and Dr. Alvin Shrier for their insightful suggestions and constructive comments in my thesis studies.

I gratefully acknowledge financial support for this study from the Canadian Institutes of Health Research, the Canadian Diabetes Association, the Fonds de la Recherche de l'Institut de Cardiologie de Montréal, the Fonds de Recherche en Santé du Québec; and the Heart and Stroke Foundation of Canada for funding me the Doctoral Research Award since 2003.

I thank my dear friends Xiao Zhang, Xiaoli Tang, and Xiang Wan for their warm-hearted support and care in spite of the thousands kilometres distance between us.

Finally I want to say 'Xiè Xiè!' to my wonderful parents Qingyun and Xiuping for their endless care and love. To my loved wife Haiqing who has been supporting me facing any obstacle and sharing our joys since our first meet; and to all others of my families. This work would not be done without their support.

Yiqiang Zhang, October 2005

CONTRIBUTION OF AUTHORS

The following is a statement regarding the contributions of co-authors and myself to the six articles which have been published or submitted for publication, and included in this thesis.

1. **Zhang Y**, Wang H*, Xiao J*, Bai Y, Wang J, Zhang H, Yang B, Wang Z. Ionic mechanisms underlying the abnormal QT prolongation and the associated arrhythmias in diabetic rabbits: Critical role of rapid delayed rectifier K^+ current. *Am.J. Physiol* Submitted, December 2005 (* indicates these two authors have equal contribution).

Dr. Zhiguo Wang and I proposed the original research plan. I designed and carried out the experiments in every step and analyzed the data and prepared for the figures and manuscripts. Dr. Huizhen Wang, Dr. Jiening Xiao, and Haiqing Zhang were involved in the experiments of Western blot. Yunlong Bai and Dr. Baofeng Yang were involved in the recording of I_{Ks} and I_{Na}. Dr. Jingxiong Wang participated in animal handling and myocyte isolation. Dr. Z. Wang had the original idea and fully supervised the work and finalized the manuscript for publication.

2. **Zhang Y**, Xiao J*, Wang H*, Wang J, Villeneuve LR, Zhang H, Lin H, Bai Y, Yang B, Wang Z. I_{Kr}/HERG as a target for experimental therapies of diabetic QT prolongation and arrhythmias. *Am.J. Physiol* Submitted December 2005 (* indicates these two authors have equal contribution).

Dr. Z. Wang and I proposed the original research plan. I designed and carried out the experiments in every step and analyzed the data and prepared for the manuscript. Drs. J. Xiao and H. Lin participated in the experiments to test the oxidative status of heart tissues. Dr. H. Wang and H. Zhang, Y. Bai and Dr. B. Yang participated in the experiments of Western blot and immunocytochemistry. Dr. J. Wang participated in the animal handling, myocyte isolation, and ion current recording. Louis R. Villeneuve contributed to the cryosectioning and the observation of immuno-histochemical and immunocytochemical specimens. Dr. Z. Wang had the original idea and fully supervised the work and finalized the manuscript for publication.

3. **Zhang Y**, Han H, Wang J, Wang H, Yang B, Wang Z. Impairments of HERG (Human *ether-à-go-go* related gene) K^+ channel function by hypoglycemia and hyperglycemia: Similar phenotype but different mechanisms *J Biol Chem* 2003;278:10417-10426

Dr. Z. Wang and I proposed the original research plan. I designed and performed the experiments in cell culture, ion current recording, and ROS staining, and analyzed the data and worked out the draft of this article. Dr. Hong Han and Dr. H. Wang participated in the experiments of ROS staining, and Dr. J. Wang worked partially on the patch-clamp recording. Dr. Yang comments on the designing of experiments. Dr. Z. Wang had the original idea and fully supervised the work and finalized the manuscript for publication.

4. **Zhang Y**, Wang H, Wang J, Han H, Nattel S, Wang Z. Normal function of HERG K^+ channels expressed in HEK293 cells requires basal protein kinase B activity. *FEBS Lett.* 2003; 534:125-132

In this paper, Dr. Z. Wang and I proposed the original research plan. I designed and did the experiments, analyzed the data and wrote the manuscript. Dr. H. Wang and Dr. H. Han participated in the immunocytochemical studies and Dr. J. Wang participated in the experiments of ion current recording. Dr. Stanley Nattel provided effective co-direction of this work and Dr. Z. Wang offered close instruction in the whole process, refining the proposal, clarifying the notion, and producing the final version of this article.

5. Wang J*, Wang H*, **Zhang Y**, Gao H, Nattel S, Wang Z. Impairment of HERG K^+ Channel Function by Tumor Necrosis Factor-α: Role of Reactive Oxygen Species as a Mediator. *J Biol Chem,* 2004; 279(14):13289 13292. (* indicates both authors have equal contribution).

In this work, I designed the protocols for detecting ROS generated by TNF-α in HEK293 cells and cardiomyocytes, performed the experiment and analyzed the data. Dr. J. Wang performed the experiment and analyzed the data about the effects of TNF-α on HERG current and on action potential in myocytes and involved in the experiments about ROS. Dr. H. Wang and Dr. Huanhuan Gao performed the Western blot experiments. Dr. Nattel provided effective

co-direction of this work and Dr. Z. Wang offered close instruction in the whole process, refining the proposal, clarifying the notion, and producing the final version of this article.

6. Wang J, **Zhang Y**, Wang H, Lin H, Yang B, Wang Z. Sphingolipid Metabolite Ceramide Causes Metabolic Perturbation Leading to HERG K^+ Channel Dysfunction and Abnormal Slowing of Cardiac Repolarization. (in preparation)

I designed and performed the experiments to detect the ROS generated by ceramide in HEK293-HERG cells, and analyzed the data. Dr. J. Wang demonstrated the depressive effects of ceramide on HERG channel in HEK293 cells using different pharmacological approaches. Dr. H. Wang and Dr. H. Lin participated in the Western blot experiments. Dr. Yang provided effective co-direction of this work. Dr. Z. Wang offered close instruction in the whole process, refining the proposal, clarifying the notion, and producing the final version of this article.

DEDICATION

I would like to dedicate this thesis to my family, my relatives, and my friends, whose continued support and encouragement along the way have meant more to me than they will ever know.

PART I. INTRODUCTION AND REVIEW OF THE LITERATURES

Unattended patients of diabetes mellitus (DM) are at high risk of developing cardiac and vascular diseases, such as arrhythmias and hypertension, which can be life-threatening; therefore, it is important to understand the mechanisms underlying the diabetic cardiac and vascular complications.

Previous studies on diabetic vascular and heart diseases have demonstrated the impaired cardiac function independent of vascular and other diseases, suggesting the existence of a primary myocardial defect in DM, so-called diabetic cardiomyopathy. Diabetic cardiomyopathy is characterized by electrical remodeling with aberrant electrophysiology, metabolic remodeling with malignant biochemical processes and anatomical remodeling with progressive loss of cardiomyocytes, which result in impaired cardiac function and increased risk of lethal arrhythmias, with the prolongation of cardiac QT interval as a predictor. These studies have suggested the transient outward K^+ channel (I_{to}) to be a contributor to the QT prolongation. However, these studies were mainly done in diabetic rat and mouse models, and it is unlikely applicable to humans. The metabolic stresses, such as increased reactive oxygen species, and the defective biochemical process including insulin insufficiency, are also considered to cause diabetic arrhythmias because of the resultant functional impairment of cardiac myocytes.

This dissertation focuses on the role of the rapid delayed rectifier K^+ channel (I_{Kr}) that is encoded mainly by human *ether-à-go-go* related gene (*HERG*) which is a critical player in maintaining regular cardiac rhythm, in the diabetic QT prolongation and arrhythmias, and deciphers the possible mechanisms using cell and animal models. The ultimate goal is to provide novel and rational approaches for the treatment of cardiac arrhythmias in DM patients.

The first chapter introduces the basis of cardioelectrophysiology and provides extended review of our understanding to the diabetic QT prolongation and arrhythmias, and the questions remained unanswered. The main parts of the thesis include: in Type 1 diabetic rabbits, how the cardioelectrophysiology changes and what are the underlying mechanisms (Chapters 3 and 4); how glucose level affects I_{Kr}/HERG function in an HEK293 cell model (Chapter 5); the role of protein kinase B (PKB), a downstream target of insulin signaling cascade, in sustaining proper I_{Kr}/HERG activity (Chapter 6); and how tumor necrosis factor-α (TNF-α) and ceramide, both of which are diabetic signaling molecules, modulate the function of I_{Kr}/HERG and change the cardiac function (Chapter 7, and 8). Overall discussion of these results is followed at the end of the dissertation (Chapter 9).

CHAPTERS

1 QT PROLONGATION AND ARRHYTHMIAS IN DIABETIC CARDIOCOMPLICATIONS

1.1 Diabetes Mellitus and Diabetic Complications

1.1.1 Diabetes, a prevalent and costly disease

Diabetes mellitus (DM), a silent killer, is a chronic metabolic disease caused by inherited and/or acquired absolute or relative deficiency in production of insulin by the pancreas, or by the ineffectiveness of the insulin produced (known as insulin resistance). Such kind of deficiency results in increased concentration of glucose in blood, which in turn damages functions of many systems of the body, in particular the heart, blood vessels, nerves, kidneys, etc.

There are mainly two common types of DM: the insulin-dependent DM (IDDM, Type 1) and the non-insulin-dependent (NIDDM, Type 2). IDDM is characterized as a symptom that the pancreas islet fails to produce insulin, which is essential for survival. This form develops most frequently in children and adolescents, but is being increasingly noted later in life. NIDDM results from the body's inability to respond properly to the action of insulin produced by the pancreas. Type 2 diabetes is much more common and accounts for around 90% of all diabetes cases worldwide.[1] It occurs most frequently in adults, but is being noted increasingly in adolescents as well.

DM is a major health problem worldwide. Now more than 2.4 million or 6.7% of Canadians,[2] and 18.2 million or 6.3% of Americans have diabetes.[3] Globally, there are currently almost 200 million diabetic patients. In Canada, more than 60,000 new cases of diabetes come to light every year. Moreover, half of people with diabetes are unaware of their condition. In some countries this figure may rise to 80%. According to the World Health Organization (WHO)'s Diabetes Program of the Division of Noncommunicable Diseases and Mental Health (NMH/DIA), recent estimates predict that if current trends continue the number of persons with diabetes will be more than double, from 175 million to 300 million in the next two decades.[4;5]

The greater proportion of the increase is likely to occur in the developing countries, the communities that can least afford the treatments.

Diabetes is a costly and even fatal disease. WHO estimates that 4~5% of health budgets is spent on diabetes-related illnesses. A person with diabetes incurs medical costs that are two to five times higher than those of a person without diabetes. This is due to more frequent medical visits, purchase of supplies and medication, and the higher likelihood of being admitted to a hospital. Health care costs for diabetes and its complications amount to more than $9 billion a year for the Canadian.[2] It is the fourth main cause of death in most developed countries, the leading cause of blindness and visual impairment in adults, and the most common cause of amputation which is not the result of an accident. It is a bit better that this disease is the seventh leading cause of death in Canada. Diabetic patients are two to four times more likely than people without diabetes, to develop cardiovascular disease, which is the number one cause of death in industrialized and most of the less developed countries. Increased risks and occurrence of heart attack, stroke, and high blood pressure are found in people with diabetes.

There is considerable scope however, to lessen the economic and social burden, and the patients' torment resulted from diabetes, provided that work continues in identifying the most effective prevention and control policy.[6-9] There is conclusive evidence that good control of blood glucose level can substantially reduce the risk of developing complications and slow their progression in all types of diabetes. The management of hypertension and hyperlipemia is equally important. In all societies, better control of these parameters would contribute to a substantial improvement of quality of life. Once diabetic complications occur, well monitored conditions such as arrhythmia-prevention will help to improve the health of the diabetics.

1.1.2 Cardiomyopathy and cardiovascular complications in diabetes

Due to the increased glucose level and insulin insufficiency and resistance, diabetes can result in a number of complications that have a major impact on the health and well-being, depending on the serious degree of the diabetic diseases. These include neuropathy or nerve problem, cardiovascular complications (e.g. hypertension, coronary heart disease, micro- and macrovascular complications), retinopathy or eye problem, nephropathy or kidney damage, diabetic foot diseases, etc (Figure 1).

Cardiovascular disease represents the major cause of morbidity and mortality in diabetic patients and heart disease is the leading cause of diabetes-related deaths. Adults with diabetes have heart disease death rates and risk for stroke, both about two to four times higher than adults without diabetes. About 65% of deaths among people with diabetes are due to heart disease and stroke. Heart disease accounts for approximately 50% of all deaths among people with diabetes.[8]

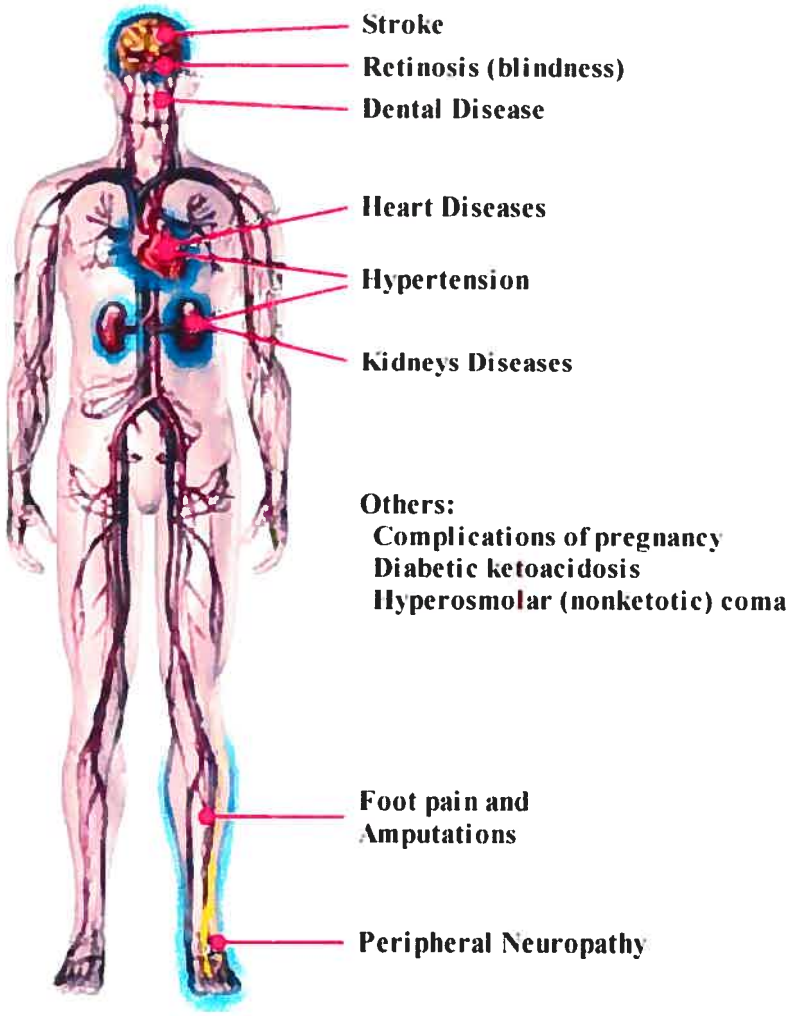

Figure 1. Diabetic Complications. (Modified from healthcentersonlin.com)

Prior to 1972, the increased cardiovascular morbidity and mortality in diabetics had been attributed to vascular diseases. In 1972, Rubler et al first described a specific type of cardiomyopathy related to diabetes,[10] suggesting that there exist myocardial disease as an independent clinical entity.[11] The term "diabetic cardiomyopathy" was thus proposed, describing

an early complication of diabetes that shows diastolic dysfunction and then followed by systolic dysfunction. Since then, a variety of disciplines including noninvasive and invasive cardiac methodologies, as well as epidemiologic studies, have provided information that has changed our view on the relation of diabetes to cardiac diseases. Instead of an exclusive focus on coronary artery disease, it is now recognized that heart muscle can be independently involved in diabetic patients. In diabetics without known cardiac diseases, abnormalities of left ventricular mechanical function have been demonstrated in 40~50% of subjects and it is primarily a diastolic phenomenon. Left ventricular hypertrophy may eventually appear in the absence of hypertension. The diastolic dysfunction appears related to interstitial collagen deposition, largely attributable to diminished degradation.[12] Clinical studies demonstrated that children and adolescents with type 1 diabetes have signs of subclinical cardiac dysfunction since their early disease stage; in this population comorbidity such as ischemic heart disease or hypertension can be considered as absent or minimal.[13]

When presenting with other cardiovascular complications (e.g., ischemic heart disease or hypertension), diabetic patients have a much worse prognosis than non-diabetic patients and are more prone to progress to congestive heart failure.[14-16] The underlying diabetic cardiomyopathy appears to contribute to accelerated heart failure. Diabetic cardiomyopathy in general is characterized by metabolic remodeling with malignant biochemical processes,[17;18] electrical remodeling with aberrant cardiac electrical and contractile functions and arrhythmias, [11;19-21] and anatomical remodeling with progressive loss of cardiomyocytes.[22] These alterations can be primary (due to loss of direct insulin action) or secondary (due to the metabolic perturbations associated with the disease). Cardiomyopathy will result in impaired cardiac performance and increased risk of lethal arrhythmias. Despite the obvious importance of diabetic cardiomyopathy, a better understanding of this complex and very likely multi-factorial problem at the cellular and molecular levels is lacking. Much of what is known about the pathogenesis of diabetic complications has been gleaned from studies using animal models, including rat, mouse, rabbit, and dogs, etc.

1.1.3 QT prolongation and arrhythmias in diabetic hearts

Electrocardiogram (ECG) recorded from diabetic patients show prominent electrical disturbance with prolonged QT interval according to more than 6 long-term epidemiological

studies (including the EURODIAB, the Neuropathy Study Group of the Italian Society for the Study of Diabetes, the 3rd National Health and Nutrition Examination Survey) involving more than 20 countries and 30 centers, and 11 thousand diabetic patients.[23-33] It was found up to 26% diabetic patients have electrical disturbance along with QT prolongation and dispersion,[34] including the diabetics of both children and adolescents.[28] The QT prolongation and dispersion are associated with an increased risk of sudden cardiac death in diabetics have been considered as a predictor of mortality in diabetic patients and,[35;36] due to the occurrence of lethal ventricular arrhythmias known as Torsade des Pointes or long Q-T syndrome (LQTS).[37;38] These findings can also be applied to type 2 diabetes.[30-32;39-41]

Studies also demonstrated that both hyperglycemia of diabetes, and hypoglycemia in diabetes therapies, can prolong cardiac QT interval.[34;42-48] Indeed, QT prolongation and heterogeneity of QT prolongation (QT dispersion) have been suggested as the predictor of mortality in both IDDM and NIDDM. [26;33;34;37;38;40]

Despite this serious reality, it is only in recent years that people start to understand the ionic and cellular/molecular basis for the diabetic QT prolongation.

1.1.4 Animal models of diabetes mellitus

There has been little progress in characterizing the ionic, cellular and molecular features of diabetic cardiomyopathy in patients, much less their mechanisms. It remains unclear whether there are differences between insulin dependent and non-insulin dependent forms of diabetes mellitus with respect to the development of diabetic cardiomyopathy. Defining cardiac changes in diabetic humans is obviously extremely important in light of the fact that diabetes is a chronic disease not well represented by animal models. However, animal models are the most used subjects to understand the mechanisms of diabetic complications.

Although we now have animal models for both type 1 and type 2 diabetes, the separation of these two categories is not total, just as these two are not completely separated in human. Most used type II diabetic animal models are: genetic, obese diabetic mouse and fatty Zucker rat, nutrition-induced diabetic sand rat and spiny mouse, rodents with decrease in β-cell mass induced by pancreatectomy and streptozocin (STZ), and diabetic offsprings of selective inbreeding of rodents.[49]

Type 1 diabetic animals can be subdivided into two groups: chemical-induced, and spontaneous/ genetic modified.[50;51] Genetic models include the nonobese diabetic (NOD) mouse model of diabetes and also the BB rat model,[52] which will not be discussed in detail in this thesis. Induced diabetes can be achieved by pancreatectomy or by destroying the pancreatic β-cell with a number of chemicals, including alloxan and STZ which are frequently used. Alloxan and STZ, initially used as active anti-tumor reagents, are deleterious and can selectively damage islet cells, thus can be used to induce IDDM.[53-56] The β-cell is uniquely sensitive to alloxan because its plasma membrane contains ionized sulphydryl (SH) groups related to insulin release which are not found in other tissues.[57] The sensitivities to alloxan or STZ in different species are not the same, e.g. guinea pig and some big-size animals including dog and rabbit, are resistant to STZ, therefore it is difficult to make diabetes in these species.[50] Functionally, both alloxan and STZ interfere the glucose transport, alter the SH groups of glucokinase, and impair mitochondrial function by inducing the formation of free radicals.[58] Repeated injections with low doses of STZ into genetically susceptible mice can induce diabetes similar to human IDDM, in which a pathogenic involvement of cell-mediated immunity and the coexistence of a marked pancreatic insulitis are encountered and apoptotic death of β-cell is a responsible mechanism. However, this model is different from the autoimmune type 1 diabetes seen in spontaneous animal models.[58]

Both chemical-induced and genetic-modified diabetic animal models have been generated to facilitate the studies in the pathology of diabetes. By far the most extensively employed animal models are the STZ-induced diabetes mellitus in rat and mouse and alloxan-induced rabbits and dogs. Rats treated with STZ for weeks to months develop hypoinsulinemic diabetes mellitus, and mice are usually treated for a single dosage of STZ in order to develop DM. Chronic diabetes diminishes contractility and, most especially, relaxation, and prolongs the duration of contraction in rabbit hearts,[59] which may due to the alteration of myosin isoenzyme composition (i.e. switch from V1 to V3 isomyosin) and are reversible with insulin.[60] Effects on "passive" diastolic compliance have been variable. These contractile abnormalities are correlated with several alterations in excitation-contraction (E-C) coupling, ion transport and exchange, including the prolongation of AP, and the depressed sarcoplasmic reticular (SR) calcium pumping and sarcolemmal Na/Ca exchange.[11;21;61] While the STZ-diabetes mellitus rat and mouse are reliable, well-characterized models, they may not be the most relevant model for human disease, particular in their different electrophysiological profiles.

1.2 QT interval, APD, and Ion Channels: Physiology and Pathology

1.2.1 QT interval as a function of cardiac repolarization

Heart rhythm is generated by sequential movement of inward and outward ion currents across the membrane of the cardiomyocyte; disturbance of the balance will result in aberrantly altered cardiac electrical activities, so called arrhythmias.

1.2.1.1 Electrocardiogram (ECG)

The electrical activity of heart can be detected using a technique called electrocardiogram (ECG) which represents the electrical current moving through the heart during heartbeat cycles. The current movement is divided into several parts, and each part is given an alphabetic designation in the ECG. Each heartbeat begins with an impulse from the heart's pacemaker (sinus or sinoatrial node) located at the entrance to the right atrium. This impulse activates the upper chambers of the heart (atria), represented as a P wave in the ECG recording. Then the excitatory stimuli pass over the atrioventricular node (AV node) to the lower chambers of the heart (ventricles) and generate the QRS complex in ECG. The electrical pulse then spreads back over the ventricles wall in the opposite direction, resulting in the recovery T wave. Therefore, the QT interval which is the duration between the onset of Q wave and the termination of T wave represents the activity of ventricular contraction. Many kinds of cardiac abnormalities can be seen on an ECG. For example, the heart rhythm may be abnormal: too fast, too slow, or irregular. By reading an ECG, doctors can usually determine where in the heart the abnormal rhythm starts and what its causes may be.

1.2.1.2 Ion channels and action potential

The basis of ECG is the ion currents passing through the protein-structured "ion channels" on cell membrane of cardiomyocytes and channels on membrane of cell organelle such as sarcoplasmic reticulum (SR) which is a pool of calcium storage. Cell plasma membranes are highly selective barriers forming the outer surface of eukaryote cells including cardiomyocytes. Inside the cell, membranes of many organelles such as the SR and the mitochondria also have similar structure as the plasma membranes. Assembled from lipids and

proteins in sheet like fashion, plasma membranes give the cell individuality and a certain level of control over its internal environment, and permit the development of concentration gradients (e.g. ions) crucial to the function of signaling molecules.

An ion channel is a pore-forming protein or more typically an assembly of several proteins on the membrane. Such "multi-subunit" assemblies usually involve a circular arrangement of identical or related proteins closely packed around a water-filled pore through the plane of the membrane or lipid bilayer. Ion channels are generally highly selective and impermeable to most ions. By conducting and controlling the flow of ions, ionic channels help establish the small negative voltage that all cells possess at rest, or fire the cell membrane when a certain voltage threshold reaches. Ion channels can generally be classified according to their "gating" (the open-close of a channel): voltage-gated and ligand-gated ion channels; or based on their permeability to ions: cation, anion, or Na^+, Ca^{2+}, K^+, Cl^- channels, etc. Ions passing though the channel will generate either inward or outward currents.

The cardiac action potential (AP) is generated by the concerted action of depolarizing (inward) and repolarizing (outward) currents conducted by different ion channels, pumps and transporters. As the ventricular activity is the main part responsible for the QT interval, it will be focused on the ventricle when discussing AP and ion channels. In ventricle, major inward currents include sodium current (I_{Na}) and calcium current (I_{Ca}), and outward currents include the Ca^{2+}-independent transient outward K^+ current (I_{to}), the rapid and the slow activating delayed rectifier outward K^+ currents (I_{Kr} and I_{Ks}, respectively), and the inward rectifier K^+ current (I_{K1}) which conducts outward current at membrane potential between –80 and 0 mV.[62-65] A small change in the potential across the cell due to various stimuli is sensed by the Na^+ channel protein (I_{Na}), which alters its conformation from resting close state to open, allowing a large, rapid Na^+ influx, producing the typical rapid rising upstroke phase 0 depolarization -- membrane potential becomes positive compared to the resting membrane potential which is between -65mV to -85 mV in different heart cells. A rapid phase 1 repolarization then ensues in some types of cells (e.g. atrial and ventricular myocytes), because of the outward movement of K^+ via the transient outward K^+ channels (I_{to}). Calcium channels open when the membrane depolarizes to the threshold during phase 0 and phase 1. Following phase 1 is the long lasting plateau (phase 2) of the action potential, reflecting a balance between inward current, largely through L-type Ca^{2+} channels (I_{CaL}), and outward current, mainly through delayed rectifier K+ channels (I_K, including

I_{Kr} and I_{Ks}). It is I_{Kr} that initiates the repolarization phase 2 in the action potential. The net outward current during Phase 3 repolarization comes from the increasing I_K, along with the inactivation of I_{CaL}. I_{Kr} reach maximum at about 90% depolarization of AP (APD_{90}). Final repolarization is accomplished by the increasing outward movement of K^+ through inward rectifier channels (I_{K1}) beginning from phase 3 and reach stable at complete repolarization. Slow response cells, for example the sinus node and the AV node have slow depolarization during phase 4 due to the activity of the pacemaker channel. In these cells, a rapid phase 1 upstroke is absent, and initial depolarization is accomplished by the opening of L-type (and perhaps also T-type) Ca^{2+} channels.

The burst and the decay of inward and outward currents during an electrical pulse cycle in a cell form different phenotypes of AP at different regions of the heart because of the different expression in ion channels. For example in ventricle, there are three distinct cell types: epicardial, midmyocardial (M) and endocardial cells particularly in species with larger size. APs of epimyocardial and M cells differ from endocardial cells with respect to the morphology of phase 1. These cells possess a prominent I_{to} which mediates the notch and is responsible for the 'spike and dome' morphology in APs. M cells are distinguished from the other cell types in that they display a smaller I_{Ks}, but a larger late sodium current (I_{NaL}) and sodium-calcium exchanger current (I_{NCx}).[66-74] These intrinsic electrical heterogeneities in ventricular myocardium underlie the longer action potential duration (APD), which is more pronounced in the presence of antiarrhythmic agents with class III actions. The preferential prolongation of the M cell action potential results in the development of a transmural dispersion of repolarization, which can be examined from the ECG showing a prolonged QT interval and a change of the T morphology. Exaggeration of these heterogeneities due to inherited (i.e. gene mutation of channels and their regulatory molecules) or acquired means (e.g. drug exposure, exercise, and secondary to diseases such as ischemia, diabetes, etc.) enhances reentrant excitation, a common mechanism for many cardiac arrhythmias.[75;76] The acute electrophysiological response of a myocyte to exogenous stressors such as drugs, myocardial ischemia, diabetes, or autonomic activation likely reflects changes in function of individual ion channels (also called remodeling), including channels activated by specific stimuli such as ATP depletion and muscarinic stimulation. More chronic responses to such exogenous stressors may also include changes in gene expression.

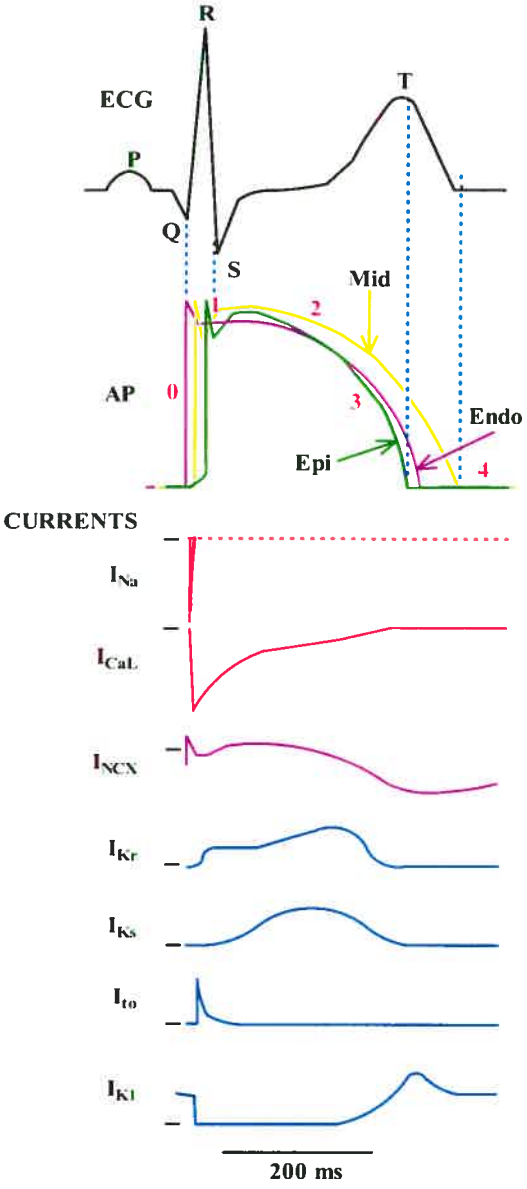

Figure 2. Relationships between ECG, APD and ion currents. (Adapted from Roden DM, et al., 2002.[65])

In theory, inward currents depolarize (meaning the membrane potential is brought to more positive) the cardiac cell membrane and maintain the APD, whereas outward currents repolarize (meaning the membrane potential is brought back to more negative) cardiac cells and shorten the APD. Therefore, decreases in outward currents and/or increased inward currents will

result in the prolongation of APD thereby the QT interval. Figure 2 describes the relationship between a typical ECG, an AP, and ion currents.

1.2.1.3 Long QT syndromes (LQTS)

LQTS is a disorder characterized by a prolongation of the QT interval on the ECG and a propensity to ventricular tachyarrhythmia, which may lead to syncope, cardiac arrest, or sudden death. Defects in the genes corresponding to certain ion channels or impairment of functions of these channels result in QT prolongation, reflecting the abnormally long delay between the electrical excitation (or depolarization) and relaxation (repolarization) of the ventricles of heart. Heart rate corrected QTc values above 0.44 seconds are generally considered abnormal in human, although age- and sex-specific abnormal QTc values have been proposed. Certain triggers such as intense physical exercise or excitement, and being suddenly startled or badly frightened, result arrhythmias, e.g. torsade de pointes (TdP), a life-threatening form of ventricular tachycardia and sudden cardiac death.

LQTS is recognized as the Romano-Ward (RW) syndrome (familial occurrence with autosomal dominant inheritance, QT prolongation, and ventricular tachyarrhythmias) or the Jervell and Lang-Nielsen (JLN) syndrome (familial occurrence with autosomal recessive inheritance, congenital deafness, QT prolongation, and ventricular arrhythmias). Conventionally, LQTS is divided into two catalogues: genetic or inherited, and acquired or drug-induced. Based on recent efforts in deciphering the arrhythmias in cardiac or noncardiac diseases, it is rational to classify a new class of QT prolongation which may also lead to LQTS. Many other syndromes or diseases have been correlated to and probably a reason of QT prolongation. This "pathological LQTS" may occur in ischemia and infarction, chronic heart failure, and noncardiac conditions, such as electrolyte abnormalities (e.g. hypokalemia, hypocalcemia), pulmonary embolism, CNS diseases (e.g. cerebrovascular disorders), hypothermia,[77] hypothyroidism,[78-81] and both IDDM and NIDDM which have been discussed in Section *1.1.3*. Yet, the ionic mechanisms underlying these pathological LQTS are just becoming understood by intensive studies in electrophysiology, cellular and molecular biology.

Genetic testing of LQTS is unfortunately still not readily available, and it may not be possible to determine with certainty a particular patient's genotype. However, at least one recent article claims that LQT 1, 2, and 3 can frequently be identified by the ECG pattern.[82] LQT 1 has

a prolonged QT interval with a normal to high T wave amplitude, a broad based T wave, and an indistinct T wave onset, caused by dysfunction of the pore-forming α-subunit of I_{Ks} channel due to either lost-function mutation or drug induced or diseases-modulated channel impairment. LQT 2 accounts for about 35% of the long QT syndrome patients, resulted from the depression of I_{Kr} current. It is characterized by a prolonged QT interval, low amplitude and bifid T waves in over 60% of cases. LQT 3 patients have a prolonged QT interval with a delayed-onset, peaked and widened T wave, and a long, isoelectric ST segment. They have a rate dependence of the QT interval prolongation and develop TdP at slow rates. The positional candidate gene approach was used to establish that the gene responsible for this chromosome 3-linked LQTS is the cardiac sodium channel gene SCN5A.[83] In 1995, Schott et al.[84] reported on a large French kindred with a complex cardiac phenotype including sinus bradycardia, abnormal heart rate variability, defects in cardiac repolarization (denoted on the ECG as prolonged QT interval), and sudden cardiac death. This report described the first finding of 'type 4 long QT syndrome' and mapped the autosomal dominant disease to human chromosome 4q25-27, a site distinct from the location of any other ion channel gene implicated in the genesis of inherited arrhythmia. LQT5 and LQT6 are diseases resulted from the dysfunction of the channel accessory subunits minK and MiRP1, of I_{Ks} and I_{Kr} channel, respectively. The Andersen syndrome is a rare, inherited disorder characterized by periodic paralysis, long QT interval with ventricular arrhythmias, and skeletal developmental abnormalities, and subtyped into LQT7 due to its prolonging QT interval and its distinct substrate for arrhythmia susceptibility: in reduced extracellular K^+, it induces delayed afterdepolarizations (DAD) and spontaneous arrhythmias. Homozygous KVLQT1 and KCNE1 mutations are associated with congenital deafness (JLN syndrome) and account for less than 1% of cases of LQTS. Approximately 200 different mutations of these genes have been found so far. Significant phenotypic variation of the ECG findings (T wave morphology), factors triggering cardiac events, and risk of cardiac events exist, depending upon which gene and which mutations are involved. Because not all known cases of LQTS are caused by mutations of the above genes, other genes causing this disorder are expected to be identified in the future.

Table 1 lists the chromosomal locus, gene and ion currents related to these LQTS.[85-87] Drug-induced and pathological QT prolongations may also lead to increased risk of ventricular tachyarrhythmias (e.g., TdP) and sudden cardiac death in a similar ionic mechanism as observed in congenital LQTS.

In sum, ionic basis in LQTS demonstrates that reduction of outward current (e.g. I_{Kr}, I_{Ks}) and/or increase of inward current (e.g. I_{Na}, I_{CaL}), will delay the repolarization of AP, lead QT prolongation and predispose to LQTS.

Table 1. Genetic Background of Inherited Forms of LQTS.

LQTS type	D/R	Chromosomal Locus	Gene	Target (channel, etc.)	Alteration
LQT1	D	11p15.5	*KVLQT1 (KCNQ1)* (heterozygotes)	I_{Ks} (α)	↓
LQT2	D	7q35-36	*HERG*	I_{Kr}	↓
LQT3	D	3p21-24	*SCN5A*	I_{Na}	↑
LQT4	D	4q25-27	*ankyrin-B, G*	calcium signalings Na/K-ATPase, I_{NCX} InsP3 receptor	$[Ca^{2+}]_i$ transient ↑
LQT5	D	21q22.1-22.2	*KCNE1* (heterozygotes)	I_{Ks} (β, minK)	↓
LQT6	D	21q22.1-22.2	*KCNE2*	I_{Kr} (β, MiRP1)	↓
LQT7 (Andersen syndrome)	D	17q23	*KCNJ2 (Kir2.1)*	I_{K1}	↓
LQT8 (Timothy syndrome)	D	12p13.3	*CACNA1c (Cav1.2)*	I_{CaL}	↑
JLN1	R	11p15.5	*KVLQT1 (KCNQ1)* (homozygotes)	I_{Ks} (α)	↓
JLN2	R	21q22.1-22.2	*KCNE1* (homozygotes)	I_{Ks} (β, minK))	↓

D: autosomal dominant inheritance; R: autosomal recessive inheritance; ↓: decrease, ↑: increase; α and β represent pore-forming subunit and auxillary subunit of ion channels, respectively.

1.2.2 Inward currents

1.2.2.1 Na^+ current: I_{Na}

Voltage-gated sodium (Na^+) channels (VGSCs) play a fundamental role in the excitability of cardiomyocytes and neurons. They mediate the influx of Na^+ into the cell in response to local membrane depolarization, resulting in a positive feedback to generate the action potential, and produce the rapid rising upstroke in a cell action potential recording (phase 0). I_{Na} expresses in both atria and ventricles in almost all species, including human, canine, rabbit, rat, mouse, guinea pig, and porcine. In heart, I_{Na} is critical in the initiation, propagation, and maintenance of normal cardiac rhythm. Alteration in VGSC expression and/or function thus has a profound effect on the excitability and conduction of stimuli in the heart. It has been demonstrated that channel dysfunctions resulted from gene mutation or blockage of the channels will render to serious cardiac problems including bradycardial arrhythmias and cardiac death.

Like most of other voltage-gated ion channels, I_{Na} heteromultimer composes of one pore-forming α-subunit and one or two regulating auxiliary (β_1 and β_2) subunits.[88;89] α-subunit determines main characteristics of the complex conveying ion selectivity and containing the ion-conducting pore, the voltage sensors, the gates for the different opened and closed channel states, and the binding sites for endogenous and exogenous ligands. It is a tetramer of a series of six transmembrane α-helical segments, numbered S1-S6, connected by both intracellular and extracellular loops called interlinkers (Figure 3). Twelve different genes have been identified that are known to encode the four-domain α-subunits of VGSC (*SCN1A* to *SCN12A*).[90;91] All α-subunits contain four internal repeat domains (DI-DIV), two large interdomain cytoplasmic loops (L1 and L2) and short interdomain loop (L3); S4 is positively charged and the others are hydrophobic. Segment S4 and loop L3 are responsible for voltage sensor and inactivation, respectively. The β subunits regulate the kinetic properties and facilitate membrane localization of sodium channels.

I_{Na} current peaks rapidly and then inactivates in just a few milliseconds. During the plateau of AP, I_{NaL} is very small yet contributes critically to the configuration of AP.[92] VGSCs are classified pharmacologically into two large groups according to their sensitivity or resistance to the block by tetrodotoxin.[93] Most sodium channels are tetrodotoxin-sensitive, but the well-studied Scn5a/SCN5A, is tetrodotoxin-resistant channels. SCN5A is expressed specifically in

cardiac muscle and brain. Its mutation is responsible for the cardiac arrhythmia of the congenital LQT3,[83;94] due to the resultant persistent noninactivating inward Na^+ current, the alterations of voltage dependence and rate and speed of inactivation of the channel throughout the plateau phase of AP.[95] The small net inward pedestal current through these channels is sufficient to distract the balance between inward and outward currents in the plateau and, hence, to prolong APD. On the other hand, mutation in SCN5A can also cause other congenital arrhythmia syndromes including idiopathic ventricular fibrillation (IVF) and conduction block, which unlike LQT3, appears to arise from reduced I_{Na}. Some patients with IVF, i.e., sudden death in the absence of any detectable heart disease (and a normal QT interval), display an unusual ECG feature at rest, J-point elevation in the right precordial leads. This distinctive ECG was first popularized by Brugada & Brugada and is termed the Brugada syndrome.[96] Some Brugada syndrome mutations result in a highly truncated, and therefore nonfunctional protein,[94] or lead to the slowing of inactivation,[97] both causing the reduction of I_{Na}. The ECG manifestations of the Brugada syndrome likely reflect a marked shortening of epicardial but not endocardial APs by loss of Na^+ channel function; the rate dependence of recovery from slow inactivation explains why these ECG findings are exaggerated at fast rates. Some other mutations, e.g. G514C in the I–II linker, have been demonstrated to cause slowed conduction by shifting the voltage dependence of activation to positive potential, and by enhancing the inactivation rate, therefore results in reduced I_{Na}.[98] Recent studies in a family case showed its mutation (D1275N, T220I, R814W, and D1595H) and truncation (2550-2551insTG) is susceptible to cause the early-onset dilated cardiomyopathy and atrial fibrillation (AF). Similar or even identical mutations of this gene may lead to heart failure, arrhythmia, or both.[99] Figure 3 shows the structure of sodium channel subunits which is shared by other voltage gated ion channels, and some sites on SCN5A responsible for Na^+ channel diseases.

Besides the mutated channel defection, I_{Na} impairment caused by drugs such as anti-arrhythmic I_{Na} blockers flecainide and encainide results in increased mortality,[100] especially in those patients with high risk of recurrent myocardial ischemia, because the I_{Na} blockers slows the conduction, and increase the chance of reentry through a scarred myocardium.[101] Moreover, in ischemic condition and I_{Na} blocking, the balance between I_{Na} and I_{to} at the end of phase 1 of AP is disrupted. Because I_{to} is expressed highly in epicardium but not in endocardium, the alteration

of AP in phase 1 generates significant heterogeneity of APDs (shorten in epicardial but not in endocardial APs), and leads to reentry.[102]

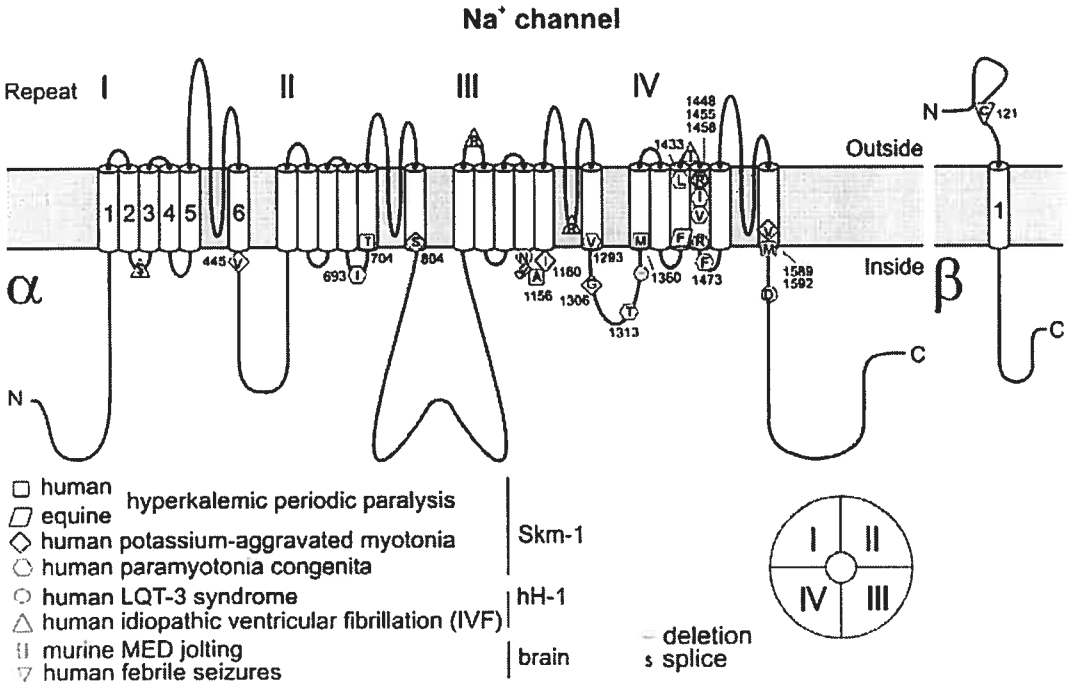

Figure 3. Subunits of voltage-gated sodium channel and sites responsible for diseases. Subunit consists of 4 highly homologous domains (repeats I-IV) containing 2 transmembrane segments each (S1-S6). S5-S6 loops form ion-selective pore, and S4 segments contain positively charged residues conferring voltage dependence to protein. Repeats are connected by intracellular loops; one of them, III-IV linker, contains supposed inactivation particle of channel. 1 and 2 are auxiliary subunits. When inserted in membrane, 4 repeats of protein fold to generate a central pore as schematically indicated on bottom right. Also listed are mutations of α-subunits of various species and tissues: human and equine adult skeletal muscle (Skm-1), human heart (hH-1), and murine brain. Conventional 1-letter abbreviations are used for replaced amino acids whose positions are given by respective numbers of human skeletal muscle channel. Different symbols used for point mutations indicate resulting diseases as explained at bottom left. (Lehmann-Horn, F and Jurkat-Rott, K[90]).

Under chronic conditions, reduction of current can be a result of channel remodeling by either decrease in expression level, or of regulation by both protein kinase C (PKC) and protein

kinase A (PKA)-mediated phosphorylation which reduce the I_{Na} function.[103] PKC effects appear to be mediated by phosphorylation of a serine in the III–IV linker, which is highly conserved among Na^+ channel isoforms.[104] Multiple PKA consensus sites are located in the I–II linker, and a role for PKA-mediated phosphorylation of the channel in mediating its trafficking to and from the cell surface has been proposed.[105] I_{Na} was found to be unchanged in heart failure in ventricular pacing dogs[106] while other studies found it decreased in heart failing dogs induced by in coronary microembolization,[107] and in pig and rabbit a reduction by 40% was found. For more details about the roles of I_{Na} in arrhythmias, refer to the reviews.[65;89;90;108-112]

1.2.2.2 Ca^{2+} currents: I_{CaL}, I_{CaT}

There are primary two types of Ca^{2+} channels in the heart: L-type (long lasting current, I_{CaL}) and T-type (tiny or low-voltage threshold, I_{CaT}). More sensitive to Ni^+ block than I_{CaL}, I_{CaT} is thought to be absent in human ventricle though it contributes to the automaticity in sinus node, AV node, and atrium and acts as a pacemaker current.[113;114] I_{CaL} is sensitive to cadmium and zinc block while more permeable to barium than Ca^{2+}. Following the activation of I_{Na} to depolarize the membrane, calcium channels open and conduct inward currents to further depolarize the membrane and maintain the membrane potential, in which way they critically determine the APD from phase 1 to 3. Ca^{2+} channel α subunit resembles that of sodium channel while α_2/δ, β_1 to β_4, and γ are auxiliary. α_{1C} encodes the L-type α-subunit, and α_{1H} (maybe also α_{1G}) encodes the I_{CaT} α subunit.[115] *Ca(V)1.2* encodes the cardiac I_{CaL} pore forming α-subunit. β-subunits for I_{CaL} increase Ca^{2+} current, accelerate activation and inactivation, and shift activation to more hyperpolarized potentials and maybe involve in α-Ca^{2+} channel trafficking as well.[116;117]

I_{CaL} is regulated by a complex of signaling molecules.[118;119] Calmodulin, a widely distributed Ca^{2+} binding protein in eukaryotic cell, also acts as the Ca^{2+} sensor for the facilitation of I_{CaL}, perhaps by directly binding to the C terminus of I_{CaL} α-subunit or through the activation of the Ca^{2+}/calmodulin–dependent protein kinase CaM kinase II.[120] CaM kinase II and PKA-mediated phosphorylation of the channel, dihydropyridine agonists (e.g. BayK8644) and β-adrenergic stimulation, can enhance the long opening of the channel which result in increased Ca^{2+} current.[121;122] I_{CaL} can be also PKC phosphorylated thus its activation curve being shifted to more positive potential, which reduces the Ca^{2+} current.[123;124] Extracellular ATP stimulates I_{CaL} by increasing the channel open probability.[125]

As a major contributor of inward current to maintain the AP and also to regulate the intracellular Ca^{2+} handling, inherited or artificial mutations of I_{CaL} channel have been shown to cause various types of neurological or cardiac diseases.[90;126;127] Dysfunction of I_{CaL} by missense mutation G406R and G402S in *Ca(V)1.2* causes Long QT syndrome with syndactyly (Timothy syndrome) which is characterized by multiorgan dysfunction including lethal arrhythmias, webbing of fingers and toes, congenital heart disease, immune deficiency, intermittent hypoglycemia, cognitive abnormalities, and autism.[127] These mutations produce sustained inward Ca^{2+} currents by causing nearly complete loss of voltage-dependent channel inactivation and induces intracellular Ca^{2+} overload in multiple cell types which can delay cardiomyocyte repolarization and increase risk of arrhythmia, the ultimate causes of death in this disorder.

Ca^{2+} channels are blocked by three major classes of drugs: dihydropyridines (nifedipine and others), phenylalkylamines (verapamil and others), and benzothiazepines (diltiazem).[128;129] Multiple binding sites for dihydropyridines have been described, including domains III and IV S6 as well as the domain IV P-loop.[130] Most Ca^{2+} channel blockers shift the steady-state inactivation toward more negative voltages.

I_{CaL} and I_{Na} are reduced in myocytes in animal models of AF, congestive heart failure, atrial tachycardia,[76;131-137] in which APD is significantly shortened, while in hypertrophy I_{CaL} is enhanced so APD prolonged due to the accelerated recovery from inactivation.[138;139] Prolongation of the AP also increases the amplitude of the $[Ca^{2+}]_i$ transient, activating CaM kinase (and thus I_{CaL} and other arrhythmogenic inward currents), thereby promoting arrhythmogenic early and delayed afterdepolarizations (EAD, DAD).[140] In addition, mutation in cardiac ryanodine release channel RYR2 causes elevated $[Ca^{2+}]_i$ transient and bursts I_{CaL} thereby prolongs APD and QT interval, result in polymorphic ventricular tachycardia.[141] Other studies showed that in hypertrophied ventricle after ischemia, I_{CaL} is reduced and β-adrenergic response is impaired,[142] which could relate to the degree and types of hypertrophy.[143]

1.2.3 Outward currents

1.2.3.1 Transient outward K^+ current: I_{to}

Cardiac potassium (K^+) ion channels constitute the most diverse class of ion channels with respect to kinetic properties, regulation, pharmacology, and structure.[63;65;144-148] They carry

outward currents in the physiological range of potentials and act to set the resting potential near the K^+ equilibrium potential or to repolarize the membrane.[144] K^+ currents are nearly involved in all phases of AP. K^+ channels can be generally classified into two types: voltage-gated K^+ channels (VGKCs) which contain six transmembrane segments and one pore in each of its four highly homologous α-subunits; and voltage insensitive or ligand-gated K^+ channels that are also tetramer of α-subunits but composing of two transmembrane segments and one pore, and are normally regulated by signaling molecules or neuronal transmitters. In heart, I_{to}, I_K (I_{Kr}, I_{Ks}) are the major VGKCs and I_{K1} is the main voltage insensitive channel that contributes to the ventricular AP configuration. There are a variety of auxillary β-subunits to modify the VGKCs' properties, e.g. channel gating.[146;149]

I_{to} expresses in human ventricular and atrial cells and acts as the principal repolarizing current in adult mouse and rat atrium and ventricle, accounting for the extraordinarily short APs in these species. There is significant transmural heterogeneity in the expression of I_{to} in ventricles, especially in large-size species including human.[66;68;71;75;150] This transmural heterogeneity results in the difference of AP in phase 1 repolarization: Epicardial and M cells possess a prominent I_{to}-mediated notch responsible for the 'spike and dome' morphology, which is absent in endocardial cells due to the lower I_{to} current density . M cells are distinguished from the other cell types in that they display smaller I_{Ks}, but larger I_{NaL} and I_{NCX}. These ionic distinctions underlie the longer APD and steeper APD-rate relationship in M cells, which is more pronounced in the presence of antiarrhythmic agents with class III actions. However, I_{to} does not function as a key current to regulate the APD in rabbit, canine, or human,[16;151] though eliminating this current in mouse results in significant APD and QT prolongations.[152;153]

I_{to} channel has very fast activation and inactivation gates and activates then inactivates rapidly, brings about only a transient of outward K^+ current that repolarizes to protect the membrane. Various cloned K^+ channel α-subunits, including Kv1.4, Kv3.3, Kv3.4, Kv4.1, Kv4.2 and Kv4.3 result in rapidly activating and inactivating K^+ currents with characteristics resembling endogenous cardiac I_{to} yet subtle difference exists.[154;155] For example, the primary difference between Kv1.4 and the two Kv4 channels is in the recovery from inactivation, with Kv1.4 recovering much more slowly than Kv4.2.[154;156] With respect to I_{to} expression in the heart, only Kv1.4, Kv1.7, Kv4.2, and Kv4.3 show substantial expression in the mammalian myocardium, while other Kvα genes (i.e. Kv3.4 and Kv4.1) encode for I_{to}-like currents, but

physiologically express in much lower level. Recent studies demonstrated that the β-subunit, K^+-channel interacting protein (KChIP), expresses differently in different regions of the heart and in different species, contributing to the biophysical properties of I_{to} and its pharmacological response, tissue distribution, as well as the trafficking of α-subunit,[145;149;157-159] even though one study considered that the phenotype differences are not likely caused by differential expression of the K^+ channel subunit genes thought to encode I_{to}, but rather may arise from differences in molecular structure and/or posttranslational modification of these subunits.[160]

In addition, the molecular basis for I_{to} varies greatly in myocytes from different species and cells from different regions of the heart in the same species. In many cases, more than one gene is responsible for the channel α-subunit conducting I_{to},[144-146;155;161] which contributes to the subtle difference in the channel properties of time- and voltage-dependence.

I_{to} is blocked by many antiarrhythmic agents such as quinidine, flecainide, propafenone, most of which are viewed as having other primary cardiac ion channel targets. Thus, the extent to which I_{to}/K_v4 block contributes to the actions of these drugs is uncertain. A common finding in human heart failure is AP prolongation, an effect that has been attributed in part to reduction of I_{to}. A remarkably good correlation has been found between the extent of reduction of I_{to} and reduction in the abundance of mRNA transcripts encoding Kv4.3 in human heart failure.[162] The mechanisms underlying this transcriptional regulation have not been elucidated. In mice expressing a dominant negative Kv4.2 construct in heart, action potentials are markedly prolonged, reflecting the primacy of I_{to} in rodent heart.[152]

I_{to} seems to be a "conventional" current that undergoes remodeling (down-regulation) in various types of diseases: heart failure,[163] diabetic cardiomyopathy,[164-167] while its correlation with clinical QT prolongation is unknown even though it has been demonstrated to prolong APD significantly in rat or mouse.[152]

1.2.3.2 Rapid delayed rectifier K^+ currents: I_{Kr}

Delayed rectifier K^+ channels (I_K) activate more slowly compared to other VGKCs, therefore generally do not play a major role in determining the balance of inward and outward currents during phases 0 and 1, while they contribute the outward currents in the later phases of AP. There are two components of I_K (the rapid component I_{Kr}, and the slow component I_{Ks}) in ventricular myocytes of human,[168-170] rabbit,[171-174] and dog.[67;175-177] These channels are

distinguished by their kinetics of activation, deactivation and inactivation, and by their highly variable sensitivity to blocking drugs.

I_{Kr} activates rapidly, and inactivates faster at more positive potential thus limits the amount of time that channels spend in the open state, showing strong inward rectification.[178] It deactivates much more slowly compared to the slow component I_{Ks} therefore shows large outward tail current (Figure 4). On repolarization the rate of recovery from inactivation through the open state is much more rapid than deactivation, which at voltages negative to 0 mV results in a large outward current and set the basis for promoting the repolarization at phase 3 of AP. It is the unique ability that I_{Kr} governs the rate of membrane potential repolarization at the end of each cardiac AP and refractoriness, and therefore is crucial for the termination of AP. In ventricular and atrial myocytes, I_{Kr} regulates the duration of the plateau phase of AP. Application of E-4031 or dofetilide prolongs APD but has little effect on the rate of final repolarization or on resting potential.[179] Figure 5 depicts the unusual kinetic of this voltage gated K^+ channel.

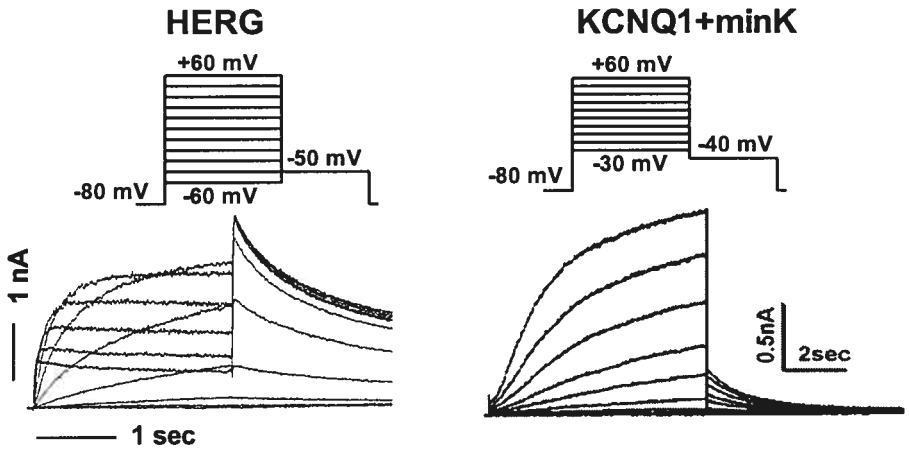

Figure 4. Comparison of cardiac delayed rectifier K^+ currents in heterogenous systems. HERG encodes I_{Kr} and KCNQ1+minK encodes I_{Ks}.

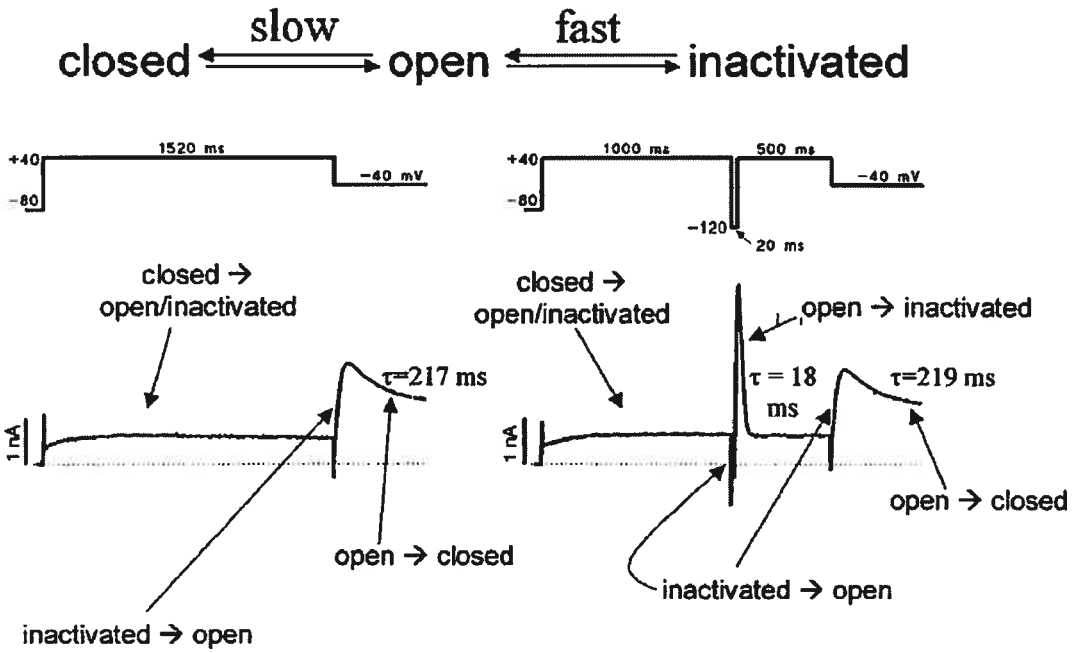

Figure 5. Unusual kinetics of I_{Kr}/HERG channel. (Modified from Roden DM, et al.[65])

The putative α-subunits of delayed rectifier K^+ channels are comparable as of I_{to} and I_{Na} (Figure 3), containing four repeats of six transmembrane segments (S1-S6) with a S5-S6 linker (loop) to form the channel pore. There are also auxiliary β-subunits for I_{Kr}, mainly to regulate the channel kinetics or sensitivity to drug blockage. Initially isolated by screening a human hippocampal cDNA library with a mouse homolog of *ether-à-go-go*, a *Drosophila* K^+ channel gene,[180] the human *either-à-go-go* related gene (*HERG*) (it is also nominated as KCNH2) encodes the α-subunits of I_{Kr} and conducts nearly identical biophysical properties as of native I_{Kr} in cardiomyocytes when it is expressed in heterogenous system, including *Xenopus* oocytes,[37] Chinese hamster oocytes,[181] COS,[182] and human embryonic kidney cell line 293 (HEK293).[183] However, when expressed in *Xenopus* oocytes, it is not blocked by drugs that specific block I_{Kr} (e.g. dofetilide),[37] as the required concentration to achieve blockage is significantly higher, probably due to the different cellular matrix in oocytes. This prompted the subsequent studies searching for the accessory subunits of HERG. The minimal K^+ channel protein (MinK) is a widely expressed protein of relative molecular mass approximately 15Kd that forms potassium channels by aggregation with other membrane proteins. MinK governs the ion channel activation,

pathway.[184] It has been shown to associate with both KVLQT1 which is the α-subunit of I_{Ks}, and HERG, to produce current resembling I_{Ks} and I_{Kr}.[185] minK-related peptide 1 (MiRP1) was initially believed to act as a β-subunit of HERG,[186] while contradictions remain on whether MiRP1 or MinK plays an essential role in pharmacology and biophysics of I_{Kr}/HERG,[187-189] even though it may serves as stabling molecular for HERG. MinK is encoded by *KCNE1*; and MiRP1 is encoded by *KCNE2*, which was cloned based on homology with minK. MiRP1 mutations are identified to cause a congenital long-QT syndrome (LQT6).[186]

HERG gene is highly conserved across mammalian species. The canine and rabbit clones are 99% identical to the human sequence at the amino acid level.[190] In some species, such as rabbits,[67;172] guinea pigs,[168] humans,[169;191] and dogs,[67] I_K is composed of both I_{Ks} and I_{Kr}. In others (e.g. cats,[192-194] fetal mice[195]), the current is almost exclusively I_{Kr}. I_{Kr} is the major repolarizing current in fetal mouse and rat heart, but it is rapidly supplanted postnatally by a very large I_{to},[196;197] resulting in the characteristically short action potential in small rodents.[195]

Because of its crucial role in determining the APD, I_{Kr}/HERG has been demonstrated to be a target of inherited and drug induced LQTS, a potentially-lethal arrhythmia. HERG is a second most common cause of LQTS2; until the year of 2000, more than 94 mutations scattered throughout this entire gene have been seen while no hot spots have been recognized.[198] Several mechanisms, including loss of channel function,[199-201] alteration of channel gating properties,[202] and defects in assembling, trafficking, and membrane targeting of channel protein,[199;203-207] have been demonstrated in heterogeneous system as mechanisms underlying the reduction of I_{Kr}/ HERG current in LQTS2. Based on these findings, gene-testing on *HERG*, and pharmacological rescuing of the channel protein, have been proposed for the prevention and therapies of LQT2 patients.

I_{Kr}/HERG is very sensitive to the block by antiarrhythmic drugs containing methanesulfonanilide group (e.g. dofetilide, D-sotalol, E-4031, ibutilide, and MK-499)[168], calcium blockers (e.g. verapamil, bepridil, and mibefradil)[182] and many noncardiovascular drugs (e.g. cisapride,[208] astemizole, terfenadine[209]) that share a potential to produce marked QT prolongation and a distinctive ventricular tachycardia, TdP, and syndromes resembling congenital LTQ2. Recent concerns on the QT prolongation and arrhythmias induced by many clinically used drugs ("pharmacological LQTS") prompt investigators to study the I_{Kr}/HERG blockage in order to prevent possible arrhythmic events.

Impairment of I_{Kr}/HERG in diseases may also serve as a cause of the pathological type LQTS, though only a few detail studies have been reported. For example, acidosis such as in ischemia, results in the reduction of I_{Kr} thus prolongs the APD.[210;211] Myocytes isolated from hypertrophied left ventricles of cats have reduced I_K density, with slowed channel activation and faster deactivation.[212] In the pacing-induced heart failure rabbit model, both I_{Kr} and I_{Ks} are smaller while not changed in the voltage dependence or the kinetics of I_K currents.[213] The reduction in the outward current over the plateau phase of AP in cells from hypertrophied feline left ventricles, exhibits a greater predisposition to developing potentially arrhythmogenic EAD.[212] I_{Kr} density and HERG mRNA levels are reduced in myocytes from infarcted canine ventricle,[214] while no change was found in the steady-state level of *HERG* mRNA in human HF.[162]

Moreover, HERG is regulated by phosphorylation by PKA and PKC. There are four putative cAMP-dependent PKA phosphorylation sites and a cyclic nucleotide binding domain in the C-terminal of HERG, which can be modulated via the cAMP-PKA phosphorylation pathway.[215;216] Activation of adrenergic receptors and increased intracellular cAMP levels regulate HERG channels both through PKA-mediated effects and by direct interaction with the protein.[215] PKA activation reduces HERG current amplitude and induces a depolarizing shift in the voltage-dependent activation curve. This shift is inhibited by specific PKA inhibitors (H89, KT5720) and in channels missing all PKA phosphorylation sites (S283A, S890A, T895A, S1137A), while coexpression of HERG with KCNE1 or KCNE2 accentuates the cAMP-induced voltage shift.[215] The net result of these effects is a reduction in HERG current. However, isoproterenol increases I_{Kr} in guinea pig ventricular myocytes, an effect that was inhibited by bisindolylmaleimide.[216] In rabbit SA cells isoproterenol increases I_{Kr} and this effect is inhibited by H89, but not by bisindolylmaleimide.[217] These results suggest that regulation of I_{Kr} might be species- and tissue-specific and might also depend strongly on experimental conditions.

HERG channels are modulated by PKC independently of direct phosphorylation of the channel.[218] PMA causes a positive shift of activation and reduces I_{Kr} and its effects can still be observed when the PKC-dependent phosphorylation sites are deleted by mutagenesis. Changes in phosphatidyl 4,5-biphosphate (PIP2) levels result from activation of several adrenergic and muscarinic receptors. PIP2 increases HERG currents and shifts the voltage-dependence of channel activation in a hyperpolarizing direction.[219] Moreover, in cells coexpressing α_{1A}-receptor

and HERG, phenylephrine reduces HERG currents and this effect is prevented by PIP2 but not by PKC inhibition. Since there are several polycationic segments in the cytoplasmic C-terminus of HERG, it is possible that an electrostatic interaction between the negatively charged phosphate groups of PIP2 and the positively charged amino acids in the channel protein can maintain the channel in an open state.[219] In human ventricular myocytes, endothelin-1 inhibits I_{Kr}, but fails to modify I_{to} and I_{K1}.[220] Lysophosphatidylcholine (LPC), a naturally occurring phospholipid metabolite, can accumulate and cause extracellular K^+ accumulation and AP shortening, via the enhancement of HERG current.[221] This may contribute to K^+ loss, abnormal electrophysiology (e.g. shortened APD and QT interval in the early phase of ischemia), and arrhythmia occurrence in the ischemic heart.[221;222] Thus, dysfunction of I_{Kr}/HERG (enhanced or defected) can result in alteration of APD and QT interval, substrates of different types of arrhythmias.

1.2.3.3 Slow Delayed rectifier K^+ currents: I_{Ks}

I_{Ks} is slowly activated at potentials above -30 mV with a linear current–voltage relationship, reaching half-maximum activation ($V_{1/2}$) at +20 mV ($V_{1/2}$ for I_{Kr} is around -25 mV).[168;169;183;224;225] I_{Ks} activates much more slowly than any other known VGKCs, and steady-state amplitude is only achieved with extremely long depolarization. Thus, I_{Ks} contributes to human atrial and ventricular repolarization, and serves as a "repolarization reserve" component,[226;227] particularly when I_{Kr} is reduced by disease or drug, preventing excessive action potential prolongation and development of arrhythmogenic early afterdepolarizations.[228] It is a dominant determinant of the physiological heart rate-dependent shortening of APD besides I_{CaL},[229] due to its incomplete deactivation and subsequent current accumulation, which is much more pronounced under beta-adrenergic activation,[230-232] while it has not significant role when the cycle length is short.[231] Pharmacologically, I_{Ks} is resistant to methanesulfonanilides,[168] but selectively blocked by chromanols (293B, HMR-1556)[233;234] and others.

The pore-forming α-subunit KvLQT1 (or KCNQ1) together with the β-subunit minK (or KCNE1) reconstitute the native I_{Ks}-like current when co-expressed in heterogeneous systems while any alone can not carry I_{Ks}-like current.[225;235-238] minK functions as a regulatory subunit to increase the KvLQT1 current by increasing the membrane targeting of KvLQT1 and eliminating

the inactivation gate of the channel.[236;239-242] Mutations in either KvLQT1 or minK can destroy the channel function and current kinetics, resulting in reduced repolarization K^+ current during the plateau phase, thus prolong APD and QT interval. Clinical and experimental studies have revealed that mutations in KvLQT1 can result in LQT1,[38;198;225;237;238;243] and minK in LQT5.[38;149;198;240;244-246]

Reduced I_{Ks} resulted from block by cardiac or noncardiac drugs leads to APD and QT prolongation,[209;247] and resembles the LQT1-like syndrome especially in the presence of beta-adrenergic activation, mainly due to the transmural heterogenous of I_{Ks} that its density is much larger in M cells compared to epi- and endo-myocardial cells,[66;67;248] and due to that I_{Ks} is regulated by sympathetic nervous stimulation, with activation of beta-adrenergic receptors PKA phosphorylating this channel,[249-252] and the colocalization of adrenergic receptors and I_{Ks} channel proteins.[249] Phosphorylation of I_{Ks} channel shifts the channel activation to negative potential, and increase the current,[249-252] thus beta-adrenergic stimulation is a frequent trigger of arrhythmias in patients with inherited KvLQT1/minK mutations or taking I_{Ks}-inhibiting drugs. PKC also enhance I_{Ks} in guinea pig ventricular myocytes.[253] The effects of PKC activation on minK are species-dependent, causing an increase in guinea pigs and a decrease in rats and mice.[254-256] Prior PKC activation prevents I_{Ks} current modulation by PKA, and vice versa, suggesting multiple interacting phosphorylation sites on KvLQT1 and/or minK subunits.[254]

There are a few studies on the remodeling of I_{Ks} by diseases or stimulations. Cells isolated from pressure-overload guinea pig ventricles demonstrate no change in I_K,[257] while chronic atrioventricular block canine hypertrophy model exhibits significant down-regulation of I_{Ks}.[258] I_{Ks} may be absent in ventricles from ischemic or dilated cardiomyopathy but present in normal heart.[191;259]

1.2.3.4 Inward rectifier K^+ currents: I_{K1}

Composed of only two membrane-spanning segments with an intervening loop homologous to the S5-P0-S6 section of voltage-gated K^+ channels, forming a homo- or hetero-tetramer, the inward rectifier K^+ channel (I_{K1}) subserves a variety of physiologic functions, including setting the resting potential, hyperpolarizing depolarized membranes, and contributing to repolarization. [63;144;147] It carries an outward current during the late phase of AP. I_{K1} shows significant inward rectification (increases of K^+ conductance under hyperpolarization and

decreases under depolarization) thus carries a substantial current at negative potentials and set a stable resting potential close to E_K at around -85 mV, while conducts very little outward current even at positive potentials. Upon depolarization this large conductance is virtually shut down by the rectification, allowing other K^+ currents to control the plateau phase. It remains closed throughout the plateau and opens again at potentials negative to −20 mV, thus contributes to terminal phase 3 of repolarization. I_{K1} density is higher in ventricular than in atrial myocytes, and is not different in epicardial, M and endocardial cells in canine and guinea pig hearts.[260]

Members of Kir2 family are the major I_{K1} channel proteins. Homo- or hetero-tetramer of Kir2.1 Kir2.2, Kir2.3 subunits resemble the native I_{K1}.[261-263] Due to the manifold roles of I_{K1}, mutation of Kir2.1 causes Andersen's syndrome (or LQT7), a rare disease characterized by periodic paralysis, dysmorphic features, QT prolongation and ventricular arrhythmias. Mutations in Kir2.1 associated with Andersen syndrome were found to cause dominant negative suppression of the wild type Kir2.1 channels when expressed in *Xenopus* oocytes thus mimicking the effects of the Kir2.1 gene knock-out which is characterized by prolonged QT interval.[264-268]

I_{K1} can be blocked by Ba^{2+} (IC_{50}=20 μM),[269] or drugs such as chloroquine and nicotine,[270] lengthening the atrial, AV node and ventricular APDs. I_{K1} blockers are effective against various types of experimental reentrant ventricular tachycardias.[271] Moreover, I_{K1} blockers produce membrane depolarization (an effect that slows conduction velocity due to a voltage-dependent inactivation of Na^+ channels) and prolong the QT interval, both actions being proarrhythmic.

Findings in guinea-pig ventricular myocytes suggest that I_{K1} can be suppressed by a PKA-mediated phosphorylation occurring in response to isoprenaline-induced beta-adrenergic receptor activation and that acetylcholine (Ach) can antagonize the suppression by mechanisms that involve both intracellular and membrane-delimited pathways. The membrane-delimited pathway appears to involve M2-cholinergic receptors, their associated G protein, Gi, and a protein phosphatase, all located in the sarcolemma in close proximity to the involved I_{K1} channels.[272] However, human Kir2.1 current is up-regulated by activation of PKA, and is inhibited by direct PKC-dependent phosphorylation.[273;274] Besides, α_{1D}-adrenergic receptor activation mediates I_{K1} regulation via CaMKII.[275]

I_{K1} is down-regulated in spontaneously hypertensive rats, in models of cardiac hypertrophy, infarcted rat heart, and in patients with severe heart failure and cardiomyopathies,[276-278] but may not at mRNA level.[279] This leads to the membrane

depolarization, the prolongation of APD, and the early and delayed afterdepolarizations.[276;277] However, I_{K1} density increases in patients with chronic AF.[131] The increase of I_{K1} results in abnormalities of excitability, including slowed heart rate, premature ventricular contractions, atrioventricular block, and atrial fibrillation, as found in transgenic mice over-expressing I_{K1} current.[280]

1.2.3.5 Other cardiac ion channels

Physiologically, the inward I_{Na} and I_{CaL} currents, and the outward I_{to}, I_{Kr}, I_{Ks}, and I_{K1} currents, are the major players setting the heart rhythm and mainly determining the APD and QT interval. There are also several catalogues of ion channels shaping the electrophysiology of heart, especially during the diseased states. Most of these ion channels are not voltage-gated while modulated by physiological ligands, e.g. ATP, adenosine, Ach. Ion exchangers such as Na^+-Ca^{2+} exchanger (I_{NCx}), contribute to the plateau phase of AP, too.

Present in various tissues, including pancreatic ß-cells, heart, skeletal muscles, vascular smooth muscles, and brain,[281] I_{KATP} channels are hetero-octameric proteins composed of pore-forming inwardly rectifying K^+ channel (Kir6.x) and regulatory sulfonylurea receptor (SUR) subunits.[282] I_{KATP} is a major regulator for insulin secretion in pancreases.[283] Physiologically, cardiac sarcolemmal I_{KATP} channels are closed by the inhibitory effect of ATP, and conduct outward K^+ current when opened due to decreased intracellular ATP but increased ADP levels, which often occur under stresses conditions such as ischemia and hypoxia,[283] thus contribute to the increase of K^+ efflux and the shortening of APD.[284] Therefore, opening of I_{KATP} channels may result in cardioprotective as well as proarrhythmic effects while blocking (e.g. by glyburide) may prevent arrhythmias in ischemia.[285] The I_{KATP} channel has been therapeutic targets for both diabetes and heart diseases.

1.3 Current Knowledge of Ionic Mechanisms for Prolonged QT Interval in Diabetic Hearts

Under pathological states such as ischemia, congestive heart failure, stress, autonomic activation, and diabetes, etc., the functions of either inward or outward ion channels, or both, are changed, due to the variation of ion channel expressions and/or functions and mal-regulation by related signalings. [34;286-288] QT Prolongation resulted from ion channel dysfunction is a common electrophysiological symptom in diseased hearts, such as heart failure resulted from ischemia, hypertension and diabetes.

APD recorded in STZ-diabetic cardiomyocytes was increased more than one fold compared to normal heart cells.[164;289-292] A net change in increased inward current and/or reduced outward current across the cell membrane can result in APD and QT prolongation as we have discussed in the Introduction. Great efforts have been made to understand the ionic mechanisms underlying diabetic APD and QT prolongations.

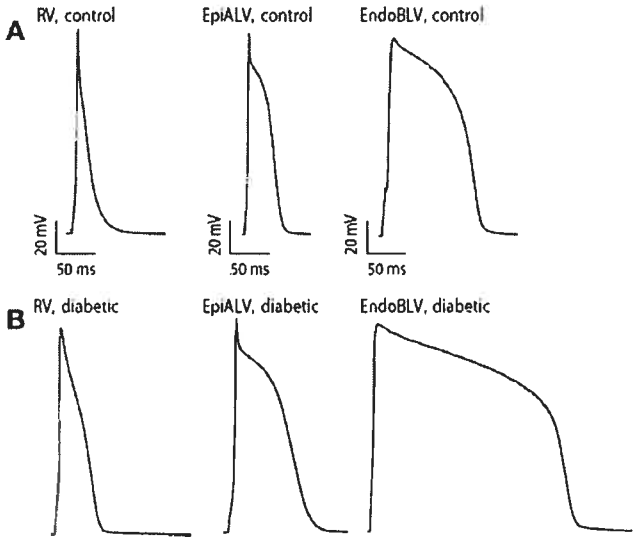

Figure 6. Action potentials of rat ventricles. APDs of three selected regions of the ventricular muscle recorded in diabetes (***B***) are remarkably longer than in control (***A***). RV: right ventricle, EpiALV: epimyocardial wall of left ventricle; EndoBLV: endomyocardial wall of left ventricle. From Casis O, et al. 2000.[292]

1.3.1 Inward currents

1.3.1.1 Sodium currents

The peak sodium current (I_{Na}) in isolated diabetic rat ventricular myocytes does not change significantly compared to that in healthy myocytes.[293] However, slowly inactivating component of Na^+ current (I_{NaL}), as a contributor to ischemic Na^+ and subsequently Ca^{2+} loading, was found to be significantly decreased in myocytes isolated from diabetic rat hearts.[293] Therefore, it is not likely that sodium current contributes to the QT prolongation in these diabetic animal models.

1.3.1.2 Calcium currents

I_{CaL} was found smaller in IDMM in some studies [294;295] but unaltered in chemical-induced or genetic diabetic animals in other studies.[296;297] The former is supported by a study showing significant decreases in maximal number of ^{3}H-nitrendipine binding to I_{CaL} channels in STZ-induced IDDM rats.[298] As activation of I_{CaL} is essential for subsequent stimulation of Na^+-Ca^{2+} exchanger (I_{NCX}) current, reduced I_{CaL} may contribute to decreasing the activation of I_{NCX} in diabetic myocytes.[294] In STZ-diabetic guinea pigs, the impaired Ca^{2+} homeostasis in the myocardium of diabetic guinea pigs may explain the increased incidents of DADs and triggered activity in this model. Even though the basal calcium current density and kinetics remain normal,[299-301] decrease in response to beta-stimulation occur in genetically diabetic rats compared with control rats.[299]

In addition, the resting levels of $[Ca^{2+}]_i$ and basal $[Ca^{2+}]_i$ transients remain normal in diabetes until the system is challenged by certain stimuli. $[Ca^{2+}]_i$ responses to isoproterenol are depressed in both resting and stimulated diabetic cells. This suggests an alteration in the beta-adrenergic pathway, possibly related to the beta-adrenoceptor deficiency reported in diabetic hearts. SR Ca-ATPase is also involved in the isoproterenol-induced $[Ca^{2+}]_i$ changes. Moreover, the decreased maximum response to 8-bromo-cAMP provides evidence of a post-receptor alteration in the pathway. Diabetic myocytes are more sensitive to ouabain, whereas the maximum response to ouabain was depressed. This may be the result of depressed Na-K ATPase and increased $[Ca^{2+}]_i$. Ryanodine binding suggests a decreased number of high-affinity binding sites in the SRs of diabetic myocytes. Additionally, there are indications that SR releasable calcium is reduced and that the major functions of SR, notably uptake, release and storage, may

be depressed in diabetic myocytes. Finally, L-type Ca^{2+}-channels are quantitatively and qualitatively altered in diabetes. Insulin treatment normalizes most of the diabetes-induced changes in cardiomyocytes, suggesting that metabolic alterations due to insulin deficiency play an important role in diabetic cardiomyopathy. Results from several studies show that in diabetes the function of major organelles that handle $[Ca^{2+}]_i$ in myocytes is depressed, which in turn causes the alteration of $[Ca^{2+}]_i$ mobilization in myocytes. Different second messenger systems involved in E-C coupling may also be altered due to metabolic impairments. The rapid advancement in our understanding of the pathophysiology of calcium homeostasis in cardiomyocytes will be forthcoming as the powerful new tools of molecular and structural biology are used to investigate the regulation of the Ca^{2+} transport system.[301] These data suggest that I_{CaL} does not likely account for diabetic APD or QT prolongation.

1.3.2 Outward currents

1.3.2.1 I_{to} and I_{ss}

Representative studies in diabetic models by Shimoni's group and other fellows contributed greatly to this area.[164-166;290;295;302-306] Their work establishes that I_{to}, and a slowly inactivating, quasi-steady-state outward K^+ current (I_{ss}), are the major electrophysiological determinants for the APD prolongation in ventricular cells from STZ-diabetic rats and mice.[164;289] It was found that in STZ-induced diabetic rats, I_{to} and I_{ss} were significantly smaller than in the age-matched rats,[166;289;292;307;308] and the reactivation kinetics of I_{to} was slowed down, [166;295;305] or the inactivation was accelerated,[309] mechanisms underlying the I_{to} reduction. These reductions are uniform in the total right ventricle, subepicardium at the apex of the left ventricle and subendocardium at the base of the left ventricle of STZ-rats.[292] By comparing I_{to} in diabetic myocytes treated with or without insulin and the inhibitors mitogen-activated protein kinase (MAPK), they believed the loss of insulin-stimulated gene expression of ion channels through MAPK kinase pathway is responsible for the malfunction of I_{to}. In addition, STZ itself has no direct effect on electrophysiological activity in the hearts of diabetic rats.[305] Similar results were reproduced by other groups using the same animal model.[289;295;296;306] Qin et al recently documented that mRNA and protein levels of Kv2.1, Kv4.2, and Kv4.3, the molecular components of cardiac I_{to}, are significantly decreased in IDMM rats.[310] Moreover, Nishiyama et

al[311] demonstrated that the density of Kv4.2 protein decreased, whereas Kv1.4 protein increased. They postulated that isoform switching from Kv4.2 to Kv1.4 is most likely the mechanism underlying the slower kinetics of I_{to} initially identified by Shimoni et al.[305] In type 2 genetic diabetic rats, ventricular I_{to} is also decreased significantly. [297; 299;312] These results reveal the molecular basis of I_{to} depression in diabetic rats and mice.

Autonomic neuropathy, including cardiac neuropathy, is a complication of chronic diabetes. Acute exposure of the α-adrenergic agonist norepinephrine (NE) reduces I_{to} current amplitude in both healthy and diabetic rat myocytes; however diabetes shifts to the right of the concentration-response curve and reduces the maximum effect of the neurotransmitter,[309] thus diabetic myocytes are more resistant to sympathetic regulation than are healthy cells. Moreover, prolonged exposure of diabetic cardiomyocytes with NE restores I_{to} current, may be by increasing its expression.[313] The reduced I_{to} and I_{ss} density is significantly restored in diabetic rat isolated ventricular myocytes treated *in vitro* with insulin or agents that activate the cellular metabolism such as by increasing the pyruvate dehydrogenase activity (e.g. by dichloroacetate). [164;314;315] This mechanism is not limited to diabetic conditions, because metabolic stimuli that up-regulate I_{to} in diabetic rat myocytes act similarly in non-diabetic models of heart failure.[316] Moreover, in diabetic rat myocytes, the integrity of cytoskeleton (e.g. β-tubulin) was disrupted remarkably in parallel with the I_{to} and I_{ss} reduction. This is mimicked by destroying the actin microfilament network with cytochalasin D, and rescued by insulin treatment.[165] It is possible that in diabetic myocytes, the significant changes in the cellular milieu result in the impaired trafficking of ion channel to the membrane. Detail electrophysiological studies of diabetic and non-diabetic disease conditions affecting the heart suggest I_{to} channels are regulated by a redox-sensitive mechanism, where glucose utilization plays an essential role in maintaining a normally reductive state of the myocyte.[314] This concept may have implications for clinical approaches aimed at reversing pathogenic electrical remodeling in a variety of cardiovascular diseases.

However, controversy was reported by Rusznak et al[317] with diabetic Bio Breeding/ Worcester (BB/Wor) rats that spontaneously develop pathologic changes characteristic of human type I diabetes. They found no significant difference between the non-diabetic and diabetic BB rats (IDDM) in the amplitude, and the rate of recovery from inactivation, of I_{to}. In ob/ob NIDDM mice, the 4-aminopyridine sensitive currents (I_{to}) were also similar and the voltage dependences of the activation and of the steady-state inactivation did not differ significantly, either.[317] This

may due to the difference in mechanisms underlying the insulin deficiency in genetic and chemical-induced diabetic models, where the former results in more complicated gene regulation and auto-immunol injuries while the later results in mainly the dysfunction of pancreas and most symptoms are secondary to the insulin insufficiency. More efforts are needed to advance our understanding in the role of I_{to} in diabetic cardiomyopathy.

1.3.2.2 I_{K1}

I_{K1} was found unchanged in the magnitude or voltage dependence around the resting membrane potential in IDDM by Shimoni et al[164] and other laboratories,[289;292;296;308] excluding the contribution of I_{K1} to APD prolongation in these animal models of diabetes. As I_{K1} is the major current setting the resting membrane potential (RMP), the preserved I_{K1} may explain the comparable RMPs in healthy and diabetic cardiomyocytes.

1.3.2.3 I_{KATP}

I_{KATP} channel opens under stress states such as ischemia or hypoxyia that results in reduction of intracellular ATP concentration.[283] When opened, it conducts outward K^+ current and influences the repolarization of AP. Evidence exists that I_{KATP} is enhanced in diabetic rat hearts, due to the increased sensitivity to ATP.[290;318] However, increase in I_{KATP} is expected to shorten, but not lengthen the APD. Thus, participation of I_{KATP} in diabetic APD prolongation can also be ruled out.

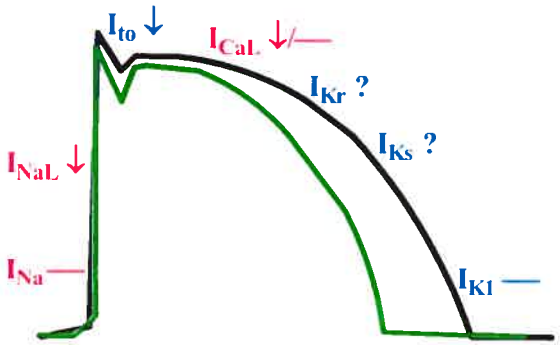

Figure 7. Current knowledge of ionic disturbance in diabetic heart. Inward Na^+ or Ca^{2+} currents are unchanged or reduced. Outward I_{to} is reduced markedly and contributes to the APD prolongation in diabetic rodents; I_{K1} is resistant to the diabetes and remains similar level as in healthy ones.

1.4 Current Knowledge of Cellular/Molecular Mechanisms in Diabetic Cardiocomplications

Although expression of a single gene, encoding a pore-forming subunit, is often sufficient to generate an ion current, recapitulation of all the physiologic features of a current in myocytes frequently requires function-modifying accessory subunits. To extend this further, it is now apparent that the generation of ion currents in cardiac myocytes requires coordinated function of not only of α and ß subunits, but also multiple other gene products that settle such functions as assembly and trafficking, phosphorylation and dephosphorylation, posttranslational modifications, and regulation by other signalling molecules. The mechanisms underlying these very important aspects of channel physiology and the roles of cellular signalling pathways are only now being delineated.

Studies on both type 1 and type 2 diabetes have revealed several important cellular/ molecular mechanisms underlying the cardiocomplications. This section outlines some of the signaling factors in diabetes closely related to the channel pathophysiology, including: glucose, insulin, phosphoinositide 3-kinase (PI3K), protein kinase B (PKB, also named Akt), tumor necrosis factor α (TNF-α) and the intermediate metabolite ceramide, and enhanced PKC activity and oxidative stress, etc. [319]

1.4.1 Hypo- and hyper-glycemia

Determination of elevated plasma glucose is a criterion to diagnose diabetes. Untreated diabetic patients have hyperglycemia with fasting plasma glucose ≥ 140 mg/dl (7 mM), or venous plasma glucose ≥ 200 mg/dl (10 mM) at 2 hours after a 75 g oral glucose challenge. However, treatments to correct this biochemical disturbance may result in ultra low level of glucose. As a major source of metabolic fuel, degradation of glucose via glycolysis and subsequent oxidative phosphorylation generates high-energy phosphates (e.g. ATP) to drive biological processes in the cell. When glucose level is reduced to less than 2.5 mM, it is diagnosed as hypoglycemia, which may be fatal when lasting for a prolonged period.

Multiple lines of studies have demonstrated that hyperglycemia can impair cellular functions. The common effect of hyperglycemia in various types of cells is increase in ROS level,

which subsequently have numerous molecular targets in the cell.[320;321] Incubation of pancreatic β-cells in mimetic hyperglycemia induces mitochondrial ROS and suppressed first-phase of glucose induced insulin secretion through the suppression of GAPDH activity.[322] Exposure of rat small coronary arteries to high glucose reduces nitric oxide activities but enhances superoxide ($O_2^{\cdot-}$) formation.[323] Hyperglycemia also enhances ROS production in rat cardiomyocytes, resulting in the increased phosphorylation on angiotensin II (AT-II) by Janus-activated kinase-2, a tyrosine kinase related with myocyte hypertrophy and cytokine and fibrogenetic growth factor overexpression, which may explain the increased hypertrophy and higher cardiovascular morbidity and mortality in diabetics, in which the AT-II activity is augmented.[324] More detailed discussion about diabetic ROS is made in *Section 1.4.4*.

1.4.2 Insulin-PI3K-PKB signaling pathway

Signaling through the insulin pathway is critical for the regulation of intracellular and blood glucose levels and the avoidance of diabetes. Insulin binds to its receptor leading to the autophosphorylation of the ß-subunits and the tyrosine phosphorylation of insulin receptor substrates (IRS). IRS activates PI3K through its SH2 domain, thus increasing the intracellular concentration of PIP2 and PIP. This, in turn, activates phosphatidylinositol phosphate-dependent kinase-1, that subsequently activates Akt/PKB. This leads to the translocation of the glucose transporter (glucose transporterase, GLUT4) from cytoplasmic vesicles to the cell membrane to carry in the glucose molecule in cardiac and other tissues.[325-328]

PKB is a serine/threonine (Ser/Thr) protein kinase which can be activated by a variety of stimuli in a PI3K-dependent or -independent manner.[329-332] PKB regulates cellular processes and promotes cell survival by the Ser/Thr phosphorylation of downstream signaling proteins, such as glycogen synthase kinase-3, GluT4, nuclear factor κB (NfκB), and TNF-α, etc.[333-337] Experiments have demonstrated that PI3K and PKB are also involved in the growth and the function of hearts,[334;338-343] and they regulate some ion channels, including L-type Ca^{2+} and M-type K^+ channel in neurons.[223;344] As a survival factor insulin prevents H_2O_2-induced apoptosis in rat neonatal cardiomyocytes via activating the PI3K/PKB pathway.[345;346] In STZ-diabetic rats, insufficient insulin results in the downregulation of heat shock protein-60 and the subsequent reduction of the downstream IGF-1 receptor signaling that protects cardiac muscle against injury via activation of PI3K/PKB.[343;347]

In chemical-induced or genetic type 1 diabetic subjects, the PKB/PI3K signaling pathway has been found being dramatically impaired.[293;336;348;349] Enhanced PKC activity resulted from hyperglycemia and diabetes also diminishes PKB function.[350] However, there are studies indicate that insulin-induced phosphorylation of Akt/PKB on Thr-308 was increased fivefold in STZ-diabetic heart, but normal on Ser-473; in contrast with PKB phosphorylation, insulin-induced phosphorylation of GSK-3, a major cellular substrate of PKB, was markedly reduced in diabetes,[340] therefore impairs other cellular functions. However, one study on rats showed unchanged PKB activity up to 9 months of IDDM.[351] Despite of the discrepancy, insulin treatment normalizes most of the diabetes-induced changes in cardiomyocytes, suggesting that metabolic alterations due to insulin deficiency play an important role in diabetic cardiomyopathy.

1.4.3 Tumor Necrosis factor-α and sphingolipid metabolites

Increased TNF-α level in cardiac tissues plays an important role in the progress of non-obese IDDM resulted from the immunol reaction of $CD8^+$ T cells.[352;353] TNF-α is also responsible for the development of human insulin resistance as found in NIDDM;[354] administration of exogenous TNF-α induces insulin resistance, whereas neutralization of TNF-α improves insulin sensitivity.[355]

On the other hand, elevated TNF-α contributes greatly to heart diseases including congestive heart failure (CHF),[356;357] ischemic and non-ischemic heart failure, myocardial infarction, arrhythmias, and apoptosis of heart cells.[358] CHF increases the APD, leading to EAD and lethal ventricular tachyarrhythmias.[213] Circulating concentrations of TNF-α and soluble TNF receptors (TNFR) are independent predictors of mortality in CHF.[359]

TNF-α reduces both the inward rectifying and outward K^+ current in oligodendrocytes.[360] In brain, it decreases the expression of Kir2.1 but upregulates Kv1.3, thus modulate the neuron firing and repolarization.[361] K^+ and Cl^- channels are activated in liver cells by TNF-α in Ca^{2+}- and PKC-dependent manners, and participate in pathways leading to TNF-mediated cell death.[362] In spite of this, the role of TNF-α in regulating cardiac ion channels is not well defined although TNF-α is a causative factor in diabetes and a deleterious factor in cardiomyopathy.

In addition, the activation of TNF-α pathway triggers the production of arrhythmogenic sphingolipid such as palmitoylcarnitine, LPC, and ceramide[363] which modulate cardiac channels, e.g. I_{CaL},[364-366] HERG,[221], and I_{K1}.[367] These lipids accumulate much more in ischemic hearts of

diabetic rats compared to the ischemic hearts of healthy ones,[368] which may explain the higher arrhythmic rate in diabetic subjects insulting an ischemic senior.

1.4.4 Oxidative stress

The well-balanced organism system has a finely controlled antioxidant system to eliminate any excessive free radioactive particles generated in disease or stress states. Elevated ROS or nitrogen species under oxidative stress have been demonstrated to be important factors responsible for the pathogenesis of both diabetes mellitus and heart diseases, hence the diabetic cardiomyopathy and cardiocomplications.[369-371]

In diabetes, hyperglycemia results in the production of reactive oxygen and nitrogen species, which brings about oxidative myocardial injury. Pancreatic beta-cells exposed to high glucose produce significantly high level of ROS due to the overwork of mitochondria, resulting in the suppression of glucose-induced insulin secretion.[322] Significant alterations in myocardial structure and function occur in the late stage of DM. These chronic changes are believed being resulted from acute cardiac responses to suddenly increased glucose levels at the early stage of diabetes. Oxidative stress derived from hyperglycemia causes abnormal gene expression and protein function, and altered signal transduction, and the activation of pathways leading to cardiomyocytes apoptosis.[336] In hearts of STZ-diabetic rats, oxidative stress starts at early stage of diabetes and increases progressively.[350] Studies on type 2 DM patients also found an increased ROS level as comparable to that in animal models.[371]

Increased ROS can prolong the APD significantly. When exposed to H_2O_2, the APD in isolated adult rat cardiomyocytes and in guinea pig cardiac muscle is significantly prolonged, which is later markedly abbreviated due to the depletion of intracellular ATP and the activation of I_{KATP}. [372;373] It was shown that within minutes of exposure to dihydroxyfumaric acid or xanthine /xanthine oxidase (X/XO), both of which produce the superoxide anion, the APD was prolonged in canine myocytes, papillary muscle or small strips of right ventricular walls of guinea pig hearts, and this effect was followed by the appearance of EAD.[374; 375] It has been previously reported that the O_2^- generated by high glucose (23 mM) or by X/XO in rat small coronary arteries impairs cAMP-mediated dilation by reducing Kv channel function,[323;376] which was partially restored by SOD and catalase.

The elevated oxidative stress in diabetes is also found to be a deleterious factor for the function of I_{to}. By incubating the diabetic rat cardiomyocytes with insulin or GSH, I_{to} current density was normalized to the level as in healthy myocytes, resulting from increased glucose utilization and enhanced insulin signaling of reductive components in the redox system.[308;377] It was not clear whether other cardiac ion channels, for instance, I_{Kr} and I_{Ks}, are modulated by the overproduction of ROS in hyperglycemia and diabetes.

1.5 Questions

Although previous studies have tremendously advanced our understanding of ionic and cellular/molecular mechanisms for the QT prolongation in diabetic animals, application of these findings to humans remain uncertain mainly because there exist some unsolved issues. There are potentially other factors contributing to the abnormal cardiac QT interval of diabetic hearts.

First, our current knowledge of ionic mechanisms of diabetic QT prolongation is acquired nearly exclusively from animal models of rats and mice that in their adulthood do not express typical and apparent I_{Kr} or I_{Ks}.[195] No studies regarding ionic mechanisms of diabetic QT prolongation have so far been reported in humans and other species whose hearts possess prominent I_{to} and significant I_{Kr} and I_{Ks} as well. Apparently, the potential role of I_{Kr} or I_{Ks} in diabetic cardiac electrical disorder has been overlooked.

Second, decreased I_{to} may prolong the APDs in rats or mice, but may not in species also possessing I_{Kr} and I_{Ks}, such as humans, dog, and rabbit, in which the APDs have been shown to be shortened by reducing I_{to}.[62;68;378-381] This phenomenon is commonly interpreted as such that depression of I_{to} elevates the plateau level so as to set the membrane potential favoring greater activation of I_{Kr} (maybe also slightly on I_{Ks}) which in turn results in a briefer APD. Therefore, the finding that depression of I_{to} accounts for the QT prolongation in diabetic rats and mice may not be directly extrapolated to humans or other I_{Kr}/I_{Ks}-possessing species. Although experiments with transgenic expression of dominant negative Kv4.2 and Kv4.3 (also named KCND2 and KCND3) constructs in murine models have indicated that a decrease of I_{to} may increase the APD and give rise to the prolongation of QT interval in ECG,[152;153] it does not contribute to determining the APD or the transmural APD dispersion in species with dominant I_{Kr} and I_{Ks}, e.g. in dogs.[16] Moreover, no clear clinical evidence indicates that patients suffering long QT syndromes have abnormal I_{to}; instead, the mutations in KCND2 and KCND3 found in LQT patients have normal function, thus I_{to} dysfunction is not a frequent cause of long QT syndrome.[151]

Third, the ion current equivalent to I_{ss} is believed to be absent in human ventricular cells although reduction of I_{ss} has been found to significantly contribute to QT prolongation in diabetic rats.[259] Hence its clinical implication in diabetic QT lengthening is uncertain.

Taken these together, it appears conceivable that besides the diminishment of I_{to}, alterations of some other ion currents may also be involved in causing diabetic QT prolongation and the associated arrhythmias. In particular, I_{Kr} or its genetic counterpart HERG as in humans has all the potentials of being one of the multi-players. Yet, the potential roles of this current in this regard, and the underlying mechanisms, have not been assessed. This thesis seeks to cast light on this area and hopes to attain a clearer view on diabetic cardiocomplications so that rational intervention is possible.

1.6 Reference

1. Edlund H. Factors controlling pancreatic cell differentiation and function. *Diabetologia*. 2001;44:1071-1079.
2. Public Health Agency of Canada / Agence de santé publique du Canada. Diabetes in Canada: National Statistics and Opportunities for Improved Surveillance, Prevention and Control/Le diabète au Canada: Statistiques nationales et possibilites d'accroitre la surveillance, la prévention et la lutte (Cat. No. H49-121/1999). 1999. Minister of Public Works and Government Services Canada.
3. National Institute of Diabetes and Digestive and Kidney Diseases. National Diabetes Statistics fact sheet: general information and national estimates on diabetes in the United States, 2003. 2004. U.S. Department of Health and Human Services, National Institutes of Health, Bethesda, MD.
4. International Diabetes Federation. Diabetes Atlas Second Edition. 2003. Imprimerie L Vanmelle SA, Gent/Mariakerke, Belgium.
5. World Health Organization DoNDS. Definition, Diagnosis and Classification of Diabetes mellitus and its Complications. Report of a WHO Consultation. WHO/NCD/NCS/99.2, ed. 1999. WHO, Geneva.
6. Turtle JR. The economic burden of insulin resistance. *Int J Clin Pract Suppl*. 2000;23-28.
7. McCarty D ZP. Diabetes 1994-2010: Global Estimates and Projections. WHO Collaborating Centre for Diabetes Mellitus Melbourne, ed. 1994. Bayer AG Publication, Leverkusen.

8. Baric L. Heart in the elderly (views and considerations at the turn of the centuries). *Acta Med Croatica*. 1999;53:171-178.
9. International Diabetes Federation. Cost-effective Approaches to Diabetes Care and Prevention. 2003.
10. Rubler S, Dlugash J, Yuceoglu YZ, Kumral T, Branwood AW, Grishman A. New type of cardiomyopathy associated with diabetic glomerulosclerosis. *Am J Cardiol*. 1972;30:595-602.
11. Fang ZY, Prins JB, Marwick TH. Diabetic cardiomyopathy: evidence, mechanisms, and therapeutic implications. *Endocr Rev*. 2004;25:543-567.
12. Shehadeh A, Regan TJ. Cardiac consequences of diabetes mellitus. *Clin Cardiol*. 1995;18:301-305.
13. Suys BE, Katier N, Rooman RP, Matthys D, Op DB, Du Caju MV, De Wolf D. Female children and adolescents with type 1 diabetes have more pronounced early echocardiographic signs of diabetic cardiomyopathy. *Diabetes Care*. 2004;27:1947-1953.
14. Bell DS. Heart failure: the frequent, forgotten, and often fatal complication of diabetes. *Diabetes Care*. 2003;26:2433-2441.
15. Kodama K, Sakagashira S, Hori M. Prognostic significance of diabetes mellitus in patients with acute myocardial infarction after recanalization. *Diabetes Res Clin Pract*. 1996;30 Suppl:71-75.
16. Sun X, Wang HS. Role of the transient outward current (I_{to}) in shaping canine ventricular action potential--a dynamic clamp study. *J Physiol*. 2005;564:411-419.
17. Lopaschuk GD. Metabolic abnormalities in the diabetic heart. *Heart Fail Rev*. 2002;7:149-159.
18. Rodrigues B, Cam MC, McNeill JH. Myocardial substrate metabolism: implications for diabetic cardiomyopathy. *J Mol Cell Cardiol*. 1995;27:169-179.
19. Hayat S, Patel B, Khattar RS, Malik RA. Diabetic cardiomyopathy: mechanisms, diagnosis and treatment. *Clin Sci (Lond)*. 2004;107:539-557.
20. Mahgoub MA, Abd-Elfattah AS. Diabetes mellitus and cardiac function. *Mol Cell Biochem*. 1998;180:59-64.
21. Casis O, Echevarria E. Diabetic cardiomyopathy: electromechanical cellular alterations. *Curr Vasc Pharmacol*. 2004;2:237-248.

22. Frustaci A, Kajstura J, Chimenti C, Jakoniuk I, Leri A, Maseri A, Nadal-Ginard B, Anversa P. Myocardial cell death in human diabetes. *Circ Res*. 2000;87:1123-1132.
23. Arildsen H, May O, Christiansen EH, Damsgaard EM. Increased QT dispersion in patients with insulin-dependent diabetes mellitus. *Int J Cardiol*. 1999;71:235-242.
24. Brown DW, Giles WH, Greenlund KJ, Valdez R, Croft JB. Impaired fasting glucose, diabetes mellitus, and cardiovascular disease risk factors are associated with prolonged QTc duration. Results from the Third National Health and Nutrition Examination Survey. *J Cardiovasc Risk*. 2001;8:227-233.
25. Ebbehoj E, Arildsen H, Hansen KW, Mogensen CE, Molgaard H, Poulsen PL. Effects of metoprolol on QT interval and QT dispersion in Type 1 diabetic patients with abnormal albuminuria. *Diabetologia*. 2004;47:1009-1015.
26. Rossing P, Breum L, Major-Pedersen A, Sato A, Winding H, Pietersen A, Kastrup J, Parving HH. Prolonged QTc interval predicts mortality in patients with Type 1 diabetes mellitus. *Diabet Med*. 2001;18:199-205.
27. Sivieri R, Veglio M, Chinaglia A, Scaglione P, Cavallo-Perin P. Prevalence of QT prolongation in a type 1 diabetic population and its association with autonomic neuropathy. The Neuropathy Study Group of the Italian Society for the Study of Diabetes. *Diabet Med*. 1993;10:920-924.
28. Suys BE, Huybrechts SJ, De Wolf D, Op DB, Matthys D, Van Overmeire B, Du Caju MV, Rooman RP. QTc interval prolongation and QTc dispersion in children and adolescents with type 1 diabetes. *J Pediatr*. 2002;141:59-63.
29. Veglio M, Sivieri R, Chinaglia A, Scaglione L, Cavallo-Perin P. QT interval prolongation and mortality in type 1 diabetic patients: a 5-year cohort prospective study. Neuropathy Study Group of the Italian Society of the Study of Diabetes, Piemonte Affiliate. *Diabetes Care*. 2000;23:1381-1383.
30. Veglio M, Chinaglia A, Cavallo PP. The clinical utility of QT interval assessment in diabetes. *Diabetes Nutr Metab*. 2000;13:356-365.
31. Veglio M, Giunti S, Stevens LK, Fuller JH, Perin PC. Prevalence of Q-T interval dispersion in type 1 diabetes and its relation with cardiac ischemia : the EURODIAB IDDM Complications Study Group. *Diabetes Care*. 2002;25:702-707.

32. Veglio M, Chinaglia A, Cavallo-Perin P. QT interval, cardiovascular risk factors and risk of death in diabetes. *J Endocrinol Invest*. 2004;27:175-181.

33. Veglio M, Borra M, Stevens LK, Fuller JH, Perin PC. The relation between QTc interval prolongation and diabetic complications. The EURODIAB IDDM Complication Study Group. *Diabetologia*. 1999;42:68-75.

34. Marfella R, Rossi F, Giugliano D. Hyperglycemia and QT interval: time for re-evaluation. *Diabetes Nutr Metab*. 2001;14:63-65.

35. Abo K, Ishida Y, Yoshida R, Hozumi T, Ueno H, Shiotani H, Matsunaga K, Kazumi T. Torsade de pointes in NIDDM with long QT intervals. *Diabetes Care*. 1996;19:1010.

36. Kahn JK, Sisson JC, Vinik AI. QT interval prolongation and sudden cardiac death in diabetic autonomic neuropathy. *J Clin Endocrinol Metab*. 1987;64:751-754.

37. Sanguinetti MC, Jiang C, Curran ME, Keating MT. A mechanistic link between an inherited and an acquired cardiac arrhythmia: HERG encodes the I_{Kr} potassium channel. *Cell*. 1995;81:299-307.

38. Splawski I, Shen J, Timothy KW, Vincent GM, Lehmann MH, Keating MT. Genomic structure of three long QT syndrome genes: KVLQT1, HERG, and KCNE1. *Genomics*. 1998;51:86-97.

39. Cardoso CR, Salles GF, Deccache W. QTc interval prolongation is a predictor of future strokes in patients with type 2 diabetes mellitus. *Stroke*. 2003;34:2187-2194.

40. Christensen PK, Gall MA, Major-Pedersen A, Sato A, Rossing P, Breum L, Pietersen A, Kastrup J, Parving HH. QTc interval length and QT dispersion as predictors of mortality in patients with non-insulin-dependent diabetes. *Scand J Clin Lab Invest*. 2000;60:323-332.

41. Sawicki PT, Kiwitt S, Bender R, Berger M. The value of QT interval dispersion for identification of total mortality risk in non-insulin-dependent diabetes mellitus. *J Intern Med*. 1998;243:49-56.

42. Heller SR. Abnormalities of the electrocardiogram during hypoglycaemia: the cause of the dead in bed syndrome? *Int J Clin Pract Suppl*. 2002;27-32.

43. D'Amico M, Marfella R, Nappo F, Di Filippo C, De Angelis L, Berrino L, Rossi F, Giugliano D. High glucose induces ventricular instability and increases vasomotor tone in rats. *Diabetologia*. 2001;44:464-470.

44. Ireland RH, Robinson RT, Heller SR, Marques JL, Harris ND. Measurement of high resolution ECG QT interval during controlled euglycaemia and hypoglycaemia. *Physiol Meas*. 2000;21:295-303.
45. Landstedt-Hallin L, Englund A, Adamson U, Lins PE. Increased QT dispersion during hypoglycaemia in patients with type 2 diabetes mellitus. *J Intern Med*. 1999;246:299-307.
46. Eckert B, Agardh CD. Hypoglycaemia leads to an increased QT interval in normal men. *Clin Physiol*. 1998;18:570-575.
47. Marques JL, George E, Peacey SR, Harris ND, Macdonald IA, Cochrane T, Heller SR. Altered ventricular repolarization during hypoglycaemia in patients with diabetes. *Diabet Med*. 1997;14:648-654.
48. Shimada R, Nakashima T, Nunoi K, Kohno Y, Takeshita A, Omae T. Arrhythmia during insulin-induced hypoglycemia in a diabetic patient. *Arch Intern Med*. 1984;144:1068-1069.
49. Rees DA, Alcolado JC. Animal models of diabetes mellitus. *Diabet Med*. 2005;22:359-370.
50. Bell RH, Jr., Hye RJ. Animal models of diabetes mellitus: physiology and pathology. *J Surg Res*. 1983;35:433-460.
51. Cheta D. Animal models of type I (insulin-dependent) diabetes mellitus. *J Pediatr Endocrinol Metab*. 1998;11:11-19.
52. Wong FS, Janeway CA, Jr. Insulin-dependent diabetes mellitus and its animal models. *Curr Opin Immunol*. 1999;11:643-647.
53. Matkovics B, Sasvari M, Kotorman M, Varga IS, Hai DQ, Varga C. Further prove on oxidative stress in alloxan diabetic rat tissues. *Acta Physiol Hung*. 1997;85:183-192.
54. Gumieniczek A, Hopkala H, Wojtowicz Z, Nikolajuk J. Changes in antioxidant status of heart muscle tissue in experimental diabetes in rabbits. *Acta Biochim Pol*. 2002;49:529-535.
55. Hadour G, Ferrera R, Sebbag L, Forrat R, Delaye J, de Lorgeril M. Improved myocardial tolerance to ischaemia in the diabetic rabbit. *J Mol Cell Cardiol*. 1998;30:1869-1875.
56. Zola BE, Miller B, Stiles GL, Rao PS, Sonnenblick EH, Fein FS. Heart rate control in diabetic rabbits: blunted response to isoproterenol. *Am J Physiol*. 1988;255:E636-E641.

57. Watkins D, Cooperstein SJ, Fiel S. Studies on the selectivity of alloxan for the beta-cells of the islets of Langerhans: effect of pH on the in vitro action of alloxan. *J Pharmacol Exp Ther*. 1979;208:184-189.

58. Bone A.J., Gwilliam D.J. Animal models of insulin-dependent diabetes mellitus. In: Textbook of Diabetes. Pickup J.C., Williams G., eds. 1997. Blackwell Science Ltd, Oxford-London.

59. Fein FS, Miller-Green B, Sonnenblick EH. Altered myocardial mechanics in diabetic rabbits. *Am J Physiol*. 1985;248:H729-H736.

60. Pollack PS, Malhotra A, Fein FS, Scheuer J. Effects of diabetes on cardiac contractile proteins in rabbits and reversal with insulin. *Am J Physiol*. 1986;251:H448-H454.

61. Severson DL. Diabetic cardiomyopathy: recent evidence from mouse models of type 1 and type 2 diabetes. *Can J Physiol Pharmacol*. 2004;82:813-823.

62. Wang Z, Fermini B, Nattel S. Delayed rectifier outward current and repolarization in human atrial myocytes. *Circ Res*. 1993;73:276-285.

63. Snyders DJ. Structure and function of cardiac potassium channels. *Cardiovasc Res*. 1999;42:377-390.

64. Shih HT. Anatomy of the action potential in the heart. *Tex Heart Inst J*. 1994;21:30-41.

65. Roden DM, Balser JR, George AL, Jr., Anderson ME. Cardiac ion channels. *Annu Rev Physiol*. 2002;64:431-475.

66. Liu DW, Gintant GA, Antzelevitch C. Ionic bases for electrophysiological distinctions among epicardial, midmyocardial, and endocardial myocytes from the free wall of the canine left ventricle. *Circ Res*. 1993;72:671-687.

67. Liu DW, Antzelevitch C. Characteristics of the delayed rectifier current (I_{Kr} and I_{Ks}) in canine ventricular epicardial, midmyocardial, and endocardial myocytes. A weaker I_{Ks} contributes to the longer action potential of the M cell. *Circ Res*. 1995;76:351-365.

68. Litovsky SH, Antzelevitch C. Transient outward current prominent in canine ventricular epicardium but not endocardium. *Circ Res*. 1988;62:116-126.

69. Cheng JH, Kodama I. Two components of delayed rectifier K^+ current in heart: molecular basis, functional diversity, and contribution to repolarization. *Acta Pharmacol Sin*. 2004;25:137-145.

70. Antzelevitch C. Electrical heterogeneity, cardiac arrhythmias, and the sodium channel. *Circ Res*. 2000;87:964-965.

71. Antzelevitch C, Fish J. Electrical heterogeneity within the ventricular wall. *Basic Res Cardiol*. 2001;96:517-527.

72. Laurita KR, Katra R, Wible B, Wan X, Koo MH. Transmural heterogeneity of calcium handling in canine. *Circ Res*. 2003;92:668-675.

73. Zygmunt AC, Goodrow RJ, Antzelevitch C. I_{NaCa} contributes to electrical heterogeneity within the canine ventricle. *Am J Physiol Heart Circ Physiol*. 2000;278:H1671-H1678.

74. Antzelevitch C, Shimizu W, Yan GX, Sicouri S, Weissenburger J, Nesterenko VV, Burashnikov A, Di Diego J, Saffitz J, Thomas GP. The M cell: its contribution to the ECG and to normal and abnormal electrical function of the heart. *J Cardiovasc Electrophysiol*. 1999;10:1124-1152.

75. Li GR, Lau CP, Ducharme A, Tardif JC, Nattel S. Transmural action potential and ionic current remodeling in ventricles of failing canine hearts. *Am J Physiol Heart Circ Physiol*. 2002;283:H1031-H1041.

76. Yue L, Feng J, Gaspo R, Li GR, Wang Z, Nattel S. Ionic remodeling underlying action potential changes in a canine model of atrial fibrillation. *Circ Res*. 1997;81:512-525.

77. Van Mieghem C, Sabbe M, Knockaert D. The clinical value of the ECG in noncardiac conditions. *Chest*. 2004;125:1561-1576.

78. Eiferman C, Chanson P, Cohen A, Lubetzki J. Torsade de pointes and Q-T prolongation in secondary hypothyroidism. *Lancet*. 1988;2:170-171.

79. Fredlund BO, Olsson SB. Long QT interval and ventricular tachycardia of "torsade de pointe" type in hypothyroidism. *Acta Med Scand*. 1983;213:231-235.

80. Izumi C, Inoko M, Kitaguchi S, Himura Y, Iga K, Gen H, Konishi T. Polymorphic ventricular tachycardia in a patient with adrenal insufficiency and hypothyroidism. *Jpn Circ J*. 1998;62:543-545.

81. Osborn LA, Skipper B, Arellano I, MacKerrow SD, Crawford MH. Results of resting and ambulatory electrocardiograms in patients with hypothyroidism and after return to euthyroid status. *Heart Dis*. 1999;1:8-11.

82. Moss AJ. T-wave patterns associated with the hereditary long QT syndrome. *Card Electrophysiol Rev*. 2002;6:311-315.

83. Wang Q, Shen J, Splawski I, Atkinson D, Li Z, Robinson JL, Moss AJ, Towbin JA, Keating MT. SCN5A mutations associated with an inherited cardiac arrhythmia, long QT syndrome. *Cell.* 1995;80:805-811.

84. Schott JJ, Charpentier F, Peltier S, Foley P, Drouin E, Bouhour JB, Donnelly P, Vergnaud G, Bachner L, Moisan JP, . Mapping of a gene for long QT syndrome to chromosome 4q25-27. *Am J Hum Genet.* 1995;57:1114-1122.

85. Mohler PJ, Bennett V. Ankyrin-based cardiac arrhythmias: a new class of channelopathies due to loss of cellular targeting. *Curr Opin Cardiol.* 2005;20:189-193.

86. Priori SG, Napolitano C. Genetics of cardiac arrhythmias and sudden cardiac death. *Ann N Y Acad Sci.* 2004;1015:96-110.

87. Tristani-Firouzi M, Jensen JL, Donaldson MR, Sansone V, Meola G, Hahn A, Bendahhou S, Kwiecinski H, Fidzianska A, Plaster N, Fu YH, Ptacek LJ, Tawil R. Functional and clinical characterization of KCNJ2 mutations associated with LQT7 (Andersen syndrome). *J Clin Invest.* 2002;110:381-388.

88. Trimmer JS. Regulation of ion channel expression by cytoplasmic subunits. *Curr Opin Neurobiol.* 1998;8:370-374.

89. Catterall W, Epstein PN. Ion channels. *Diabetologia.* 1992;35 Suppl 2:S23-S33.

90. Lehmann-Horn F, Jurkat-Rott K. Voltage-gated ion channels and hereditary disease. *Physiol Rev.* 1999;79:1317-1372.

91. Jeong SY, Goto J, Hashida H, Suzuki T, Ogata K, Masuda N, Hirai M, Isahara K, Uchiyama Y, Kanazawa I. Identification of a novel human voltage-gated sodium channel alpha subunit gene, SCN12A. *Biochem Biophys Res Commun.* 2000;267:262-270.

92. Kiyosue T, Arita M. Late sodium current and its contribution to action potential configuration in guinea pig ventricular myocytes. *Circ Res.* 1989;64:389-397.

93. Catterall WA. Neurotoxins that act on voltage-sensitive sodium channels in excitable membranes. *Annu Rev Pharmacol Toxicol.* 1980;20:15-43.

94. Chen Q, Kirsch GE, Zhang D, Brugada R, Brugada J, Brugada P, Potenza D, Moya A, Borggrefe M, Breithardt G, Ortiz-Lopez R, Wang Z, Antzelevitch C, O'Brien RE, Schulze-Bahr E, Keating MT, Towbin JA, Wang Q. Genetic basis and molecular mechanism for idiopathic ventricular fibrillation. *Nature.* 1998;392:293-296.

95. Wang DW, Yazawa K, George AL, Jr., Bennett PB. Characterization of human cardiac Na^+ channel mutations in the congenital long QT syndrome. *Proc Natl Acad Sci U S A.* 1996;93:13200-13205.

96. Brugada P, Brugada J. Right bundle branch block, persistent ST segment elevation and sudden cardiac death: a distinct clinical and electrocardiographic syndrome. A multicenter report. *J Am Coll Cardiol.* 1992;20:1391-1396.

97. Veldkamp MW, Viswanathan PC, Bezzina C, Baartscheer A, Wilde AA, Balser JR. Two distinct congenital arrhythmias evoked by a multidysfunctional Na^+ channel. *Circ Res.* 2000;86:E91-E97.

98. Tan HL, Bink-Boelkens MT, Bezzina CR, Viswanathan PC, Beaufort-Krol GC, van Tintelen PJ, van den Berg MP, Wilde AA, Balser JR. A sodium-channel mutation causes isolated cardiac conduction disease. *Nature.* 2001;409:1043-1047.

99. Olson TM, Michels VV, Ballew JD, Reyna SP, Karst ML, Herron KJ, Horton SC, Rodeheffer RJ, Anderson JL. Sodium channel mutations and susceptibility to heart failure and atrial fibrillation. *JAMA.* 2005;293:447-454.

100. The Cardiac Arrhythmia Suppression Trial (CAST) Investigators. Preliminary report: effect of encainide and flecainide on mortality in a randomized trial of arrhythmia suppression after myocardial infarction. *N Engl J Med.* 1989;321:406-412.

101. Coromilas J, Saltman AE, Waldecker B, Dillon SM, Wit AL. Electrophysiological effects of flecainide on anisotropic conduction and reentry in infarcted canine hearts. *Circulation.* 1995;91:2245-2263.

102. Lukas A, Antzelevitch C. Differences in the electrophysiological response of canine ventricular epicardium and endocardium to ischemia. Role of the transient outward current. *Circulation.* 1993;88:2903-2915.

103. Qu Y, Rogers JC, Tanada TN, Catterall WA, Scheuer T. Phosphorylation of S1505 in the cardiac Na^+ channel inactivation gate is required for modulation by protein kinase C. *J Gen Physiol.* 1996;108:375-379.

104. Li M, West JW, Numann R, Murphy BJ, Scheuer T, Catterall WA. Convergent regulation of sodium channels by protein kinase C and cAMP-dependent protein kinase. *Science.* 1993;261:1439-1442.

105. Zhou J, Yi J, Hu N, George AL, Jr., Murray KT. Activation of protein kinase A modulates trafficking of the human cardiac sodium channel in Xenopus oocytes. *Circ Res.* 2000;87:33-38.

106. Kaab S, Nuss HB, Chiamvimonvat N, O'Rourke B, Pak PH, Kass DA, Marban E, Tomaselli GF. Ionic mechanism of action potential prolongation in ventricular myocytes from dogs with pacing-induced heart failure. *Circ Res.* 1996;78:262-273.

107. Zicha S, Maltsev VA, Nattel S, Sabbah HN, Undrovinas AI. Post-transcriptional alterations in the expression of cardiac Na^+ channel subunits in chronic heart failure. *J Mol Cell Cardiol.* 2004;37:91-100.

108. Roberts R, Brugada R. Genetic aspects of arrhythmias. *Am J Med Genet.* 2000;97:310-318.

109. Clancy CE, Kass RS. Inherited and acquired vulnerability to ventricular arrhythmias: cardiac Na^+ and K^+ channels. *Physiol Rev.* 2005;85:33-47.

110. Viswanathan PC, Balser JR. Inherited sodium channelopathies: a continuum of channel dysfunction. *Trends Cardiovasc Med.* 2004;14:28-35.

111. Vizgirda VM. The genetic basis for cardiac dysrhythmias and the long QT syndrome. *J Cardiovasc Nurs.* 1999;13:34-45.

112. Catterall WA. From ionic currents to molecular mechanisms: the structure and function of voltage-gated sodium channels. *Neuron.* 2000;26:13-25.

113. Benitah JP, Gomez AM, Fauconnier J, Kerfant BG, Perrier E, Vassort G, Richard S. Voltage-gated Ca^{2+} currents in the human pathophysiologic heart: a review. *Basic Res Cardiol.* 2002;97 Suppl 1:I11-I18.

114. Beuckelmann DJ, Nabauer M, Erdmann E. Characteristics of calcium-current in isolated human ventricular myocytes from patients with terminal heart failure. *J Mol Cell Cardiol.* 1991;23:929-937.

115. Perez-Reyes E, Cribbs LL, Daud A, Lacerda AE, Barclay J, Williamson MP, Fox M, Rees M, Lee JH. Molecular characterization of a neuronal low-voltage-activated T-type calcium channel. *Nature.* 1998;391:896-900.

116. Chien AJ, Zhao X, Shirokov RE, Puri TS, Chang CF, Sun D, Rios E, Hosey MM. Roles of a membrane-localized beta subunit in the formation and targeting of functional L-type Ca^{2+} channels. *J Biol Chem.* 1995;270:30036-30044.

117. Hullin R, Khan IF, Wirtz S, Mohacsi P, Varadi G, Schwartz A, Herzig S. Cardiac L-type calcium channel beta-subunits expressed in human heart have differential effects on single channel characteristics. *J Biol Chem.* 2003;278:21623-21630.

118. Yamaoka K, Kameyama M. Regulation of L-type Ca^{2+} channels in the heart: overview of recent advances. *Mol Cell Biochem.* 2003;253:3-13.

119. Keef KD, Hume JR, Zhong J. Regulation of cardiac and smooth muscle Ca^{2+} channels (Ca(V)1.2a,b) by protein kinases. *Am J Physiol Cell Physiol.* 2001;281:C1743-C1756.

120. Anderson ME. Calmodulin kinase and L-type calcium channels; a recipe for arrhythmias? *Trends Cardiovasc Med.* 2004;14:152-161.

121. Perets T, Blumenstein Y, Shistik E, Lotan I, Dascal N. A potential site of functional modulation by protein kinase A in the cardiac Ca^{2+} channel alpha 1C subunit. *FEBS Lett.* 1996;384:189-192.

122. Dzhura I, Wu Y, Zhang R, Colbran RJ, Hamilton SL, Anderson ME. C terminus L-type Ca^{2+} channel calmodulin-binding domains are 'auto-agonist' ligands in rabbit ventricular myocytes. *J Physiol.* 2003;550:731-738.

123. Ko JH, Park WS, Earm YE. The protein kinase inhibitor, staurosporine, inhibits L-type Ca^{2+} current in rabbit atrial myocytes. *Biochem Biophys Res Commun.* 2005;329:531-537.

124. Kamp TJ, Hell JW. Regulation of cardiac L-type calcium channels by protein kinase A and protein kinase C. *Circ Res.* 2000;87:1095-1102.

125. Liu QY, Rosenberg RL. Stimulation of cardiac L-type calcium channels by extracellular ATP. *Am J Physiol Cell Physiol.* 2001;280:C1107-C1113.

126. Liu L, Zwingman TA, Fletcher CF. In vivo analysis of voltage-dependent calcium channels. *J Bioenerg Biomembr.* 2003;35:671-685.

127. Splawski I, Timothy KW, Sharpe LM, Decher N, Kumar P, Bloise R, Napolitano C, Schwartz PJ, Joseph RM, Condouris K, Tager-Flusberg H, Priori SG, Sanguinetti MC, Keating MT. Ca(V)1.2 calcium channel dysfunction causes a multisystem disorder including arrhythmia and autism. *Cell.* 2004;119:19-31.

128. Romero M, Sanchez I, Pujol MD. New advances in the field of calcium channel antagonists: cardiovascular effects and structure-activity relationships. *Curr Med Chem Cardiovasc Hematol Agents.* 2003;1:113-141.

129. Clusin WT, Anderson ME. Calcium channel blockers: current controversies and basic mechanisms of action. *Adv Pharmacol.* 1999;46:253-296.

130. Schuster A, Lacinova L, Klugbauer N, Ito H, Birnbaumer L, Hofmann F. The IVS6 segment of the L-type calcium channel is critical for the action of dihydropyridines and phenylalkylamines. *EMBO J.* 1996;15:2365-2370.

131. Van Wagoner DR. Electrophysiological remodeling in human atrial fibrillation. *Pacing Clin Electrophysiol.* 2003;26:1572-1575.

132. Nattel S. Atrial electrophysiological remodeling caused by rapid atrial activation: underlying mechanisms and clinical relevance to atrial fibrillation. *Cardiovasc Res.* 1999;42:298-308.

133. Li D, Melnyk P, Feng J, Wang Z, Petrecca K, Shrier A, Nattel S. Effects of experimental heart failure on atrial cellular and ionic electrophysiology. *Circulation.* 2000;101:2631-2638.

134. Li D, Zhang L, Kneller J, Nattel S. Potential ionic mechanism for repolarization differences between canine right and left atrium. *Circ Res.* 2001;88:1168-1175.

135. Hill JA. Electrical remodeling in cardiac hypertrophy. *Trends Cardiovasc Med.* 2003;13:316-322.

136. Clozel JP, Ertel EA, Ertel SI. Voltage-gated T-type Ca^{2+} channels and heart failure. *Proc Assoc Am Physicians.* 1999;111:429-437.

137. Cha TJ, Ehrlich JR, Zhang L, Nattel S. Atrial ionic remodeling induced by atrial tachycardia in the presence of congestive heart failure. *Circulation.* 2004;110:1520-1526.

138. Wang Z, Kutschke W, Richardson KE, Karimi M, Hill JA. Electrical remodeling in pressure-overload cardiac hypertrophy: role of calcineurin. *Circulation.* 2001;104:1657-1663.

139. Bryant SM, Shipsey SJ, Hart G. Regional differences in electrical and mechanical properties of myocytes from guinea-pig hearts with mild left ventricular hypertrophy. *Cardiovasc Res.* 1997;35:315-323.

140. Wu Y, Roden DM, Anderson ME. Calmodulin kinase inhibition prevents development of the arrhythmogenic transient inward current. *Circ Res.* 1999;84:906-912.

141. Laitinen PJ, Swan H, Kontula K. Molecular genetics of exercise-induced polymorphic ventricular tachycardia: identification of three novel cardiac ryanodine receptor mutations

and two common calsequestrin 2 amino-acid polymorphisms. *Eur J Hum Genet.* 2003;11:888-891.

142. Saraiva RM, Chedid NG, Quintero HC, Diaz GL, Masuda MO. Impaired beta-adrenergic response and decreased L-type calcium current of hypertrophied left ventricular myocytes in postinfarction heart failure. *Braz J Med Biol Res.* 2003;36:635-648.
143. Nuss HB, Houser SR. Voltage dependence of contraction and calcium current in severely hypertrophied feline ventricular myocytes. *J Mol Cell Cardiol.* 1991;23:717-726.
144. Barry DM, Nerbonne JM. Myocardial potassium channels: electrophysiological and molecular diversity. *Annu Rev Physiol.* 1996;58:363-394.
145. Coetzee WA, Amarillo Y, Chiu J, Chow A, Lau D, McCormack T, Moreno H, Nadal MS, Ozaita A, Pountney D, Saganich M, Vega-Saenz dM, Rudy B. Molecular diversity of K^+ channels. *Ann N Y Acad Sci.* 1999;868:233-285.
146. Nerbonne JM. Molecular basis of functional voltage-gated K^+ channel diversity in the mammalian myocardium. *J Physiol.* 2000;525 Pt 2:285-298.
147. Deal KK, England SK, Tamkun MM. Molecular physiology of cardiac potassium channels. *Physiol Rev.* 1996;76:49-67.
148. Tamargo J, Caballero R, Gomez R, Valenzuela C, Delpon E. Pharmacology of cardiac potassium channels. *Cardiovasc Res.* 2004;62:9-33.
149. Pourrier M, Schram G, Nattel S. Properties, expression and potential roles of cardiac K^+ channel accessory subunits: MinK, MiRPs, KChIP, and KChAP. *J Membr Biol.* 2003;194:141-152.
150. Wang Z. Ionic mechanisms and molecular basis of human cardiac repolarization: Implication for drug development. *Current Topics in Pharmacology in RESEARCH TRENDS.* 1998;19-35.
151. Frank-Hansen R, Larsen LA, Andersen P, Jespersgaard C, Christiansen M. Mutations in the genes KCND2 and KCND3 encoding the ion channels Kv4.2 and Kv4.3, conducting the cardiac fast transient outward current (ITO,f), are not a frequent cause of long QT syndrome. *Clin Chim Acta.* 2005;351:95-100.
152. Barry DM, Xu H, Schuessler RB, Nerbonne JM. Functional knockout of the transient outward current, long-QT syndrome, and cardiac remodeling in mice expressing a dominant-negative Kv4 alpha subunit. *Circ Res.* 1998;83:560-567.

153. Hoppe UC, Marban E, Johns DC. Molecular dissection of cardiac repolarization by in vivo Kv4.3 gene transfer. *J Clin Invest*. 2000;105:1077-1084.

154. Patel SP, Campbell DL. Transient Outward Potassium Current, "I_{to}", Phenotypes in the Mammalian Left Ventricle: Underlying Molecular, Cellular and Biophysical Mechanisms. *J Physiol*. 2005.

155. Oudit GY, Kassiri Z, Sah R, Ramirez RJ, Zobel C, Backx PH. The molecular physiology of the cardiac transient outward potassium current (I_{to}) in normal and diseased myocardium. *J Mol Cell Cardiol*. 2001;33:851-872.

156. Wickenden AD, Jegla TJ, Kaprielian R, Backx PH. Regional contributions of Kv1.4, Kv4.2, and Kv4.3 to transient outward K^+ current in rat ventricle. *Am J Physiol*. 1999;276:H1599-H1607.

157. Patel SP, Parai R, Parai R, Campbell DL. Regulation of Kv4.3 voltage-dependent gating kinetics by KChIP2 isoforms. *J Physiol*. 2004;557:19-41.

158. Patel SP, Campbell DL, Morales MJ, Strauss HC. Heterogeneous expression of KChIP2 isoforms in the ferret heart. *J Physiol*. 2002;539:649-656.

159. Lin YL, Chen CY, Cheng CP, Chang LS. Protein-protein interactions of KChIP proteins and Kv4.2. *Biochem Biophys Res Commun*. 2004;321:606-610.

160. Akar FG, Wu RC, Deschenes I, Armoundas AA, Piacentino V, III, Houser SR, Tomaselli GF. Phenotypic differences in transient outward K^+ current of human and canine ventricular myocytes: insights into molecular composition of ventricular I_{to}. *Am J Physiol Heart Circ Physiol*. 2004;286:H602-H609.

161. Kawano S, Hirayama Y, Hiraoka M. Activation mechanism of Ca^{2+}-sensitive transient outward current in rabbit ventricular myocytes. *J Physiol*. 1995;486 (Pt 3):593-604.

162. Kaab S, Dixon J, Duc J, Ashen D, Nabauer M, Beuckelmann DJ, Steinbeck G, McKinnon D, Tomaselli GF. Molecular basis of transient outward potassium current downregulation in human heart failure: a decrease in Kv4.3 mRNA correlates with a reduction in current density. *Circulation*. 1998;98:1383-1393.

163. Janse MJ. Electrophysiological changes in heart failure and their relationship to arrhythmogenesis. *Cardiovasc Res*. 2004;61:208-217.

164. Shimoni Y, Ewart HS, Severson D. Type I and II models of diabetes produce different modifications of K^+ currents in rat heart: role of insulin. *J Physiol.* 1998;507 (Pt 2):485-496.

165. Shimoni Y, Ewart HS, Severson D. Insulin stimulation of rat ventricular K^+ currents depends on the integrity of the cytoskeleton. *J Physiol.* 1999;514 (Pt 3):735-745.

166. Shimoni Y. Inhibition of the formation or action of angiotensin II reverses attenuated K^+ currents in type 1 and type 2 diabetes. *J Physiol.* 2001;537:83-92.

167. Shimoni Y, Liu XF. Sex differences in the modulation of K^+ currents in diabetic rat cardiac myocytes. *J Physiol.* 2003;550:401-412.

168. Sanguinetti MC, Jurkiewicz NK. Two components of cardiac delayed rectifier K^+ current. Differential sensitivity to block by class III antiarrhythmic agents. *J Gen Physiol.* 1990;96:195-215.

169. Wang Z, Fermini B, Nattel S. Rapid and slow components of delayed rectifier current in human atrial myocytes. *Cardiovasc Res.* 1994;28:1540-1546.

170. Wang Z, Fermini B, Nattel S. Effects of flecainide, quinidine, and 4-aminopyridine on transient outward and ultrarapid delayed rectifier currents in human atrial myocytes. *J Pharmacol Exp Ther.* 1995;272:184-196.

171. Wang Z, Feng J, Shi H, Pond A, Nerbonne JM, Nattel S. Potential molecular basis of different physiological properties of the transient outward K^+ current in rabbit and human atrial myocytes. *Circ Res.* 1999;84:551-561.

172. Cheng J, Kamiya K, Liu W, Tsuji Y, Toyama J, Kodama I. Heterogeneous distribution of the two components of delayed rectifier K^+ current: a potential mechanism of the proarrhythmic effects of methanesulfonanilideclass III agents. *Cardiovasc Res.* 1999;43:135-147.

173. Salata JJ, Jurkiewicz NK, Jow B, Folander K, Guinosso PJ, Jr., Raynor B, Swanson R, Fermini B. I_K of rabbit ventricle is composed of two currents: evidence for I_{Ks}. *Am J Physiol.* 1996;271:H2477-H2489.

174. Lei M, Brown HF. Two components of the delayed rectifier potassium current, I_K, in rabbit sino-atrial node cells. *Exp Physiol.* 1996;81:725-741.

175. Burashnikov A, Mannava S, Antzelevitch C. Transmembrane action potential heterogeneity in the canine isolated arterially perfused right atrium: effect of I_{Kr} and I_{Kur}/I_{to} block. *Am J Physiol Heart Circ Physiol.* 2004;286:H2393-H2400.

176. Fedida D, Eldstrom J, Hesketh JC, Lamorgese M, Castel L, Steele DF, Van Wagoner DR. Kv1.5 is an important component of repolarizing K^+ current in canine atrial myocytes. *Circ Res.* 2003;93:744-751.

177. Yue L, Feng J, Li GR, Nattel S. Characterization of an ultrarapid delayed rectifier potassium channel involved in canine atrial repolarization. *J Physiol.* 1996;496 (Pt 3):647-662.

178. Tseng GN. I_{Kr}: the hERG channel. *J Mol Cell Cardiol.* 2001;33:835-849.

179. Clay JR, Ogbaghebriel A, Paquette T, Sasyniuk BI, Shrier A. A quantitative description of the E-4031-sensitive repolarization current in rabbit ventricular myocytes. *Biophys J.* 1995;69:1830-1837.

180. Warmke JW, Ganetzky B. A family of potassium channel genes related to eag in Drosophila and mammals. *Proc Natl Acad Sci U S A.* 1994;91:3438-3442.

181. Hancox JC, Levi AJ, Witchel HJ. Time course and voltage dependence of expressed HERG current compared with native "rapid" delayed rectifier K current during the cardiac ventricular action potential. *Pflugers Arch.* 1998;436:843-853.

182. Chouabe C, Drici MD, Romey G, Barhanin J, Lazdunski M. HERG and KvLQT1/IsK, the cardiac K^+ channels involved in long QT syndromes, are targets for calcium channel blockers. *Mol Pharmacol.* 1998;54:695-703.

183. Zhou Z, Gong Q, Ye B, Fan Z, Makielski JC, Robertson GA, January CT. Properties of HERG channels stably expressed in HEK 293 cells studied at physiological temperature. *Biophys J.* 1998;74:230-241.

184. Busch AE, Suessbrich H. Role of the ISK protein in the IminK channel complex. *Trends Pharmacol Sci.* 1997;18:26-29.

185. McDonald TV, Yu Z, Ming Z, Palma E, Meyers MB, Wang KW, Goldstein SA, Fishman GI. A minK-HERG complex regulates the cardiac potassium current I_{Kr}. *Nature.* 1997;388:289-292.

186. Abbott GW, Sesti F, Splawski I, Buck ME, Lehmann MH, Timothy KW, Keating MT, Goldstein SA. MiRP1 forms I_{Kr} potassium channels with HERG and is associated with cardiac arrhythmia. *Cell.* 1999;97:175-187.

187. Anantharam A, Lewis A, Panaghie G, Gordon E, McCrossan ZA, Lerner DJ, Abbott GW. RNA interference reveals that endogenous Xenopus MinK-related peptides govern mammalian K^+ channel function in oocyte expression studies. *J Biol Chem.* 2003;278:11739-11745.

188. Weerapura M, Nattel S, Chartier D, Caballero R, Hebert TE. A comparison of currents carried by HERG, with and without coexpression of MiRP1, and the native rapid delayed rectifier current. Is MiRP1 the missing link? *J Physiol.* 2002;540:15-27.

189. Anantharam A, Abbott GW. Does hERG coassemble with a beta subunit? Evidence for roles of MinK and MiRP1. *Novartis Found Symp.* 2005;266:100-112.

190. Wymore RS, Gintant GA, Wymore RT, Dixon JE, McKinnon D, Cohen IS. Tissue and species distribution of mRNA for the I_{Kr}-like K^+ channel, erg. *Circ Res.* 1997;80:261-268.

191. Veldkamp MW, van Ginneken AC, Opthof T, Bouman LN. Delayed rectifier channels in human ventricular myocytes. *Circulation.* 1995;92:3497-3504.

192. Brahmajothi MV, Morales MJ, Reimer KA, Strauss HC. Regional localization of ERG, the channel protein responsible for the rapid component of the delayed rectifier, K^+ current in the ferret heart. *Circ Res.* 1997;81:128-135.

193. Follmer CH, Colatsky TJ. Block of delayed rectifier potassium current, I_K, by flecainide and E-4031 in cat ventricular myocytes. *Circulation.* 1990;82:289-293.

194. Veldkamp MW. Is the slowly activating component of the delayed rectifier current, I_{Ks}' absent from undiseased human ventricular myocardium? *Cardiovasc Res.* 1998;40:433-435.

195. Wang L, Feng ZP, Kondo CS, Sheldon RS, Duff HJ. Developmental changes in the delayed rectifier K^+ channels in mouse heart. *Circ Res.* 1996;79:79-85.

196. Dukes ID, Morad M. Tedisamil inactivates transient outward K^+ current in rat ventricular myocytes. *Am J Physiol.* 1989;257:H1746-H1749.

197. Tseng-Crank JC, Tseng GN, Schwartz A, Tanouye MA. Molecular cloning and functional expression of a potassium channel cDNA isolated from a rat cardiac library. *FEBS Lett.* 1990;268:63-68.

198. Splawski I, Shen J, Timothy KW, Lehmann MH, Priori S, Robinson JL, Moss AJ, Schwartz PJ, Towbin JA, Vincent GM, Keating MT. Spectrum of mutations in long-QT syndrome genes. KVLQT1, HERG, SCN5A, KCNE1, and KCNE2. *Circulation.* 2000;102:1178-1185.

199. Hoorntje T, Alders M, van Tintelen P, van der LK, Sreeram N, van der WA, Mannens M, Wilde A. Homozygous premature truncation of the HERG protein : the human HERG knockout. *Circulation.* 1999;100:1264-1267.

200. Li H, Chen Q, Moss AJ, Robinson J, Goytia V, Perry JC, Vincent GM, Priori SG, Lehmann MH, Denfield SW, Duff D, Kaine S, Shimizu W, Schwartz PJ, Wang Q, Towbin JA. New mutations in the KVLQT1 potassium channel that cause long-QT syndrome. *Circulation.* 1998;97:1264-1269.

201. Sanguinetti MC, Curran ME, Spector PS, Keating MT. Spectrum of HERG K^+-channel dysfunction in an inherited cardiac arrhythmia. *Proc Natl Acad Sci U S A.* 1996;93:2208-2212.

202. Sasano T, Ueda K, Orikabe M, Hirano Y, Kawano S, Yasunami M, Isobe M, Kimura A, Hiraoka M. Novel C-terminus frameshift mutation, 1122fs/147, of HERG in LQT2: additional amino acids generated by frameshift cause accelerated inactivation. *J Mol Cell Cardiol.* 2004;37:1205-1211.

203. Thomas D, Kiehn J, Katus HA, Karle CA. Defective protein trafficking in hERG-associated hereditary long QT syndrome (LQT2): molecular mechanisms and restoration of intracellular protein processing. *Cardiovasc Res.* 2003;60:235-241.

204. Ficker E, Obejero-Paz CA, Zhao S, Brown AM. The binding site for channel blockers that rescue misprocessed human long QT syndrome type 2 ether-a-gogo-related gene (HERG) mutations. *J Biol Chem.* 2002;277:4989-4998.

205. Ficker E, Dennis AT, Obejero-Paz CA, Castaldo P, Taglialatela M, Brown AM. Retention in the endoplasmic reticulum as a mechanism of dominant-negative current suppression in human long QT syndrome. *J Mol Cell Cardiol.* 2000;32:2327-2337.

206. Furutani M, Trudeau MC, Hagiwara N, Seki A, Gong Q, Zhou Z, Imamura S, Nagashima H, Kasanuki H, Takao A, Momma K, January CT, Robertson GA, Matsuoka R. Novel mechanism associated with an inherited cardiac arrhythmia: defective protein trafficking by the mutant HERG (G601S) potassium channel. *Circulation.* 1999;99:2290-2294.

207. Akhavan A, Atanasiu R, Noguchi T, Han W, Holder N, Shrier A. Identification of the cyclic-nucleotide-binding domain as a conserved determinant of ion-channel cell-surface localization. *J Cell Sci*. 2005;118:2803-2812.

208. Rampe D, Roy ML, Dennis A, Brown AM. A mechanism for the proarrhythmic effects of cisapride (Propulsid): high affinity blockade of the human cardiac potassium channel HERG. *FEBS Lett*. 1997;417:28-32.

209. Salata JJ, Jurkiewicz NK, Wallace AA, Stupienski RF, III, Guinosso PJ, Jr., Lynch JJ, Jr. Cardiac electrophysiological actions of the histamine H1-receptor antagonists astemizole and terfenadine compared with chlorpheniramine and pyrilamine. *Circ Res*. 1995;76:110-119.

210. Carmeliet E. Cardiac ionic currents and acute ischemia: from channels to arrhythmias. *Physiol Rev*. 1999;79:917-1017.

211. Vereecke J, Carmeliet E. The effect of external pH on the delayed rectifying K^+ current in cardiac ventricular myocytes. *Pflugers Arch*. 2000;439:739-751.

212. Furukawa T, Bassett AL, Furukawa N, Kimura S, Myerburg RJ. The ionic mechanism of reperfusion-induced early afterdepolarizations in feline left ventricular hypertrophy. *J Clin Invest*. 1993;91:1521-1531.

213. Tsuji Y, Opthof T, Kamiya K, Yasui K, Liu W, Lu Z, Kodama I. Pacing-induced heart failure causes a reduction of delayed rectifier potassium currents along with decreases in calcium and transient outward currents in rabbit ventricle. *Cardiovasc Res*. 2000;48:300-309.

214. Jiang M, Cabo C, Yao J, Boyden PA, Tseng G. Delayed rectifier K currents have reduced amplitudes and altered kinetics in myocytes from infarcted canine ventricle. *Cardiovasc Res*. 2000;48:34-43.

215. Cui J, Melman Y, Palma E, Fishman GI, McDonald TV. Cyclic AMP regulates the HERG K^+ channel by dual pathways. *Curr Biol*. 2000;10:671-674.

216. Kiehn J. Regulation of the cardiac repolarizing HERG potassium channel by protein kinase A. *Trends Cardiovasc Med*. 2000;10:205-209.

217. Lei M, Brown HF, Terrar DA. Modulation of delayed rectifier potassium current, iK, by isoprenaline in rabbit isolated pacemaker cells. *Exp Physiol*. 2000;85:27-35.

218. Thomas D, Zhang W, Wu K, Wimmer AB, Gut B, Wendt-Nordahl G, Kathofer S, Kreye VA, Katus HA, Schoels W, Kiehn J, Karle CA. Regulation of HERG potassium channel activation by protein kinase C independent of direct phosphorylation of the channel protein. *Cardiovasc Res.* 2003;59:14-26.

219. Bian J, Cui J, McDonald TV. HERG K^+ channel activity is regulated by changes in phosphatidyl inositol 4,5-bisphosphate. *Circ Res.* 2001;89:1168-1176.

220. Magyar J, Iost N, Kortvely A, Banyasz T, Virag L, Szigligeti P, Varro A, Opincariu M, Szecsi J, Papp JG, Nanasi PP. Effects of endothelin-1 on calcium and potassium currents in undiseased human ventricular myocytes. *Pflugers Arch.* 2000;441:144-149.

221. Wang J, Wang H, Han H, Zhang Y, Yang B, Nattel S, Wang Z. Phospholipid metabolite 1-palmitoyl-lysophosphatidylcholine enhances human ether-a-go-go-related gene (HERG) K^+ channel function. *Circulation.* 2001;104:2645-2648.

222. Wang J, Zhang Y, Wang H, Han H, Nattel S, Yang B, Wang Z. Potential mechanisms for the enhancement of HERG K^+ channel function by phospholipid metabolites. *Br J Pharmacol.* 2004;141:586-599.

223. Blair LA, Bence-Hanulec KK, Mehta S, Franke T, Kaplan D, Marshall J. Akt-dependent potentiation of L channels by insulin-like growth factor- 1 is required for neuronal survival. *J Neurosci.* 1999;19:1940-1951.

224. Kurokawa J, Abriel H, Kass RS. Molecular basis of the delayed rectifier current I_{Ks} in heart. *J Mol Cell Cardiol.* 2001;33:873-882.

225. Sanguinetti MC, Zou A. Molecular physiology of cardiac delayed rectifier K^+ channels. *Heart Vessels.* 1997;Suppl 12:170-172.

226. Silva J, Rudy Y. Subunit Interaction Determines I_{Ks} Participation in Cardiac Repolarization and Repolarization Reserve. *Circulation.* 2005.

227. Jost N, Virag L, Bitay M, Takacs J, Lengyel C, Biliczki P, Nagy Z, Bogats G, Lathrop DA, Papp JG, Varro A. Restricting Excessive Cardiac Action Potential and QT Prolongation. A Vital Role for I_{Ks} in Human Ventricular Muscle. *Circulation.* 2005.

228. Silva J RY. Subunit Interaction Determines I_{Ks} Participation in Cardiac Repolarization and Repolarization Reserve. *Circulation.* 2005.

229. Li GR, Yang B, Feng J, Bosch RF, Carrier M, Nattel S. Transmembrane I_{Ca} contributes to rate-dependent changes of action potentials in human ventricular myocytes. *Am J Physiol.* 1999;276:H98-H106.

230. Jurkiewicz NK, Sanguinetti MC. Rate-dependent prolongation of cardiac action potentials by a methanesulfonanilide class III antiarrhythmic agent. Specific block of rapidly activating delayed rectifier K^+ current by dofetilide. *Circ Res.* 1993;72:75-83.

231. Stengl M, Volders PG, Thomsen MB, Spatjens RL, Sipido KR, Vos MA. Accumulation of slowly activating delayed rectifier potassium current (I_{Ks}) in canine ventricular myocytes. *J Physiol.* 2003;551:777-786.

232. Wang ZG, Pelletier LC, Talajic M, Nattel S. Effects of flecainide and quinidine on human atrial action potentials. Role of rate-dependence and comparison with guinea pig, rabbit, and dog tissues. *Circulation.* 1990;82:274-283.

233. Busch AE, Suessbrich H, Waldegger S, Sailer E, Greger R, Lang H, Lang F, Gibson KJ, Maylie JG. Inhibition of I_{Ks} in guinea pig cardiac myocytes and guinea pig IsK channels by the chromanol 293B. *Pflugers Arch.* 1996;432:1094-1096.

234. Gogelein H, Bruggemann A, Gerlach U, Brendel J, Busch AE. Inhibition of I_{Ks} channels by HMR 1556. *Naunyn Schmiedebergs Arch Pharmacol.* 2000;362:480-488.

235. Suessbrich H, Busch AE. The I_{Ks} channel: coassembly of IsK (minK) and KvLQT1 proteins. *Rev Physiol Biochem Pharmacol.* 1999;137:191-226.

236. Romey G, Attali B, Chouabe C, Abitbol I, Guillemare E, Barhanin J, Lazdunski M. Molecular mechanism and functional significance of the MinK control of the KvLQT1 channel activity. *J Biol Chem.* 1997;272:16713-16716.

237. Wang Q, Curran ME, Splawski I, Burn TC, Millholland JM, VanRaay TJ, Shen J, Timothy KW, Vincent GM, de Jager T, Schwartz PJ, Toubin JA, Moss AJ, Atkinson DL, Landes GM, Connors TD, Keating MT. Positional cloning of a novel potassium channel gene: KVLQT1 mutations cause cardiac arrhythmias. *Nat Genet.* 1996;12:17-23.

238. Sanguinetti MC, Curran ME, Zou A, Shen J, Spector PS, Atkinson DL, Keating MT. Coassembly of K(V)LQT1 and minK (IsK) proteins to form cardiac I_{Ks} potassium channel. *Nature.* 1996;384:80-83.

239. Ohyama H, Kajita H, Omori K, Takumi T, Hiramoto N, Iwasaka T, Matsuda H. Inhibition of cardiac delayed rectifier K^+ currents by an antisense oligodeoxynucleotide

against IsK (minK) and over-expression of IsK mutant D77N in neonatal mouse hearts. *Pflugers Arch.* 2001;442:329-335.

240. Bianchi L, Shen Z, Dennis AT, Priori SG, Napolitano C, Ronchetti E, Bryskin R, Schwartz PJ, Brown AM. Cellular dysfunction of LQT5-minK mutants: abnormalities of I_{Ks}, I_{Kr} and trafficking in long QT syndrome. *Hum Mol Genet.* 1999;8:1499-1507.
241. Tristani-Firouzi M, Sanguinetti MC. Voltage-dependent inactivation of the human K^+ channel KvLQT1 is eliminated by association with minimal K^+ channel (minK) subunits. *J Physiol.* 1998;510 (Pt 1):37-45.
242. Krumerman A, Gao X, Bian JS, Melman YF, Kagan A, McDonald TV. An LQT mutant minK alters KvLQT1 trafficking. *Am J Physiol Cell Physiol.* 2004;286:C1453-C1463.
243. Russell MW, Dick M, Collins FS, Brody LC. KVLQT1 mutations in three families with familial or sporadic long QT syndrome. *Hum Mol Genet.* 1996;5:1319-1324.
244. Sesti F, Goldstein SA. Single-channel characteristics of wild-type I_{Ks} channels and channels formed with two minK mutants that cause long QT syndrome. *J Gen Physiol.* 1998;112:651-663.
245. Duggal P, Vesely MR, Wattanasirichaigoon D, Villafane J, Kaushik V, Beggs AH. Mutation of the gene for IsK associated with both Jervell and Lange-Nielsen and Romano-Ward forms of Long-QT syndrome. *Circulation.* 1998;97:142-146.
246. Splawski I, Tristani-Firouzi M, Lehmann MH, Sanguinetti MC, Keating MT. Mutations in the hminK gene cause long QT syndrome and suppress I_{Ks} function. *Nat Genet.* 1997;17:338-340.
247. Balser JR, Bennett PB, Hondeghem LM, Roden DM. Suppression of time-dependent outward current in guinea pig ventricular myocytes. Actions of quinidine and amiodarone. *Circ Res.* 1991;69:519-529.
248. Shimizu W, Antzelevitch C. Cellular basis for the ECG features of the LQT1 form of the long-QT syndrome: effects of beta-adrenergic agonists and antagonists and sodium channel blockers on transmural dispersion of repolarization and torsade de pointes. *Circulation.* 1998;98:2314-2322.
249. Dilly KW, Kurokawa J, Terrenoire C, Reiken S, Lederer WJ, Marks AR, Kass RS. Overexpression of beta2-adrenergic receptors cAMP-dependent protein kinase phosphorylates and modulates slow delayed rectifier potassium channels expressed in

murine heart: evidence for receptor/channel co-localization. *J Biol Chem.* 2004;279:40778-40787.

250. Kathofer S, Rockl K, Zhang W, Thomas D, Katus H, Kiehn J, Kreye V, Schoels W, Karle C. Human beta(3)-adrenoreceptors couple to KvLQT1/MinK potassium channels in Xenopus oocytes via protein kinase C phosphorylation of the KvLQT1 protein. *Naunyn Schmiedebergs Arch Pharmacol.* 2003;368:119-126.
251. Yang T, Kanki H, Roden DM. Phosphorylation of the I_{Ks} channel complex inhibits drug block: novel mechanism underlying variable antiarrhythmic drug actions. *Circulation.* 2003;108:132-134.
252. Marx SO, Kurokawa J, Reiken S, Motoike H, D'Armiento J, Marks AR, Kass RS. Requirement of a macromolecular signaling complex for beta adrenergic receptor modulation of the KCNQ1-KCNE1 potassium channel. *Science.* 2002;295:496-499.
253. Walsh KB, Kass RS. Distinct voltage-dependent regulation of a heart-delayed I_K by protein kinases A and C. *Am J Physiol.* 1991;261:C1081-C1090.
254. Lo CF, Numann R. Independent and exclusive modulation of cardiac delayed rectifying K^+ current by protein kinase C and protein kinase A. *Circ Res.* 1998;83:995-1002.
255. Lo CF, Numann R. PKC modulation of minK current involves multiple phosphorylation sites. *Ann N Y Acad Sci.* 1999;868:431-433.
256. Varnum MD, Busch AE, Bond CT, Maylie J, Adelman JP. The min K channel underlies the cardiac potassium current I_{Ks} and mediates species-specific responses to protein kinase C. *Proc Natl Acad Sci U S A.* 1993;90:11528-11532.
257. Ryder KO, Bryant SM, Hart G. Membrane current changes in left ventricular myocytes isolated from guinea pigs after abdominal aortic coarctation. *Cardiovasc Res.* 1993;27:1278-1287.
258. Volders PG, Sipido KR, Vos MA, Spatjens RL, Leunissen JD, Carmeliet E, Wellens HJ. Downregulation of delayed rectifier K^+ currents in dogs with chronic complete atrioventricular block and acquired torsades de pointes. *Circulation.* 1999;100:2455-2461.
259. Li GR, Feng J, Yue L, Carrier M, Nattel S. Evidence for two components of delayed rectifier K^+ current in human ventricular myocytes. *Circ Res.* 1996;78:689-696.

260. Schram G, Pourrier M, Melnyk P, Nattel S. Differential distribution of cardiac ion channel expression as a basis for regional specialization in electrical function. *Circ Res.* 2002;90:939-950.

261. Nakamura TY, Artman M, Rudy B, Coetzee WA. Inhibition of rat ventricular I_{K1} with antisense oligonucleotides targeted to Kir2.1 mRNA. *Am J Physiol.* 1998;274:H892-H900.

262. Zobel C, Cho HC, Nguyen TT, Pekhletski R, Diaz RJ, Wilson GJ, Backx PH. Molecular dissection of the inward rectifier potassium current (I_{K1}) in rabbit cardiomyocytes: evidence for heteromeric co-assembly of Kir2.1 and Kir2.2. *J Physiol.* 2003;550:365-372.

263. Liu GX, Derst C, Schlichthorl G, Heinen S, Seebohm G, Bruggemann A, Kummer W, Veh RW, Daut J, Preisig-Muller R. Comparison of cloned Kir2 channels with native inward rectifier K^+ channels from guinea-pig cardiomyocytes. *J Physiol.* 2001;532:115-126.

264. Lange PS, Er F, Gassanov N, Hoppe UC. Andersen mutations of KCNJ2 suppress the native inward rectifier current I_{K1} in a dominant-negative fashion. *Cardiovasc Res.* 2003;59:321-327.

265. Fodstad H, Swan H, Auberson M, Gautschi I, Loffing J, Schild L, Kontula K. Loss-of-function mutations of the K(+) channel gene KCNJ2 constitute a rare cause of long QT syndrome. *J Mol Cell Cardiol.* 2004;37:593-602.

266. Ai T, Fujiwara Y, Tsuji K, Otani H, Nakano S, Kubo Y, Horie M. Novel KCNJ2 mutation in familial periodic paralysis with ventricular dysrhythmia. *Circulation.* 2002;105:2592-2594.

267. Preisig-Muller R, Schlichthorl G, Goerge T, Heinen S, Bruggemann A, Rajan S, Derst C, Veh RW, Daut J. Heteromerization of Kir2.x potassium channels contributes to the phenotype of Andersen's syndrome. *Proc Natl Acad Sci U S A.* 2002;99:7774-7779.

268. Plaster NM, Tawil R, Tristani-Firouzi M, Canun S, Bendahhou S, Tsunoda A, Donaldson MR, Iannaccone ST, Brunt E, Barohn R, Clark J, Deymeer F, George AL, Jr., Fish FA, Hahn A, Nitu A, Ozdemir C, Serdaroglu P, Subramony SH, Wolfe G, Fu YH, Ptacek LJ. Mutations in Kir2.1 cause the developmental and episodic electrical phenotypes of Andersen's syndrome. *Cell.* 2001;105:511-519.

269. Miake J, Marban E, Nuss HB. Functional role of inward rectifier current in heart probed by Kir2.1 overexpression and dominant-negative suppression. *J Clin Invest.* 2003;111:1529-1536.

270. Sanchez-Chapula JA, Salinas-Stefanon E, Torres-Jacome J, Benavides-Haro DE, Navarro-Polanco RA. Blockade of currents by the antimalarial drug chloroquine in feline ventricular myocytes. *J Pharmacol Exp Ther.* 2001;297:437-445.

271. Warren M, Guha PK, Berenfeld O, Zaitsev A, Anumonwo JM, Dhamoon AS, Bagwe S, Taffet SM, Jalife J. Blockade of the inward rectifying potassium current terminates ventricular fibrillation in the guinea pig heart. *J Cardiovasc Electrophysiol.* 2003;14:621-631.

272. Koumi S, Wasserstrom JA, Ten Eick RE. Beta-adrenergic and cholinergic modulation of inward rectifier K^+ channel function and phosphorylation in guinea-pig ventricle. *J Physiol.* 1995;486 (Pt 3):661-678.

273. Karle CA, Zitron E, Zhang W, Wendt-Nordahl G, Kathofer S, Thomas D, Gut B, Scholz E, Vahl CF, Katus HA, Kiehn J. Human cardiac inwardly-rectifying K^+ channel Kir(2.1b) is inhibited by direct protein kinase C-dependent regulation in human isolated cardiomyocytes and in an expression system. *Circulation.* 2002;106:1493-1499.

274. Zitron E, Kiesecker C, Luck S, Kathofer S, Thomas D, Kreye VA, Kiehn J, Katus HA, Schoels W, Karle CA. Human cardiac inwardly rectifying current IKir2.2 is upregulated by activation of protein kinase A. *Cardiovasc Res.* 2004;63:520-527.

275. Wang H, Yang B, Zhang Y, Han H, Wang J, Shi H, Wang Z. Different subtypes of alpha1-adrenoceptor modulate different K^+ currents via different signaling pathways in canine ventricular myocytes. *J Biol Chem.* 2001;276:40811-40816.

276. Tomaselli GF, Marban E. Electrophysiological remodeling in hypertrophy and heart failure. *Cardiovasc Res.* 1999;42:270-283.

277. Nabauer M, Kaab S. Potassium channel down-regulation in heart failure. *Cardiovasc Res.* 1998;37:324-334.

278. Yao JA, Jiang M, Fan JS, Zhou YY, Tseng GN. Heterogeneous changes in K currents in rat ventricles three days after myocardial infarction. *Cardiovasc Res.* 1999;44:132-145.

279. Wang Z, Yue L, White M, Pelletier G, Nattel S. Differential distribution of inward rectifier potassium channel transcripts in human atrium versus ventricle. *Circulation.* 1998;98:2422-2428.

280. Li J, McLerie M, Lopatin AN. Transgenic upregulation of I_{K1} in the mouse heart leads to multiple abnormalities of cardiac excitability. *Am J Physiol Heart Circ Physiol.* 2004;287:H2790-H2802.

281. Ashcroft FM. Adenosine 5'-triphosphate-sensitive potassium channels. *Annu Rev Neurosci.* 1988;11:97-118.

282. Inagaki N, Gonoi T, Clement JP, Namba N, Inazawa J, Gonzalez G, Aguilar-Bryan L, Seino S, Bryan J. Reconstitution of I_{KATP}: an inward rectifier subunit plus the sulfonylurea receptor. *Science.* 1995;270:1166-1170.

283. Ashcroft FM. ATP-sensitive potassium channelopathies: focus on insulin secretion. *J Clin Invest.* 2005;115:2047-2058.

284. Nakaya H, Takeda Y, Tohse N, Kanno M. Effects of ATP-sensitive K^+ channel blockers on the action potential shortening in hypoxic and ischaemic myocardium. *Br J Pharmacol.* 1991;103:1019-1026.

285. Wolleben CD, Sanguinetti MC, Siegl PK. Influence of ATP-sensitive potassium channel modulators on ischemia-induced fibrillation in isolated rat hearts. *J Mol Cell Cardiol.* 1989;21:783-788.

286. Ackerman MJ. The long QT syndrome: ion channel diseases of the heart. *Mayo Clin Proc.* 1998;73:250-269.

287. Keating MT, Sanguinetti MC. Molecular and cellular mechanisms of cardiac arrhythmias. *Cell.* 2001;104:569-580.

288. Nattel S, Li D. Ionic remodeling in the heart: pathophysiological significance and new therapeutic opportunities for atrial fibrillation. *Circ Res.* 2000;87:440-447.

289. Magyar J, Rusznak Z, Szentesi P, Szucs G, Kovacs L. Action potentials and potassium currents in rat ventricular muscle during experimental diabetes. *J Mol Cell Cardiol.* 1992;24:841-853.

290. Shimoni Y, Light PE, French RJ. Altered ATP sensitivity of ATP-dependent K^+ channels in diabetic rat hearts. *Am J Physiol.* 1998;275:E568-E576.

291. Nobe S, Aomine M, Arita M, Ito S, Takaki R. Chronic diabetes mellitus prolongs action potential duration of rat ventricular muscles: circumstantial evidence for impaired Ca^{2+} channel. *Cardiovasc Res*. 1990;24:381-389.

292. Casis O, Gallego M, Iriarte M, Sanchez-Chapula JA. Effects of diabetic cardiomyopathy on regional electrophysiologic characteristics of rat ventricle. *Diabetologia*. 2000;43:101-109.

293. Chattou S, Coulombe A, Diacono J, Le Grand B, John G, Feuvray D. Slowly inactivating component of sodium current in ventricular myocytes is decreased by diabetes and partially inhibited by known Na^{+}-H^{+}-change blockers. *J Mol Cell Cardiol*. 2000;32:1181-1192.

294. Chattou S, Diacono J, Feuvray D. Decrease in sodium-calcium exchange and calcium currents in diabetic rat ventricular myocytes. *Acta Physiol Scand*. 1999;166:137-144.

295. Wang DW, Kiyosue T, Shigematsu S, Arita M. Abnormalities of K^{+} and Ca^{2+} currents in ventricular myocytes from rats with chronic diabetes. *Am J Physiol*. 1995;269:H1288-H1296.

296. Jourdon P, Feuvray D. Calcium and potassium currents in ventricular myocytes isolated from diabetic rats. *J Physiol*. 1993;470:411-429.

297. Tsuchida K, Watajima H. Potassium currents in ventricular myocytes from genetically diabetic rats. *Am J Physiol*. 1997;273:E695-E700.

298. Lee SL, Ostadalova I, Kolar F, Dhalla NS. Alterations in Ca^{2+}-channels during the development of diabetic cardiomyopathy. *Mol Cell Biochem*. 1992;109:173-179.

299. Tsuchida K, Watajima H, Otomo S. Calcium current in rat diabetic ventricular myocytes. *Am J Physiol*. 1994;267:H2280-H2289.

300. Yu JZ, Quamme GA, McNeill JH. Altered $[Ca^{2+}]_i$ mobilization in diabetic cardiomyocytes: responses to caffeine, KCl, ouabain, and ATP. *Diabetes Res Clin Pract*. 1995;30:9-20.

301. Yu JZ, Rodrigues B, McNeill JH. Intracellular calcium levels are unchanged in the diabetic heart. *Cardiovasc Res*. 1997;34:91-98.

302. Shimoni Y, Severson D, Giles W. Thyroid status and diabetes modulate regional differences in potassium currents in rat ventricle. *J Physiol*. 1995;488 (Pt 3):673-688.

303. Shimoni Y, Rattner JB. Type 1 diabetes leads to cytoskeleton changes that are reflected in insulin action on rat cardiac K^+ currents. *Am J Physiol Endocrinol Metab.* 2001;281:E575-E585.

304. Shimoni Y. Protein kinase C regulation of K^+ currents in rat ventricular myocytes and its modification by hormonal status. *J Physiol.* 1999;520 Pt 2:439-449.

305. Shimoni Y, Firek L, Severson D, Giles W. Short-term diabetes alters K^+ currents in rat ventricular myocytes. *Circ Res.* 1994;74:620-628.

306. Magyar J, Cseresnyes Z, Rusznak Z, Sipos I, Szucs G, Kovacs L. Effects of insulin on potassium currents of rat ventricular myocytes in streptozotocin diabetes. *Gen Physiol Biophys.* 1995;14:191-201.

307. Thorneloe KS, Liu XF, Walsh MP, Shimoni Y. Transmural differences in rat ventricular protein kinase C epsilon correlate with its functional regulation of a transient cardiac K^+ current. *J Physiol.* 2001;533:145-154.

308. Xu Z, Patel KP, Rozanski GJ. Metabolic basis of decreased transient outward K^+ current in ventricular myocytes from diabetic rats. *Am J Physiol.* 1996;271:H2190-H2196.

309. Gallego M, Casis O. Regulation of cardiac transient outward potassium current by norepinephrine in normal and diabetic rats. *Diabetes Metab Res Rev.* 2001;17:304-309.

310. Qin D, Huang B, Deng L, El Adawi H, Ganguly K, Sowers JR, El Sherif N. Downregulation of K^+ channel genes expression in type I diabetic cardiomyopathy. *Biochem Biophys Res Commun.* 2001;283:549-553.

311. Nishiyama A, Ishii DN, Backx PH, Pulford BE, Birks BR, Tamkun MM. Altered K^+ channel gene expression in diabetic rat ventricle: isoform switching between Kv4.2 and Kv1.4. *Am J Physiol Heart Circ Physiol.* 2001;281:H1800-H1807.

312. Aomine M, Yamato T. Electrophysiological properties of ventricular muscle obtained from spontaneously diabetic mice. *Exp Anim.* 2000;49:23-33.

313. Gallego M, Casis E, Izquierdo MJ, Casis O. Restoration of cardiac transient outward potassium current by norepinephrine in diabetic rats. *Pflugers Arch.* 2000;441:102-107.

314. Li X, Xu Z, Li S, Rozanski GJ. Redox regulation of I_{to} remodeling in diabetic rat heart. *Am J Physiol Heart Circ Physiol.* 2005;288:H1417-H1424.

315. Rozanski GJ, Xu Z. A metabolic mechanism for cardiac K^+ channel remodelling. *Clin Exp Pharmacol Physiol.* 2002;29:132-137.

316. Rozanski GJ, Xu Z, Zhang K, Patel KP. Altered K^+ current of ventricular myocytes in rats with chronic myocardial infarction. *Am J Physiol*. 1998;274:H259-H265.

317. Rusznak Z, Cseresnyes Z, Sipos I, Magyar J, Kovacs L, Szucs G. Characteristics of the ventricular transient outward potassium current in genetic rodent models of diabetes. *Gen Physiol Biophys*. 1996;15:225-238.

318. Smith JM, Wahler GM. ATP-sensitive potassium channels are altered in ventricular myocytes from diabetic rats. *Mol Cell Biochem*. 1996;158:43-51.

319. Hupfeld CJ, Wong GA. Molecular mechanisms of diabetic cardiovascular disease. *Prev Cardiol*. 2002;5:183-187.

320. Hintz KK, Ren J. Phytoestrogenic isoflavones daidzein and genistein reduce glucose-toxicity-induced cardiac contractile dysfunction in ventricular myocytes. *Endocr Res*. 2004;30:215-223.

321. Marfella R, Esposito K, Giugliano D. Effect of high glucose on vasculature. *Circulation*. 2003;108:e74.

322. Sakai K, Matsumoto K, Nishikawa T, Suefuji M, Nakamaru K, Hirashima Y, Kawashima J, Shirotani T, Ichinose K, Brownlee M, Araki E. Mitochondrial reactive oxygen species reduce insulin secretion by pancreatic beta-cells. *Biochem Biophys Res Commun*. 2003;300:216-222.

323. Liu Y, Terata K, Rusch NJ, Gutterman DD. High glucose impairs voltage-gated K^+ channel current in rat small coronary arteries. *Circ Res*. 2001;89:146-152.

324. Modesti A, Bertolozzi I, Gamberi T, Marchetta M, Lumachi C, Coppo M, Moroni F, Toscano T, Lucchese G, Gensini GF, Modesti PA. Hyperglycemia activates JAK2 signaling pathway in human failing myocytes via angiotensin II-mediated oxidative stress. *Diabetes*. 2005;54:394-401.

325. Huisamen B, van Zyl M, Keyser A, Lochner A. The effects of insulin and beta-adrenergic stimulation on glucose transport, glut 4 and PKB activation in the myocardium of lean and obese non-insulin dependent diabetes mellitus rats. *Mol Cell Biochem*. 2001;223:15-25.

326. Rondinone CM, Carvalho E, Wesslau C, Smith UP. Impaired glucose transport and protein kinase B activation by insulin, but not okadaic acid, in adipocytes from subjects with Type II diabetes mellitus. *Diabetologia*. 1999;42:819-825.

327. Wymann MP, Bulgarelli-Leva G, Zvelebil MJ, Pirola L, Vanhaesebroeck B, Waterfield MD, Panayotou G. Wortmannin inactivates phosphoinositide 3-kinase by covalent modification of Lys-802, a residue involved in the phosphate transfer reaction. *Mol Cell Biol*. 1996;16:1722-1733.

328. Bevan P. Insulin signalling. *J Cell Sci*. 2001;114:1429-1430.

329. Chan TO, Rittenhouse SE, Tsichlis PN. AKT/PKB and other D3 phosphoinositide-regulated kinases: kinase activation by phosphoinositide-dependent phosphorylation. *Annu Rev Biochem*. 1999;68:965-1014.

330. Coffer PJ, Woodgett JR. Molecular cloning and characterisation of a novel putative protein-serine kinase related to the cAMP-dependent and protein kinase C families. *Eur J Biochem*. 1991;201:475-481.

331. Jones PF, Jakubowicz T, Pitossi FJ, Maurer F, Hemmings BA. Molecular cloning and identification of a serine/threonine protein kinase of the second-messenger subfamily. *Proc Natl Acad Sci U S A*. 1991;88:4171-4175.

332. Vanhaesebroeck B, Alessi DR. The PI3K-PDK1 connection: more than just a road to PKB. *Biochem J*. 2000;346 Pt 3:561-576.

333. Alessi DR, Cohen P. Mechanism of activation and function of protein kinase B. *Curr Opin Genet Dev*. 1998;8:55-62.

334. Duan J, Zhang HY, Adkins SD, Ren BH, Norby FL, Zhang X, Benoit JN, Epstein PN, Ren J. Impaired cardiac function and IGF-I response in myocytes from calmodulin-diabetic mice: role of Akt and RhoA. *Am J Physiol Endocrinol Metab*. 2003;284:E366-E376.

335. Lawlor MA, Alessi DR. PKB/Akt: a key mediator of cell proliferation, survival and insulin responses? *J Cell Sci*. 2001;114:2903-2910.

336. Storz P, Doppler H, Wernig A, Pfizenmaier K, Muller G. Cross-talk mechanisms in the development of insulin resistance of skeletal muscle cells palmitate rather than tumour necrosis factor inhibits insulin-dependent protein kinase B (PKB)/Akt stimulation and glucose uptake. *Eur J Biochem*. 1999;266:17-25.

337. Wang H, Zhang Y, Cao L, Han H, Wang J, Yang B, Nattel S, Wang Z. HERG K^+ channel, a regulator of tumor cell apoptosis and proliferation. *Cancer Res*. 2002;62:4843-4848.

338. Diez C, Nestler M, Friedrich U, Vieth M, Stolte M, Hu K, Hoppe J, Simm A. Down-regulation of Akt/PKB in senescent cardiac fibroblasts impairs PDGF-induced cell proliferation. *Cardiovasc Res*. 2001;49:731-740.

339. Dobrzynski E, Montanari D, Agata J, Zhu J, Chao J, Chao L. Adrenomedullin improves cardiac function and prevents renal damage in streptozotocin-induced diabetic rats. *Am J Physiol Endocrinol Metab*. 2002;283:E1291-E1298.

340. Laviola L, Belsanti G, Davalli AM, Napoli R, Perrini S, Weir GC, Giorgino R, Giorgino F. Effects of streptozocin diabetes and diabetes treatment by islet transplantation on in vivo insulin signaling in rat heart. *Diabetes*. 2001;50:2709-2720.

341. Matsui T, Tao J, del Monte F, Lee KH, Li L, Picard M, Force TL, Franke TF, Hajjar RJ, Rosenzweig A. Akt activation preserves cardiac function and prevents injury after transient cardiac ischemia in vivo. *Circulation*. 2001;104:330-335.

342. Miao W, Luo Z, Kitsis RN, Walsh K. Intracoronary, adenovirus-mediated Akt gene transfer in heart limits infarct size following ischemia-reperfusion injury in vivo. *J Mol Cell Cardiol*. 2000;32:2397-2402.

343. Yamashita K, Kajstura J, Discher DJ, Wasserlauf BJ, Bishopric NH, Anversa P, Webster KA. Reperfusion-activated Akt kinase prevents apoptosis in transgenic mouse hearts overexpressing insulin-like growth factor-1. *Circ Res*. 2001;88:609-614.

344. Tokimasa T, Ito M, Simmons MA, Schneider CR, Tanaka T, Nakano T, Akasu T. Inhibition by wortmannin of M-current in bullfrog sympathetic neurones. *Br J Pharmacol*. 1995;114:489-495.

345. Han H, Wang H, Long H, Nattel S, Wang Z. Oxidative preconditioning and apoptosis in L-cells. Roles of protein kinase B and mitogen-activated protein kinases. *J Biol Chem*. 2001;276:26357-26364.

346. Aikawa R, Nawano M, Gu Y, Katagiri H, Asano T, Zhu W, Nagai R, Komuro I. Insulin prevents cardiomyocytes from oxidative stress-induced apoptosis through activation of PI3 kinase/Akt. *Circulation*. 2000;102:2873-2879.

347. Chen HS, Shan YX, Yang TL, Lin HD, Chen JW, Lin SJ, Wang PH. Insulin deficiency downregulated heat shock protein 60 and IGF-1 receptor signaling in diabetic myocardium. *Diabetes*. 2005;54:175-181.

348. Oku A, Nawano M, Ueta K, Fujita T, Umebayashi I, Arakawa K, Kano-Ishihara T, Saito A, Anai M, Funaki M, Kikuchi M, Oka Y, Asano T. Inhibitory effect of hyperglycemia on insulin-induced Akt/protein kinase B activation in skeletal muscle. *Am J Physiol Endocrinol Metab*. 2001;280:E816-E824.

349. Huisamen B. Protein kinase B in the diabetic heart. *Mol Cell Biochem*. 2003;249:31-38.

350. Shizukuda Y, Buttrick PM. Protein kinase C-zeta modulates thromboxane A_2-mediated apoptosis in adult ventricular myocytes via Akt. *Am J Physiol Heart Circ Physiol*. 2002;282:H320-H327.

351. Marzban L, Bhanot S, McNeill JH. In vivo effects of insulin and bis(maltolato)-ovanadium (IV) on PKB activity in the skeletal muscle and liver of diabetic rats. *Mol Cell Biochem*. 2001;223:147-157.

352. Green EA, Flavell RA. Tumor necrosis factor-alpha and the progression of diabetes in non-obese diabetic mice. *Immunol Rev*. 1999;169:11-22.

353. Green EA, Wong FS, Eshima K, Mora C, Flavell RA. Neonatal tumor necrosis factor alpha promotes diabetes in nonobese diabetic mice by CD154-independent antigen presentation to $CD8^+$ T cells. *J Exp Med*. 2000;191:225-238.

354. Saghizadeh M, Ong JM, Garvey WT, Henry RR, Kern PA. The expression of TNF alpha by human muscle. Relationship to insulin resistance. *J Clin Invest*. 1996;97:1111-1116.

355. Moller DE. Potential role of TNF-alpha in the pathogenesis of insulin resistance and type 2 diabetes. *Trends Endocrinol Metab*. 2000;11:212-217.

356. Zhao SP, Zeng LH. Elevated plasma levels of tumor necrosis factor in chronic heart failure with cachexia. *Int J Cardiol*. 1997;58:257-261.

357. Zhao SP, Xu TD. Elevated tumor necrosis factor alpha of blood mononuclear cells in patients with congestive heart failure. *Int J Cardiol*. 1999;71:257-261.

358. Feuerstein GZ. Apoptosis in cardiac diseases--new opportunities for novel therapeutics for heart diseases. *Cardiovasc Drugs Ther*. 1999;13:289-294.

359. Deswal A, Petersen NJ, Feldman AM, Young JB, White BG, Mann DL. Cytokines and cytokine receptors in advanced heart failure: an analysis of the cytokine database from the Vesnarinone trial (VEST). *Circulation*. 2001;103:2055-2059.

360. Soliven B, Szuchet S, Nelson DJ. Tumor necrosis factor inhibits K^+ current expression in cultured oligodendrocytes. *J Membr Biol*. 1991;124:127-137.

361. Vicente R, Coma M, Busquets S, Moore-Carrasco R, Lopez-Soriano FJ, Argiles JM, Felipe A. The systemic inflammatory response is involved in the regulation of K^+ channel expression in brain via TNF-alpha-dependent and -independent pathways. *FEBS Lett.* 2004;572:189-194.

362. Nietsch HH, Roe MW, Fiekers JF, Moore AL, Lidofsky SD. Activation of potassium and chloride channels by tumor necrosis factor alpha. Role in liver cell death. *J Biol Chem.* 2000;275:20556-20561.

363. Malagarie-Cazenave S, Andrieu-Abadie N, Ségui B, ouazé V, ardy C, uvillier O, Levade T. Sphingolipid signalling: molecular basis and role in TNF-α induced cell death. *Exp Rev Mol Med.* 2002;20 December:http://www.expertreviews.org/0200546X.

364. McDonough PM, Yasui K, Betto R, Salviati G, Glembotski CC, Palade PT, Sabbadini RA. Control of cardiac Ca^{2+} levels. Inhibitory actions of sphingosine on Ca^{2+} transients and L-type Ca^{2+} channel conductance. *Circ Res.* 1994;75:981-989.

365. Schreur KD, Liu S. Involvement of ceramide in inhibitory effect of IL-1 beta on L-type Ca^{2+} current in adult rat ventricular myocytes. *Am J Physiol.* 1997;272:H2591-H2598.

366. Sugishita K, Kinugawa K, Shimizu T, Harada K, Matsui H, Takahashi T, Serizawa T, Kohmoto O. Cellular basis for the acute inhibitory effects of IL-6 and TNF- alpha on excitation-contraction coupling. *J Mol Cell Cardiol.* 1999;31:1457-1467.

367. Kiyosue T, Aomine M, Arita M. Lysophosphatidylcholine decreases single channel conductance of inward rectifier K channel in mammalian ventricular myocytes. *Jpn J Physiol.* 1984;34:369-373.

368. Ziolo MT, Sondgeroth KL, Harshbarger CH, Smith JM, Wahler GM. Effects of arrhythmogenic lipid metabolites on the L-type calcium current of diabetic vs. non-diabetic rat hearts. *Mol Cell Biochem.* 2001;220:169-175.

369. Mohamed AK, Bierhaus A, Schiekofer S, Tritschler H, Ziegler R, Nawroth PP. The role of oxidative stress and NF-kappaB activation in late diabetic complications. *Biofactors.* 1999;10:157-167.

370. Giugliano D, Ceriello A, Paolisso G. Diabetes mellitus, hypertension, and cardiovascular disease: which role for oxidative stress? *Metabolism.* 1995;44:363-368.

371. Aydin A, Orhan H, Sayal A, Ozata M, Sahin G, Isimer A. Oxidative stress and nitric oxide related parameters in type II diabetes mellitus: effects of glycemic control. *Clin Biochem*. 2001;34:65-70.

372. Bhatnagar A. Contribution of ATP to oxidative stress-induced changes in action potential of isolated cardiac myocytes. *Am J Physiol*. 1997;272:H1598-H1608.

373. Satoh H, Matsui K. Electrical and mechanical modulations by oxygen-derived free-radical generating systems in guinea-pig heart muscles. *J Pharm Pharmacol*. 1997;49:505-510.

374. Barrington PL, Meier CF, Jr., Weglicki WB. Abnormal electrical activity induced by free radical generating systems in isolated cardiocytes. *J Mol Cell Cardiol*. 1988;20:1163-1178.

375. Aiello EA, Jabr RI, Cole WC. Arrhythmia and delayed recovery of cardiac action potential during reperfusion after ischemia. Role of oxygen radical-induced no-reflow phenomenon. *Circ Res*. 1995;77:153-162.

376. Liu Y, Gutterman DD. Oxidative stress and potassium channel function. *Clin Exp Pharmacol Physiol*. 2002;29:305-311.

377. Xu Z, Patel KP, Lou MF, Rozanski GJ. Up-regulation of K^+ channels in diabetic rat ventricular myocytes by insulin and glutathione. *Cardiovasc Res*. 2002;53:80-88.

378. Escande D, Coulombe A, Faivre JF, Deroubaix E, Coraboeuf E. Two types of transient outward currents in adult human atrial cells. *Am J Physiol*. 1987;252:H142-H148.

379. Kenyon JL, Gibbons WR. 4-Aminopyridine and the early outward current of sheep cardiac Purkinje fibers. *J Gen Physiol*. 1979;73:139-157.

380. Shibata EF, Drury T, Refsum H, Aldrete V, Giles W. Contributions of a transient outward current to repolarization in human atrium. *Am J Physiol*. 1989;257:H1773-H1781.

381. Van Bogaert PP, Snyders DJ. Effects of 4-aminopyridine on inward rectifying and pacemaker currents of cardiac Purkinje fibres. *Pflugers Arch*. 1982;394:230-238.

PART II. ORIGINAL CONTRIBUTIONS

In this part, the working hypothesis and specific objectives of studies are proposed (chapter 2), followed by the results of studies in animal and cellular models, which form 6 manuscripts (chapters 3 to 8). General discussion is addressed in the last chapter.

2 AIMS OF THE STUDIES

This project focused on the ionic and cellular/molecular mechanisms of QT prolongation in IDDM hearts. It is anticipate that the result of this study, at least partially, can be extrapolated in the diabetic QT prolongation in NIDDM.

2.1 Working Hypothesis

Based on the current knowledge of ionic and molecular mechanisms in the diabetic QT prolongation, and the roles of different ion channels (in particular the I_{Kr}/HERG K^+ channel) in governing the action potential duration and the QT interval, we hypothesized that I_{Kr}/I_{HERG} is impaired in IDDM cardiomyocytes; Depression of I_{Kr}/I_{HERG} results from down-regulation of I_{Kr} protein and mRNA expressions, and from negative functional modulation of I_{Kr}/I_{HERG} by metabolic stresses and signaling molecules; The modulation is a net outcome between enhancing and suppressing factors; Impairment of I_{Kr}/I_{HERG} is an important causative factor in QT prolongation and arrhythmogenesis in IDDM subjects; Thus, enhancing I_{Kr}/I_{HERG} by manipulating HERG gene expression and cellular signaling molecules can retard and even reverse, at least partially, the electrical disorders in IDDM hearts.

2.2 Specific Aims of the Project

The overall purpose of this project is to establish the roles of I_{Kr}/I_{HERG} in QT prolongation in IDDM hearts and to decipher the underlying cellular signaling and molecular mechanisms. The ultimate goal of these studies is to provide novel and rational approaches for the treatment of cardiac arrhythmias in DM patients. To reach this goal, the following specific studies will be carried out:

(1) To investigate systemically the remodeling of ion channels in diabetic rabbit hearts (Chapter 3).

(2) To examine whether I_{Kr} function is impaired or its density is reduced in hearts of alloxan-induced diabetic rabbits and if yes, whether I_{Kr} depression correlates to the APD and QT prolongations (Chapters 3 and 4).

(3) To decipher the molecular mechanisms underlying the I_{Kr} depression by studying if HERG expression is down-regulated in diabetic hearts and whether insulin or vitamin E treatment can rescue I_{Kr} functions thus prevent diabetic QT prolongation and the associated arrhythmias (Chapters 3 and 4).

(4) To elucidate the signaling mechanisms for I_{Kr} depression by studying the modulations of I_{Kr} by glucose, insulin, PKB, O^{2-} and antioxidant vitamin E, TNF-α and ceramide, which are actively contributors to diabetic signaling pathways and to cardiac diseases as well (Chapters 5~8).

3 CRITICAL ROLE OF I_{Kr} IN DIABETIC QT PROLONGATION AND THE ASSOCIATED ARRHYTHMIAS

In this study, we established a type I diabetic rabbit model induced by alloxan. IDDM rabbit model was used for this project because reliable diabetes have been demonstrated by other groups, and it has been shown that alloxan-rabbit has significant cardiomyopathy. In addition, the rabbit heart possesses ionic channels akin to that in humans. Moreover, I_{Kr}, which could be a promising contributor to the diabetic QT prolongation, can be reasonably separated from other ion currents in rabbit myocytes; in functional and protein level, rabbit shares many similiarities of I_{Kr} with human, e.g. voltage dependence, pharmacological properties. To simplify the content, we use HERG to describe both human and rabbit I_{Kr} channel protein.

We compared the QT intervals and APDs recorded in diabetic and healthy rabbit hearts. The inward (I_{Na}, I_{CaL}) and outward currents (I_{to}, I_{Kr}, I_{Ks}, I_{K1}) were then studied by patch-clamp, with Western blot analysis on their respective channel proteins. Based on the ionic alterations, simulation using software LabHEART developed by Drs. José L. Puglisi and Donald M. Bers for rabbit ventricular myocytes, was performed to assess the contribution of each ion current to the diabetic APD prolongation.

This manuscript has been submitted to *American Journal of Physiology* for review.

Ionic mechanisms underlying abnormal QT prolongation and the associated arrhythmias in diabetic rabbits: Critical role of rapid delayed rectifier K^+ current

Yiqiang Zhang,[1,2] Huizhen Wang,[1,3]§ Jiening Xiao,[1,4]§ Yunlong Bai,[3,4] Jingxiong Wang,[1,2] Haiqing Zhang,[1]¶ Baofeng Yang,[3,4] and Zhiguo Wang[1,2,4,*]

[1]Research Center, Montreal Heart Institute, Montreal, PQ H1T 1C8 Canada

[2]Department of Medicine, University of Montreal, Montreal, PQ H3C 3J7 Canada

[3]Department of Pharmacology (State-Province Key Laboratory of China), Harbin Medical University, Harbin, Heilongjiang 150086, P.R. China

[4]Institute of Cardiovascular Research, Harbin Medical University, Harbin, Heilongjiang 150086, P.R. China

Short Title: **I_{Kr} and Diabetic QT prolongation**

Subject Codes: [189] [130] [132] [152] [91]

---

§Authors with equal contributions to the present study.

¶Current address: Institute of Parasitology, McGill University, Montreal, PQ H9X 3V9, Canada

***Address correspondence to:** Dr. Zhiguo Wang, Research Center, Montreal Heart Institute, 5000 Belanger East, Montreal, PQ H1T 1C8, Canada; Tel.: (514) 376-3330. Fax: (514) 376-4452. E-mail: [redacted] or Prof. Baofeng Yang, Department of Pharmacology (State-Province key lab of China), Harbin Medical University, Harbin, Heilongjiang 150086, P.R. China. E-mail: [redacted]

3.1 Abstract

Abnormal QT prolongation with associated arrhythmias is considered the major cardiac electrical disorder and the significant predictor of mortality in diabetic patients. The precise ionic mechanisms for diabetic QT prolongation remained unclear. We performed whole-cell patch-clamp studies in the rabbit model of alloxan-induced insulin-dependent diabetes mellitus. We demonstrated that heart rate-corrected QT interval and action potential duration (APD) were prolonged by ~20% with frequent occurrence of ventricular tachyarrhythmias. Several K^+ currents were found decreased in diabetic rabbits including transient outward K^+ current (I_{to}) that was reduced by ~60%, rapid delayed rectifier K^+ current (I_{Kr}) reduced by ~70% and slow delayed rectifier K^+ current (I_{Ks}) reduced by ~40%. The time-dependent kinetics of these currents remained unaltered. The peak amplitude of L-type Ca^{2+} current (I_{CaL}) was reduced by ~22% and the inactivation kinetics was slowed. The integration of these two effects yielded ~15% reduction of total I_{CaL}. The inward rectifier K^+ current (I_{K1}) and fast sodium current (I_{Na}) were unaffected. Simulation with LabHEART, a computer model of rabbit ventricular action potnetials, revealed that inhibition of I_{to} or I_{Ks} alone fails to alter APD whereas inhibition of I_{Kr} alone results in 30% APD prolongation and inhibition of I_{CaL} alone causes 10% APD shortening. Integration of changes of all these currents leads to ~20% APD lengthening. Protein levels of the pore-forming subunits for these ion channels were decreased to varying extents, as revealed by immunoblotting analysis. Our study represents the first documentation of I_{Kr} channelopathy as the major ionic mechanism for diabetic QT prolongation.

Keywords: diabetes; QT prolongation; arrhythmias; ion currents.

3.2 Introduction

The most prominent cardiac electrical disturbance in diabetic mellitus (DM) is the abnormality of QT interval. When QT interval is corrected for heart rate (QTc), values longer than 440 ms are considered abnormal, and this limiting value is commonly exceeded in diabetic patients. A prolongation of the QT interval has been associated with an increased risk of sudden cardiac death in patients with diabetes due to occurrence of lethal ventricular arrhythmias known as *Torsade de Pointes* or long QT syndrome (LQTS) (1, 3, 5, 6, 8, 11, 18, 20, 30, 35, 37, 39, 53, 59-62). Particularly noticeable is that in recent years there has been increasing incidences of the appearance of ECG disorders with no association between QT alterations and neuropathy, micro- or macro-vascular diseases, cardiovascular drugs, age or gender, being these situations additional risk factors (44,59). LQTS occurs in both insulin-dependent type I (IDDM) and insulin-independent type II DM (NIDDM) patients and the prevalence is as high as some 25%. Indeed, QT prolongation has been suggested as the predictor of mortality in both IDDM and NIDDM (4, 11, 37, 44, 59-62).

QT interval reflects the total duration of ventricular depolarization and repolarization or integrated action potential duration (APD) of heart cells. Cardiac APD is determined by the rate of membrane repolarization which is governed by delicate balance between inward and outward ion currents. Increase in inward currents and/or decrease in outward currents tend to prolong APD thereby QT interval. L-type of Ca^{2+} current (I_{CaL}) is the key inward current responsible for maintaining membrane depolarization or the duration of plateau phase (31). The fast Na^{+} current ($I_{Na,}$) is mainly responsible for the initial upstroke of an AP, but its sustained component and the window current resulted from overlapping of activation and inactivation can contribute to the length of plateau phase (69). The outward currents in a ventricular myocyte include a number of K^{+} channels that are of critical importance in determining cardiac repolarization thereby QT interval. They are transient outward K^{+} current (I_{to}) (70) rapid delayed rectifier K^{+} current (I_{Kr}) (24,42,43,71), slow delayed rectifier K^{+} current (I_{Ks}) (24,41-43) and inward rectifier K^{+} current (I_{K1}) (75). I_{to} is mainly responsible for the initial (phase 1) rapid membrane repolarization, due to its rapidly activating and inactivating properties. Moreover, I_{to} also has indirect impacts on APD by setting the time-voltage trajectory for the activation of subsequent ion currents in line. I_{Kr} is a key repolarizing current responsible for terminating phase 2 plateau and initiating phase 3

repolarization in cardiac cells of many species such as human (24,42,71,72) and rabbit (15,17, 25,27,40,55,58,63). Human *ether-a-go-go* related gene (*HERG*) is the pore-forming α-subunit of I_{Kr} and is well recognized as the molecular target for mutations and pharmacological target for drug actions that generate inherited and acquired LQTS, respectively. The slow component of delayed rectifier K^+ current (I_{Ks}) regulates only the late phase repolarization owing to its slow activation kinetics (41,43). Inward rectifier K^+ current (I_{K1}) contributes to the final phase of repolarization (21,75).

The roles of several of above mentioned ion currents in diabetic APD/QT prolongation have been studies with experimental animal models. I_{to} and I_{ss} (steady-state outward K^+ current) were found reduced in IDDM animals in most studies (14,28,46,48,56,64) and unaltered in others (38). I_{K1} was found unchanged in IDDM (28,47,49), excluding the contribution of I_{K1} to the APD prolongation in these animal models of diabetes. I_{CaL} was found smaller in IDMM in some studies (10,64) but unaltered in other studies (14,57). I_{Na} was also found to be decreased (9). These studies contribute significantly to our current understanding of the ionic mechanisms for diabetic QT prolongation, but several important issues remained unresolved. First, previous studies were conducted nearly exclusively in rats and mice, the species in their adulthood not expressing phenotypic and physiologically significant I_{Kr} and I_{Ks} that are otherwise the major repolarizing current determining the plateau phase and total APD in humans. Second, inhibition of I_{to}, though expected to lengthen APD, has been shown to paradoxically shorten APD in many species such as humans and rabbits (12,19,52,74). Third, I_{ss} or the equivalent has not been thus far identified in ventricular cells from species other than rats and mice, such as humans, canines, rabbits, guinea pigs and other I_{Kr}/I_{Ks}-bearing species. Therefore, its physiological function and pathological role in diabetic QT prolongation remain questionable. Finally, reduction of I_{CaL} and I_{Na} in diabetic hearts should, if anything, shorten, but not lengthen APD/QT interval. Obviously, our understanding of the ionic mechanisms underlying diabetic QT prolongation is still far from complete and there is an urgent need for further investigations into the issue in an animal model that possesses a similar set of ion current components as humans. This study was designed (1) to have an overall picture of alterations of ion currents/channels in diabetic hearts under identical or similar experimental conditions in rabbit model of diabetes, a species that possesses similar profiles of ion currents as humans and (2) to dissect the relative contribution of these ion

currents/channels in diabetic QT/APD prolongation and to shed some light on the potential underlying mechanisms.

3.3 Methods

3.3.1 Preparation of rabbit model of type I insulin-dependent diabetes mellitus

Male New Zealand white rabbits weighing 1.6~2.0 Kg (Charles River Canada Inc) were housed individually in stainless steel wire-bottomed cages in a room with a 12:12-hrs light-dark cycle with standard laboratory rabbit chow and drinking water *ad libitum*. The animals were randomly assigned to control (Ctl) and IDDM groups. To establish diabetes, a single injection of 140 mg/kg (body weight) of pre-warmed (37°C) alloxan monohydrate (Sigma-Aldrich) was administrated via marginal ear vein under local anesthesia. Alloxan was freshly dissolved in saline at a concentration of 100 mg/ml. To prevent fatal hypoglycemia from massive insulin release, 10% glucose solution (100 mg/kg, s.c.) was administered 4 and 6 hrs after alloxan treatment. The blood was collected via marginal ear vein after local anesthesia for determining the plasma level of glucose with a glucometer (TheraSense, USA) and the insulin level with colorimetric assay and radioimmunoassay in non-anesthetized rabbits before and 2-3 days after alloxan injection, and the blood glucose level was monitored weekly thereafter till 10 weeks. Only those animals with serum glucose concentrations ≥15 mM were considered diabetic and were used for further studies. All procedures were in accordance with the guidelines set by the Animal Ethics Committee of the Montreal Heart Institute.

3.3.2 Implantation of telemeters and ECG recording in conscious rabbits

Rabbits were anesthetized with ketamine (Vetalar®, BioNiche Animal Health Canada, Belleville, Ontario) and xylazine (Rompun®, Bayer Inc, Toronto, Ontario) mixture (7:1) at a dosage of 1.2 ml/3 Kg (i.m.). Abdominal hair was shaved and skin was cleaned and sterilized with antiseptic. A small incision was then made on the skin for subcutaneous implantation of ECG telemeter (EMKA Technologie, Paris, France) and the probes of the telemeter were fixed to the right and left underarm positions. Antibiotic cream (Polytopic®, Sabex Inc, Boucherville, QC, Canada) was applied to the closed skin wounds followed by adherent surgical dressing. Bondages were then used to protect the wounds. Antibiotic solution (0.5 ml, Longisil®, Vétoquinol N.-A. Inc) containing penicillin G benzathine (150,000 IU/ml) and penicillin G

procaine (150,000 IU/ml) was applied i.m. daily for 5 days after the surgery. Seven days after implantation, the transducer was activated to record the real-time ECG in conscious rabbits before induction of diabetes as the basal measurement. The ECG signal was acquired and analyzed by the EMKA Technilogies's IOX acquisition software and ECG-Auto, respectively. ECG was monitored continuously for 24 hrs immediately after treatment with alloxan. From day 2 after alloxan treatment, ECG was recorded for 20 min at an interval of every 3 hrs. ECG recorded in this way is equivalent to the standard lead II ECG.

3.3.3 *Isolation of rabbit ventricular myocytes*

Myocytes were isolated from rabbit left ventricular endocardium via enzymatic digestion with the procedures similar to previously described (73). Rabbits were anesthetized by sodium pentobarbital (60 mg/kg, i.v.). Hearts were rapidly excised and mounted on a Langendorff apparatus and perfused retrogradely with the following four solutions in sequential order: 1 mM Ca^{2+} Tyrode (2 min), Ca^{2+}-free Tyrode (3-5 min), Ca^{2+}-free Tyrode containing collagenase (Worthington type II) for 25-35 min. The left ventricular wall was shaved to obtain endocardial layer and the samples were minced in KB solution and filtered. The freshly isolated myocytes were gently centrifuged and resuspended in either KB solution for patch-clamp studies. KB solution for cell storage contained (mM): 20 KCl, 10 KH_2PO_4, 25 glucose, 70 K-glutamate, 5 β-hydroxybutyric acid, 20 taurine, EGTA, 40 mannitol, and 0.1% albumin (pH 7.4).

3.3.4 *Whole-cell patch-clamp recording*

Patch-clamp techniques have been described in detail elsewhere (66-68, 70-77). Currents were recorded with whole-cell voltage-clamp and action potentials (APs) were recorded with current-clamp, with an Axopatch-200B amplifier (Axon Instruments). Borosilicate glass electrodes had tip resistances of 1-3 MΩ when filled with the internal pipette solution. The pipette solution for I_{to} and I_{K1} recording contained (mM): 130 KCl, 1 $MgCl_2$, 5 Mg-ATP, 10 EGTA, and 10 HEPES (pH adjusted to 7.25 with KOH). The pipette solution used for recording I_{Na} contained (mM) 135 CsF, 5 NaCl, 10 EGTA and 5 Mg-ATP, 5 HEPES, and that for I_{CaL} contained (mM): 20 CsCl, 110 Cesium aspartate, 1 $MgCl_2$, 5 Mg-ATP, 10 EGTA, and 10 HEPES (pH 7.25 with CsOH). The internal pipette solution for AP recording contained same components as for K^+ currents recording, except that EGTA was 0.05 mM. The extracellular

(normal Tyrode's) solution for I_{to} and I_{K1} currents and AP recording contained (mM): 136 NaCl, 5.4 KCl, 1 $CaCl_2$, 1 $MgCl_2$, 5 glucose, and 10 HEPES (pH 7.4 with NaOH). The extracellular solutions used for recording I_{Na} contained (mM) 132.5 CsCl, 5.0 NaCl, 1.0 $MgCl_2$, 1.0 $CaCl_2$, 11 glucose, and 10 HEPES. For I_{CaL} recordings, the solution contained (mM): 136 TEA-Cl, 5.4 CsCl, 1 $CaCl_2$, 1 $MgCl_2$, 5 glucose, and 10 HEPES (pH adjusted to 7.25 with CsOH). For I_K recordings, the superfusate was changed to an NMG solution composed of the following (in mM): 149 N-methyl-D-glucamine, 5 $MgCl_2$, 0.9 $CaCl_2$, and 5 HEPES (pH adjusted to 7.4 with HCl). In addition to the use of different solutions for optimize the recordings of the currents of interest and for avoiding unwanted currents, ion channel blockers were also used to prevent the contaminating currents. For studies on K^+ currents, I_{Na} was inactivated by holding the membrane at -50 mV and I_{CaL} was blocked by $CdCl_2$ 200 μM in the bathing solution. 4-aminopyridine (1 mM) was used to inhibit I_{to} for recording other currents and glyburide (10 mM) plus Mg-ATP (5 mM) in the pipette solution to prevent ATP-sensitive K^+ current. Dofetilide (1 μM) and HMR1556 (1 μM) (Aventis) were used to separate I_{Kr} and I_{Ks}, respectively. Experiments were conducted at 36 ± 1°C except that I_{Na} was recorded at 18 ± 1°C. Junction potentials were zeroed before formation of the membrane-pipette seal. Series resistance and capacitance were compensated and leak currents were subtracted.

The voltage protocols for current recordings are shown in the insets of the respective figures. Since group comparisons of experimental results were made for our data analysis, the currents were all recorded immediately after membrane rupture and series resistance compensation in order to minimize the possible time-dependent rundown, run-up, or negative shift of currents. Individual currents were normalized to the membrane capacity to control for differences in cell size, being expressed as current density pA/pF. The amplitude of I_{to} was measured as the difference between the initial peak of I_{to} and the current level remaining at the end of the pulse. I_{K1} was measured as the magnitude of the current at the end of the pulse relative to zero reference. I_{Kr} was expressed as dofetilide-sensitive currents by subtracting the currents recorded 10 min after dofetilide (1 μM) from the baseline currents before dofetilide. I_{Ks} was taken as dofetilide-resistant currents. The amplitude of I_{Kr} and I_{Ks} was measured from both step currents at various test potentials (the difference between the current level at the end of the pulse and zero level) and tail currents (the difference between the peak tail current and zero level) at a repolarizing potential of -40 mV for I_{Kr} or at -20 mV for I_{Ks}. The amplitude of I_{CaL} and I_{Na} was

measured as the difference between the peak inward currents and the currents remaining at the end of the pulse.

3.3.5 Western blot

The membrane protein samples were extracted from rabbit ventricles for immunoblotting analysis of ion channel proteins, with the procedures essentially the same as described in detail elsewhere (65). The protein content was determined with Bio-Rad Protein Assay Kit (Bio-Rad, Mississauga, ON) using bovine serum albumin as the standard.

Membrane protein sample (~150 μg) was fractionated by SDS-PAGE (7.5%-10% polyacrylamide gels) and transferred to PVDF membrane (Millipore, Bedford, MA). The sample was incubated overnight at 4°C with the primary antibodies in 1:50~1:200. Affinity purified polyclonal primary antibodies against C-termini of human SCN5A (the pore-forming α-subunit of I_{Na}), $Ca_v1.2$ (for the α_{1c} subunit of I_{CaL}), Kv4.3 (the pore-forming α -subunit of I_{to}), Kir2.1 (for I_{K1}), HERG (the pore-forming α -subunit of I_{Kr}), or KCNQ1 (KvLQT1, the pore-forming α-subunit of I_{Ks}), and N-terminus of KCNE1 (minK, the β-subunit of I_{Ks}), were raised in goat. HERG is used for rbERG throughout the manuscript for simplicity as the amino sequences of them are mostly identical. Inhibitory peptide for each antibody was used to test the antibody specificity. Next day, the membrane was washed in TTBS three times (10 min/each) and incubated for 2 hrs with the HRP-conjugated donkey anti-goat IgG (H+L) (1:600) in the blocking buffer. Both primary and secondary antibodies were purchased from Santa Cruz Biotechnology (Santa Cruz, CA). Bound antibodies were detected using the chemiluminescent substrate (Western Blot Chemiluminescence Reagent Plus, NEN Life Science Products, Boston, USA). GAPDH was used as an internal control for equal input of protein samples, using anti-GAPDH antibody purchased from RDI (Flanders, NJ). Coomassie staining was also performed to verify the sample quantity. Western blot bands were quantified using QuantityOne software by measuring the band intensity (Area x OD) for each group and normalizing to GAPDH. The results are expressed as fold changes by normalizing the data to the control values.

3.3.6 Data analysis

Group data are expressed as mean ± S.E. Statistical comparisons (performed using ANOVA followed by Dunnett's method) were carried out using Microsoft Excel. A two-tailed

$p< 0.05$ was taken to indicate a statistically significant difference. Nonlinear least square curve fitting was performed with CLAMPFIT in pCLAMP 8.0 or GraphPad Prism.

3.4 Results

3.4.1 Diabetic QT prolongation and the associated arrhythmias

A total of 55 rabbits were used in this study, among which 22 were in the control group, and 33 in the IDDM group. Twenty-nine out of 33 rabbits (38/42, 91%) developed typical characteristics of type I diabetes 12-24 hrs after single injection of alloxan, as indicated by the elevated non-fasting blood glucose level (22.6 ± 1.1 mM) as compared with the normal value (5.4 ± 0.7 mM) in age-matched healthy animals and by the reduced plasma insulin level. The induced IDDM stabilized from day 3 after the onset and lasted for at least 10 weeks (the maximum period of our experiments). Four of 33 rabbits of IDDM group (4/33, 12%) were resistant to the alloxan treatment, either failed to develop diabetes (blood glucose <12 mM) or recovered from diabetes shortly after the onset. In addition, among the 29 IDDM rabbits, 10 died before complete data collection. Treatment of the IDDM rabbits with insulin partially but significantly corrected high blood glucose.

Remarkably, QT interval and heart rate-corrected QT interval (QTc interval) were consistently prolonged in rabbits after treatment with alloxan (188 ± 5 ms) for 10 weeks compared with the baseline values obtained before treatment (155 ± 2 ms, $p<0.05$, $n=19$), but not in healthy animals (159 ± 3 ms for baseline vs. 158 ± 4 ms for time-matched comparison). These data indicate a 21% prolongation of QTc interval in the IDDM rabbits over the age-matched healthy animals. Also noticeable is that in the rabbits that failed to develop IDDM, their QTc interval was normal (167 ± 3 ms) and comparable to that of control rabbits ($p>0.05$). The QTc data are shown in Figure 1A. In the present study, the heart rate of diabetic rabbits (205 ± 6 bpm) was only slightly slower than that of the age-matched healthy ones (211 ± 8 bpm, $p>0.05$).

Excessive QTc prolongation creates the substrates for arrhythmogenesis. This was indeed demonstrated in our experiments with the IDDM rabbits. As depicted in Figure 1B, arrhythmias, mainly of ventricular tachycardia (VT), occurred frequently in the IDDM rabbits, which was otherwise absent in healthy animals. Of the 19 IDDM rabbits used for data analyses, 12 developed VT (12/19, 63%). The VT often predisposed to ventricular fibrillation (VF) leading to

sudden death. We were able to record ECG with telemetry from 4 out of 10 rabbits right before they died five days after development of IDDM. The ECG clearly showed runs of polymorphic VT and VF.

To delineate the cellular mechanism underlying the QTc prolongation in our IDDM model, single cell action potentials (APs) were recorded in enzymetically dispersed myocytes from left ventricular endocardium. As illustrated in Figure 1C and 1D, APD at 50% repolarization (APD_{50}) and 90% repolarization (APD_{90}) was approximately 35% and 24%, respectively, longer in IDDM than in healthy subjects, which are somewhat longer than the 21% lengthening of QTc interval.

3.4.2 Functional alterations of cardiac ion currents in diabetic hearts

To unravel the changes of ion currents that may account for the QTc/APD prolongation and the associated arrhythmias in our IDDM animals, we performed whole-cell patch-clamp studies of the ion currents operating under physiological conditions in ventricular myocytes, including I_{to}, I_{K1}, I_{Kr}, I_{Ks}, I_{CaL} and I_{Na}. Our results revealed reduction of multiple ion currents (I_{to}, I_{Kr}, I_{Ks}, and I_{CaL}) in cells isolated from IDDM rabbits, compared with healthy rabbits.

I_{to} current density was approximately 60% smaller in diabetic myocytes than in control ones and similar percentage of reduction was seen at all test potentials ranging from -40 mV to +60 mV (Fig. 2A). The activation and inactivation kinetics remained unaltered (data not shown).

I_{K1} current density was found to be smaller in IDDM myocytes only at non-physiological potentials negative to -90 mV and no difference was seen at potential between -90 mV and +10 mV, where I_{K1} channels conduct outward currents (the inset of Fig. 2B).

I_{Kr} was substantially depressed in IDDM cells, as illustrated in Figure 2C. Intriguingly, the depression of I_{Kr} appears to be inversely voltage-dependent with greater reduction at more negative potentials. For instance, at -40 mV I_{Kr} was some 80% smaller in IDDM than in control animals, whereas at +10 mV, I_{Kr} was only 60% smaller in IDDM than in control animals. The steady-state voltage-dependent activation property of I_{Kr} was not changed and the kinetics of I_{Kr} did not seem to differ between control and IDDM either (data not shown).

I_{Ks} was also reduced in IDDM rabbits relative to healthy control animals (Fig. 2D), but to a much less extent compared to I_{Kr}. Similar to other K^+ currents, the gating properties of I_{Ks} were unaltered by pathological conditions of IDDM.

I_{CaL} was also reduced in IDDM hearts, albeit to a smaller extent compared to the K^+ currents described above. The reduction was voltage-independent with around 20% decreases at potentials ranging from -40 mV to +50 mV. Noticeably, the inactivation process of I_{CaL} was moderately but significantly slowed in IDDM, relative to control, myocytes (Fig. 3A). For example, at +10 mV the inactivation time constant, obtained by the mono-exponential fit to the decaying phase of I_{CaL}, was 29.0 ± 1.2 ms (n=5 cells) for control myocytes and 24.0 ± 1.3 ms (n=7 cells) for IDDM myocytes ($p<0.05$). Since slowing of I_{CaL} inactivation tends to increase Ca^{2+} entry through the channels so as to counteract the reduction of I_{CaL} amplitude, we calculated the total Ca^{2+} current by integrating the area under I_{CaL} traces at 0 and +10 mV in order to better quantify the changes of I_{CaL} (Fig. 3A). In this way, we found that I_{CaL} was reduced by ~15% in IDDM hearts.

I_{Na} density, by comparison, was not significantly changed by the pathological process of IDDM (Fig. 3B), neither was the inactivation kinetics (Data not shown).

3.4.3 Relative contributions of various ion currents to APD lengthening in IDDM

To estimate the relative contributions of various ion currents to diabetic QTc/APD prolongation, we performed the following analyses. First, we compared the relative changes of the ion currents that demonstrated differences between IDDM and control cells at the selected test potentials: +10 mV and -40 mV. The voltage of +10 mV was chosen for it roughly represents the phase 2 plateau level, and -40 mV was chosen because this potential falls roughly into the middle of phase 3 repolarization, of a rabbit ventricular AP. As illustrated in Figure 4A and 4B, at +10 mV the current densities of I_{to}, I_{Kr} and I_{Ks} are within the same range, around 1.5 pA/pF, and the degrees of depression of I_{to} and I_{Kr} in IDDM cells are also quite comparable (around 60%) and I_{Ks} was decreased by approximately 37%. At the same potential, I_{CaL} density (4.2 pA/pF) is roughly the sum of the three K^+ currents mentioned above and the reduction of I_{CaL} density was around 15% when the slowing of inactivation was taken into consideration. Evidently, the total decreases in K^+ currents were much greater than the decrease in I_{CaL} at +10 mV, which is expected to result in net lengthening of the plateau phase or APD_{50}. At -40 mV, the overall density of all currents studied was considerably smaller than at +10 mV; for I_{Ks} -10 mV was used for analysis because I_{Ks} was minimal at -40 mV. Among the various ion currents, I_{Kr} density was the greatest and more importantly, I_{Kr} depression in IDDM cells was also to the

greatest extent, ~80%. By comparison, the reduction of I_{Ks} at -10 mV was smaller than at +10 mV (~27% at -10 mV vs. 37% at +10mV). Decreases in I_{to} and I_{CaL} at -40 mV were to a similar degree as at +10 mV, ~60% and 23%, respectively. Obviously, the total reduction of outward K^+ currents tremendously exceeded that of inward currents, and slowing of phase 3 repolarization is expected; hence, decrease in I_{Kr} seems to be the major contributor.

To go further insight into the above analysis, we investigated the changes of APD by simulation of AP with LabHEART, an interactive computer model designed for ion channels rabbit ventricular myocyte (33). The model allows us the opportunity for predicting changes of APD based on the changes of ion currents, simply by inputting the percent changes of each individual current or of any combinations of different currents. In this way, we were able to obtain the predicted APs as shown in Figure 4C. Reduction of I_{to} (60%) alone hardly changes APD. 40% decrease in I_{Ks} fails to alter APD either. I_{Kr} suppression by 70% (roughly the average between 60% and 80% at +10 mV and -40 mV, respectively), however, produces remarkable lengthening (~30%) of APD_{50} and APD_{90}. In contrast, depression of I_{CaL} by only 22% results in the abbreviation of APD (changes of I_{CaL} amplitude, instead of the integrated area, was used for maximum effect), approximately 10% shortening of APD_{50} and APD_{90}. APD prolongation caused by I_{Kr} inhibition and APD shortening caused by I_{CaL} inhibition should partially cancel out each other. This was indeed verified when changes of all currents were incorporated into simulation; APD was less prolonged than when only I_{Kr} was taken into account: APD_{50} was lengthened by 19% and APD_{90} by 23%.

3.4.4 Altered protein levels of various ion channel subunits

To investigate whether the reduced densities of the ion currents tested in our experiments was due to decreases in expression levels of the responsible channel proteins, we went on to carry out Western blot analysis and the results are depicted in Figure 5. Kv4.3 (75 kDa), the major pore-forming α-subunit of I_{to} in humans and rabbits (70), was reduced by ~30% in IDDM rabbits. Kir2.1 (110 kDa), the major component of the inward rectifier K^+ channels I_{K1} (75), remained unchanged in IDDM hearts. HERG, the pore-forming α-subunit of I_{Kr} (42), demonstrated two discrete bands with molecular mass of 155 kDa and 135 kDa, respectively. The former represents the N-glycosylated form and the latter is non-N-glycosylated portion of the channels. The N-glycosylated HERG was reduced by around 45% and the non-N-

glycosylated HERG was reduced by some 55%, in IDDM relative to healthy rabbits. Unexpectedly, KvLQT1 (80 kDa), the pore-forming α-subunit of I_{Ks} (41), decreased by approximately 25% in IDDM hearts. Moreover, minK (14 kDa), the auxiliary β-subunit of KvLQT1, decreased by as high as 85%. The pore-forming α_{1c}-subunit of I_{CaL} $Ca_v1.2$ (210 kDa) was reduced by some 15%. No difference was found for $Na_v1.5$ (200 kDa), the α-subunit of cardiac I_{Na} (54) between IDDM and healthy hearts (Fig. 6).

3.5 Discussion

Here we report the study on the electrical disturbances in the rabbit model of type I diabetes (IDDM) and the related ionic and molecular alterations as possible mechanisms. The diabetic animals had abnormal QT prolongation and high incidence of ventricular tachyarrhythmias, resembling the clinical observations with diabetic patients. Our study revealed alterations of multiple ion currents/channels in IDDM hearts. While some of the results reproduced the observations from previous studies by other laboratories, several novel findings are documented in the present study. First, this is the first published study thus far to take I_{Kr} and I_{Ks} into account for the diabetic QT prolongation and the associated arrhythmias. Second, our study is also the first to evaluate the relative contributions of various ion currents to the diabetic APD lengthening under identical or similar experimental conditions. Finally, I_{Kr}/HERG K^+ channel dysfunction in diabetic heart is caused by functional impairment and expression down-regulation. Our study suggests that diabetic QT prolongation results from dysfunction of multiple ion currents/channels and depression of I_{Kr}/HERG is the major ionic contributor.

3.5.1 Dysfunction of I_{Kr}/HERG as the major ionic mechanism for diabetic QT prolongation and the associated arrhythmias

Here we demonstrated remarkable depression of I_{Kr} and I_{Ks} in IDDM animals, in addition to depression of I_{to} and I_{CaL} as already known, which has not been previously reported in the literature. In agreement with the functional depression, the protein levels of HERG and KvLQT1/minK were also significantly reduced. These findings open up an opportunity for evaluating the relative contributions of the alterations of all these ion currents to diabetic QT/APD prolongation. We used the LabHEART computer model written for rabbit ventricular

myocytes (33) to address the issue. With the simulation, we showed that 60% reduction of I_{to} alone does not produce any visible alterations of APD. This is not surprising for direct demonstration of I_{to} inhibition causing LQTS has been missing to date, particularly in the clinical settings (52). While inhibition of I_{to} indeed can result in APD prolongation in species devoid of I_{Kr} such as rats and mice, it paradoxically shortens APD in the species expressing I_{Kr} like humans and rabbits (12,19,52,74). This phenomenon is commonly interpreted as such that depression of I_{to} elevates the plateau level so as to set the membrane potential to the levels favoring greater activation of I_{Kr} and disfavoring I_{CaL} (at potentials positive to 0 mV, I_{CaL} amplitude is smaller and I_{CaL} inactivation is faster), leading to a briefer APD. Furthermore, a recent elegant study with dynamic clamp techniques provides convincing experimental data and persuading theoretical reasoning for APD shortening as a result of I_{to} inhibition in canine myocytes (52). Therefore, the finding that depression of I_{to} accounts for QT prolongation in diabetic rats and mice may not be directly extrapolated to humans or other I_{Kr}-bearing species like dogs and rabbits.

Most prominently, I_{Kr} was found decreased by around 70% in our study and this depression alone theoretically causes some 30% lengthening of rabbit APD based on the simulation with the LabHEART model (33). This is expected based on our current understanding of the role of I_{Kr} in cardiac repolarization. I_{Kr} is known to be a critical repolarizing current in cardiac myocytes and the drugs which produce acquired LQTS nearly exclusively target I_{Kr} or HERG K^+ channel, the major molecular composition of I_{Kr}. However, the potential role of I_{Kr} in diabetic QT prolongation has somehow been overlooked, mainly owing to the use of animal species lacking of I_{Kr} for studying diabetic electrophysiology.

Depression of I_{Ks} alone by 40% fails to alter rabbit ventricular APD either. This is also understandable since I_{Ks} has been believed to have limited role in cardiac repolarization under physiological conditions, presumably due to its strong depolarization requirement for activation and slow activation kinetics. I_{Ks} also has the potential to contribute to diabetic APD/QT prolongation although it has limited role in cardiac repolarization under physiologic conditions. I_{Ks} acts as repolarization reserve to limit excess slowing of repolarization (16,36), and when it is depressed this safety factor is removed so that inhibition of other repolarizing current such as I_{Kr} could lead to more pronounced APD/QT prolongation.

Our study demonstrates that I_{CaL} decreases in its current density and slows in its inactivation kinetics in diabetic rabbits. While the former is expected to shorten APD, the latter

tends to lengthen it. To take both factors into account, we analyzed the areas under the I_{CaL} traces to estimate the amount of Ca^{2+} movement across the membrane and this yielded ~15% decrease in I_{CaL}. This reduction alone predicts, by the LabHEART model, <10% shortening of rabbit APD. This is consistent with the role of I_{CaL} in determining the plateau phase of cardiac myocytes.

The combinational account of the altered ion currents in our IDDM rabbits yielded approximately 20% lengthening of APD.

Taken together all these data along with previous studies, there is hardly any doubt that dysfunction of I_{Kr}/HERG is an important ionic pathway for the lengthening of APD/QT in diabetic subjects. The prolongation of APD/QT due to dysfunction of I_{Kr}/HERG and other K^+ currents causes the cell to remain longer at the depolarized plateau phase. During this long plateau phase plus the slowing of inactivation of L-type Ca^{2+} channels in IDDM, Ca^{2+} ions have increased probability to enter into the cell leading to prolongation of APD. It is conceivable that this prolongation is offset by the shortening due to reduction of I_{CaL}. Decrease in I_{to} shifts the plateau level to more positive potential that might favor activation of L-type Ca^{2+} channels, indirectly leading to APD lengthening. I_{Ks}, normally acting to limit excessive prolongation of APD, experiences weakened ability to do so when reduced. This would facilitate the prolonging effects of I_{Kr} depression. In a whole, the diabetic QT/APD prolongation in rabbit is primarily the net outcome between lengthening factor of I_{Kr}/HERG depression and the shortening factor of I_{CaL} depression, with indirect but maybe important contributions from I_{to} and I_{Ks} inhibition to favoring the prolongation. Our study represents the first documentation of I_{Kr}/HERG channelopathy as an ionic mechanism for diabetic QT prolongation.

The lack of changes of I_{K1} and I_{Na} is in agreement with the lack of changes in their protein levels and the functional depression of I_{to}, I_{Kr}, I_{Ks} and I_{CaL} is consistent with the decreases in their protein levels. Intriguingly, the degree of reduction at the functional level did not match with the extent of reduction at the protein level, except for I_{CaL}/$Ca_v1.2$ with equivalent decreases in function and protein levels. Specifically, I_{to} and I_{Kr} decreased to a greater extent than Kv4.3 and HERG levels, respectively, whereas, I_{Ks} decreased to a much smaller extent than KvLQT1 and mink protein levels did. The most plausible explanation for the discrepancy is that decrease in the protein level may not be the only cause of the current depression and other factors such as altered cellular environment and metabolic status may well serve to modulate the channel function. We have indeed documented that HERG function is critically impaired by

hyperglycemia (76), enhanced oxidative stress (67,68) or accumulation of tumor necrosis factor-alpha (TNF-α) (67) the conditions encountered in diabetic cardiomyopathy.

3.5.2 Potential implications of the findings

In recent years there is increasing evidence of the appearance of ECG disorders with no association between QT prolongation and neuropathy, micro- or macro-vascular diseases, cardiovascular drugs, age or gender, being these situations additional risk factors. Understanding the exact ionic mechanisms for diabetic QT prolongation has become a timely and imperative task of basic scientists in order to develop more rational approaches for the prevention and treatment of electrical disorders and the resultant sudden cardiac death in diabetic patients. The present study revealed that multiple ion currents/channels are involved in the development of QT/APD prolongation in diabetic subjects with the balance between I_{Kr}/HERG and I_{CaL}/$Ca_v1.2$ as the major determinant. Our finding is the first to document I_{Kr}/HERG as the major ionic pathway leading to the abnormal QT prolongation in diabetic hearts. This implies that I_{Kr}/HERG may be the best target for interventions that enhance the channel function and/or expression to shorten or reverse prolonged QT interval. Indeed, several endogenous signaling molecules and metabolites including insulin (unpublished observation), protein kinase B (PKB) (77), phosphatidylinositol-4,5-bisphosphate (PIP2) (2) and lysophosphatidylcholine (66) have been shown to be able to enhance HERG function and protein level. Among these, PKB is of best approach because it is a downstream mediator of the insulin signaling pathway involving glucose metabolism and cell survival and its basal activity is the requirement for the normal function of HERG channels (77). PKB approach will not only enhance HERG function but also suppress apoptotic cell death that is one of the characteristics of diabetic cardiomyopathy. In diabetic hearts, PKB activity and expression were found decreased in many studies, which might be one of the mechanisms leading to enhanced apoptosis, and I_{Kr} depression as well.

3.5.3 Possible limitations of the study

Several issues might limit the clinical application of the results in this study. First, the animal model we used is typical type I insulin-dependent diabetes, and the ionic and metabolic mechanisms for APD/QT prolongation in type II insulin-resistant diabetes may not be exactly the same. In reality, type II diabetes consists of 95% of the total diabetic patients in the clinical

settings. However, APD/QT prolongation observed in type I diabetes is also known to be present at the similar percentage in type II diabetics. Except for the difference between insulin insufficiency and insulin resistance, the basic metabolic perturbations are quite similar between type I and type II diabetes. Hence, it is not unreasonable to believe that I_{Kr}/HERG dysfunction is also the cause for the APD/QT prolongation existing in type II diabetes. Second, our data obtained from rabbits may not be applicable to humans considering the interspecies difference, e.g. the heart rate which may affects the ion channel activities. Nevertheless, our rabbit model reproduces nearly all the phenotypes pertinent to the electrophysiological alterations seen in clinical diabetes. Also important are that rabbit I_{Kr} shares many similarities to human I_{Kr} in term of their biophysical characteristics and pharmacological properties and that rabbit ERG channel sequence (Genbank accession U87513) is highly similar to human ERG, around 93% and 96% homologous at the nucleotide and the amino acid levels, respectively. Even the expression levels of ERG gene under normal conditions are quite comparable between the two species (78). Thus, I_{Kr}/HERG dysfunction in our type I diabetic rabbit model may also exist in diabetic patients.

3.6 Acknowledgement

The authors wish to thank XiaoFan Yang and Marc-Antoine Gillis for excellent technical supports.

This work was supported in part by the Late Marion L. Munro grant from the Canadian Diabetes Association, and the Fonds de la Recherche de l'Institut de Cardiologie de Montreal, awarded to Dr. Z Wang. Dr. Z Wang is a senior research scholar of the Fonds de Recherche en Sante de Quebec and a recipient of Scholarship of Quebec Diabetes Society (2004). Y Zhang is a recipient of Doctoral-Studentship of the Heart and Stroke Foundation of Canada. J Wang was a recipient of Doctoral-Studentship of the Fonds de Recherche en Sante de Quebec.

3.7 References

1. **Abo K, Ishida Y, Yoshida R, Hozumi T, Ueno H, Shiotani H, Matsunaga K, and Kazumi T.** Torsade de pointes in NIDDM with long QT intervals. *Diabetes Care* 19: 1010, 1996.
2. **Bian J, Cui J, and Mcdonald TV.** HERG K^+ channel activity is regulated by changes in phosphatidyl inositol 4,5-bisphosphate. *Circ Res* 89: 1168 1176, 2001.
3. **Brown DW, Giles WH, Greenlund KJ, Valdez R, and Croft JB.** Impaired fasting glucose, diabetes mellitus, and cardiovascular disease risk factors are associated with prolonged QTc duration. Results from the Third National Health and Nutrition Examination Survey. *J Cardiovasc Risk* 8: 227 233, 2001.
4. **Cardoso C, Salles G, Bloch K, Deccache W, and Siqueira-Filho AG.** Clinical determinants of increased QT dispersion in patients with diabetes mellitus. *Int J Cardiol* 79: 253 262, 2001.
5. **Cardoso CR, Salles GF, and Deccache W.** Prognostic value of QT interval parameters in type 2 diabetes mellitus: results of a long-term follow-up prospective study. *J Diabetes Complications* 17: 169 178, 2003.
6. **Cardoso CR, Salles GF, and Deccache W.** QTc interval prolongation is a predictor of future strokes in patients with type 2 diabetes mellitus. *Stroke* 34: 2187 -2194, 2003.
7. **Carlsson L, Abrahamsson C, Andersson B, Duker G, and Schiller-Linhardt G.** Proarrhythmic effects of the class III agent almokalant: importance of infusion rate, QT dispersion, and early afterdepolarisations. *Cardiovasc Res* 27: 2186-2193, 1993.
8. **Casis O, and Echevarria E.** Diabetic cardiomyopathy: electromechanical cellular alterations. *Curr Vasc Pharmacol* 2: 237 248, 2004.
9. **Chattou S, Coulombe A, Diacono J, Le Grand B, John G, and Feuvray D.** Slowly inactivating component of sodium current in ventricular myocytes is decreased by diabetes and partially inhibited by known Na^+-H^+ exchange blockers. *J Mol Cell Cardiol* 32: 1181-1192, 2000.

10. **Chattou S, Diacono J, and Feuvray D.** Decrease in sodium-calcium exchange and calcium currents in diabetic rat ventricular myocytes. *Acta Physiol Scand* 166: 137 144, 1999.

11. **Christensen PK, Gall MA, Major-Pedersen A, Sato A, Rossing P, Breum L, Pietersen A, Kastrup J, and Parving HH.** QTc interval length and QT dispersion as predictor of mortality in patients with non-insulin-dependent diabetes. *Scand J Clin Lab Invest* 60: 323 -332, 2000.

12. **Escande D, Coulombe A, Faivre JF, Deroubaix E, and Coraboeuf E.** Two types of transient outward currents in adult human atrial cells. *Am J Physiol* 252: H142-H148, 1987.

13. **Grossmann G, Schwentikowski M, Keck FS, Hoher M, Steinbach G, Osterhues H, and Hombach V.** Signal-averaged electrocardiogram in patients with insulin-dependent (type 1) diabetes mellitus with and without diabetic neuropathy. *Diabet Med* 14: 364 369, 1997.

14. **Jourdon P, and Feuvray D.** Calcium and potassium currents in ventricular myocytes isolated from diabetic rats. *J Physiol* 470: 411 429, 1993.

15. **Howarth FC, Levi AJ, and Hancox JC.** Characteristics of the delayed rectifier K current compared in myocytes isolated from the atrioventricular node and ventricle of the rabbit heart. *Pflugers Arch* 431: 713 722, 1996.

16. **Jost N, Virág L, Bitay M, Takács J, Lengyel C, Biliczki P, Nagy Z, Bogáts G, Lathrop DA, Papp JG, and Varró A.** Restricting excessive cardiac action potential and QT prolongation: a vital role for I_{ks} in human ventricular muscle. *Circulation* 112: 1392-1399, 2005.

17. **Kamiya K, Nishiyama A, Yasui K, Hojo M, Sanguinetti MC, and Kodama I.** Short- and long-term effects of amiodarone on the two components of cardiac delayed rectifier K^+ current. *Circulation* 103: 1317 1324, 2001.

18. **Kahn JK, Sisson JC, and Vinik AI.** QT interval prolongation and sudden cardiac death in diabetic autonomic neuropathy. *J Clin Endocrinol Metab* 64: 751 754, 1987.

19. **Kenyon JL, and Gibbons WR.** 4-Aminopyridine and the early outward current of sheep cardiac Purkinje fibres. *J Gen Phsyiol* 73: 139-157, 1979.

20. **Ko GT, Chan JC, Critchley JA, and Cockram CS.** Cardiovascular disease in Chinese type 2 diabetic women is associated with a prolonged QTc interval. *Int J Cardiol* 76: 75 80, 2000.

21. **Koumi S, Backer CL, and Arentzen CE.** Characterization of inwardly rectifying K^+ channel in human cardiac myocytes: alterations in channel behavior in myocytes isolated from patients with idiopathic dilated cardiomyopathy. *Circulation* 92: 164 174, 1995.

22. **Kowalewski MA, Urban M, Florys B, and Pezcynska J.** Late potentials. Are they related to cardiovascular complications in children with type 1 diabetes? *J Diabet Compl* 16: 263 270, 2002.

23. **Lee SL, Ostadalova I., Kolar F, and Dhalla NS.** Alterations in Ca^{2+}-channels during the development of diabetic cardiomyopathy. *Mol Cell Biochem* 109: 173 179, 1992.

24. **Li GR, Feng J, Yue L, Carrier M, and Nattel S.** Evidence for two components of delayed rectifier K^+ current in human ventricular myocytes. *Circ Res* 78: 689-696, 1996.

25. **Liu XK, Katchman A, Ebert SN, and Woosley RL.** The antiestrogen tamoxifen blocks the delayed rectifier potassium current, I_{Kr}, in rabbit ventricular myocytes. *J Pharmacol Exp Ther* 287: 877 883, 1998.

26. **Lu Y, and Wang Z.** Terfenadine block of sodium current in canine atrial myocytes. *J Cardiovasc Pharmacol* 33: 507-513, 1999.

27. **Lu Z, Kamiya K, Opthof T, Yasui K, and Kodama I.** Density and kinetics of I_{Kr} and I_{Ks} in guinea pig and rabbit ventricular myocytes explain different efficacy of I_{Ks} blockade at high heart rate in guinea pig and rabbit: implications for arrhythmogenesis in humans. *Circulation* 104: 951 956, 2001.

28. **Magyar J, Rusznak Z, Szentesi P, Szucs G, and Kovacs L.** Action potentials and potassium currents in rat ventricular muscle during experimental diabetes. *J Mol Cell Cardiol* 24: 841 -853, 1992.

29. **Nishiyama A, Ishii DN, Backx PH, Pulford BE, Birks BR, and Tamkun MM.** Altered K^+ channel gene expression in diabetic rat ventricle: isoform switching between Kv4.2 and Kv1.4. *Am J Physiol* 281: H1800-H1807, 2001.

30. **Okin PM, Devereux RB, Lee ET, Galloway JM, and Howard BV. Strong Heart Study.** Electrocardiographic repolarization complexity and abnormality predict all-cause

and cardiovascular mortality in diabetes: the strong heart study. *Diabetes* 53: 434 40, 2004.

31. **Pang L, Koren G, Wang Z, and Nattel S.** Tissue-specific expression of two human $Ca_v1.2$ isoforms under the control of distinct 5 -flanking regulatory elements. *FEBS Lett* 546: 349-354, 2003.
32. **Pearson WR, Wood T, Zhang Z, and Miller W.** Comparison of DNA sequences with protein sequences. *Genomics* 46: 24 36, 1997.
33. **Puglisi JL, and Bers DM.** LabHEART: an interactive computer model of rabbit ventricular myocyte ion channels and Ca transport. *Am J Physiol* 281: C2049-2060, 2001.
34. **Qin D, Huang B, Deng L, El-Adawi H, Ganguly K, Sowers JR, and El-Sherif N.** Downregulation of K^+ channel genes expression in type I diabetic cardiomyopathy. *Biochem Biophys Res Commun* 283: 549-553, 2001.
35. **Rana BS, Lim PO, Naas AAO, Ogston SA, Newton RW, Jung RT, Morris AD, and Struthers AD.** QT interval abnormalities are often present at diagnosis in diabetes and are better predictors of cardiac death than ankle brachial pressure index and autonomic function tests. *Heart* 91: 44 50, 2005.
36. **Roden DM, and Yang T.** Protecting the heart against arrhythmias: potassium current physiology and repolarization reserve. *Circulation* 112:1376-1378, 2005.
37. **Rossing P, Breum L, Major-Peteresen A, Sato A, Winding H, Pietersen A, Kastrup J, and Parving HH.** Prolonged QTc interval predicts mortality in patients with type 1 diabetes mellitus. *Diabet Med* 18: 199 205, 2001.
38. **Rusznak Z, Cseresnyes Z, Sipos I, Magyar J, Kovacs L, and Szucs G.** Characteristics of the ventricular transient outward potassium current in genetic rodent models of diabetes. *Gen Physiol Biophys* 15: 225 238, 1996.
39. **Rutter MK, Viswanath S, McComb JM, Kesteven P, and Marshall SM.** QT prolongation in patients with Type 2 diabetes and microalbuminuria. *Clin Auton Res* 12: 366 372, 2002.
40. **Salata JJ, Jurkiewicz NK, Jow B, Folander K, Guinosso PJ Jr, Raynor B, Swanson R, and Fermini B.** I_K of rabbit ventricle is composed of two currents: evidence for I_{Ks}. *Am J Physiol* 271: H2477-H2489, 1996.

41. **Sanguinetti MC, Curran ME, Zou A, Shen J, Spector PS, Atkinson DL, and Keating MT.** Coassembly of K_VLQT1 and minK (IsK) proteins to form cardiac I_{Ks} potassium channel. *Nature* 384: 80 83, 1996.

42. **Sanguinetti MC, Jiang C, Curran ME, and Keating MT.** A mechanistic link between an inherited and an acquired cardiac arrhythmia: HERG encodes the I_{Kr} potassium channel. *Cell* 81: 299-307, 1995.

43. **Sanguinetti MC, and Jurkiewicz NK.** Two components of cardiac delayed rectifier K^+ current. Differential sensitivity to block by class III antiarrhythmic agents. *J Gen Physiol* 96: 195 215, 1990.

44. **Sawicki PT, Dahne R, Bender R, and Berger M.** Prolonged QT interval as a predictor of mortality in diabetic nephropathy. *Diabetologia* 39: 77 81, 1996.

45. **Shi H, Wang H, Han H, Xu D, Yang B, Nattel S, and Wang Z.** Ultrarapid delayed rectifier K^+ current in the myogenic H9c2 cells: biophysical property and molecular identify. *Cell Physiol Biochem* 12: 215-226, 2002.

46. **Shimoni Y.** Inhibition of the formation or action of angiotensin II reverses attenuated K^+ currents in type 1 and type 2 diabetes. *J Physiol* 537: 83 92, 2001.

47. **Shimoni Y, Ewart HS, and Severson D.** Type I and II models of diabetes produce different modifications of K^+ currents in rat heart: role of insulin. *J Physiol* 507: 485 496, 1998.

48. **Shimoni Y, Firek L, Severson D, and Giles W.** Short-term diabetes alters K^+ currents in rat ventricular myocytes. *Circ Res* 74: 620 628, 1994.

49. **Shimoni Y, Light PE, and French RJ.** Altered ATP sensitivity of ATP-dependent K^+ channels in diabetic rat hearts. *Am J Physiol* 275: E568 E576, 1998.

50. **Shiono J, Horigome H, Kamoda T, and Matsui A.** Signal-averaged electrocardiogram in children and adolescents with insulin-dependent diabetes mellitus. *Acta Paediatr* 90: 1244 1248, 2001.

51. **Smith JM, and Wahler GM.** ATP-sensitive potassium channels are altered in ventricular myocytes from diabetic rats. *Mol Cell Biochem* 158: 43 51, 1996.

52. **Sun X, and Wang HS.** Role of the transient outward current (I_{to}) in shaping canine ventricular action potential - a dynamic clamp study. *J Physiol* 564: 411-419, 2005.

53. **Suys BE, Huybrechts, SJ, De Wolf D, Op De Beeck, Matthys D, Van Overmeire B, Du Caju MV, and Rooman RP.** QTc interval prolongation and QTc dispersion in children and adolescents with type 1 diabetes. *J Pediatr* 141: 59 63, 2002.

54. **Szabo G, Szentandrassy N, Biro T, Toth BI, Czifra G, Magyar J, Banyasz T, Varro A, Kovacs L, and Nanasi PP.** Asymmetrical distribution of ion channels in canine and human left-ventricular wall: epicardium versus midmyocardium. *Pflugers Arch* 450: 307-316, 2005.

55. **Toyama J, Kamiya K, Cheng J, Lee JK, Suzuki R, and Kodama I.** Vesnarinone prolongs action potential duration without reverse frequency dependence in rabbit ventricular muscle by blocking the delayed rectifier K^+ current. *Circulation* 96: 3696 3703, 1997.

56. **Tsuchida K, and Watajima H.** Potassium currents in ventricular myocytes from genetically diabetic rats. *Am J Physiol* 273: E695 E700, 1997.

57. **Tsuchida K, Watajima H, and Otomo S.** Calcium current in rat diabetic ventricular myocytes. *Am J Physiol* 267: H2280 H2289, 1994.

58. **Tsuji Y, Opthof T, Yasui K, Inden Y, Takemura H, Niwa N, Lu Z, Lee JK, Honjo H, Kamiya K, and Kodama I.** Ionic mechanisms of acquired QT prolongation and torsades de pointes in rabbits with chronic complete atrioventricular block. *Circulation* 106: 2012 2018, 2002.

59. **Veglio M, Borra M, Stevens LK, Fuller JH, and Perin PC.** The relation between QTc interval prolongation and diabetic complications. The EURODIAB IDDM Complication Study Group. *Diabetologia* 42: 68 75, 1999.

60. **Veglio M, Sivieri R, Chinaglia A, Scaglione L, and Cavallo-Perin P.** QT interval prolongation and mortality in type 1 diabetic patients: a 5-year cohort prospective study. Neuropathy Study Group of the Italian Society of the Study of Diabetes, Piemonte Affiliate. *Diabetes Care* 23: 1381 1383, 2000.

61. **Veglio M, Bruno G, Borra M, Macchia G, Bargero G, D'Errico N, Pagano GF, and Cavallo-Perin P.** Prevalence of increased QT interval duration and dispersion in type 2 diabetic patients and its relationship with coronary heart disease: a population-based cohort. *J Intern Med* 251: 317 324, 2002.

62. **Veglio M, Chinaglia A, and Cavallo-Perin P.** QT interval, cardiovascular risk factors and risk of death in diabetes. *J Endocrinol Invest* 27: 175 81, 2004.

63. **Veldkamp MW, van Ginneken AC, and Bouman LN.** Single delayed rectifier channels in the membrane of rabbit ventricular myocytes. *Circ Res* 72: 865 878, 1993.

64. **Wang DW, Kiyosue T, Shigematsu S, and Arita M.** Abnormalities of K^+ and Ca^{2+} currents in ventricular myocytes from rats with chronic diabetes. *Am J Physiol* 1269: H1288 H1296, 1995.

65. **Wang H, Zhang Y, Cao L, Han H, Wang J, Yang B, Nattel S, and Wang Z.** HERG K^+ channel, a regulator of tumor cell apoptosis and proliferation. *Cancer Res* 62: 4843-4848, 2002.

66. **Wang J, Wang H, Han H, Zhang Y, Yang B, Nattel S, and Wang Z.** The phospholipid metabolite 1-palmitoyl-lysophosphatidylcholine enhances human *ether-a-go-go* related gene (HERG) K^+ channel function. *Circulation* 104: 2645-2648, 2001.

67. **Wang J, Wang H, Zhang Y, Gao H, Nattel S, and Wang Z.** Impairment of HERG K^+ channel function by tumor necrosis factor-α: role of reactive oxygen species as a mediator. *J Biol Chem* 279: 13289-13292, 2004.

68. **Wang J, Zhang Y, Wang H, Han H, Nattel S, Yang B, and Wang Z.** Modulation of human *ether-a-go-go* related gene (HERG) K^+ channel function by lysophospholipids: Direct interaction as a mechanism. *Br J Pharmacol* 141: 586-599, 2004.

69. **Wang Q, Shen J, Splawski I, Atkinson D, Li Z, Robinson JL, Moss AJ, Towbin JA, and Keating MT.** SCN5A mutations associated with an inherited cardiac arrhythmia, long QT syndrome. *Cell* 80: 805-811, 1995.

70. **Wang Z, Feng J, Shi H, Pond A, Nerbonne JM, and Nattel S.** The potential molecular basis of different physiological properties of transient outward K^+ current in rabbit and human hearts. *Circ Res* 84: 551 561, 1999.

71. **Wang Z, Fermini B, and Nattel S.** Rapid and slow components of delayed rectifier current in human atrial myocytes. *Cardiovasc Res* 28: 1540-1546, 1994.

72. **Wang Z, Fermini B, and Nattel S.** Delayed rectifier outward current and repolarization in human atrial myocytes. *Circ Res* 73: 276-285, 1993.

73. **Wang Z, Fermini B, and Nattel S.** Role of chloride currents in repolarizing rabbit atrial myocytes. *Am J Physiol* 268: H1992-H2002, 1995.

74. **Wang Z, Fermini B, and Nattel S.** Sustained depolarization-induced outward current in human atrial myocytes: Evidence for a novel delayed rectifier potassium current similar to Kv1.5 cloned channel currents. *Circ Res* 73: 1061-1076, 1993.

75. **Wang Z, Yue L, White M, Pelletier G, and Nattel S.** Differential expression of inward rectifier potassium channel mRNA in human atrium versus ventricle and in normal versus failing hearts. *Circulation* 98: 2422-2428, 1998.

76. **Zhang Y, Han H, Wang J, Wang H, Yang B, Wang Z.** Impairment of HERG (Human *ether-a-go-go* Related Gene) K^+ channel function by hypoglycemia and hyperglycemia: similar phenotypes but different mechanisms. *J Biol Chem* 278: 10417-10426, 2003.

77. **Zhang Y, Wang H, Wang J, Han H, Nattel S, and Wang Z.** Normal function of HERG K^+ channels expressed in HEK293 cells requires basal protein kinase B activity. *FEBS Lett* 534: 125-132, 2003.

78. **Zicha S, Moss I, Allen B, Varro A, Papp J, Dumaine R, Antzelevich C, and Nattel S.** Molecular basis of species-specific expression of repolarizing K^+ currents in the heart. *Am J Physiol* 285: H1641- H1649, 2003.

3.8 Figures and Figure Legends

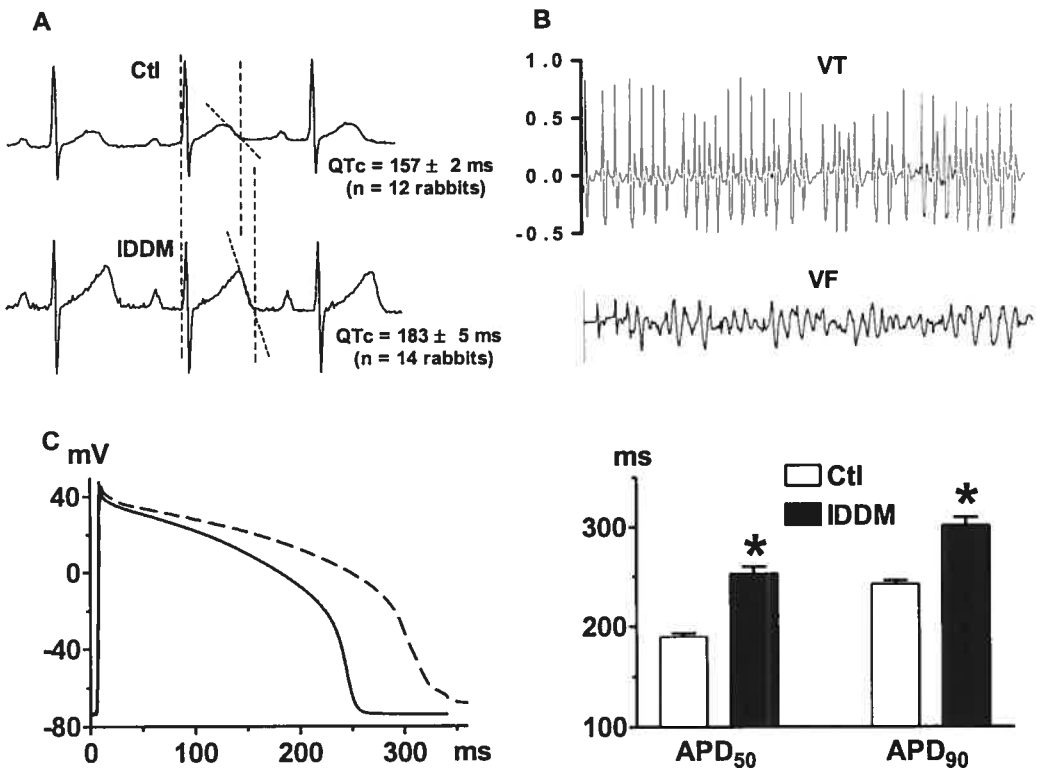

Figure 1. Electrical disorders in rabbits with insulin-dependent diabetes mellitus (IDDM). (**A**) Abnormal prolongation of QT interval in IDDM rabbits. Shown are representative ECG recordings from a control (Ctl) and an IDDM (10 weeks) rabbits, and the mean data (n=12 rabbits for Ctl and n=14 for IDDM) of heart rate-corrected QT interval (QTc interval). The dash lines define the measurements of QT interval. *p<0.05 IDDM *vs.* Ctl. (**B**) Ventricular arrhythmias in IDDM rabbits. The examples of ventricular tachycardia (VT) and ventricular fibrillation (VF) were recorded by an ECG telemeter from an IDDM rabbit 2 min before sudden death. (**C**) Prolongation of action potential duration (APD) in IDDM rabbits. Mean data are from n=12 cells from 4-5 rabbits. *p<0.05 *vs.* Ctl.

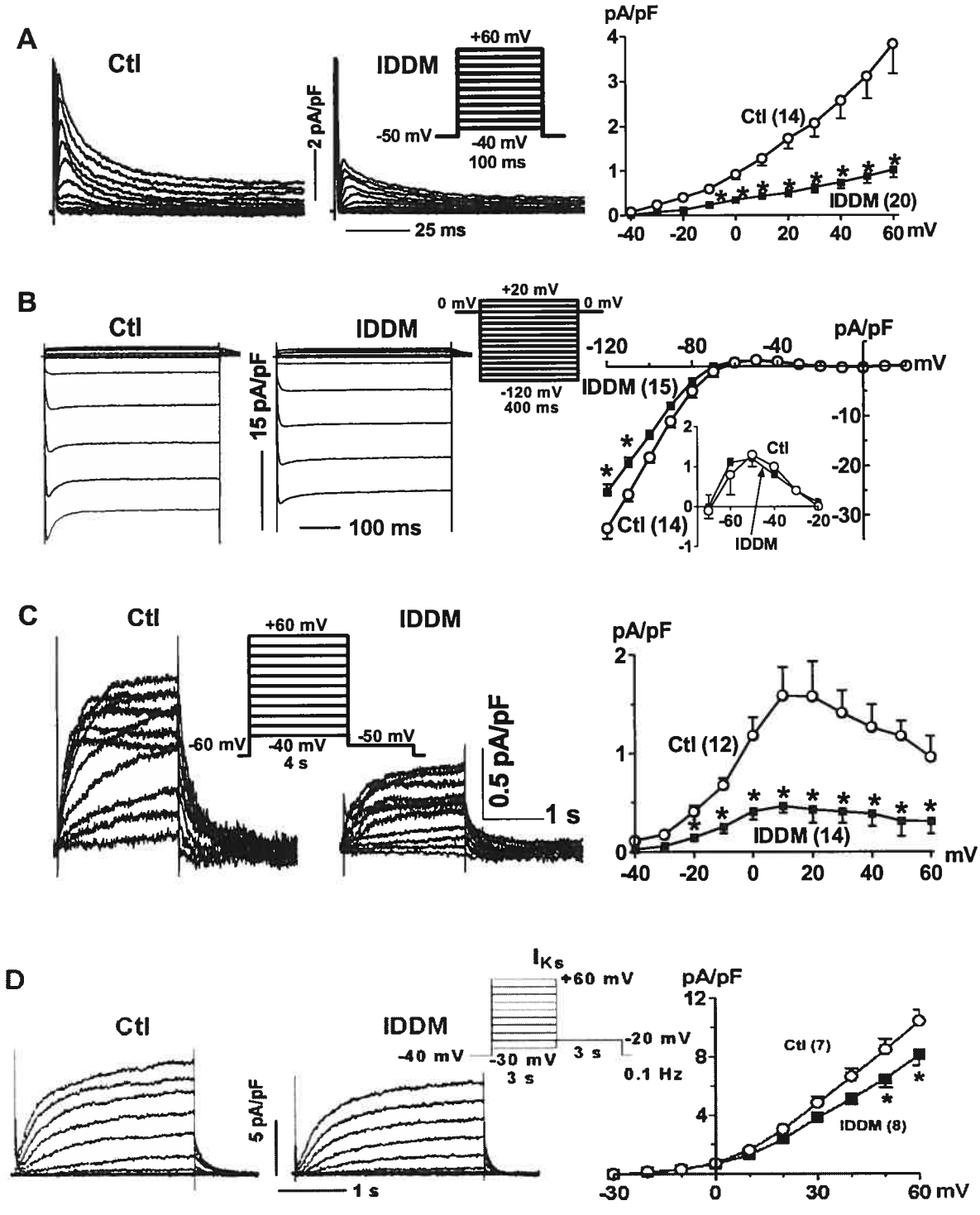
A
Ctl
IDDM
+60 mV
-50 mV
-40 mV
100 ms
2 pA/pF
25 ms
pA/pF
Ctl (14)
IDDM (20)
mV
B
Ctl
IDDM
+20 mV
0 mV
0 mV
-120 mV
400 ms
15 pA/pF
100 ms
pA/pF
IDDM (15)
Ctl (14)
Ctl
IDDM
mV
C
Ctl
IDDM
+60 mV
-60 mV
-40 mV
4 s
-50 mV
0.5 pA/pF
1 s
pA/pF
Ctl (12)
IDDM (14)
mV
D
Ctl
IDDM
I_{Ks}
+60 mV
-40 mV
-30 mV
3 s
-20 mV
3 s
0.1 Hz
5 pA/pF
1 s
pA/pF
Ctl (7)
IDDM (8)
mV

Figure 2

Figure 2. Comparison of various K^+ currents in ventricular cardiomyocytes between healthy and diabetic rabbits. Currents were recorded with the voltage protocols shown in the insets. Left panels: representative recording of I_{to}, I_{K1}, I_{Kr}, and I_{Ks} in healthy (Ctl) and IDDM rabbit hearts, and right panels: averaged I (current density)-V relationships (right panels). The inset in the I_{K1} I-V curves shows the outward portion of I_{K1}. I_{Kr} is defined as the dofetilide (1 μM)-sensitive currents and I_{Ks} the dofetilide-resistant currents. The values within the brackets indicate the number of cells included for data analysis (the same below). *p<0.05 IDDM *vs.* Ctl.

Figure 3

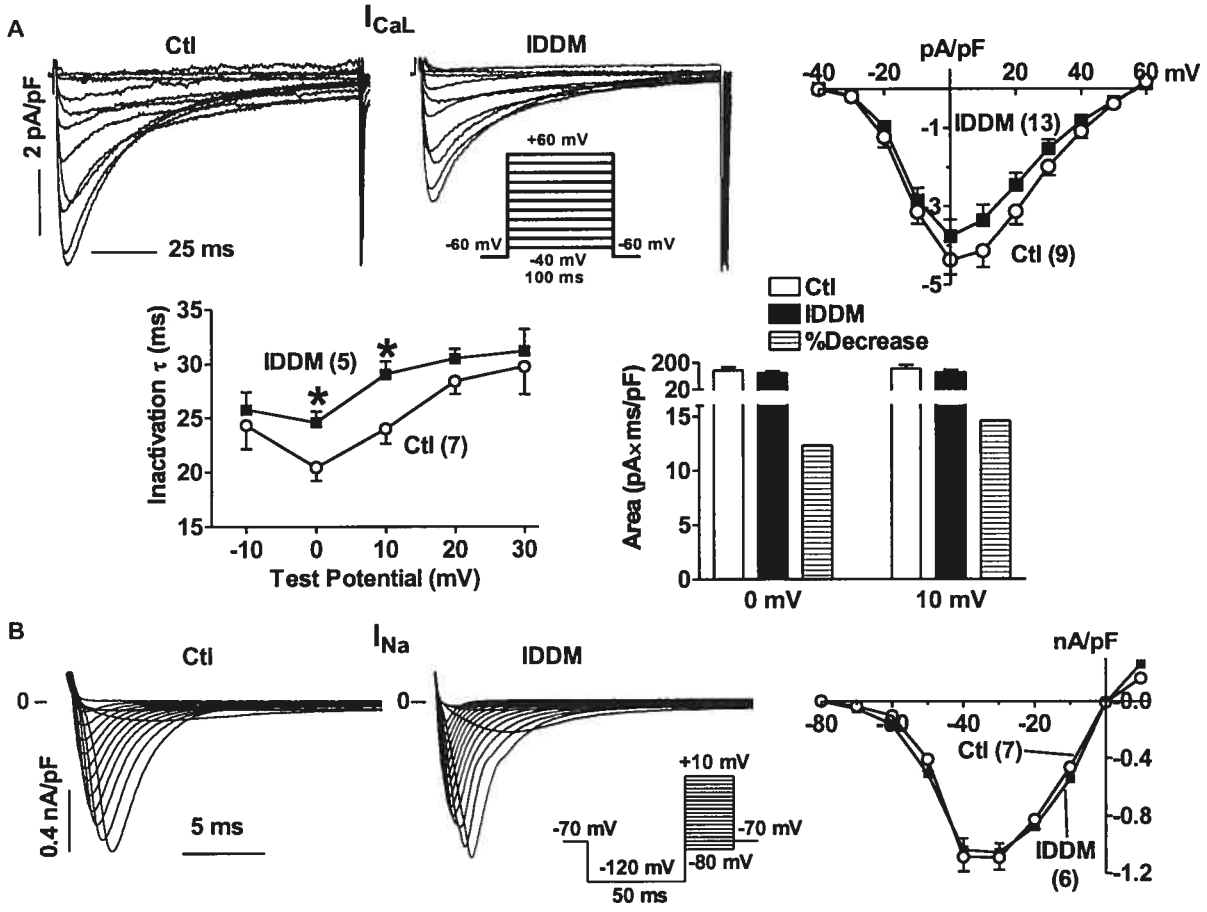

Figure 3. Comparison of L-type Ca^{2+} current (I_{CaL}) and fast Na^{+} current (I_{Na}) in ventricular myocytes between healthy and IDDM rabbits. Currents were recorded with the voltage protocols shown in the insets. (**A**) The inactivation time constants (τ) of I_{CaL} were obtained by a single exponential fit to the decaying phase of the currents at potentials from -10 to +30 mV. To integrate the changes of amplitude and inactivation kinetics, the areas under the I_{CaL} traces were calculated for more rational comparison of I_{CaL} sizes between healthy and IDDM rabbits. *p<0.05 IDDM *vs.* Ctl.

Figure 4

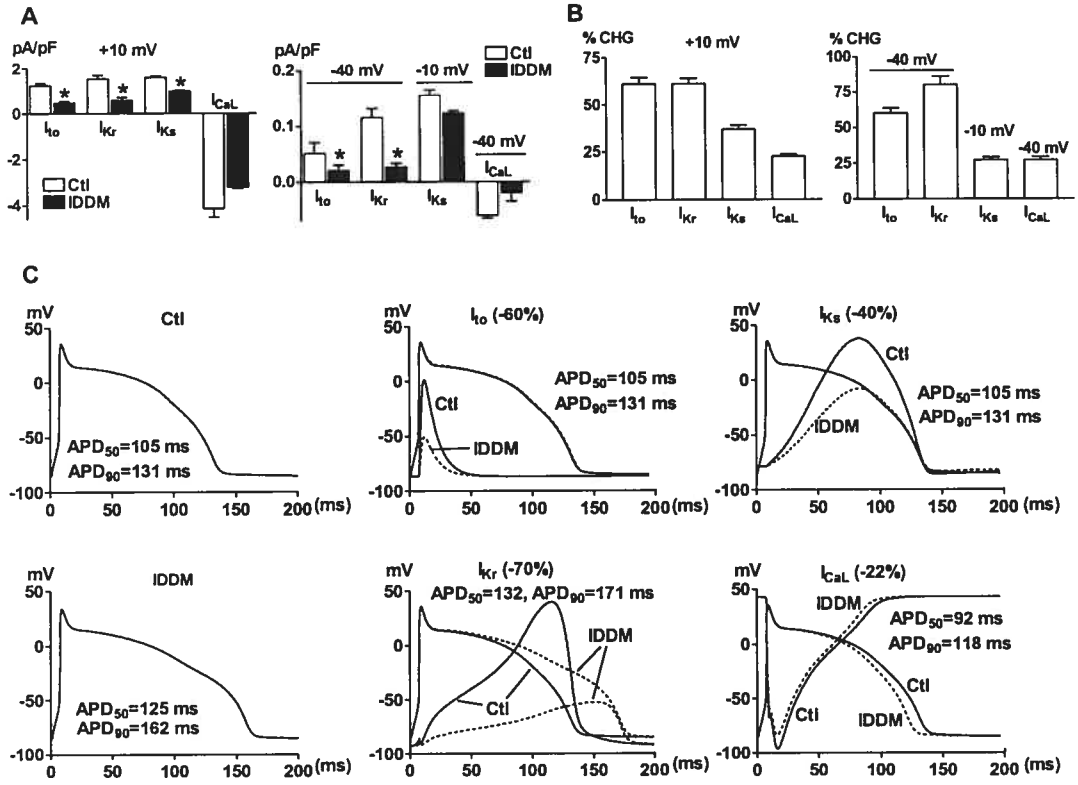

Figure 4. Relative contributions of various ion currents to APD prolongation in ventricular myocytes from IDDM rabbits. (**A** and **B**) Comparison of various ion currents at selected test potentials (+10 mV and -40 mV or -10 mV for I_{Ks}). *p<0.05 IDDM *vs.* Ctl. (**C**) Simulation of action potentials based on the changes of ion currents in IDDM hearts, using LabHEART software. The labels in each panel indicate the simulation with the inhibition of a given current and the percent reduction of currents is indicated in the brackets. Bottom left panel (IDDM) represents AP simulated with combinational changes of all ion currents examined.

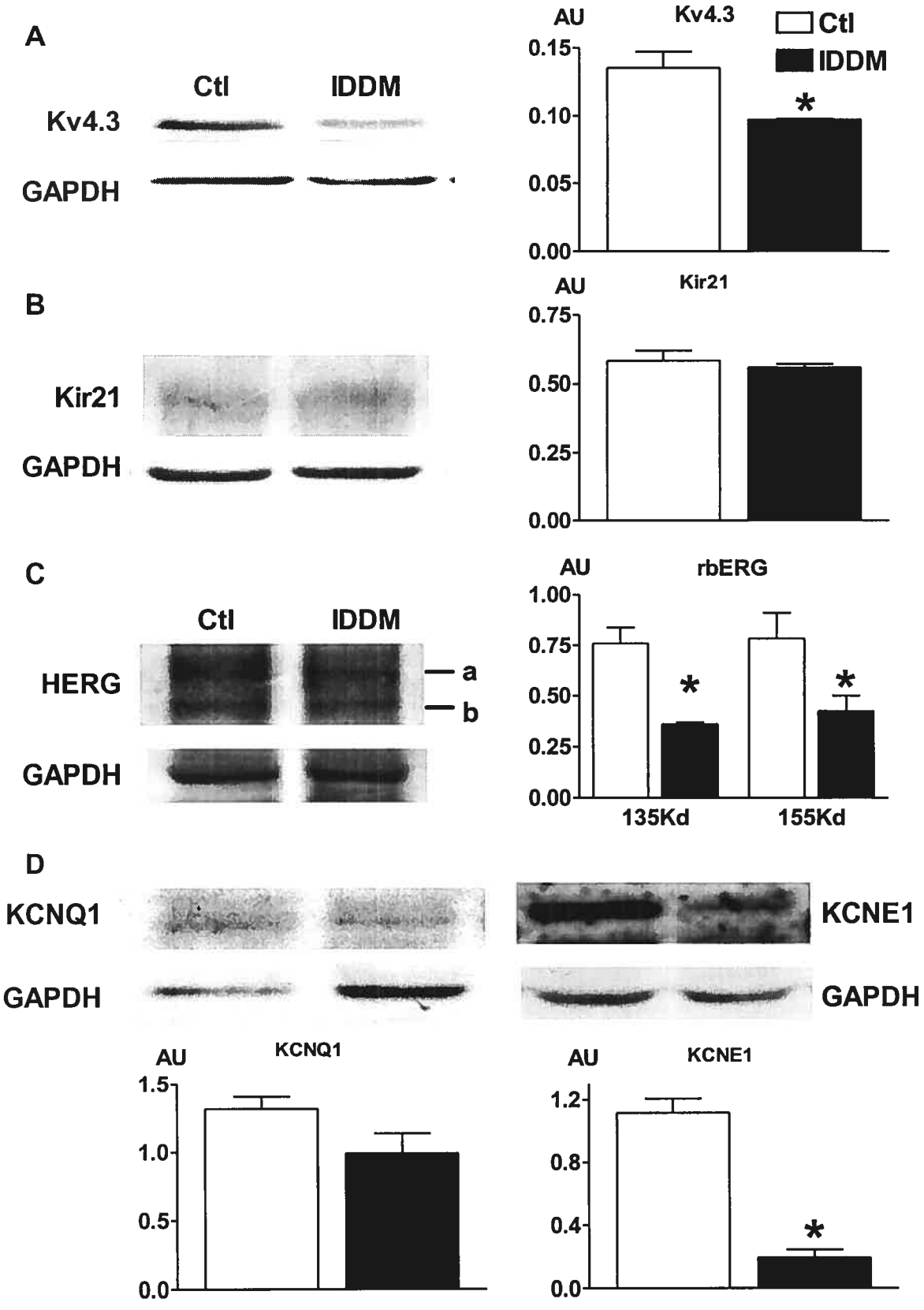
A
Ctl
IDDM
Kv4.3
GAPDH
AU
Kv4.3
Ctl
IDDM
0.15
0.10
0.05
0.00
*
B
Kir21
GAPDH
AU
Kir21
0.75
0.50
0.25
0.00
C
Ctl
IDDM
HERG
a
b
GAPDH
AU
rbERG
1.00
0.75
0.50
0.25
0.00
*
*
135Kd
155Kd
D
KCNQ1
KCNE1
GAPDH
GAPDH
AU
KCNQ1
1.5
1.0
0.5
0.0
AU
KCNE1
1.2
0.8
0.4
0.0
*

Figure 5

Figure 5. Alterations of protein levels of outward ion channel subunits revealed by Western blot analysis. The relative quantification of protein levels was attained by normalizing the band densities to GAPDH, followed by further normalization to the values from control hearts. The data were averaged from experiments in triplicate with 5 hearts of healthy and IDDM rabbits, respectively, and are expressed as fold changes. *$p<0.05$ IDDM *vs.* Ctl.

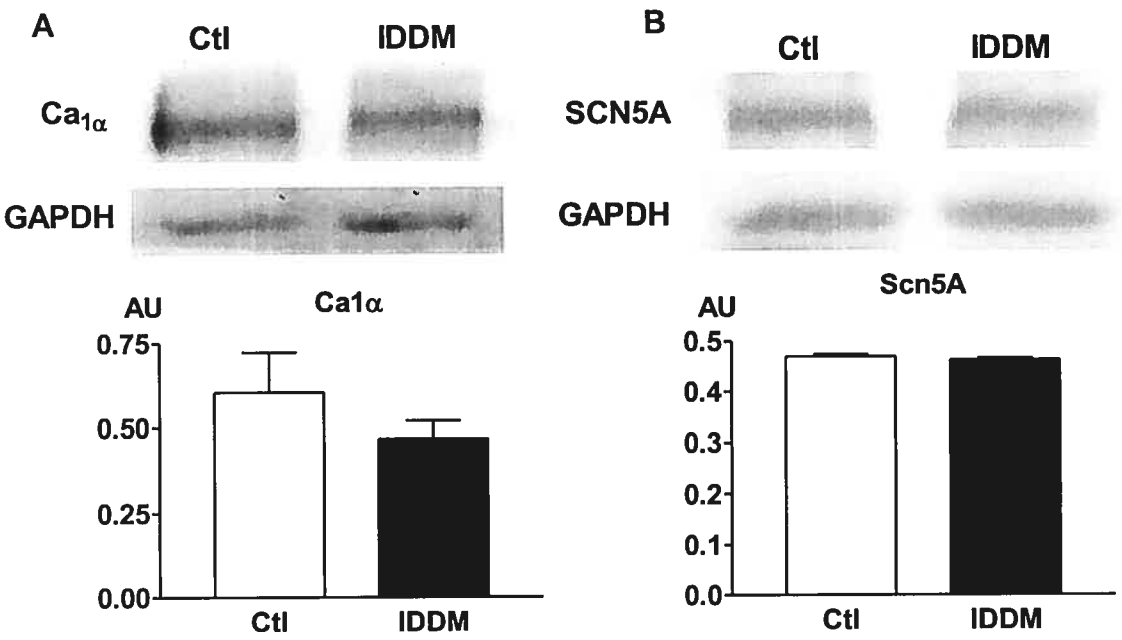

Figure 6. Alterations of protein levels of α-subunits of I_{CaL} (*A*) and I_{Na} (*B*) revealed by Western blot analysis. The relative quantification of protein levels was attained by normalizing the band densities to GAPDH, followed by further normalization to the values from control hearts. The data were averaged from experiments in triplicate with 5 hearts of healthy and IDDM rabbits, respectively, and are expressed as fold changes. *p<0.05 IDDM *vs.* Ctl. *p<0.05 IDDM *vs.* Ctl.

4 EXPERIMENTAL THERAPIES OF DIABETIC QT PROLONGATION AND ARRHYTHMIAS

According to the prediction on the contributions of ion channels to the APD lengthening in diabetic cardiomyocytes by the software LabHEART, APD is mostly prolonged by reduction of I_{Kr} but not I_{Ks} or I_{to}. We continued to explore the mechanisms underlying the diabetic channelopathy of I_{Kr}/HERG using both IDDM rabbits and cell models expressing HERG channels under mimicked hyperglycemia.

The major metabolic disturbances in diabetes include increased glucose level, reduced insulin level (in IDDM) and impaired insulin signaling. Previous studies have also shown levels of reactive oxygen species increase dramatically in diabetes. We describe here the experimental therapy for the diabetic QT prolongation and arrhythmias using insulin to decrease glucose and vitamin E to reduce the oxidative stress, and decipher the potential mechanisms.

This manuscript has been submitted to *American Journal of Physiology* for review.

I_{Kr}/HERG as a Therapeutic Target for Diabetic QT Prolongation and Arrhythmias

Yiqiang Zhang,[1,2] Jiening Xiao,[1,4§] Huizhen Wang,[1,3§] Jingxiong Wang,[1,2] Louis R. Villeneuve,[1] Haiqing Zhang,[1¶] Huixian Lin,[1,4] Yunlong Bai,[3,4] Baofeng Yang,[3,4] and Zhiguo Wang[1,2,4,*]

From the [1]Research Center, Montreal Heart Institute, Montreal, PQ H1T 1C8 Canada, [2]Department of Medicine, University of Montreal, Montreal, PQ H3C 3J7 Canada, [3]Department of Pharmacology (State-Province Key Laboratory of China), Harbin Medical University, Harbin, Heilongjiang 150086, P.R. China, [4]Institute of Cardiovascular Research, Harbin Medical University, Harbin, Heilongjiang 150086, P.R. China

Running Title: **Insulin and vitamin E treatments for diabetic QT prolongation**

§ Authors with equal contributions to the present study.

¶ Current address: Institute of Parasitology, McGill University, Montreal, PQ H9X 3V9, Canada.

Address correspondence to: Dr. Zhiguo Wang, Research Center, Montreal Heart Institute, 5000 Belanger East, Montreal, PQ H1T 1C8, Canada; Tel.: (514) 376-3330. Fax: (514) 376-4452. E-mail: [redacted] or Prof. Baofeng Yang, Department of Pharmacology (State-Province key lab of China), Harbin Medical University, Harbin, Heilongjiang 150086, P.R. China. E-mail: [redacted]

4.1 Summary

Abnormal QT prolongation in diabetic patients has become a non-negligible clinical problem and attracted increasing attention from basic scientists, due to its resultant increases in the risk of lethal ventricular arrhythmias. Correction of QT interval may be an important measure in minimizing sudden cardiac death in diabetic patients. Herein we report the efficacies of insulin and vitamin E in preventing QT prolongation and the associated arrhythmias and the mechanisms underlying the effects in a rabbit model of type I insulin-dependent diabetes mellitus (IDDM). The heart rate-corrected QT interval (QTc interval) and action potential duration (APD) were considerably prolonged with frequent occurrence of ventricular tachyarrhythmias. The rapid delayed rectifier K^+ current (I_{Kr}) was markedly reduced in DM hearts and hyperglycemia depressed the function of HERG that encodes I_{Kr}. Impairment of I_{Kr}/HERG function in diabetic animals and hyperglycemic cells was primarily ascribed to the enhanced oxidative damages to the myocardium as indicated by the increased intracellular level of reactive oxygen species and simultaneously decreased endogenous antioxidant reserve and by the increased lipid peroxidation and protein oxidation. Moreover, DM or hyperglycemia resulted in downregulation of HERG protein level and loss of HERG protein stability. Insulin or vitamin E restored the depressed I_{Kr}/HERG and prevented QTc/APD prolongation and the associated arrhythmias and our data further indicate that the beneficial actions of insulin and vitamin E are likely due to their anti-oxidant ability. Our study represents the first documentation of I_{Kr}/HERG K^+ channelopathy as the ionic mechanism for diabetic QT prolongation and oxidative stress caused by hyperglycemia as the major metabolic mechanism for diabetic HERG K^+ channelopathy, and of I_{Kr}/HERG as a therapeutic target for the treatment of diabetic electrical disturbances.

Abbreviations used: AP, action potential; APD, action potential duration; APD_{50} and APD_{90}, action potential duration to 50% and 90% full repolarization, respectively; DM, diabetes mellitus; Dof, dofetilide; INS, insulin; G5, 5 mM glucose; G20, 20 mM glucose; HERG, human *ether-a-go-go*-related gene; IDDM, type I insulin-dependent diabetes mellitus; I_{Kr}, rapid delayed rectifier K^+ current; I_{Ks}, slow delayed rectifier K^+ current; NIDDM, type II insulin-independent NIDDM; QTc interval, heart rate-corrected QT interval; rbERG, rabbit *ether-a-go-go*-related gene; ROS, reactive oxygen species; VF, ventricular fibrillation; VT, ventricular tachycardia; VitE: vitamin E; X/XO, xanthine/xanthine oxidase.

4.2 Introduction

Diabetes mellitus (DM) is one of the most prevalent chronic conditions associated with significant morbidity and mortality from cardiovascular diseases. Increasing evidence indicates that impaired cardiac function in diabetes can be independent of vascular diseases, suggesting the existence of myocardial defect in diabetic subjects, so-called diabetic cardiomyopathy (3, 14, 35). Diabetic cardiomyopathy is characterized by electrical remodeling with aberrant electrophysiology (11, 14, 20, 26), metabolic remodeling with malignant biochemical processes (25, 33), and anatomical remodeling with progressive loss of cardiomyocytes (15), which result in impaired cardiac contractile and increased risk of lethal arrhythmias. The abnormal prolongation of the QT interval is the most prominent electrical remodeling in diabetic hearts; clinically, it accounts for some 25% DM patients including both type I insulin-dependent (IDDM) and type II insulin-independent (NIDDM) populations (27, 44). QT prolongation has been considered as a predictor of mortality in diabetic subjects because it is associated with an increased risk of ventricular arrhythmias and the consequent sudden cardiac death (9, 13, 41, 49, 50). Correction of QT prolongation therefore is an important step towards reducing cardiac death of lives suffering from DM.

To achieve the therapeutic goal, sufficient knowledge about the ionic mechanisms underlying diabetic QT prolongation is critical. We have recently identified depression of multiple ion currents in diabetic rabbits, including transient outward K^+ current (I_{to}), L-type Ca^{2+} current (I_{CaL}), rapid delayed rectifier K^+ current (I_{Kr}) and slow delayed rectifier K^+ current (I_{Ks}). Our data on I_{to} and I_{CaL} are consistent with the results from earlier studies carried out with animal models of rats and mice (12, 42, 43, 46, 52). However, our finding that I_{Kr} is the major ionic determinant, while other ion currents play a minimal role, in diabetic QT prolongation is unique and bears significant implications for therapeutic interventions (39). Moreover, our previous studies have revealed that HERG (human *ether-a-go-go* related gene), the pore-forming α-subunit of the native I_{Kr}, is negatively modulated by hyperglycemia, tumor necrosis factor-alpha (TNF-α), ceramide and reactive oxygen species (ROS) (55, 60), the cellular metabolites accumulating in diabetic tissues (16, 17, 37, 64). Also pertinent to the diabetic QT-P is our finding that basal activities of protein kinase B (PKB), a down-stream mediator of the insulin signaling pathway, are crucial for maintaining the normal function of HERG K^+ channels (61).

Our current understanding of diabetic QT prolongation, though still incomplete, allows us to develop rational therapeutic approaches. The present study was designed to shed some light on this issue, evaluating the potential of I_{Kr}/HERG as the therapeutic target. In IDDM model of rabbits, we examined whether reducing metabolic stress by insulin therapy and antioxidant therapy with vitamin E (VitE) could restore the prolonged QT interval and prevent the associated arrhythmias, and decipher the underlying mechanisms.

4.3 Methods

4.3.1 Rabbit model of type I insulin-dependent diabetes mellitus (DM)

Male New Zealand white rabbits weighing 1.6~2.0 Kg (Charles River Canada Inc) were housed individually in stainless steel wire-bottomed cages in a room with a 12:12-hrs light-dark cycle with standard laboratory rabbit chow and drinking water *ad libitum*. The animals were randomly assigned to control, DM, and DM/insulin (INS) and DM/vitamin E (VitE) groups. To establish diabetes, a single injection of 140 mg/kg (body weight) of pre-warmed (37°C) alloxan monohydrate (Sigma-Aldrich) was administrated via marginal ear vein under local anesthesia (19, 65). Alloxan was freshly dissolved in saline at a concentration of 100 mg/ml. To prevent fatal hypoglycemia from massive insulin release, 10% glucose solution (100 mg/kg, s.c.) was administered 4 and 6 hrs after alloxan treatment. For DM/INS group, after establishment of stable diabetes for 3 days, animals were administered with diluted insulin zinc (first dosage 7-10 IU/kg, s.c., and 5-7 IU/kg every 2-3 days thereafter, to clamp the glucose level between 8-12 mM) to lower the rabbit plasma glucose level while still maintaining the diabetic condition. For DM/VitE group, diabetic rabbits were administered with VitE acetate (100 mg/kg/day, i.m.). The blood was collected via marginal ear vein after local anesthesia for determining the plasma level of glucose with a glucometer (TheraSense, USA) and the insulin level with colorimetric assay and radioimmunoassay in non-anaesthetized rabbits before and 2-3 days after alloxan injection, and the blood glucose level was monitored weekly thereafter till 10 weeks. Only those animals with serum glucose concentrations $\geqslant$15 mM were considered diabetic and were used for further studies. All procedures are in accordance with the guidelines set by the Animal Ethics Committee of the Montreal Heart Institute.

4.3.2 Implantation of telemeters and ECG recording in conscious rabbits

Rabbits were anesthetized with ketamine (Vetalar®, BioNiche Animal Health Canada, Belleville, Ontario) and xylazine (Rompun®, Bayer Inc, Toronto, Ontario) mixture (7:1) at a dosage of 1.2 ml/3 Kg (i.m.). Abdominal hair was shaved and skin was cleaned and sterilized with antiseptic. A small incision was then made on the skin for subcutaneous implantation of ECG telemeter (EMKA Technologie, Paris, France) and the probes of the telemeter were fixed to the right and left underarm positions. Antibiotic cream (Polytopic®, Sabex Inc, Boucherville, QC, Canada) was applied to the closed skin wounds followed by adherent surgical dressing. Bondages were then used to protect the wounds. Antibiotic solution (0.5 ml, Longisil®, Vétoquinol N.-A. Inc) containing penicillin G benzathine (150,000 IU/ml) and penicillin G procaine (150,000 IU/ml) was applied i.m. daily for 5 days after the surgery. Seven days after implantation, the transducer was activated to record the real-time ECG in conscious rabbits. The ECG signal was acquired and analyzed by the EMKA Technilogies's IOX acquisition software and ECG-Auto, respectively. ECG was monitored continuously for 24 hrs immediately after treatment with alloxan. From day 2 after alloxan treatment, ECG was recorded for 20 min at an interval of every 3 hrs when necessary (at least 2 days every week). ECG recorded in this way is equivalent to the standard lead II ECG.

4.3.3 Surface ECG recording in anesthetized rabbits

Standard ECG was recorded before and after establishment of diabetes in rabbits. Sedation and induction of anesthesia were obtained with intramuscular injections of ketamine (65 mg/kg) and xylazine (13 mg/kg). Three-lead surface ECGs were recorded with silver electrodes placed under the skin at the optimized positions to obtain maximal amplitude recordings, enabling accurate measurements of QT intervals. ECGs were recorded from standard lead II and the QT measurements and simultaneously recorded RR intervals were used to derive heart rate corrected QT intervals using Carlsson's formula (QTc=QT - 0.175 (RR-300)) (10).

4.3.4 Isolation and primary culture of rabbit ventricular myocytes

Myocytes were isolated from rabbit left ventricular endocardium via enzymatic digestion of the whole heart on a Langendorff apparatus with the procedures similar to previously described (58). Rabbits were anaesthetized by sodium pentobarbital (60 mg/kg i.v.). Hearts were

rapidly excised and mounted on a Langendorff apparatus and perfused retrogradely with the following four solutions in sequential order: 1 mM Ca^{2+} Tyrode (2 min), Ca^{2+}-free Tyrode (3-5 min), Ca^{2+}-free Tyrode containing collagenase (Worthington type II) for 20-30 min. The ventricle was cut off and minced in enzyme solution and incubated at 37°C while shaking for 3-4 min, then filtered to remove big piece of tissue. The freshly isolated myocytes were gently centrifuged and resuspended in either KB solution for patch-clamp studies or in standard culture medium (M199 with Earl's salts and L-glutamine; Gibco) for ROS measurement and patch-clamp experiments involving signaling molecules, supplemented with penicillin (50 U/ml; Sigma) and 2% FBS (Gibco). Cells were maintained at 37°C in a humidified atmosphere of 5% CO_2 and 95% air. KB solution for cell storage (at 4 °C) contained (mM): 20 KCl, 10 KH_2PO4, 10 glucose, 70 K-glutamate, β-hydroxybutyric acid, 20 taurine, EGTA, 40 mannitol, and 0.1% albumin (pH 7.4).

4.3.5 HEK293 cell culture

HEK293 cells stably-expressing HERG were a kind gift from Drs. Zhou and January (62). Cell culture and handling procedures have been described previously (53-55).

4.3.6 Whole-cell patch-clamp recording

Patch-clamp of I_{Kr} and HERG currents have been described in detail elsewhere (53-57). Briefly, currents were recorded with whole-cell patch-clamp and action potential-clamp (AP-clamp) techniques in the voltage-clamp mode and single cell action potentials were recorded in the current-clamp mode, using an Axopatch-200B amplifier (Axon Instruments). For AP-clamp, the AP waveforms were collected from single myocytes of rabbit left ventricular endocardium using current-clamp methods. Borosilicate glass electrodes had tip resistances of 1-3 MΩ when filled with the internal pipette solution. The pipette solution contained (mM): 130 KCl, 1 $MgCl_2$, 5 Mg-ATP, 10 EGTA, and 10 HEPES (pH adjusted to 7.3 with KOH). The internal pipette solution for AP recording contained the same components, except that EGTA was reduced to 0.05 mM. The extracellular solution for I_{HERG} recording contained (mM): 136 NaCl, 5.4 KCl, 1 $CaCl_2$, 1 $MgCl_2$, 10 HEPES, 5 glucose (pH 7.4 with NaOH). For I_{Kr} recordings, the superfusate was changed to NMG solution containing (mM): 149 N-methyl-D-glutamine, 5 $MgCl_2$, 0.9 $CaCl_2$, and 5 HEPES (pH adjusted to 7.4 with HCl). All experiments were conducted at 36±1°C.

Junction potentials were zeroed before formation of the membrane-pipette seal. Series resistance and capacitance were compensated and leak currents were subtracted.

For myocyte studies, the following were included in the bath to block contaminating currents: nisodipine (3 μM, L-type Ca^{2+}-current), glyburide (10 μM, ATP-sensitive K^+-current) and 293B (10 μM, slow delayed-rectifier K^+-current). I_{Kr} was expressed as dofetilide-sensitive current by subtracting the currents recorded 10 min after dofetilide (1 μM) from the baseline currents before dofetilide. The voltage protocols for current recordings are shown in the figures.

4.3.7 Western blot

The membrane and cytosolic protein samples were extracted from rabbit hearts and HERG-expressing HEK293 cells and were used for immunoblotting analysis of membrane HERG protein, with the procedures essentially the same as described in detail elsewhere (53). The protein content was determined with Bio-Rad Protein Assay Kit (Bio-Rad, Mississauga, ON) using bovine serum albumin as the standard.

Membrane proteins (150 μg for rabbit heart samples and 20 μg for HEK293 cell samples) were fractionated by SDS-PAGE (10% polyacrylamide gels) and transferred to PVDF membrane (Millipore, Bedford, MA). The membrane was incubated overnight at 4°C with the primary antibody, polyclonal anti-HERG (diluted 1:50) raised in goat against the highly purified peptide corresponding to residues within 1100-1200 of human HERG. The overall rabbit ERG clone (Genbank accession U87513) is 96% identical to the human sequence at the amino acid level and is 100% identical to HERG within the region where the antigenic peptide is generated for the antibody (24; 30; 59). Therefore, HERG is used for rbERG throughout the manuscript. Next day, the membrane was washed in TTBS three times (10 min/each) and incubated for 2 hrs with the HRP-conjugated donkey anti-goat IgG (H+L) (1:600) in the blocking buffer. Both primary and secondary antibodies were purchased from Santa Cruz Biotechnology (Santa Cruz, CA). Bound antibodies were detected using the chemiluminescent substrate (Western Blot Chemiluminescence Reagent Plus, NEN Life Science Products, Boston, USA). GAPDH was used as an internal control for equal input of protein samples, using anti-GAPDH antibody purchased from RDI (Flanders, NJ). Coomassie staining was also performed to verify the sample quantity. Western blot results were quantified using QuantityOne software by measuring the

band intensity (Area x OD) for each group and normalizing to GAPDH. The final results are expressed as fold changes by normalizing the data to the value for control 155 kDa band.

4.3.8 Immunohistochemistry

Hearts of 4 to 6 week-diabetic rabbits or age-matched healthy rabbits were rapidly removed from heparinized animals after sedated with sodium pentobarbital and washed in ice-cool Tyrode's solution. Left ventricle was dissected and immersed in 2-methylbutane (2-MB) pre-chilled with liquid nitrogen. Samples were then frozen in liquid nitrogen and stored at -80°C for later use.

Left ventricular apexes were continuously cryo-cut in 14 μm section at -20 °C with a Leica CM19000 cryostat and mounted onto slides, dried and stored at -80°C before immunohistochemical studies. Specimens were fixed with acetone at -20°C for 5 min followed by three washes in phosphate-based buffer (PBS) at room temperature (RT). Samples were then blocked with 2% normal donkey serum (NDS in PBS) for 1 hr, and reacted overnight at 4°C with goat polyclonal antibodies against HERG and mouse monoclonal antibody against BIP (ER marker) diluted in 1:50 in 1% NDS. Donkey anti-goat, Alexa Fluor 546-conjugated and donkey anti-mouse, Alexa Fluor 647-conjugated antibodies, purchased from Molecular Probes (Eugene, OR), were used as secondary antibodies. Anti-fading medium was applied to the specimens to prevent color bleaching. The samples were examined under a confocal microscope and analyzed by Zeiss LSM software suite, using control group for optimization.

4.3.9 Immunocytochemistry

Immunocytochemical procedures have been described previously (53, 61). Briefly, left ventricular cardiomyocytes enzymatically isolated from hearts of both healthy and diabetic rabbits as already described above were seeded onto coverslips coated with laminin and incubated in M199 medium for 1 hr at 37°C. The cells were washed twice in ice cooled PBS before being fixed with freshly prepared 1% paraformaldehyde (pH 7.35 in PBS) at RT for 30 min, followed by three washes in PBS. 1% Triton X-100 (in PBS) was used to permeabilize the cell membrane by incubating at RT for 5 min, followed by blocking with 1% NDS for 1.5 hrs at RT. Goat polyclonal primary antibodies against HERG (and rbERG, Santa Cruz Biotechnology, Santa Cruz, CA) and mouse monoclonal antibody (IgG_{2a}) against BIP (ER marker protein, BD

Biosciences Pharmingen, San Jose, CA) were diluted 1:50 in antibody dilution buffer (ADB, containing 1% NDS in PBS) and reacted with cells on coverslips at 4°C overnight. The specificity of antibodies was verified using antigenic blocking peptides. Donkey anti-goat, Alexa Fluor 594-conjugated and Alexa Fluor 647-conjugated donkey anti-mouse IgG (H+L), purchased from Molecular Probes (Eugene, OR), were used as secondary antibodies (1:600). After blocking with 1% BSA, cell membrane was stained with Alexa Fluor 488-conjugated wheat germ agglutinin (WGA, 10 μg/ml) (Molecular Probes) for 30 min. Coverslips were then mounted onto slides with anti-fading medium and subjected to confocal microscopic examination. The images were deconvolved to minimize the background noise.

4.3.10 Measurement of intracellular reactive oxygen species (ROS)

Detailed procedures have been described previously (60, 61). Briefly, 5-(and-6)-chloromethyl-2 , 7 -dichlorodihydrofluoresceinp diacetate (CM-H2DFDA) from Molecular Probes was used to detect oxidative activity in living cells, according to the manufacturer's protocols. The cells were examined under a laser scanning confocal microscope (Zeiss LSM 510), with an excitation wavelength of 480 nm and an emission wavelength at 505 530 nm. The percentage of positively stained cells and the fluorescence intensity of staining were determined by densitometric scanning with LSM software (Zeiss).

4.3.11 Lipid peroxidation assay

Lipid peroxidation was measured using a Lipid Hydroperoxide (LPO) Assay kit from Cayman Chemical (Arbor, Michigan). Rabbit left ventricular preparation of 0.2 g was homogenized in HPLC grade H_2O on ice and LPO was immediately extracted from the sample into chloroform and assayed in a 96-well plate in triplicate according to the manufacture's protocols. The standard curve was generated with the materials provided with the kit using a microplate reader (Power Wave x 340, Biotec Instrument, Inc.) by measuring the absorbance at 500 nm, for calculating the LPO amount. LPO was expressed as hydroperoxide in nM per gram heart tissue.

4.3.12 Protein oxidation assay

Protein Carbonyl Assay kit from Cayman Chemical was used for quantifying protein oxidation in the samples extracted from the hearts of DM and age-matched healthy rabbits, according to the manufacturer's protocols. Briefly, 0.2 g of ventricular tissue was homogenized and total proteins were extracted. The reactions were carried out in a 96-well plate and the absorbance was measured at a wavelength of 370 nm in duplicate using a microplate reader (Power Wave x 340, Biotec Instrument, Inc.). The relative OD values were calculated for comparison and protein oxidation was expressed as protein carbonyl in nM per mg total protein.

4.3.13 Total endogenous antioxidant assay

Blood was collected from ear edge vein in citrate containing tubes. Plasma was obtained by centrifuging blood at 1000 x g for 20 min at 4°C. Plasma total antioxidant status was measured using the Antioxidant Status Assay kit from Cayman Chemical according to the manufacturer's instructions. The reactions were read at 750 nm in duplicate.

4.3.14 Data analysis

Group data are expressed as mean ± S.E. Statistical comparisons (performed using ANOVA followed by Dunnett's method) were carried out using Microsoft Excel. A two-tailed $p< 0.05$ was taken to indicate a statistically significant difference. Nonlinear least square curve fitting was performed with CLAMPFIT in pCLAMP 8.0 or GraphPad Prism.

4.4 Results

4.4.1 Insulin corrects diabetic QT prolongation and suppresses arrhythmias

Rabbits developed typical characteristics of type I diabetes 12-24 hrs after single injection of alloxan, as indicated by the elevated non-fasting blood glucose level as compared with the normal value in age-matched healthy animals and by the reduced plasma insulin level. The induced DM usually stabilized from day 3 after the onset and lasted for at least 10 weeks. Four of 33 rabbits allocated for DM group (4/33, 12%) were resistant to the alloxan treatment, either failed to develop diabetes (blood glucose <12 mM) or recovered from diabetes shortly after the onset. In addition, among the 29 DM rabbits, 10 died before complete data collection. Treatment of the DM rabbits with insulin partially but significantly corrected high blood glucose. The average blood glucose concentration was 5.4 ± 0.7 mM for control group (n=22), 22.6 ± 1.1 mM (n=29) for DM group, 11.4 ± 1.8 mM (n=5) for DM/INS group, and 23.1 ± 2.3 mM (n=4) for DM/VitE group.

QT interval and heart rate-corrected QT interval (QTc interval) (188 ± 5 ms) were consistently prolonged in rabbits developed stable IDDM as compared with the baseline values obtained before treatment (155 ± 2 ms, $p<0.05$, n=19), but not in healthy animals (159 ± 3 ms for baseline *vs.* 158 ± 4 ms for time-matched comparison). These data indicate a 21% prolongation of QTc interval in the DM rabbits over the age-matched healthy animals. Particularly important is that insulin administration prevented QTc prolongation (165 ± 7 ms, $p<0.05$ *vs.* DM group, n=5) (Fig. 1A). Also noticeable is that in the rabbits that failed to develop DM, their QTc interval was normal (167 ± 3 ms) and comparable to that of control rabbits ($p>0.05$). The effects of VitE will be discussed in a later section. In the present study, there is not significant change of heart rate in diabetic or healthy rabbits (205 ± 6 vs 211 ± 8 bpm, $p>0.05$).

Excessive QTc prolongation creates the substrates for arrhythmogenesis. As depicted in Fig. 1B, arrhythmias, mainly ventricular tachycardia (VT), occurred frequently in DM rabbits, which was otherwise absent in healthy animals. An episode of VT was defined as a run of extra-excitations with at least three consecutive beats. The VT often predisposed to ventricular fibrillation (VF) leading to sudden death. Of the 19 DM rabbits used for data analyses, 12 developed VT (12/19, 63%). We were able to record ECG with telemetry from 4 out of 10 rabbits right before they died five days after development of DM. The ECG clearly showed runs

of polymorphic VT and VF. Consistent with the correction of QTc prolongation, no arrhythmias of any sorts were seen in DM rabbits with insulin treatment (Fig. 1B).

To decipher the cellular mechanism underlying the QTc prolongation in our IDDM model, single cell action potential (AP) was recorded in enzymatically dispersed myocytes from left ventricular endocardium. As illustrated in Fig. 1C, AP duration at 50% repolarization (APD_{50}) and at 90% repolarization (APD_{90}) was approximately 35% and 24%, respectively, longer in DM than in healthy subjects, which are somewhat longer than the 20% lengthening of QTc interval.

We have previously demonstrated that high glucose suppresses HERG channel activity and based on the data, we proposed that impairment of I_{Kr}/HERG function by hyperglycemia accounts for diabetic QT prolongation. To examine this hypothesis and to decipher the ionic mechanism for the abnormal lengthening of APD and QTc in our diabetic rabbits, we went on to study the native I_{Kr}, the physiological counterpart of HERG, in isolated rabbit ventricular cells with whole-cell patch-clamp techniques. I_{Kr} was elicited by conventional voltage-clamp protocols with depolarizing pulses of 2.5-s duration from a holding potential of –50 mV to various potentials ranging from –40 to +60 mV to record the step I_{Kr}, followed by 2-s repolarizing pulses to –40 mV to observe the tail I_{Kr}. I_{Kr} was measured as dofetilide-sensitive component and expressed as current density by dividing the current amplitude by the cell capacitance. The data are displayed in Fig. 1D, where both raw current traces and averaged values are shown. Strikingly, I_{Kr} current density was considerably smaller (40~55% at test potentials between -20 mV and +40 mV) in DM rabbits relative to healthy animals. Consistent to its effects on shortening the prolonged APD, insulin treated to diabetic rabbit significantly restored I_{Kr} density in isolated myocytes significantly.

4.4.2 *HERG K^+ channel dysfunction as the ionic mechanism for diabetic QT prolongation: role of high glucose*

Evidently, depression of I_{Kr} accounts for, at least partially, the observed APD/QT prolongation and the associated arrhythmias in DM subjects. It is known that diabetes is a pathological process caused by, and resulting in, metabolic disorders in the cell: diminished glucose metabolism, impaired insulin signaling, increased oxidative stress, etc. To elucidate the metabolic and molecular mechanisms underlying the reduced I_{Kr} function, we investigated the effects of glucose on I_{Kr} and APD. Since the results from the above experiments also

demonstrated that insulin completely prevented QT prolongation and arrhythmias despite that insulin at the dosage used in our study only partly corrected the blood glucose level, effects of insulin on I_{Kr} and APD were also evaluated.

Dispersed ventricular myocytes of healthy rabbits were divided into three groups: control group, hyperglycemia group, and hyperglycemia/insulin group. Cells of hyperglycemia group were incubated with 20 mM glucose (G20) in Tyrode solution for 40 min before patch-clamp recordings. Cells of hyperglycemia/insulin group were preincubated with insulin (100 nM) for 1 hr and then incubated with 20 mM glucose (G20/INS) in insulin-containing solution for 40 min before patch-clamp recordings. Both APD_{50} and APD_{90} were significantly prolonged in G20-treated myocytes, which was prevented by insulin (Fig 2A). When dofetilide (1 μM) was present to block I_{Kr}, insulin lost the ability of shortening the APD prolongation induced by G20. Consistently, I_{Kr} in myocytes treated with G20 was reduced by 50% relative to untreated control cells, and the G20-induced I_{Kr} depression was restored by insulin (Fig 2B).

Moreover, the effects of glucose and insulin on I_{Kr} were reproduced in the *in vitro* expression system with HERG-expressing HEK293 cells. Depolarizing pulses of 2.5-s duration were delivered from a holding potential of –80 mV to various potentials ranging from –60 to +40 mV to record the step I_{HERG}. G20 produced substantial reduction (60% decrease) of I_{HERG} step current, as illustrated in Fig. 2C, and the effect was abolished in cells pretreated with insulin.

The possibility that I_{Kr} depression in DM rabbits is a consequence of direct toxic action of alloxan on HERG channels was excluded by our data demonstrating the failure of alloxan to affect I_{HERG} at concentrations up to 1 mM (data not shown).

4.4.3 *Oxidative stress leading to impairment of HERG K^+ channel: vitamin E treatment*

As already mentioned above, oxidative stress as a result of metabolic perturbation is a pivotal deleterious factor for diabetic cardiomyopathy. Moreover, we have previously identified HERG channel as a target for the action of ROS; specifically, superoxide anion ($O_2^{\cdot-}$) depresses I_{HERG} in the heterologous expression system. However, whether the same results can be applied to *in vivo* diabetic conditions remained yet to be established. To this end, we confirmed the presence of oxidative damage to the myocardium in our rabbit DM model by measuring the degree of lipid peroxidation and protein oxidation of the myocardium.

As depicted in Fig. 3A, the degree of lipid peroxidation was increased by ~45% in diabetic heart relative to control heart. This increase was nearly abolished by insulin (100 nM) and ~50% abrogated by vitamin E (100 mg/kg).

It is known that protein carbonyls are covalent modification of a protein induced by reactive oxygen intermediates or by-products of oxidative stress, such as xanthine oxidase, superoxide anion, lipid peroxide adducts, etc. Carbonyls can result in protein aggregation and are often associated with dysfunction but may require more stringent oxidative conditions. As illustrated in Fig. 3B, the protein oxidation, determined by carbonyl assay, was significantly increased in DM rabbit relative to healthy animals (Fig. 3B), the effects abrogated by insulin or vitamin E.

The oxidative damages might be caused by decreased endogenous antioxidant reserve or increased ROS production or both. To clarify the issue, we went on to quantify the total antioxidant capacity and intracellular ROS concentration.

Figure 3C shows that in six-week diabetes antioxidant concentration was diminished to some 45% of the level in age-matched healthy rabbits. This reduction was likely due to depletion of endogenous antioxidant molecules by intracellular ROS because pretreatment with insulin or vitamin E partially restored the endogenous antioxidant level; antioxidant concentrations were 75% and 65% of the control value with insulin and vitamin E, respectively. More direct evidence came from the experiments with intracellular ROS staining shown in Fig. 3D. The myocytes treated with high level of glucose had considerably higher percentage of positive ROS staining and strikingly stronger staining, indicating an elevated level or over-production of ROS in the cell, compared to the cells in normal glucose level. Strikingly, in the myocytes under hyperglycemic condition treated with insulin, the ROS level was restored to nearly identical to the healthy animals. The increased ROS level in hyperglycemia may be produced by hyperglycemia for the healthy myocytes and normal HEK293 cells treated with 20 mM glucose also had high levels of intracellular ROS that was diminished by incubation with insulin (Fig. 3E, 3G).

If, as revealed by the above results, the elevated intracellular ROS level and diminished endogenous antioxidant reserve are indeed the key for the functional impairment of I_{Kr}/HERG and if I_{Kr}/HERG is indeed the major ionic determinant for diabetic QT prolongation, then treatment of DM rabbits with vitamin E alone should, as insulin does, allow for alleviation of the

diabetic electrical disorders. This notion was examined by the following experiments carried out with both *in vivo* animal model and *in vitro* cell system. We first demonstrated that the abnormal QT prolongation and arrhythmias in diabetic rabbits were prevented by VitE, as indicated by virtually identical QTc interval between DM rabbits with VitE and healthy rabbits (159±4 ms, n=4). Consistently, the APD lengthening seen in single cells isolated from diabetic hearts was substantially smaller after the rabbits had been treated with VitE. These results are shown in Fig. 4A and 4B. We then observed that VitE prevented impairment of I_{Kr} in DM myocytes (Fig. 4C) and hyperglycemia-induced I_{HERG} depression in HEK293 cells (Fig. 4D). The point was further reinforced by the results showing the efficacy of another antioxidant MnTBAP to counteract with ROS so as to rescue the depressed HERG function (Fig. 4E). Moreover, the $O_2^{\cdot-}$-generating system xanthine/xanthine oxidase (X/XO) produced similar inhibitory effect on I_{HERG} as high glucose did (Fig. 4F), another evidence for the role of oxidative stress in functional impairment of HERG channels and the resultant diabetic QT prolongation.

4.4.4 Reduced protein level and membrane density of HERG K^+ channels

There is a possibility that the diabetic conditions can result in down-regulation of HERG expression contributing to the HERG dysfunction thereby QT prolongation in diabetic heart. This was indeed supported by our Western blotting analysis with membrane protein samples extracted from the hearts of healthy or diabetic rabbits and from HERG-expressing HEK293 cells. The anti-HERG antibody recognized two separate HERG bands, one with a molecular mass of 135 kDa representing the non-N-glycosylated protein and the other of 155 kDa for the N-glycosylated form of HERG. When normalized to the internal control with GAPDH for protein sample input, the densities of both bands were found to be approximately 25% smaller in DM rabbit relative to healthy animals, despite that the decrease in 135 kDa band did not reach statistical significance, indicating that HERG protein expression level was overall diminished. This decrease in HERG protein expression was diminished in DM rabbits treated with insulin or vitamin E (Fig. 5A).

To see whether the observed down-regulation of HERG expression in DM hearts was attributable to hyperglycemia, we carried out further investigations in HERG-expressing HEK293 cells. As depicted in Fig. 5B, the samples from the cells treated with 20 mM glucose

had markedly lower levels of HERG protein compared to non-treated cells. Insulin (100 nM) reversed the hyperglycemia-induced downregulation of HERG protein.

Noticeably from the immunoblotting bands and mean data in Fig. 5, the decrease in the glycosylated form was more significant than the non-glycosylated form of HERG proteins, indicating that there might be trafficking deficiency of HERG proteins. To resolve this issue, we performed immunostaining analyses as to be described below.

Cellular localization of HERG channel proteins was analyzed first by immunohistochemistry with double staining for HERG (red) and endoplasmic reticulum (ER, green) using confocal microscopy. As displayed in Fig. 6A, HERG proteins were stained along the cytoplasmic membrane with stronger staining at the intercalated discs, and ER was stained scattered in the cytosol as rod-shaped objects or punctates. Clearly, HERG staining was overall weakened in diabetic heart compared to that in healthy heart, particularly at the intercalated discs. HERG staining in ER (co-localization of HERG and ER, stained yellow) was minimal. Also, in the diabetic heart, no clear HERG retention in ER was observed as expected for trafficking deficiency. There was a possibility that the non-glycosylated form of HERG channels observed in our Western blotting bands represents the internalized portion of the proteins. To test this notion, we then performed more detailed investigation on the subcellular distribution of HERG proteins using immunocytochemistry.

To make it possible to see subcellular localization of HERG proteins, triple stainings for HERG (red), membrane (green) and nucleus (blue) were performed for our immunocytochemistry and Fig. 6B presents some typical examples of such staining. A punctate staining pattern was detected for HERG channels on the cytoplasmic membrane and intercalated discs; consistent with our immunohistochemical data, the strongest staining was found in the intercalated discs. This staining pattern was overall kept in myocytes from DM rabbits, but the density of staining was remarkably diminished, especially at the region of intercalated discs. Intriguingly, with close look at the images using higher magnifications, we found that in DM myocytes, there was a significant amount punctate staining of HERG in the cytosol adjacent to the cytoplasmic membrane (or sub-membrane localization) together with some staining in the perinuclear locations consistent with retention in the ER for misfolded proteins. However, no appreciable localization of HERG to ER was observed. By comparison, in myocytes from healthy hearts, there was little intracellular staining of HERG proteins. Consistent with the

results from immunoblotting analysis, insulin reversed the DM-induced decrease in HERG proteins as shown in Figure 6B (middle panels). Vitamin E also partially restored the density of HERG proteins in the cytoplasmic membrane.

4.5 Discussion

The results presented here reveal first time the ionic, molecular and metabolic mechanism of the QT prolongation and arrhythmias in IDDM model of rabbits. The diabetic animals had prolonged QTc, with high incidence of ventricular tachyarrhythmias and increased risk of sudden death, resembling the clinical findings with diabetic patients. The present work allowed us to get some insights into the diabetic QT prolongation with several novel and important findings. First of all, the diabetic QT prolongation and the associated arrhythmias are mainly the consequence of I_{Kr}/HERG K^+ channel dysfunction. Second, I_{Kr} K^+ channel dysfunction in diabetic heart is caused by defects at multiple levels, including functional impairment, trafficking deficiency, and probably also expression down-regulation. The metabolic perturbation in diabetic heart, especially the increased ROS presumably generated by hyperglycemia and the consequent lipid and protein oxidations, is the key factor causing I_{Kr}/HERG K^+ channel dysfunction. Finally, I_{Kr} K^+ channel dysfunction in diabetic heart is reversible and the diabetic electrical disturbances are efficiently corrected by treatment with insulin or with vitamin E. The mechanism for the beneficial actions of insulin and vitamin E is primarily ascribed to their anti-oxidant ability. Our study represents the first documentation of I_{Kr}/HERG K^+ channelopathy as an ionic mechanism for diabetic QT prolongation and oxidative stress caused by hyperglycemia as the major metabolic mechanism for I_{Kr} /HERG K^+ channelopathy.

4.5.1 I_{Kr}/HERG K^+ channelopathy as an ionic mechanism for diabetic QT prolongation and the associated arrhythmias

In the present study with alloxan-induced DM in rabbits, we reproduced the electrical disorders typical of diabetic conditions as encountered in the clinical settings. These include excessive QT prolongation (20% lengthening in our model *vs.* 18~25% lengthening in patients (1, 7-9, 11, 13, 21, 22, 29, 31, 34, 36, 44, 47, 48, 50, 51), ventricular tachyarrhythmias (5, 23, 45) and increased risk of sudden death (8, 13, 21, 29, 31, 34, 40, 50, 51). The diabetic QT

prolongation and arrhythmias (ventricular tachycardias) were entirely prevented by treatment with insulin and significantly abrogated by vitamin E. In the cellular level, APD was substantially increased to the similar extent as QTc prolongation in DM rabbits relative to age-matched healthy rabbits, an effect reversed by either insulin or vitamin E. The native I_{Kr} was suppressed in primary myocytes from DM rabbits and consistently the genetic counterpart I_{HERG} was suppressed in the expression system of HEK293 cells treated with high glucose. Either insulin or vitamin E reversed the depression of I_{Kr} and I_{HERG} in both *in vivo* and *in vitro* models. These results clearly indicate suppression of I_{Kr}/HERG as an ionic mechanism for diabetic QTc prolongation and the associated arrhythmias. The dysfunction of I_{Kr}/HERG in our models is mainly due to Impairment of HERG K^+ channel function and downregulation of HERG protein level and membrane density.

In human or rabbit ventricular cells, there are several kinds of K^+ current contributing to repolarization, including transient outward current (I_{to}), delayed rectifier currents (I_{Kr} and I_{Ks}) and inward rectifier currents (I_{K1}). All of these currents participate in one or more phases of a cardiac action potential. I_{to} initiates phase 1 repolarization and regulates the amplitude and duration of phase 2 (plateau phase). I_{Kr} terminate the plateau. The final repolarization to resting potential is produced primarily by I_{K1}. I_{Ks} may contribute to the final phase of repolarization but its role is limited under normal conditions; only when there is excessive slowing of repolarization the role of I_{Ks} becomes manifested, so-called repolarization reserve. In rat and mouse, there are additional two K^+ current components I_K and I_{ss}. Previous work aimed to elucidate ionic mechanisms of diabetic APD prolongation was performed exclusively in rats and mice. It was found that I_{to}, I_K and I_{ss} are reduced by diabetes, whereas the inward rectifier I_{K1} is not affected. As already described in Introduction, while I_{to} is important to cardiac repolarization as a major repolarizing current in rats and mice lacking I_{Kr} and when suppressed, may be responsible for diabetic APD prolongation in these species, I_{to} inhibition in human and canine hearts paradoxically shortens APD, instead of lengthening it. Thus, the claim that I_{to} inhibition underlies diabetic APD prolongation remains uncertain in humans and other mammals such as dogs and rabbits that possess I_{Kr}.

L-type Ca^{2+} current has been found either unaltered or decreased in diabetic myocytes. This is expected to result in APD shortening, instead of lengthening. Interestingly, however, it

has also been shown that the fast inactivation time constant of I_{CaL} is slowed (by ~40%) in the chronic model of diabetes (12), which may cause APD prolongation.

Based on all these previous studies and the present work, it seems plausible that dysfunction of I_{Kr}/HERG is an important ionic pathway, in addition to I_{to}, for the lengthening of APD/QT in diabetic subjects. The prolongation of APD/QT due to dysfunction of I_{Kr}/HERG and other K^+ currents causes the cell to remain longer at the depolarized plateau potential. During this long plateau phase, the slowed inactivation of L-type Ca^{2+} channels have sufficient time to become reactivated, thus provoking the renewed depolarization of the cell, leading to frequent appearance of afterpotentials. These changes could explain the increased predisposition of the diabetic patients to episodes of ventricular tachyarrhythmia. We therefore proposed that diabetic QT prolongation is primarily a HERG K^+ channelopathy.

4.5.2 Metabolic perturbation as the mechanism for dysfunction of HERG K^+ channels

Diabetes mellitus is a syndrome characterized by chronic hyperglycemia and alterations in carbohydrate, fat and protein metabolisms associated with total or partial deficiencies in insulin secretion or activity. Metabolic changes in diabetes are directly triggered by hyperglycemia.

Hyperglycemia may mediate its damaging effects through a series of secondary transducers and a common element linking hyperglycemia-induced damage is overproduction of superoxide by the mitochondrial electron-transport chain (28).

Because of the importance of insulin in the regulation of myocardial metabolism, chronic insulin deficiency or resistance results in a marked reduction in cardiac glucose utilization such that the heart relies almost exclusively on fatty acids to generate energy. High rates of fatty acid utilization in the diabetic heart could lead to functional derangements related to accumulation of lipid intermediates, excessive oxygen consumption, etc. Chronic derangements in myocardial cell metabolism, as well as impairment of various intracellular signaling pathways, may therefore have maladaptive consequences, including functional abnormalities. We have recently documented that sphingolipid metabolite ceramide that accumulates in diabetic myocardium impairs HERG function (unpublished observation). Similarly, TNF-α that is also known to elevate in its concentration and activity in diabetic myocardium suppresses I_{HERG} (55).

Intriguingly, we found that the common mechanism for HERG dysfunction induced by ceramide and TNF-α is overproduction of ROS, especially superoxide anion ($O_2^{\cdot-}$). Studies from other laboratories demonstrated that PKC phosphorylation reduces HERG activity (4) and we found that PKC activators increase intracellular ROS level and depress I_{HERG} (unpublished observation). Conversely, the intracellular substances important to maintaining HERG function such as Akt, PIP2 (6) and ATP are diminished in diabetic myocardium. Reduction of these substances can cause decrease in HERG function.

Taken together, it is conceivable that metabolic perturbations are the causal factor for the diabetic I_{Kr}/HERG dysfunction and ROS is the common pathway or key element linking metabolic perturbation with HERG dysfunction in diabetic myocardium. The direct and indirect evidence supportive of the notion from the present study include increased lipid peroxidation and protein oxidation, increased intracellular ROS level and decreased endogenous antioxidant reserve, and X/XO mimicking, while exogenous antioxidants (vitamin E and MnTBAP) alleviating, hyperglycemia-induced depression of I_{HERG}.

4.5.3 Insulin and vitamin E treatment of diabetic APD/QT prolongation and the associated arrhythmias

One of the most significant findings of the present study is that I_{Kr}/HERG dysfunction and the resultant APD/QT prolongation in diabetic hearts are preventable and reversible with treatment of either insulin or vitamin E. Strikingly, arrhythmias frequently occurring in diabetic rabbits were also abolished by insulin or vitamin E treatment. Insulin restores the diabetic depression of I_{Kr} and hyperglycemia-induced impairment of HERG activity. The mechanisms determining the efficacy of insulin are likely multiple. First of all, insulin corrects hyperglycemia by improving cellular metabolism. We show that insulin efficiently lowers blood glucose level in diabetic rabbits despite that complete restoration was not achieved at the dosage used in our experiments. Second, insulin possesses antioxidant effects; it reduces intracellular ROS level and reverses HERG depression induced by oxidative stress. Third, insulin activates its downstream component Akt that we have shown to be essential for maintaining normal HERG activity (61). Moreover, Akt mediates insulin's effects on glucose transport and metabolism, which is also important in modulating I_{Kr}/HERG function.

Perhaps the most significant observation of this study is the efficacy of antioxidant vitamin E against I_{Kr}/HERG dysfunction and APD/QT prolongation. Though surprising, this antioxidant alone is sufficient for reversing the I_{Kr}/I_{HERG} depression and the resultant APD/QT prolongation. Although the beneficial effect of vitamin E appears smaller than insulin in our model, our data simplify the complex nature of diabetic electrical disorders to primarily oxidative stress.

4.5.4 Potential implications of the findings

Accumulating data from experimental, pathological, epidemiological, and clinical studies have shown that diabetes mellitus results in cardiac functional and structural changes, independent of hypertension, coronary artery disease, autonomic neuropathy, or any other known cardiac disease, which support the existence of diabetic cardiomyopathy (2, 14). The ECG of diabetic patients shows a variety of alterations with respect to healthy people. Among these alterations, the most frequent are those related to cardiac repolarization. When QT interval is corrected for heart rate (QTc), values longer than 0.44s are considered abnormal, and this limiting value is commonly exceeded in diabetic patients (1, 7-9, 11, 13, 21, 22, 29, 31, 34, 36, 44, 47, 48, 50, 51). Prolonged QTc is associated with a higher risk of ventricular arrhythmias. Thus, these alterations can be the cause of the higher incidence of ventricular afterpotentials, the marked increase in complex arrhythmias and the higher incidence of sudden death that have been demonstrated in patients with diabetes mellitus (18, 23, 32, 45). In recent years there is increasing evidence of the appearance of ECG disorders with no association between QT prolongation and neuropathy, micro- or macro-vascular diseases, cardiovascular drugs, age or gender, being these situations additional risk factors (2, 14). Therefore, understanding the exact ionic mechanisms for diabetic QT prolongation is of pivotal importance to developing more rational approaches for the prevention and treatment of the electrical disorders and the associated arrhythmias and sudden cardiac death. The present study is the first to document I_{Kr}/HERG as the major ionic pathway through which the diabetic heart acquires abnormal QT prolongation and ventricular tachyarrhythmias.

Increasing evidence from both experimental and clinical studies suggests that oxidative stress plays a major role in the pathogenesis of both types of diabetes mellitus (28). Free radicals are formed disproportionately in diabetes by glucose oxidation, nonenzymatic glycation of

proteins, and the subsequent oxidative degradation of glycated proteins. Abnormally high levels of free radicals and the simultaneous decline of antioxidant defense mechanisms can lead to damages of cellular organelles and enzymes, increased lipid peroxidation, and development of insulin resistance. Our study represents the first to show that oxidative stress as a result of metabolic perturbations is the major cause for I_{Kr}/HERG dysfunction and the consequent QT prolongation in diabetes. Pathophysiologically important is that I_{Kr}/HERG dysfunction and the resultant APD/QTc prolongation in diabetic heart are reversible; treatment with insulin or vitamin E rescues I_{Kr}/HERG and prevents APD/QT prolongation. While the efficacy of insulin may be limited to type I insulin-dependent diabetes with suboptimal value for type II insulin-resistant diabetes, our finding that vitamin E has similar effects as insulin at least on I_{Kr}/HERG dysfunction and the resultant APD/QT prolongation suggests an alternative approach for the therapy of diabetic electrical disturbances. Antioxidants, albeit with minimal therapeutic value for diabetes *per se*, can be used for correcting the abnormal APD/QT prolongation. This is particularly important considering that I_{Kr}/HERG enhancer is currently unavailable. Alternatively, any interventions that can boost up Akt level and activity should enhance I_{Kr}/HERG function on one hand and improve cellular metabolism on the other hand since we have demonstrated that Akt serves to maintain the normal I_{Kr}/HERG function (60) and Akt is known to be critical to the insulin signaling pathway. These points imply that "metabolic correction" may be considered a more rational therapeutic approach for QT prolongation and the associated arrhythmias in diabetic patients.

4.5.5 Possible limitations of the study

Several issues that might limit the application of the results from this study to clinical practice should be mentioned. First, our model deals with only type I insulin-dependent diabetes, and the ionic and metabolic mechanisms for APD/QT prolongation in type II insulin-resistant diabetes may not be exactly the same. In reality, type II diabetes consists of more than 90% of the total diabetic patients in clinics. Nonetheless, APD/QT prolongation observed in type I diabetes is also known to be present at the similar percentage in type II diabetic patients. And the trigger of metabolic perturbations, hyperglycemia, and the key element for HERG impairment, ROS, are present in both type I and type II diabetic subjects. Moreover, except for the difference between insulin insufficiency and insulin resistance, other metabolic perturbations are quite

similar between type I and type II diabetes. Hence, it is not unreasonable to believe that I_{Kr}/ HERG dysfunction is also the cause for the APD/QT prolongation existing in type II diabetes. Second, our data obtained from rabbits may not be applicable to humans since there exist interspecies differences. Nevertheless, our rabbit model reproduces nearly all the phenotypes pertinent to the electrophysiological alterations seen in clinical diabetes. Also important are that rabbit I_{Kr} shares many similarities to human I_{Kr} in term of their biophysical characteristics and pharmacological properties (38) and that rabbit ERG channel sequence (Genbank accession U87513) is around 93% and 96% homologous to human ERG at the nucleotide and amino acid levels, respectively (55-57). Even the expression levels of *ERG* gene are quite comparable between the two species (63). These facts suggest that the I_{Kr}/HERG dysfunction observed in our rabbit model may also be applied to patients. Finally, I_{Ks} also has the potential to contribute to diabetic APD/QT prolongation although it has limited role in cardiac repolarization under physiologic conditions. I_{Ks} acts as repolarization reserve to limit excess slowing of repolarization and when it is depressed this safety factor is removed so that inhibition of other repolarizing current such as I_{Kr} could lead to tremendous APD/QT prolongation. However, whether I_{Ks} plays a role in diabetic APD/QT prolongation remained unknown and the present study cannot resolve the issue; it is an on-going research project in our laboratory.

4.5.6 Conclusion

Based on our data and above discussion, we were able to draw the following conclusions. First, the abnormal APD/QT prolongation in diabetic subjects is partly a HERG K^+ channelopathy; or in other words, HERG dysfunction is an important or even the major ionic mechanism underlying diabetic APD/QT prolongation, which forms the electrophysiologic substrate for increased propensity of arrhythmias in diabetic hearts. HERG dysfunction includes functional impairment, expression down-regulation and metabolic alteration. Second, cellular metabolic perturbations are the direct mechanism underlying dysfunction of HERG channels. The diabetic metabolic perturbations are triggered mainly by hyperglycemia and the latter, besides resulting in deficiency of energy metabolism and accumulation of glycolysis end-products, stimulates over-production of ROS. ROS appears the common pathway linking metabolic perturbations to HERG dysfunction. Finally, of particular significance is our finding that correction of abnormal metabolic status by insulin reverses HERG dysfunction thereby

diabetic APD/QT prolongation and more so is our data showing the efficacy of vitamin E in protecting HERG function and preventing diabetic APD/QT prolongation. These imply that antioxidants, albeit with little value for the treatment of diabetes *per se*, may find their value in antagonizing diabetic electrical disturbances thereby alleviating diabetic cardiocomplications or cardiomyopathy.

A schematic chart is presented in Figure 7 which illustrates the changes of metabolic status in diabetic myocardium with increases or decreases in an array of enzymes, signaling molecules and metabolic substances that have been shown to modulate HERG function. In principle, the factors positively modulate HERG (such as insulin, Akt) decrease and those produce negative modulation of HERG (such as TNF-α, ceramide, PKC) increase in diabetic hearts. Thus, the metabolic status is shifted towards the direction in favor of ROS production leading to HERG dysfunction. Evidently, "metabolic correction" may be a better therapeutic approach for diabetic QT prolongation and the associated arrhythmias. It should be emphasized that by proposing this theme, we are in no way trying to exclude the role of other ion currents/channels in contributing to diabetic QT prolongation and arrhythmias. Instead, we consider I_{Kr}/HERG as a part of the multiple players including I_{to}, I_{ss}, I_{CaL}, etc.

4.6 Acknowledgements

The authors wish to thank XiaoFan Yang and Marc-Antoine Gillis for excellent technical supports. This work was supported in part by the Canadian Diabetes Association and the Fonds de la Recherche de l'Institut de Cardiologie de Montreal, awarded to Dr. Z Wang. Dr. Z Wang is a senior research scholar of the Fonds de Recherche en Sante de Quebec and a recipient of Scholarship of Quebec Diabetes Society (2004). Y Zhang is a recipient of Doctoral-Studentship of the Heart and Stroke Foundation of Canada. J Wang is a recipient of Doctoral-Studentship of the Fonds de Recherche en Sante de Quebec.

4.7 References

1. **Abo K, Ishida Y, Yoshida R, Hozumi T, Ueno H, Shiotani H, Matsunaga K and Kazumi T**. Torsade de pointes in NIDDM with long QT intervals. *Diabetes Care* 19: 1010, 1996.
2. **Avogaro A, Vigili dK, Negut C, Tiengo A and Scognamiglio R**. Diabetic cardiomyopathy: a metabolic perspective. *Am J Cardiol* 93: 13A-16A, 2004.
3. **Baric L**. Heart in the elderly (views and considerations at the turn of the centuries). *Acta Med Croatica* 53: 171-178, 1999.
4. **Barros F, Gomez-Varela D, Viloria CG, Palomero T, Giraldez T and de la PP**. Modulation of human erg K^+ channel gating by activation of a G protein-coupled receptor and protein kinase C. *J Physiol* 511 (Pt 2): 333-346, 1998.
5. **Benjamin EJ, Levy D, Vaziri SM, D'Agostino RB, Belanger AJ and Wolf PA**. Independent risk factors for atrial fibrillation in a population-based cohort. The Framingham Heart Study. *JAMA* 271: 840-844, 1994.
6. **Bian J, Cui J and McDonald TV**. HERG K^+ channel activity is regulated by changes in phosphatidyl inositol 4,5-bisphosphate. *Circ Res* 89: 1168-1176, 2001.
7. **Brown DW, Giles WH, Greenlund KJ, Valdez R and Croft JB**. Impaired fasting glucose, diabetes mellitus, and cardiovascular disease risk factors are associated with prolonged QTc duration. Results from the Third National Health and Nutrition Examination Survey. *J Cardiovasc Risk* 8: 227-233, 2001.
8. **Cardoso CR, Salles GF and Deccache W**. Prognostic value of QT interval parameters in type 2 diabetes mellitus: results of a long-term follow-up prospective study. *J Diabetes Complications* 17: 169-178, 2003.
9. **Cardoso CR, Salles GF and Deccache W**. QTc interval prolongation is a predictor of future strokes in patients with type 2 diabetes mellitus. *Stroke* 34: 2187-2194, 2003.
10. **Carlsson L, Abrahamsson C, Andersson B, Duker G and Schiller-Linhardt G**. Proarrhythmic effects of the class III agent almokalant: importance of infusion rate, QT dispersion, and early afterdepolarisations. *Cardiovasc Res* 27: 2186-2193, 1993.

11. **Casis O and Echevarria E.** Diabetic cardiomyopathy: electromechanical cellular alterations. *Curr Vasc Pharmacol* 2: 237-248, 2004.
12. **Chattou S, Diacono J and Feuvray D.** Decrease in sodium-calcium exchange and calcium currents in diabetic rat ventricular myocytes. *Acta Physiol Scand* 166: 137-144, 1999.
13. **Christensen PK, Gall MA, Major-Pedersen A, Sato A, Rossing P, Breum L, Pietersen A, Kastrup J and Parving HH.** QTc interval length and QT dispersion as predictors of mortality in patients with non-insulin-dependent diabetes. *Scand J Clin Lab Invest* 60: 323-332, 2000.
14. **Fang ZY, Prins JB and Marwick TH.** Diabetic cardiomyopathy: evidence, mechanisms, and therapeutic implications. *Endocr Rev* 25: 543-567, 2004.
15. **Frustaci A, Kajstura J, Chimenti C, Jakoniuk I, Leri A, Maseri A, Nadal-Ginard B and Anversa P.** Myocardial cell death in human diabetes. *Circ Res* 87: 1123-1132, 2000.
16. **Green EA and Flavell RA.** Tumor necrosis factor-alpha and the progression of diabetes in non-obese diabetic mice. *Immunol Rev* 169: 11-22, 1999.
17. **Green EA, Wong FS, Eshima K, Mora C and Flavell RA.** Neonatal tumor necrosis factor alpha promotes diabetes in nonobese diabetic mice by CD154-independent antigen presentation to $CD8^+$-T cells. *J Exp Med* 191: 225-238, 2000.
18. **Grossmann G, Schwentikowski M, Keck FS, Hoher M, Steinbach G, Osterhues H and Hombach V.** Signal-averaged electrocardiogram in patients with insulin-dependent (type 1) diabetes mellitus with and without diabetic neuropathy. *Diabet Med* 14: 364-369, 1997.
19. **Gumieniczek A, Hopkala H, Wojtowicz Z and Nikolajuk J.** Changes in antioxidant status of heart muscle tissue in experimental diabetes in rabbits. *Acta Biochim Pol* 49: 529-535, 2002.
20. **Hayat S, Patel B, Khattar RS and Malik RA.** Diabetic cardiomyopathy: mechanisms, diagnosis and treatment. *Clin Sci (Lond)* 107: 539-557, 2004.
21. **Kahn JK, Sisson JC and Vinik AI.** QT interval prolongation and sudden cardiac death in diabetic autonomic neuropathy. *J Clin Endocrinol Metab* 64: 751-754, 1987.
22. **Ko GT, Chan JC, Critchley JA and Cockram CS.** Cardiovascular disease in Chinese type 2 diabetic women is associated with a prolonged QTc interval. *Int J Cardiol* 76: 75-80, 2000.

23. **Kowalewski MA, Urban M, Florys B and Peczynska J**. Late potentials: are they related to cardiovascular complications in children with type 1 diabetes? *J Diabetes Complications* 16: 263-270, 2002.

24. **Liu XK, Katchman A, Drici MD, Ebert SN, Ducic I, Morad M and Woosley RL**. Gender difference in the cycle length-dependent QT and potassium currents in rabbits. *J Pharmacol Exp Ther* 285: 672-679, 1998.

25. **Lopaschuk GD**. Metabolic abnormalities in the diabetic heart. *Heart Fail Rev* 7: 149-159, 2002.

26. **Mahgoub MA and Abd-Elfattah AS**. Diabetes mellitus and cardiac function. *Mol Cell Biochem* 180: 59-64, 1998.

27. **Marfella R, Rossi F and Giugliano D**. Hyperglycemia and QT interval: time for re-evaluation. *Diabetes Nutr Metab* 14: 63-65, 2001.

28. **Maritim AC, Sanders RA and Watkins JB, III**. Diabetes, oxidative stress, and antioxidants: a review. *J Biochem Mol Toxicol* 17: 24-38, 2003.

29. **Okin PM, Devereux RB, Lee ET, Galloway JM and Howard BV**. Electrocardiographic repolarization complexity and abnormality predict all-cause and cardiovascular mortality in diabetes: the strong heart study. *Diabetes* 53: 434-440, 2004.

30. **Pearson WR, Wood T, Zhang Z and Miller W**. Comparison of DNA sequences with protein sequences. *Genomics* 46: 24-36, 1997.

31. **Rana BS, Lim PO, Naas AA, Ogston SA, Newton RW, Jung RT, Morris AD and Struthers AD**. QT interval abnormalities are often present at diagnosis in diabetes and are better predictors of cardiac death than ankle brachial pressure index and autonomic function tests. *Heart* 91: 44-50, 2005.

32. **Robillon JF, Sadoul JL, Jullien D, Morand P and Freychet P**. Abnormalities suggestive of cardiomyopathy in patients with type 2 diabetes of relatively short duration. *Diabete Metab* 20: 473-480, 1994.

33. **Rodrigues B, Cam MC and McNeill JH**. Myocardial substrate metabolism: implications for diabetic cardiomyopathy. *J Mol Cell Cardiol* 27: 169-179, 1995.

34. **Rossing P, Breum L, Major-Pedersen A, Sato A, Winding H, Pietersen A, Kastrup J and Parving HH**. Prolonged QTc interval predicts mortality in patients with Type 1 diabetes mellitus. *Diabet Med* 18: 199-205, 2001.

35. **Rubler S, Dlugash J, Yuceoglu YZ, Kumral T, Branwood AW and Grishman A.** New type of cardiomyopathy associated with diabetic glomerulosclerosis. *Am J Cardiol* 30: 595-602, 1972.

36. **Rutter MK, Viswanath S, McComb JM, Kesteven P and Marshall SM.** QT prolongation in patients with Type 2 diabetes and microalbuminuria. *Clin Auton Res* 12: 366-372, 2002.

37. **Saghizadeh M, Ong JM, Garvey WT, Henry RR and Kern PA.** The expression of TNF alpha by human muscle. Relationship to insulin resistance. *J Clin Invest* 97: 1111-1116, 1996.

38. **Salata JJ, Jurkiewicz NK, Jow B, Folander K, Guinosso PJ, Jr., Raynor B, Swanson R and Fermini B.** I_K of rabbit ventricle is composed of two currents: evidence for I_{Ks}. *Am J Physiol* 271: H2477-H2489, 1996.

39. **Sanguinetti MC, Jiang C, Curran ME and Keating MT.** A mechanistic link between an inherited and an acquired cardiac arrhythmia: HERG encodes the I_{Kr} potassium channel. *Cell* 81: 299-307, 1995.

40. **Sawicki PT, Dahne R, Bender R and Berger M.** Prolonged QT interval as a predictor of mortality in diabetic nephropathy. *Diabetologia* 39: 77-81, 1996.

41. **Sawicki PT, Kiwitt S, Bender R and Berger M.** The value of QT interval dispersion for identification of total mortality risk in non-insulin-dependent diabetes mellitus. *J Intern Med* 243: 49-56, 1998.

42. **Shimoni Y.** Inhibition of the formation or action of angiotensin II reverses attenuated K^+ currents in type 1 and type 2 diabetes. *J Physiol* 537: 83-92, 2001.

43. **Shimoni Y, Ewart HS and Severson D.** Type I and II models of diabetes produce different modifications of K^+ currents in rat heart: role of insulin. *J Physiol* 507 (Pt 2): 485-496, 1998.

44. **Suys BE, Huybrechts SJ, De Wolf D, Op DB, Matthys D, Van Overmeire B, Du Caju MV and Rooman RP.** QTc interval prolongation and QTc dispersion in children and adolescents with type 1 diabetes. *J Pediatr* 141: 59-63, 2002.

45. **Tong NW, Yang TG and Liang JZ.** [Ventricular late potentials in patients with diabetes mellitus]. *Zhonghua Nei Ke Za Zhi* 32: 464-466, 1993.

46. **Tsuchida K and Watajima H.** Potassium currents in ventricular myocytes from genetically diabetic rats. *Am J Physiol* 273: E695-E700, 1997.

47. **Veglio M, Borra M, Stevens LK, Fuller JH and Perin PC**. The relation between QTc interval prolongation and diabetic complications. The EURODIAB IDDM Complication Study Group. *Diabetologia* 42: 68-75, 1999.

48. **Veglio M, Bruno G, Borra M, Macchia G, Bargero G, D'Errico N, Pagano GF and Cavallo-Perin P**. Prevalence of increased QT interval duration and dispersion in type 2 diabetic patients and its relationship with coronary heart disease: a population-based cohort. *J Intern Med* 251: 317-324, 2002.

49. **Veglio M, Chinaglia A and Cavallo PP**. The clinical utility of QT interval assessment in diabetes. *Diabetes Nutr Metab* 13: 356-365, 2000.

50. **Veglio M, Chinaglia A and Cavallo-Perin P**. QT interval, cardiovascular risk factors and risk of death in diabetes. *J Endocrinol Invest* 27: 175-181, 2004.

51. **Veglio M, Sivieri R, Chinaglia A, Scaglione L and Cavallo-Perin P**. QT interval prolongation and mortality in type 1 diabetic patients: a 5-year cohort prospective study. Neuropathy Study Group of the Italian Society of the Study of Diabetes, Piemonte Affiliate. *Diabetes Care* 23: 1381-1383, 2000.

52. **Wang DW, Kiyosue T, Shigematsu S and Arita M**. Abnormalities of K^+ and Ca^{2+} currents in ventricular myocytes from rats with chronic diabetes. *Am J Physiol* 269: H1288-H1296, 1995.

53. **Wang H, Zhang Y, Cao L, Han H, Wang J, Yang B, Nattel S and Wang Z**. HERG K^+ channel, a regulator of tumor cell apoptosis and proliferation. *Cancer Res* 62: 4843-4848, 2002.

54. **Wang J, Wang H, Han H, Zhang Y, Yang B, Nattel S and Wang Z**. Phospholipid metabolite 1-palmitoyl-lysophosphatidylcholine enhances human ether-a-go-go-related gene (HERG) K^+ channel function. *Circulation* 104: 2645-2648, 2001.

55. **Wang J, Wang H, Zhang Y, Gao H, Nattel S and Wang Z**. Impairment of HERG K^+ channel function by tumor necrosis factor-alpha: role of reactive oxygen species as a mediator. *J Biol Chem* 279: 13289-13292, 2004.

56. **Wang Z, Fermini B and Nattel S**. Delayed rectifier outward current and repolarization in human atrial myocytes. *Circ Res* 73: 276-285, 1993.

57. **Wang Z, Fermini B and Nattel S**. Rapid and slow components of delayed rectifier current in human atrial myocytes. *Cardiovasc Res* 28: 1540-1546, 1994.

58. **Wang Z, Fermini B and Nattel S.** Effects of flecainide, quinidine, and 4-aminopyridine on transient outward and ultrarapid delayed rectifier currents in human atrial myocytes. *J Pharmacol Exp Ther* 272: 184-196, 1995.

59. **Wymore RS, Gintant GA, Wymore RT, Dixon JE, McKinnon D and Cohen IS.** Tissue and species distribution of mRNA for the I_{Kr}-like K^+ channel, erg. *Circ Res* 80: 261-268, 1997.

60. **Zhang Y, Han H, Wang J, Wang H, Yang B and Wang Z.** Impairment of HERG (human ether-a-go-go related gene) K^+ channel function by hypoglycemia and hyperglycemia: Similar phenotypes but different mechanisms. *J Biol Chem* 278: 10417-10426, 2003.

61. **Zhang Y, Wang H, Wang J, Han H, Nattel S and Wang Z.** Normal function of HERG K^+ channels expressed in HEK293 cells requires basal protein kinase B activity. *FEBS Lett* 534: 125-132, 2003.

62. **Zhou Z, Gong Q, Ye B, Fan Z, Makielski JC, Robertson GA and January CT.** Properties of HERG channels stably expressed in HEK 293 cells studied at physiological temperature. *Biophys J* 74: 230-241, 1998.

63. **Zicha S, Moss I, Allen B, Varro A, Papp J, Dumaine R, Antzelevich C and Nattel S.** Molecular basis of species-specific expression of repolarizing K^+ currents in the heart. *Am J Physiol Heart Circ Physiol* 285: H1641-H1649, 2003.

64. **Ziolo MT, Sondgeroth KL, Harshbarger CH, Smith JM and Wahler GM.** Effects of arrhythmogenic lipid metabolites on the L-type calcium current of diabetic vs. non-diabetic rat hearts. *Mol Cell Biochem* 220: 169-175, 2001.

65. **Zola BE, Miller B, Stiles GL, Rao PS, Sonnenblick EH and Fein FS.** Heart rate control in diabetic rabbits: blunted response to isoproterenol. *Am J Physiol* 255: E636-E641, 1988.

4.8 Figures and Figure Legends

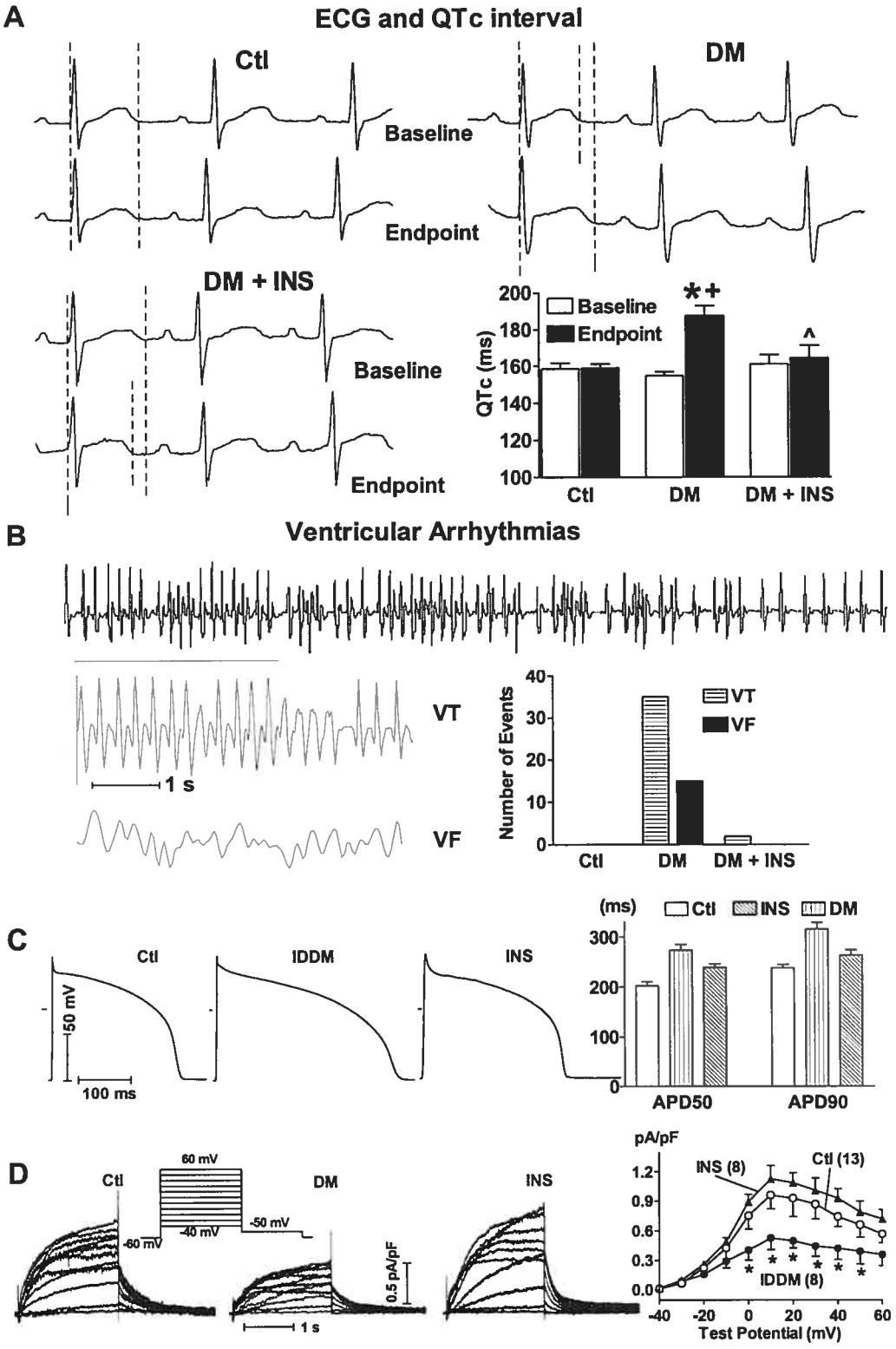

Figure 1. Electrical disorders and the ionic mechanism in rabbits with insulin-dependent diabetes mellitus (DM) and insulin treatment. *A*, Abnormal prolongation of QT interval in DM rabbits. Upper panel: Representative ECG recordings before alloxan injection for baseline data and 10 weeks after alloxan for endpoint data in anesthetized rabbits, showing prolongation of QT interval. Ctl: control sham-treated and age-matched rabbits; DM: rabbit with diabetes mellitus; INS: insulin. Lower panel: Mean data (n=12 rabbits for Ctl, n=14 for DM, and n=5 for DM/INS) of heart rate-corrected QT interval (QTc interval). **p*<0.05 *vs.* Ctl (endpoint); +*p*<0.05 *vs.* DM (baseline); ^p<0.05 *vs.* DM (endpoint). *B*, Ventricular arrhythmias in DM rabbits. Upper panel and lower left panels: Examples of polymorphic ventricular tachy-arrhythmias (VT, *Torsade de Pointes*) in a DM rabbit and of ventricular fibrillation (VF) occurring 2 min before sudden death of a DM rabbit, recorded by an ECG telemeter. Lower right panel: Mean data of incidence of VT and VF. Data in each group are from 3 rabbits with telemetry ECG recordings. *C*, Prolongation of action potential duration (APD) in DM rabbits. Left panels: Analog data of APs recorded from single ventricular myocytes. Right panel: Mean data of APD at 50% (APD_{50}) and 90% (APD_{90}) repolarization, respectively (n=12 cells from 4-5 rabbits). **p*<0.05 *vs.* Ctl; +*p*<0.05 *vs.* DM alone. *D*, Depression of rapid delayed rectifier K^+ current (I_{Kr}) in DM rabbits. Left panels: Cell-capacitance normalized I_{Kr} traces recorded from isolated ventricular myocytes with the voltage protocols shown in the inset. Shown are dofetilide (1 μM)-sensitive currents. Right panel: Mean data of current density as a function of testing potential. Cell numbers from 4 to 6 hearts are indicated in brackets. **p*<0.05 *vs.* Ctl.

Figure 2

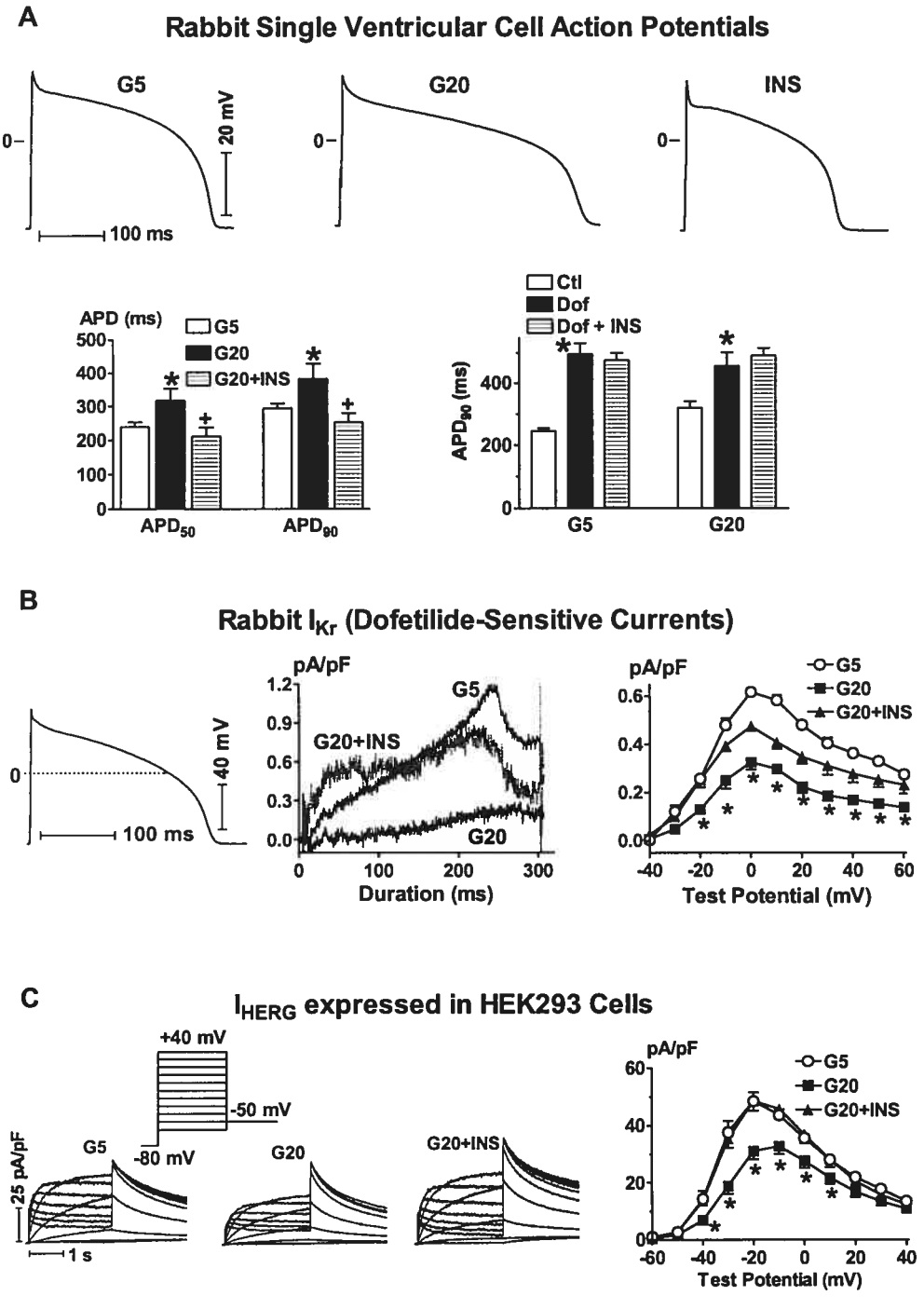
A
Rabbit Single Ventricular Cell Action Potentials
G5
G20
INS
0
20 mV
100 ms
APD (ms)
G5
G20
G20+INS
APD50
APD90
Ctl
Dof
Dof + INS
APD90 (ms)
G5
G20
B
Rabbit IKr (Dofetilide-Sensitive Currents)
40 mV
100 ms
pA/pF
G5
G20+INS
G20
Duration (ms)
Test Potential (mV)
C
IHERG expressed in HEK293 Cells
+40 mV
-50 mV
-80 mV
G5
G20
G20+INS
25 pA/pF
1 s
Test Potential (mV)

Figure 2. Metabolic mechanisms for diabetic APD prolongation: high glucose and insulin treatment. Metabolic mechanisms for diabetic APD prolongation: high glucose and insulin treatment. *A*, Insulin reverses hyperglycemia-induced abnormal APD prolongation in rabbit ventricular myocytes. Upper panels: Raw traces of action potentials (APs). G5: glucose 5 mM; G20 glucose 20 mM; INS: insulin 100 nM. Lower left panel: Mean data of APD_{50} and APD_{90}, showing the effects of INS on G20-induced APD prolongation. *$p<0.05$ *vs.* G5; +$p<0.05$ *vs.* G20. n=20 for G5; n=16 for G20; n=13 for G20+INS. Lower right panel: Mean data showing the effects of INS on APD in the presence of dofetilide (Dof, 1 μM). Ctl: Dof-untreated cells. *$p<0.05$ *vs.* Dof alone. *B*, Insulin reverses hyperglycemia-induced impairment of I_{Kr} in rabbit ventricular myocytes. I_{Kr} was elicited either by action potential-clamp (AP-clamp) techniques or by conventional pulse protocols. Left panel: The AP waveform from a left ventricular myocyte used for evoking I_{Kr}. Middle panel: The raw I_{Kr} traces (dofetilide-sensitive currents) recorded with AP-clamp techniques. Right panel: Mean I (density)-V relationships of I_{Kr} (dofetilide-sensitive currents) obtained using conventional pulse protocols as shown in the inset of Figure 1D. *$p<0.05$ *vs.* G5. *C*, Effects of insulin on I_{HERG} in HERG-expressing HEK293 cells. I_{HERG} was recorded with the voltage protocols shown in the inset. Left panels: The capacitance-normalized I_{HERG} traces. Right panel: Mean data on I-V relationships. *$p<0.05$ *vs.* G5, and +$p<0.05$ *vs.* G20. n=14 cells for G5, n=16 cells for G20, and n=14 for G20+INS.

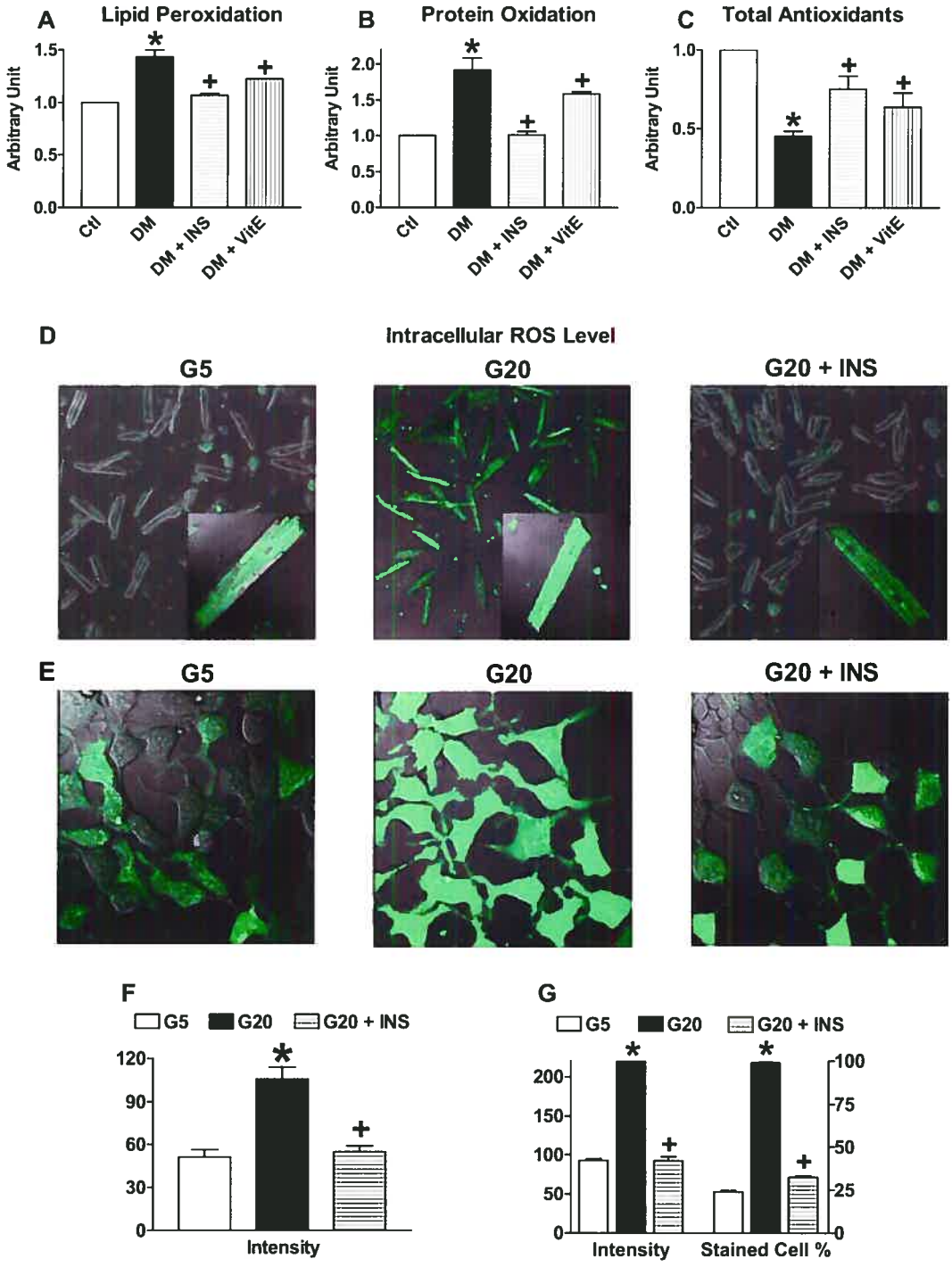
A
Lipid Peroxidation
Arbitrary Unit
1.5
1.0
0.5
0.0
Ctl
DM
DM + INS
DM + VitE
B
Protein Oxidation
Arbitrary Unit
2.0
1.5
1.0
0.5
0.0
Ctl
DM
DM + INS
DM + VitE
C
Total Antioxidants
Arbitrary Unit
1.0
0.5
0.0
Ctl
DM
DM + INS
DM + VitE
D
Intracellular ROS Level
G5
G20
G20 + INS
E
G5
G20
G20 + INS
F
G5
G20
G20 + INS
120
90
60
30
0
Intensity
G
G5
G20
G20 + INS
200
150
100
50
0
100
75
50
25
0
Intensity
Stained Cell %

Figure 3

Figure 3. Metabolic mechanisms for diabetic APD prolongation and insulin treatment. *A*, Lipid hydroperoxidation in myocardium from healthy (Ctl), DM, DM+insulin (INS) or DM+vitamin E (VitE) rabbits. Shown are averaged data obtained from experiments performed in duplicate from three hearts for each group. *p<0.05 *vs.* Ctl; +p<0.05 *vs.* DM alone. *B*, Protein carbonyl oxidation in myocardium from healthy (Ctl), DM, DM+INS or DM+VitE rabbits. Shown are averaged data obtained from experiments performed in triplicate from three hearts for each group. *p<0.05 *vs.* Ctl; +p<0.05 *vs.* DM alone. *C*, Total endogenous antioxidant level in the plasma. Shown are averaged data obtained from experiments performed in duplicate from 3-4 hearts for each group. *p<0.05 *vs.* Ctl; +p<0.05 *vs.* DM alone. *D-G*, Overproduction of intracellular reactive oxygen species (ROS) induced by high glucose (G20, glucose 20 mM) in myocytes isolated from left ventricular endocardium of rabbit hearts (*D* and *F*) or in HERG-expressing HEK293 cells (*E* and *G*). Example images are shown and the green fluorescence indicates ROS staining (*D* and *E*). The mean data were acquired from 24-26 cardiomyocytes (*F*) and from 85-126 HEK293 cells (*G*). *p<0.05 *vs.* G5; +p<0.05 *vs.* G20 alone.

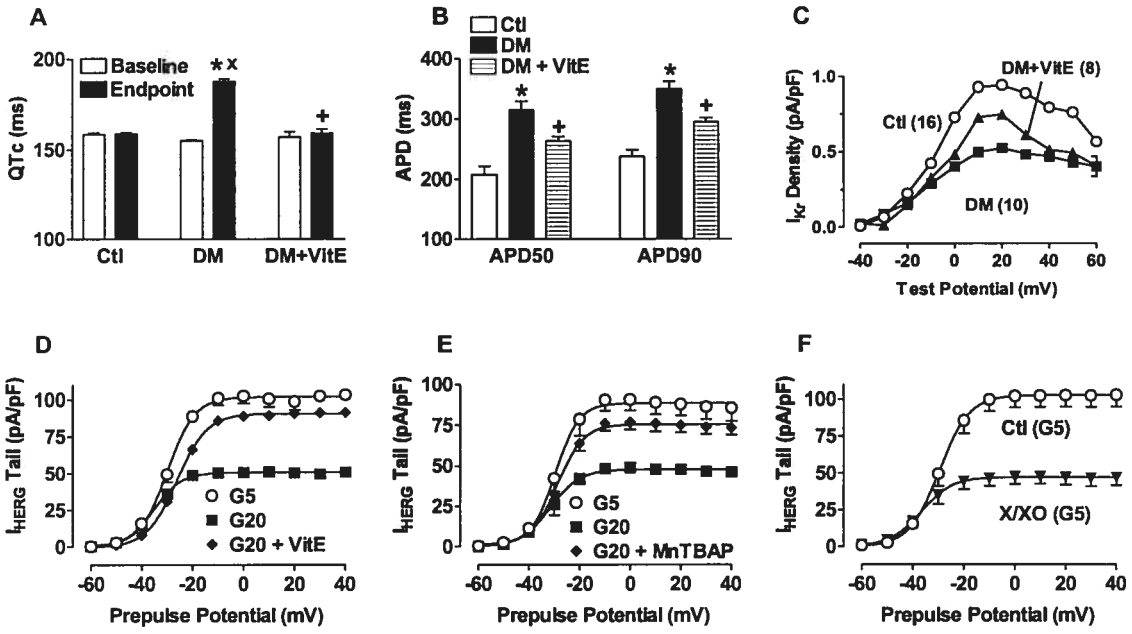

Figure 4. Role of oxidative stress in diabetic QT/APD prolongation and vitamin E treatment. *A,* Effects of vitamin E (VitE) on QTc interval and arrhythmias in DM rabbits. **p*<0.05 *vs.* Ctl (endpoint); ^{+}p<0.05 *vs.* DM (baseline); ^p<0.05 *vs.* DM (endpoint). n=12 for Ctl, n=14 for DM and n=4 for DM+VitE. *B*, Effects of VitE on APD in myocytes isolated from left ventricular endocardium of DM rabbits. Shown are mean data of APD at 50% (APD_{50}) and 90% (APD_{90}) repolarization, respectively (n=12 cells from 4-5 rabbits). **p*<0.05 *vs.* Ctl; +*p*<0.05 *vs.* DM alone. n=12 for Ctl, n=12 for DM and n=10 for DM+VitE. *C*, Averaged I (density)-V relationships of I_{Kr} (dofetilide-sensitive currents) in myocytes isolated from left ventricular endocardium of DM rabbits, showing the effects of VitE on DM-induced depression of I_{Kr}. **p*<0.05 *vs.* Ctl; +*p*<0.05 *vs.* DM alone. Values in the brackets indicate the number of cells studied. *D-E,* Effects of antioxidants VitE (100 μM) or MnTBAP (5 μM) on I_{HERG} impairment induced by hyperglycemia (G20, glucose 20 mM) in HERG-expressing HEK293 cells. n=5 for each group. *F*, Effects of the superoxide anion-generating system xanthine/xanthine oxidase (X/XO) on I_{HERG} in HERG-expressing HEK293 cells. X: 500 μM and XO: 5mU/ml, n=5 for each group.

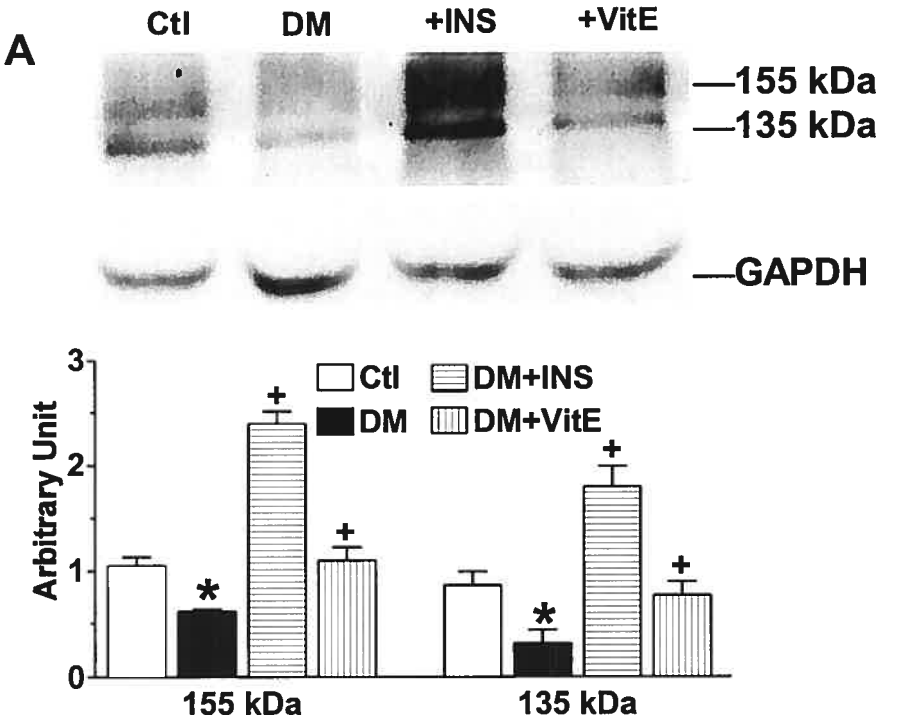
A
Ctl
DM
+INS
+VitE
—155 kDa
—135 kDa
—GAPDH
Arbitrary Unit
Ctl
DM
DM+INS
DM+VitE
155 kDa
135 kDa

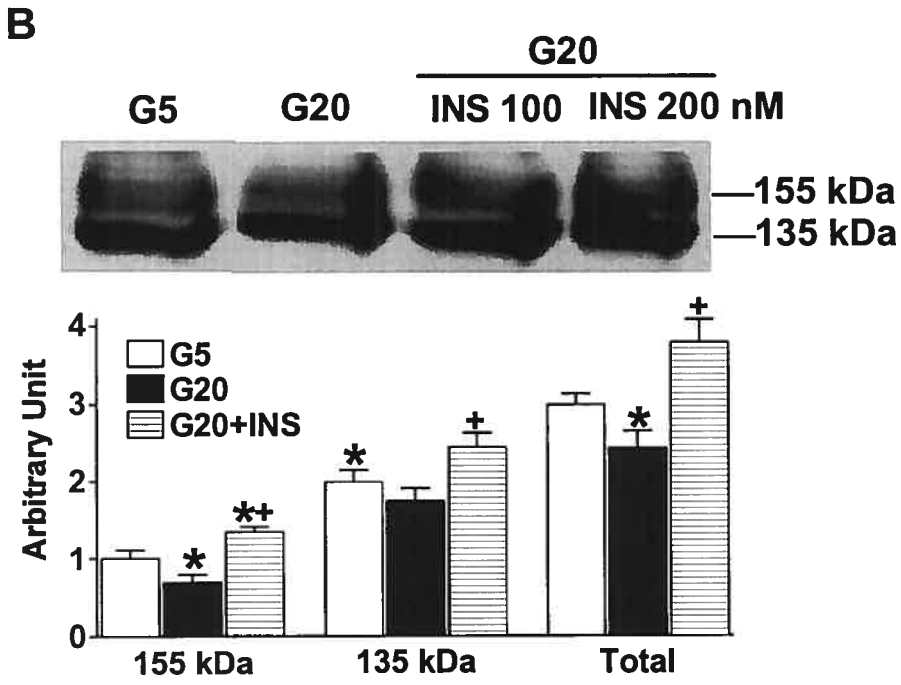
B
G5
G20
G20
INS 100
INS 200 nM
—155 kDa
—135 kDa
Arbitrary Unit
G5
G20
G20+INS
155 kDa
135 kDa
Total

Figure 5

Figure 5. Alterations of protein levels of HERG K^+ channels. *A,* HERG protein level assessed by Western blot analysis with the membrane samples extracted from rabbit hearts. Upper panel: Examples of Western blot bands with anti-HERG and anti-GAPDH antibodies. Lower panel: Mean data of densitometric analysis of the bands corresponding to the non-N-glycosylated form (135 kDa) and N-glycosylated (155 kDa) forms of HERG; the data were normalized to GAPDH and expressed as fold changes over control 155 kDa band. n=6 hearts for Ctl, n=7 hearts for DM, n=4 for DM+INS and n=3 for DM+VitE. *$p<0.05$ *vs.* Ctl; +$p<0.05$ *vs.* DM alone. *B*, HERG protein level assessed by Western blot analysis with the membrane samples extracted from HERG-expressing HEK293 cells. Upper panel: Examples of Western blot bands. Lower panel: Mean data of band density normalized to the G5-155 kDa band; the concentration of insulin for the mean data is 100 nM. *$p<0.05$ *vs.* Ctl; +$p<0.05$ *vs.* G20 alone; n=4 independent experiments for each group.

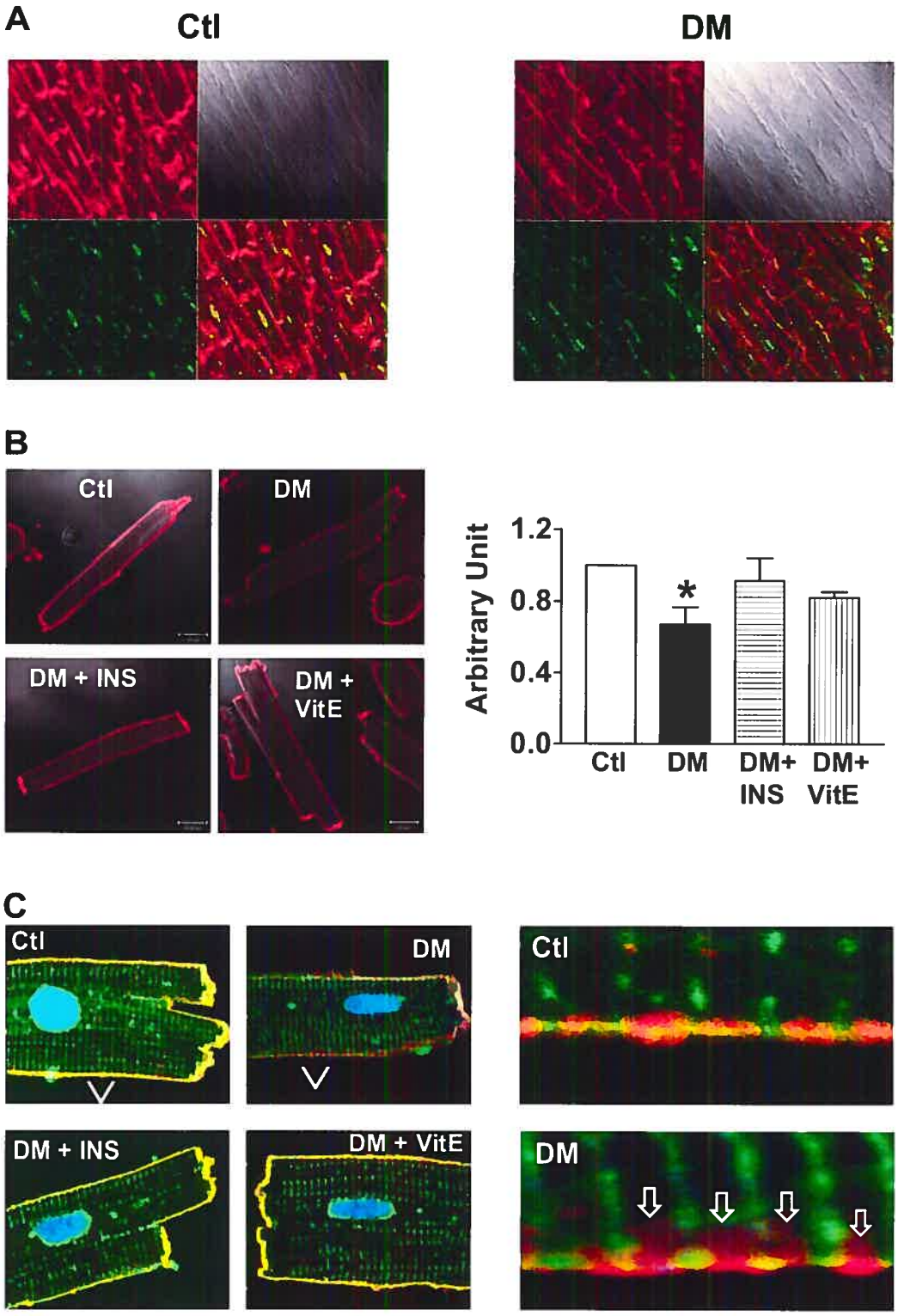
A
Ctl
DM
B
Ctl
DM
DM + INS
DM + VitE
Arbitrary Unit
1.2
0.8
0.4
0.0
*
Ctl
DM
DM+ INS
DM+ VitE
C
Ctl
DM
DM + INS
DM + VitE
Ctl
DM

Figure 6

Figure 6. Subcellular distribution and membrane density of HERG channel protein. *A,* Immunohistochemical analysis of HERG with left ventricular samples from healthy and DM rabbits. HERG is stained in red with anti-HERG antibody and endoplasmic reticulum (ER) is stained in green with anti-BIP antibody. Note that the intensity of HERG staining is weaker in the DM tissue than in the healthy tissue, particularly at the intercalated disks. *B*, Immunocytochemical analysis of HERG in the ventricular myocytes isolated from healthy and DM rabbits. Left panels: Examples of laser scanning confocal microscopic images showing the alterations of the cytoplasmic membrane density of HERG K^+ channel proteins (red). Right panel: Mean values on fold changes of HERG staining on the cell membrane. *$p<0.05$ *vs.* Ctl; +$p<0.05$ *vs.* DM alone. Data are from 2-3 three rabbits in each group and 5-8 cells for each rabbit. *C*, Left panels: Examples of triple staining showing the subcellular distribution of HERG K^+ channel proteins (red), ER (BIP blue) and cytoplasmic membrane (green, Alexa Fluor 488-conjugated wheat germ agglutinin). "V" indicate the areas chosen to display in a high magnification (right panels) the typical sub-membrane distribution of HERG proteins (red punctate staining in the cytosol adjacent to cytoplasmic membrane indicated by the white arrows) in the cells from DM rabbits as opposed to the restricted membrane distribution in the cells from healthy once.

Figure 7

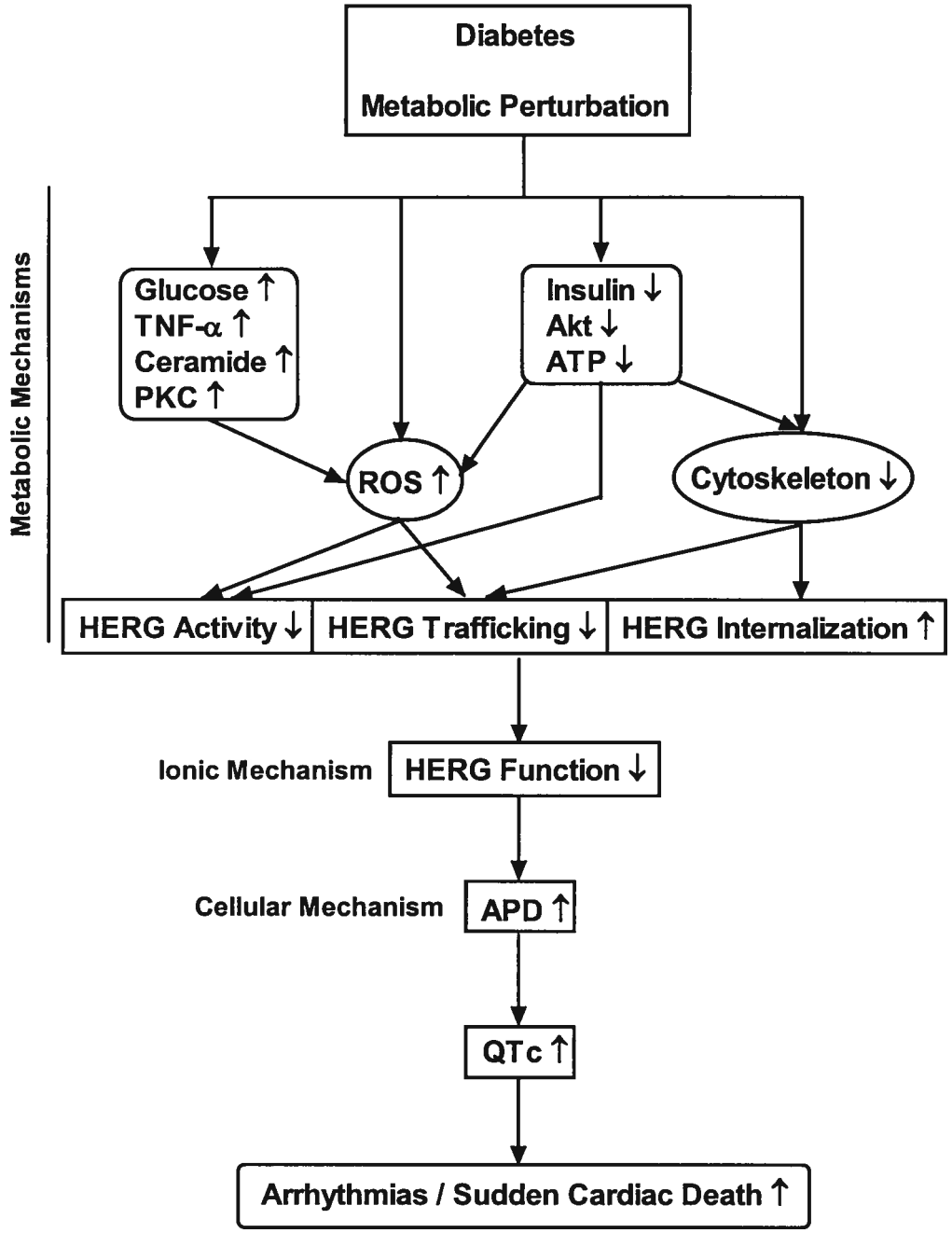

Figure 7. Schematic chart of the proposed mechanisms of diabetic QTc prolongation. ↑: increase in function or level; ↓: decrease in function or level. Akt: protein kinase B; PKC; protein kinase C; TNF-α: tumor necrosis factor-alpha; ROS: reactive oxygen species.

5 IMPAIRMENT OF HERG K^+ CHANNEL FUNCTION BY HYPOGLYCEMIA AND HYPERGLYCEMIA

Elevated glucose level is one of the results of insulin insufficiency and deficiency, but also a causative factor for many of the diabetic complications. High level of glucose can be toxic to many cellular events while shortage of glucose can render the cell working abnormally. This work was designed to test the effects of mimicked hyperglycemia and hypoglycemia on the function of HERG K^+ channel expressed in HEK293 cells, and the underlying mechanisms. It is demonstrated that both hypo- and hyper-glycemia impair HERG function, due to the underproduction of ATP in the former, and overproduction of reactive oxygen species in the latter.

This work has been published in the *Journal of Biological Chemistry* 2003; **278**:10417-26.

Impairment of HERG (Human *ether-a-go-go* Related Gene) K^+ Channel Function by Hypoglycemia and Hyperglycemia: Similar Phenotypes but Different Mechanisms*

Yiqiang Zhang‡¶, Hong Han‡, Jingxiong Wang‡¶, Huizhen Wang‡§, Baofeng Yang, and Zhiguo Wang‡ ¶ §§**

From the ‡Research Center, Montreal Heart Institute, Montreal, PQ H1T 1C8, the ¶Department of Medicine, University of Montreal, Montreal, PQ H3C 3J7, Canada, and the
***Department of Pharmacology, Harbin Medical University, Harbin, Heilongjiang, P. R. China*

First Author's surname: Zhang

Short Title: **Metabolic Mechanisms of HERG Modulation by Glucose**

---

* This work was supported in part by the Canadian Institute of Health Research, the Heart and Stroke Foundation of Quebec, and the Fonds de la Recherche de l'Institut de Cardiologie de Montreal, awarded to Dr. Z Wang.

§ A research fellow of the Canadian Institute of Health Research.

§§ A research scholar of the Fonds de Recherche en Sante de Quebec. To whom correspondence should be addressed: Research Center, Montreal Heart Institute, 5000 Belanger East, Montreal, PQ H1T 1C8, Canada; Tel.: (514) 376-3330. Fax: (514) 376-4452. E-mail: [redacted]

5.1 Summary

Hyperglycemia and hypoglycemia both can cause prolongation of Q-T interval and ventricular arrhythmias. Here we studied modulation of HERG K^+ channel, the major molecular component of delayed rectifier K^+ current responsible for cardiac repolarization, by glucose in HEK293 cells using whole-cell patch-clamp techniques. We found that both hyperglycemia (extracellular glucose concentration $[Glu]_o$=10 or 20 mM) and hypoglycemia ($[Glu]_o$=2.5, 1 or 0 mM) impaired HERG function by reducing HERG current (I_{HERG}) density, as compared with normoglycemia ($[Glu]_o$=5 mM). Complete inhibition of glucose metabolism (glycolysis and oxidative phosphorylation) by 2-deoxy-D-glucose mimicked the effects of hypoglycemia, but inhibition of glycolysis or oxidative phosphorylation alone did not cause I_{HERG} depression. Depletion of intracellular ATP mimicked the effects of hypoglycemia and replacement of ATP by GTP or non-hydrolysable ATP failed to prevent the effects. Inhibition of oxidative phosphorylation by NaCN or application of antioxidants vitamin E or superoxide dismutase mimetic (MnTBAP) abrogated, and incubation with xanthine/xanthine oxidase (X/XO) mimicked, the effects of hyperglycemia. Hyperglycemia or X/XO markedly increased intracellular level of reactive oxygen species (ROS), as measured by CM-H_2DCFDA fluorescence dye, and this increase was prevented by NaCN, vitamin E or MnTBAP. We conclude that ATP, derived from either glycolysis or oxidative phosphorylation, is critical for normal HERG function; depression of I_{HERG} in hypoglycemia results from underproduction of ATP and in hyperglycemia from overproduction of ROS. Impairment of HERG function might contribute to Q-T prolongation caused by hypoglycemia and hyperglycemia.

Keywords: HERG K^+ channel, glucose, glycolysis, oxidative phosphorylation, intracellular ATP, reactive oxygen species

5.2 Introduction

Glucose, the primary end product of the digestion of glycogen, is essential for maintaining life activities in organisms. As a major source of metabolic fuel, degradation of glucose via glycolysis and subsequent oxidative phosphorylation generates high-energy phosphates to power the biological processes in the cell. Yet, through an exquisitely complex network of control mechanisms, the rate of glucose metabolism is only as great as needed by the organisms. Moreover, glucose also has other regulatory effects on many cellular functions. Either inadequate or excessive glucose can be harmful to the living system. Therefore, the blood glucose level is dynamically controlled. However, under pathological conditions like diabetes, glucose cannot be efficiently utilized and the blood glucose level rises. When the blood level of glucose maintains higher than 7 mM it is considered as hyperglycemia. Diabetes therapy, on the other hand, can lead to an overly low level of blood glucose, which is referred to as hypoglycemia when the level falls below 3 mM.

Either hypoglycemia or hyperglycemia can have deleterious effects on the cells. One common feature of electrophysiological alterations caused by both hypoglycemia and hyperglycemia in the heart is prolongation of Q-T interval and the associated ventricular arrhythmias which are presumably responsible for sudden cardiac death in diabetic patients (1-10). However, the ionic mechanisms by which hyperglycemia and hypoglycemia prolong Q-T interval remained unclear, which is at least a part of the reasons why diabetic patients die of mainly cardiac complications.

The human *either-a-go-go* related gene (*HERG*) encodes the rapid component of delayed rectifier K^+ current in the heart, being the major repolarizing current in the plateau voltage range of cardiac action potentials. HERG K^+ channels are susceptible to genetic defects and environmental cues, the consequence being depression of HERG function in most situations (9). Indeed, most of the cases of long Q-T syndrome are ascribed to dysfunction of HERG channels, particularly that induced by therapeutic drugs (13). It is conceivable that HERG alteration might also be involved in the Q-T prolongation induced by hyperglycemia and hypoglycemia. This thought prompted us to carry out a series of experiments to study the effects of glucose on HERG K^+ channels and the potential mechanisms.

5.3 Experimental Procedures

5.3.1 Cell culture

HEK293 cells stably expressing HERG (a kind gift from Drs. Zhou and January) (14) were grown in Dulbecco's Modified Eagle's Medium supplemented with 10% heat-inactivated fetal bovine serum, 200 μM G418, 100 U/ml penicillin and 100 μg/ml streptomycin. The cells subcultured to ~85% confluency were harvested by trypsinization and stored in the Tyrode solution containing 0.5% bovine serum albumin at 4°C (12). Electrophysiological recordings were conducted within 10 hrs of storage.

5.3.2 Whole-cell patch-clamp recording

Patch-clamp techniques have been described in detail elsewhere (15-16). Currents were recorded with whole-cell voltage-clamp with an Axopatch-200B amplifier (Axon Instruments). Borosilicate glass electrodes had tip resistances of 1-3 MΩ when filled with the internal solution containing (mM): 130 KCl, 1 $MgCl_2$, 5 Mg-ATP, 10 EGTA, and 10 HEPES (pH 7.3). The extracellular (Tyrode) solution contained (mM): 136 NaCl, 5.4 KCl, 1 $CaCl_2$, 1 $MgCl_2$, 10 HEPES (pH 7.4), and glucose at concentrations as to be specified. Experiments were conducted at 36±1°C. Junction potentials were zeroed before formation of the membrane-pipette seal. Series resistance and capacitance were compensated and leak currents were subtracted.

5.3.3 Pharmacological probes

D-glucose (Glu), 2-deoxy-D-glucose (2dG), sodium cyanide (NaCN), pyruvate, ATP, GTP, β,γ-methyleneadenosine 5 -triphosphate (AMP-PCP, non-hydrolysable analogue of ATP), xanthine (X), xanthine oxidase (XO), and vitamin E (VitE) were all purchased from Sigma. Xanthine was prepared in 2N NaOH and diluted in the Tyrode solution by 800 times with pH adjusted to 7.4 with HCl. Xanthine oxidase was added to the xanthine preparation to form the X/XO reactive oxygen species (ROS) generating system. VitE was dissolved in ethanol and diluted by 1000 times to reach the final concentration. Pyruvate in liquid was diluted into the Tyrode solution and pH was adjusted to 7.4 with NaOH before use. All other compounds were directly dissolved into the patch-clamp recording solutions as to be specified. Mn(III) tetrakis (4-benzoic acid) porphyrin chloride (MnTBAP) purchased from Calbiochem was dissolved in 1N

NaOH and diluted by 5000 times to reach the desired experimental concentrations. All compounds and reagents were prepared freshly before experiments.

5.3.4 Intracellular reactive oxygen species (ROS) measurement

CM-H_2DCFDA (Molecular Probe) is a ROS sensitive probe that can be used to detect oxidative activity in living cells. It passively diffuses into cells, where its acetate groups are cleaved by intracellular esterases, releasing the corresponding dichlorodihydrofluorescein derivative. Its thiol-reactive chloromethyl group reacts with intracellular glutathione and other thiols. Subsequent oxidation yields a fluorescent adduct that is trapped inside the cell. When it is excited at 480 nm its emissions at 505-530 nm can be captured. CM-H_2DCFDA is prepared in dimethyl sulfoxide immediately prior to loading. Glass coverslips were coated with laminin and placed in the wells of a 12-well culture plate before the cells were seeded into the well in a density of 5.0 x 10^4/well. After overnight incubation, the cells were washed with pre-warmed (37°C) phosphate buffered saline (PBS) once and then incubated in the Tyrode solution containing glucose of varying concentrations or exogenous superoxide generating system (xanthine/xanthine oxidase) or the reagents as to be otherwise specified, together with the fluorescence dye CM-H_2DCFDA (10 μM). After 30 min incubation, the coverslips were washed with pre-warmed PBS twice before being mounted to the glass slides with anti-fading mounting medium and were examined immediately under a laser scanning confocal microscope (Zeiss LSM 510). The percentage of positively stained cells and the fluorescence intensity of staining were determined by densitometric scanning with LSM software suite (Zeiss).

5.3.5 Data analysis

Group data are expressed as mean±SE. Comparisons among groups were made by ANOVA (F-test) and Bonferroni adjusted t-tests were used for multiple group comparisons and paired or unpaired t-test was used, as appropriate, for single comparisons. A two-tailed $p<0.05$ was taken to indicate a statistically-significant difference. Nonlinear least-square curve fitting was performed with CLAMPFIT in pCLAMP 8.0 or Graphpad Prism.

5.4 Results

5.4.1 *Effects of glucose on I_{HERG}*

To study the effects of varying concentrations of glucose (Glu, ranging from 0 to 20 mM) on I_{HERG}, our experiments were designed for group comparisons. For each experiment, HERG-expressing HEK293 cells were divided into six groups each superfused with the Tyrode solution containing a given concentration of Glu for 30 min prior to patch-clamp recordings. In addition, recordings were performed immediately after formation of whole-cell configuration and adjustments of capacitance and series resistance compensation, and all recordings were made complete within 3 min. In this manner, there was minimal dialysis through the recording pipette thereby minimal current rundown (time-dependent current decay), and the data best reflect the effects of Glu on I_{HERG} in cells with intact intracellular contents. In addition, such an experimental design also allowed us to study the effect of Glu on I_{HERG} under the condition devoid of influence from exogenous ATP included in the pipette, which is an important issue as to be described later. I_{HERG} was elicited by 2.5-s depolarizing steps from –60 mV to +40 mV to record the activating current, followed by a repolarizing pulse to –50 mV for another 2.5 s to observe the deactivating tail current, before being returned to a holding potential of –80 mV. The results are illustrated in Fig. 1 with both representative raw data and analyzed mean data. Glucose produced two characteristic alterations of HERG channel functions: changes of I_{HERG} amplitude and density and shifts of I-V relationships and activation curves.

Comparison of I_{HERG} recorded at varying extracellular concentrations of Glu ($[Glu]_o$=0, 1, 2.5, 5, 10, or 20 mM) consistently showed that I_{HERG} density was maximal at a physiological $[Glu]_o$ (5 mM) and it was depressed at $[Glu]_o$ below or above 5 mM (Fig. 1A-1C). In other words, under normoglycemia ($[Glu]_o$=5 mM) the HERG K^+ channel operates at its maximum function level, whereas under hypoglycemia ($[Glu]_o$=0, 1 or 2.5 mM) or hyperglycemia ($[Glu]_o$= 10 or 20 mM), the HERG channel function is impaired and the degree of functional impairment is proportional to the degrees of hypoglycemia or hyperglycemia (Fig. 1D). For example, with 5 mM $[Glu]_o$ the I_{HERG} current density was 88.5 ± 7.4 pA/pF (n=25) at a test potential of 0 mV, while with 0 mM and 20 mM, the values were 35.4 ± 3.0 pA/pF (n=22, $p < 0.05$ *vs.* 5 mM $[Glu]_o$) and 35.8 ± 4.9 (n=15, $p < 0.05$ *vs.* 5 mM $[Glu]_o$), respectively, approximately a 2-fold difference. The HERG tail current density at –10 mV was also significantly depressed by hypoglycemia (0, 1 and 2.5 mM $[Glu]_o$) or hyperglycemia (10 and 20 mM $[Glu]_o$) (data not shown).

Also noticeable is the hypolarization shifts of I_{HERG} I-V relationships (Fig. 1E) and the activation curves by hypoglycemia (Fig. 1F). For example, the half activation voltage ($V_{1/2}$) was -25.4±2.7 mV (n=19) for 5 mM $[Glu]_o$ and -34.3±3.8 mV (n=22) for 0 mM $[Glu]_o$ ($p<0.05$, unpaired *t*-test), which accounted for around 10 mV shift of the steady-state voltage-dependent activation of I_{HERG}. This negative shift resulted in a crossover of the I-V curves between normoglycemia and hypoglycemia. Only slight (~4 mV) hyperpolarization shift of activation was seen with hyperglycemia (20 mM $[Glu]_o$).

Several potential mechanisms could explain the observed effects of $[Glu]_o$ on I_{HERG}. First, there was a possibility that the effects were a consequence of alterations of extracellular osmolarity with varying $[Glu]_o$. Alternatively, Glu might act directly on HERG proteins to modify the channel function. Finally, Glu metabolism which generates ATP as well as other metabolic intermediates also has the potential to modulate I_{HERG}. The following experiments were set out to clarify these issues.

To test the first possibility, we performed experiments in which cells were first superfused with a given concentration of Glu (1, 5 or 20 mM) for >30 min, followed by I_{HERG} recording within 3 min bathing in the Tyrode solution containing 10 mM Glu. Under such conditions, I_{HERG} demonstrated the same pattern of changes as described above: cells pre-exposed to 1 or 20 mM Glu had markedly smaller I_{HERG} density than those pre-exposed to 5 mM Glu (Fig. 2A), despite that all recordings were made under isotonic conditions with 10 mM $[Glu]_o$. For instance, at 0 mV, the I_{HERG} density was 56.1 ± 6.9 pA/pF (n=8) with 5 mM $[Glu]_o$, while with 1 mM and 20 mM $[Glu]_o$, the values were 32.4 ± 3.2 pA/pF (n=7, $p < 0.05$ vs. 5 mM $[Glu]_o$) and 35.8 ± 2.2 (n=7, $p< 0.05$ vs. 5 mM $[Glu]_o$), respectively. Consistently, the activation curve of I_{HERG} was also shifted to more negative potentials by hypoglycemia (Fig. 2B). Similar difference of I_{HERG} between 5 and 20 mM $[Glu]_o$ was also consistently seen when 15 mM cellobiose was added to the Tyrode solution containing 5 mM Glu (Fig. 2D).

The above data indicate that changes of osmolarity is unlikely the mechanism by which glucose modulates I_{HERG}. Apart from that, the fact that differences of I_{HERG} among the cells pretreated with three different concentrations of Glu (1, 5 and 20 mM) persisted even though I_{HERG} was recorded 10 min after superfusion with the normal Tyrode solution containing 10 mM $[Glu]_o$ suggest that the effects of glucose on I_{HERG} are mediated by some intracellular events and direct interactions between glucose and HERG channels do not likely play a major role.

5.4.2 *Role of glycolysis and oxidative phosphorylation on glucose-induced I_{HERG} enhancement*

Glucose, once being taken up into the cell, is metabolized via glycolysis to generate 2 molecules of ATP and 2 molecules of pyruvate (a substrate for oxidative phosphorylation) which is further metabolized via oxidative phosphorylation to produce more ATP molecules. To investigate whether the effects of Glu on I_{HERG} are associated with glucose metabolism, we studied the effects of the glycolysis inhibitor 2-deoxy-D-glucose (2dG). Glucose was replaced by the non-hydrolysable analogue of glucose 2dG to eliminate the glucose metabolism (both glycolysis and subsequent oxidative phosphorylation). Cells were superfused with the Glu-free Tyrode solution containing 5 mM 2dG for 30 min before patch-clamp recordings. I_{HERG} recorded under such a condition was compared with I_{HERG} recorded with the Tyrode solution containing 5 mM Glu. As shown in Fig. 3, 2dG substitution for Glu reproduced the two characteristic changes of I_{HERG} as observed under hypoglycemia. First, marked depression of I_{HERG} was seen in the presence of 2dG, with I_{HERG} density only ~38% of that in the presence of 5 mM $[Glu]_o$ at 0 mV. Second, similar to the results with 0 mM $[Glu]_o$, the I-V relationship and activation curve were shifted by 10 mV towards hyperpolarizing potentials by 2dG (-28.2±3.4 mV for 5 mM $[Glu]_o$ and -37.6±4.5 mV for 5 mM 2dG, $p<0.05$, $n=8$ for both groups) (Fig. 3B). Since 2dG is a competitive inhibitor of glycolysis, its effects on I_{HERG} in the presence of 5 mM Glu were also investigated. Cells were superfused with the Glu-containing Tyrode solution with or without 5 mM 2dG for 30 min before patch-clamp recordings. The I_{HERG} density was approximately 45% smaller in cells treated with 2dG than in untreated cells (Fig. 3C). For example, the I_{HERG} density at 0 mV was 40.2±4.1 pA/pF for cells treated with 2dG at 5 mM $[Glu]_o$ ($n=14$) and was 75.6±6.6 pA/pF for cells without 2dG treatment ($n=14$, $p<0.05$). These results indicate the importance of glucose metabolism in maintaining the normal HERG function. Intriguingly, when 2dG was added to the hyperglycemic solution containing 20 mM $[Glu]_o$, I_{HERG} was increased as compared with that measured in the hyperglycemic solution without 2dG (Fig. 3E). In other words, 2dG partly reversed the depressed I_{HERG} caused by hyperglycemia towards the normal HERG function seen under normoglycemia.

To further dissect which of the two, glycolysis or oxidative phosphorylation, is truly responsible for HERG modulation, the following experiments were carried out. In the first set of

experiments, pyruvate was supplied to the 2dG-containing Glu-free Tyrode solution. Under such a condition, the glycolysis was inhibited but the oxidative phosphorylation was maintained. As displayed in Fig. 3A, addition of pyruvate at a concentration of 5 mM restored the depressed I_{HERG} induced by glycolysis inhibition. However, the negative shifts of I-V relationship and activation curve, as seen with hypoglycemia or 2dG substitution for Glu, were still consistently observed with pyruvate (Fig. 3B). In contrast, elevation of pyruvate to 20 mM weakened the ability to restore the suppressed I_{HERG} caused by glycolysis inhibition with 2dG substitution for Glu. Thus, the I_{HERG} density with 20 mM pyruvate in the 2dG-containing Glu-free Tyrode solution was considerably smaller than that with normal $[Glu]_o$ (5 mM). However, this high concentration of pyruvate still failed to prevent the negative shifts of I_{HERG} I-V relationship and activation curve produced by glycolysis inhibition (Fig. 3B).

In the second set of experiments, the oxidative phosphorylation was inhibited by inclusion of NaCN (2 mM), an uncoupler of oxidative phosphorylation, in the bathing solution and the glycolysis was kept intact with 5 mM or 20 mM $[Glu]_o$. Under normoglycemia (5 mM $[Glu]_o$), inhibition of oxidative phosphorylation by NaCN produced a slight non-significant decrease in I_{HERG} (Fig. 4A). Under hyperglycemia (20 mM $[Glu]_o$), however, I_{HERG} was markedly diminished and NaCN restored the depressed I_{HERG} towards the I_{HERG} amplitude seen under normoglycemia (5 mM). For instance, the step and tail I_{HERG} densities in 20 mM glucose were 50.4±5.9 pA/pF and 56.4±5.3 pA/pF (n=14) at –10 mV, and were restored by NaCN to 73.9±7.9 pA/pF and 81.6±6.4 pA/pF (n=13, $p<0.05$ *vs.* 20 mM $[Glu]_o$), respectively. Also important is that the oxidative phosphorylation inhibition did not produce any significant voltage shifts of I-V relationships and activation curves, regardless of different $[Glu]_o$ (5 mM or 20 mM) (Fig. 4B). It appears from the above data that either glycolysis or oxidative phosphorylation was sufficient to sustain the normal function of HERG channels and significant negative shifts of I_{HERG} I-V relationships and activation curves occurred when glycolysis was inhibited, regardless of whether oxidative phosphorylation was maintained or not.

5.4.3 Role of intracellular ATP in maintaining HERG function

The above experiments indicate that glucose metabolism (glycolysis and oxidative phosphorylation) is critical for I_{HERG} modulation by Glu. Yet, it was unclear whether the I_{HERG} modulation by glucose metabolism is associated with the generation of high energy phosphates

(i.e. ATP), and if yes whether the ATP generated from the glucose metabolism is glycolysis-derived, or oxidative phosphorylation-derived. To clarify this issue, we first assessed the influence of intracellular ATP depletion on HERG function in the presence of 5 mM Glu, by omitting ATP from the pipette (internal) solution. I_{HERG} recorded immediately after membrane rupture and capacitance/resistance compensation was taken as baseline control data and the same measurement was repeated every 5 min up to 15 min. Under our experimental conditions, 10 min is sufficient to allow complete dialysis thereby the equilibrium between pipette solution and cytoplasm. As illustrated in Fig. 5, the I_{HERG} recorded with the normal ATP-containing pipette showed only slight rundown over a 15-min period, whereas the I_{HERG} recorded with ATP-free pipette was found significantly reduced with time. There was ~46% decrease in I_{HERG} at 10 min after dialysis at -10 mV (Fig. 5C), being similar to the reduction of I_{HERG} under hypoglycemia or with the inhibition of glucose metabolism by 2dG. Also consistent with the hypoglycemia and metabolic inhibition was the negative shifts of the I-V relationship (Fig. 5D) and voltage-dependent activation (Fig. 5E) of I_{HERG} with ATP depletion; the $V_{1/2}$ was changed by ~8 mV from -31.2±3.6 mV before to -38.9±8.1 mV ($p<0.05$, $n=7$) after $[ATP]_i$ depletion.

To investigate whether the requirement of intracellular ATP for HERG function relies on hydrolysis of ATP or simply due to nucleotide interaction with the nucleotide binding domain of HERG channels (17), we carried out the following series of experiments. We first used the pipette containing the non-hydrolysable β,γ-methyleneadenosine 5 -triphosphate (AMP-PCP) to replace ATP. With 5 mM AMP-PCP in the pipette, the I_{HERG} demonstrated a rapid rundown as observed with the ATP-free internal solution (Fig. 6C). For instance, at -10 mV the I_{HERG} recorded 10 min after dialysis was 32.2±2.1% smaller than the basal current recorded right after membrane rupture. We then went on to test if substitution of GTP for ATP could prevent I_{HERG} rundown. With 5 mM GTP in the ATP-free pipette solution, the I_{HERG} developed a similar degree of rapid rundown to what was seen with the intracellular ATP-depletion alone (Fig. 6F). For example, at -10 mV, there were 34.4±5.1 % decreases in the I_{HERG} amplitude 10 min after dialysis. Moreover, the negative shifts of I-V relationships and activation curves were also seen with AMP-PCP or GTP (Fig. 6B and 6E). For instance, $V_{1/2}$ was changed from -33.4±0.8 mV for baseline to -37.3±1.0 mV for 10 min dialysis with AMP-PCP and similarly, $V_{1/2}$ was shifted from -31.4±1.5 mV to -38.9±2.2 mV by GTP ($p<0.05$).

The same effects of ATP depletion on I_{HERG} were consistently reproduced when glyburide (10 μM) was included in the superfusate to inhibit ATP-sensitive K^+ current (K_{ATP}), if any (data not shown).

5.4.4 Role of ROS on hyperglycemia-induced I_{HERG} depression

Collectively from the above experiments, glucose metabolism is necessary for maintaining the HERG channel function and the ATP produced by either glycolysis or oxidative phosphorylation seems to be a key factor for the regulation; on the other hand, the fact that NaCN restores the depressed I_{HERG} induced by 20 mM $[Glu]_o$ or by 20 mM pyruvate suggests that oxidative phosphorylation also produces negative (suppressive) regulation on HERG function. This would imply that the I_{HERG} suppression by high glucose via oxidative phosphorylation is ATP-independent, or is the balance between the enhancement by ATP and the suppression by other factors associated with oxidative phosphorylation. It has been well established that mitochondria produce most of the endogenous reactive oxygen species (ROS) through oxidative phosphorylation (18-23) and hyperglycemia stimulates massive ROS production (24-30). It is therefore rational to propose that the endogenously produced ROS via oxidative phosphorylation stimulated by hyperglycemia could impair HERG channel function to suppress I_{HERG}. To test this hypothesis, we performed the following experiments. We first evaluated the effects of an antioxidant vitamin E (VitE) on 20 mM $[Glu]_o$ -induced I_{HERG} depression. Cells were divided into 3 groups: 5 mM $[Glu]_o$, 20 mM $[Glu]_o$, and 20 mM $[Glu]_o$ + 0.1 mM VitE. As illustrated in Fig. 7A and 7B, pretreatment of cell with VitE effectively prevented the I_{HERG} suppression by hyperglycemia; the I_{HERG} density in VitE group was virtually identical to that in the normaglycemia group. There was no significant shift of the activation curve along the voltage axis. These data suggest a participation of ROS in the HERG regulation by hyperglycemia. Next, we studied the effects of another antioxidant, superoxide dismutase (SOD) mimetic MnTBAP, on the I_{HERG} depression induced by 20 mM $[Glu]_o$. Since the compound does not readily penetrate the cells, it was intracellularly applied through dialysis of the pipette solution at a concentration of 5 μM. Cells were superfused with 20 mM Glu for 30 min prior to formation of the whole-cell membrane patch. To correct for the potential current rundown, the I_{HERG} recorded at various time points after membrane rupture was normalized to the I_{HERG} recorded with the normal Tyrode solution without MnTBAP at the corresponding time

points. As shown in Fig. 7C, MnTBAP caused a time-dependent increase in the I_{HERG} amplitude, indicating a restoration of the depressed HERG function. By comparison, no alterations of I_{HERG}, or virtually a slight decrease (presumably representing rundown of the current), were found with catalase in the pipette (data not shown). These results indicate that the ROS involved in the I_{HERG} suppression by hyperglycemia was of mainly superoxide anion (O_2^-).

To obtain further evidence for this notion, we assess the effects of exogenously produced O_2^- by the ROS generating system xanthine/xanthine oxidase (X/XO) on I_{HERG}. Cells were incubated with or without X/XO (500 μM/5 mU/ml) in the Tyrode solution containing 5 mM $[Glu]_o$ for 40 min before I_{HERG} was recorded under 5 mM $[Glu]_o$. The I_{HERG} density was consistently smaller in X/XO treated cells than in X/XO non-treated cells (Fig. 8A and 8B).

To confirm that ROS production was indeed increased by 20 mM $[Glu]_o$ and the hyperglycemia-induced ROS was mainly of O_2^-, we went on to measure the intracellular ROS levels using CM-H_2DCFDA fluorescence dye. The ROS level was measured in cells preincubated with the Tyrode solution containing 5 or 20 mM glucose for 30 min. The staining of the cells demonstrated two distinct patterns: one localized to the defined rod-shaped structures and the other one diffused evenly throughout the cytoplasm. The former presumably represents the physiological production of ROS as a byproduct of oxidative phosphorylation in mitochondria and the latter indicates overproduction of ROS as a result of metabolic stress and damage to mitochondria. The cells with diffused staining and with fluorescence intensity ≥ 5 times the background were defined as positive staining and the number of cells with positive staining was pooled from 5 fields. The intensity of staining by the fluorescent probe for ROS was analyzed by densitometric scanning using LSM program suite and cells with either localized or diffused staining were taken for analysis, and the data were normalized to the control (5 mM $[Glu]_o$) values. Under normoglycemia, a majority of cells which were stained by CM-H_2DCFDA demonstrated the localized pattern and the diffused staining was sparse. Yet in the cells treated with 20 mM Glu, the number of the cells with positive staining as well as the intensity of staining was consistently higher, as compared with the cells treated with 5 mM Glu (Fig. 9). This high level of ROS production was markedly suppressed in the cells pretreated with NaCN (2 mM, Fig. 9), an uncoupler of oxidative phosphorylation, indicating that the mitochondrion is most likely where the ROS was massively produced. Since we have demonstrated that pyruvate at high concentrations decreased I_{HERG} (Fig. 3A), the ROS level in the cells pretreated with 20 mM

pyruvate was also measured. As shown in Fig. 9, like 20 mM Glu, 20 mM pyruvate also significantly increased the ROS production though to a less extent. Moreover, the glycolysis inhibitor 2dG (5 mM) also reduced the ROS level in high glucose (20 mM), which is indicated by fewer positively stained cells and lower intensity of staining (Fig. 9). The results explain why 2dG partly restored the depressed I_{HERG} in 20 mM Glu (Fig. 3E).

We have shown that VitE prevented, and MnTBAP partly reversed, the I_{HERG} depression in hyperglycemia (Fig. 7). To see whether this is indeed attributable to their antioxidant actions, effects of VitE and MnTBAP on hyperglycemia-induced ROS production were also studied. As shown in Fig. 10A and 10B, the ROS level was significantly lower, as indicated by the smaller number of cells with positive staining and the weaker intensity of staining in individual cells, in the cells pretreated with VitE than in non-treated cells, at 20 mM $[Glu]_o$. Consistently, MnTBAP abolished the hyperglycemia-induced ROS generation; the number of stained cells and the intensity of staining in the presence of MnTBAP were nearly the same as those under normoglycemia.

It has been well documented that the X/XO ROS generating system stimulates mainly the generation of $O_2^{\cdot-}$. To test whether this is also true in our conditions, the ROS which was exogenously generated by X/XO and penetrated cells was measured and the effect of MnTBAP was studied at 5 mM $[Glu]_o$. As displayed in Fig. 11, the ROS level was significantly higher in the cells treated with X/XO alone and this increase in ROS level was prevented in the cells pretreated with MnTBAP.

5.5 Discussion

The work described here documents a heretofore-unreported role of glucose in regulating the function of HERG K^+ channels. Our data revealed that glucose produces two characteristic effects on the HERG channel function: changes of HERG current (I_{HERG}) amplitude/density and activation voltage. The maximum HERG function operates under physiological $[Glu]_o$ (5 mM, normoglycemia), and depressed HERG function occurs with $[Glu]_o < 5$ mM (hypoglycemia) or with $[Glu]_o > 5$mM (hyperglycemia); hypoglycemia but not hyperglycemia causes shifts of HERG activation towards hyperpolarizing voltages. The modulation of HERG by glucose is critically

mediated by glucose metabolism (glycolysis and oxidative phosphorylation), and ATP and ROS are crucial in defining the HERG function with changing extracellular glucose levels.

5.5.1 *Depression of HERG function in hypoglycemia likely results from underproduction of ATP*

In our study, lower glucose levels and inhibition of glucose metabolism both produced similar suppression of HERG function as reflected by the substantial diminishment of HERG current (I_{HERG}), pointing to a requirement of glucose metabolism for HERG modulation by glucose. Our data allowed us to reach the following conclusions.

Either Glycolysis- or Oxidative Phosphorylation-Derived ATP Is Sufficient for Maintaining the Normal HERG Function — The end point of glucose metabolism is generation of high-energy phosphates for maintaining cellular functions and depletion of ATP could impair cellular processes dependent on high-energy phosphates. One of the major findings of this study is that the normal HERG function critically relies on the level of intracellular ATP; depletion of intracellular ATP impairs HERG function to an extent similar to what severe hypoglycemia (0 mM $[Glu]_o$) does (see Figs. 1, 2 and 5). Complete inhibition of glucose metabolism by 2-d-deoxyglucose (2dG) substitution for glucose reproduces the effects of hypoglycemia or ATP depletion on I_{HERG}. Yet, neither inhibition of glycolysis alone by 2dG substitution of Glu with a supply of pyruvate to sustain oxidative phosphorylation nor inhibition of oxidative phosphorylation alone by NaCN in the presence of 5 mM Glu to maintain glycolysis is able to cause depression of HERG function. The results imply that the ATP generated by glucose metabolism plays an important role in maintaining HERG function and either the glycolytic or oxidative ATP is adequate for the regulation.

ATP synthesis and utilization are subcellularly compartmentalized; glycolysis-derived ATP primarily regulates membrane proteins because glycolytic pathway is associated with the sarcolemma (31) whereas oxidative phosphorylation-derived ATP preferentially supports cytosolic processes because oxidative ATP is generated within the mitochondria and subsequently transported to the cytoplasm (32). Regulation of cardiac ATP-sensitive K^+ channel (K_{ATP}) (34) and L-type Ca^{2+} channel (I_{Ca}) (33) by intracellular ATP has been well documented by some previous studies. It was found that both K_{ATP} and I_{Ca} were preferentially regulated by glycolytic ATP (33-34).

Glycolysis-Derived ATP May Be Responsible for Maintaining the Normal Voltage-Dependent Activation of I_{HERG}—Although as above-mentioned, either glycolytic or oxidative ATP is sufficient for maintaining the normal HERG current amplitude/density, only glycolysis-derived ATP seems to affect the steady-state voltage-dependent activation property of HERG channels. This notion is supported by several lines of evidence from our experiments: (1) Hypoglycemia (0 or 1 mM $[Glu]_o$), a situation with inadequate ATP production, but not hyperglycemia (10 or 20 mM $[Glu]_o$), causes negative shifts of I-V relationships and voltage-dependent activation curves; (2) Inhibition of glycolysis (Fig. 3), but not oxidative phosphorylation (Fig. 4), abolishes the negative shifts of the HERG activation; (3) When glycolysis is inhibited by 2dG, preservation of oxidative phosphorylation by addition of pyruvate fails to prevent the negative shift caused by hypoglycemia (see Fig. 3); and (4) Depletion of intracellular ATP reproduces negative shifts similar to those seen with hypoglycemia. Similar dependence of glycolytic ATP regulation of K_{ATP} and I_{Ca} has been documented (33-34).

Role of ATP in Maintaining HERG Function Is Most Likely due to the Phosphorylation-Dependent Mechanisms —Two alternative mechanisms could account for intracellular ATP regulation of ion channels: ATP acts as a substrate for phosphorylation of channel proteins by protein kinase which requires ATP hydrolysis and ATP interacts with the nucleotide binding domains of channel proteins to produce allosteric regulation not requiring ATP hydrolysis. The latter mechanism has been shown to operate for K_{ATP} and I_{Ca} regulation (33, 35). In our case, neither the non-hydrolysable analog of ATP AMP-PCP nor GTP prevented the I_{HERG} rundown caused by ATP depletion (Fig. 6); instead substitution of AMP-PCP or GTP for ATP in the internal solution produced nearly identical effects as seen with ATP depletion alone. The results suggest that the HERG regulation by ATP under our experimental conditions is phosphorylation-dependent requiring ATP hydrolysis. In other words, ATP serves as a substrate for phosphorylation of HERG channels by protein kinases. Indeed, we have recently found that the normal HERG function requires basal activity of protein kinase B (PKB) and inhibition of PKB markedly suppresses I_{HERG} and shifts HERG activation along the voltage axis towards more negative potentials (36). These results are in good agreement with the HERG regulation by ATP. Studies are currently undertaken to clarify the link between ATP and PKB modulation of HERG channels.

5.5.2 *Depression of HERG function in hyperglycemia results from overproduction of ROS*

Consequence of the physiological role in oxidative phosphorylation is the generation of ROS as byproducts of the consumption of molecular oxygen in the electron transport chain (23). Physiologically, these ROS are mostly trapped within mitochondria and rapidly scavenged by endogenous antioxidants like superoxide dismutase (SOD), catalase, glutathione, etc. Yet under metabolic stress, ROS can be overproduced and can cause damages to mitochondria. Consequently, the ROS may diffuse throughout the cytoplasm and cause further deleterious effects on other cellular processes. Abnormally high concentrations of glucose can enhance ROS damage at least in three different manners. It has been known that high glucose (25 mM) evoked ROS generation, which was blocked by antioxidants, inhibitors of mitochondrial electron transport chain complex, inhibitors of glycolysis-derived pyruvate transport into mitochondria, uncouplers of oxidative phosphorylation, SOD mimetics, catalase, etc (30). Superoxide anion (O_2^-) is found to be the major ROS produced under hyperglycemia (37-42) and increases in ROS can be prevented by SOD. Second, glucose itself can auto-oxidize to form ROS including O_2^-, OH^-, and H_2O_2 (43). Finally, acute elevations in glucose also depress natural antioxidant defenses. It has been found that incubation of purified bovine CuZn SOD with 10 to 100 mM glucose reduces the enzyme activity by 60% (44).

Elevated glucose or pyruvate level is expected to enhance oxidative phosphorylation and produce more ATP molecules to support HERG function or increase I_{HERG}. However, our observations are on the contrary to this expectation. Our results showed that hyperglycemia or excessive pyruvate markedly depressed the HERG function. A reasonable explanation for this is that the ROS produced under hyperglycemia counteract the effects of ATP and the net outcome is a balance between enhancing effects of ATP and suppressing effects of ROS. Evidently, under our experimental conditions, the effects of increased ROS overwrite the effects of increased ATP, resulting in suppression of I_{HERG}. This notion is supported by the following evidence. First, the depression of I_{HERG} induced by hyperglycemia was prevented or reversed by the antioxidants vitamin E and MnTBAP (SOD mimetic). Second, inhibition of the glycolysis thereby the subsequent oxidative phosphorylation by 2-D-deoxyglucose (2dG) partially reversed the depressed I_{HERG} under hyperglycemia (Fig. 3). Weakened oxidative phosphorylation due to inhibition of the glycolysis would reduce both ATP and ROS productions but the net result was

an increase in I_{HERG}, indicating again that in our experimental conditions ROS overweighs ATP in terms of their effects on I_{HERG}. This is in agreement with the notion that the suppressing effects of ROS overproduction overwhelm the effects of ATP increase. Moreover, 2dG also can compete with glucose for access to glucose transporters, thus decreases glucose uptake which in turn can result in reduction of ROS production in the cells. Finally, our data indeed demonstrated the ability of high glucose to stimulate an overproduction of ROS (see Fig. 9). The fact that a high concentration of pyruvate mimicked, while VitE or NaCN abrogated, the ROS overproduction suggests that the ROS were mainly produced via the oxidative phosphorylation in mitochondria in our cells.

It has been reported that the ROS, which generate highly reactive hydroxyl group (OH^-), such as H_2O_2 or $FeSO_4$/ascorbic acid (an oxidative stimulus analogous to H_2O_2), increased I_{HERG} at negative potentials by shifting the HERG activation to more negative voltages (45-46). These results are opposite to our observation. One explanation is that the ROS generated under our experimental conditions may different from the OH^- generating system (H_2O_2 or $FeSO_4$/ascorbic acid). As already mentioned, previous studies have confirmed that the ROS induced by hyperglycemia is mainly of O_2^-. Here, we also showed that the SOD mimetic MnTBAP reduced the hyperglycemia-induced ROS overproduction (Fig. 10) and the O_2^--generating system xanthine/xanthine oxidase (X/XO) produced ROS which were also abolished by MnTBAP, an evidence for O_2^- as a major ROS generated in our cells. Consistently, depressive effects of hyperglycemia or X/XO on I_{HERG} were significantly weakened by MnTBAP. Indeed, it has been reported that the O_2^- generated by high glucose (23 mM) or by X/XO in rat small coronary arteries impairs voltage-gated K^+ (Kv) current (39, 47); reducing the current density by around 60%, which was partially restored by SOD and catalase. Together all these, we believe that different ROS might have different effects on I_{HERG}; OH^- enhances, while O_2^- depresses, I_{HERG}. Moreover, it has been shown that excessive ROS inhibits glycolysis and the subsequent glycolytic ATP production, and even depletes intracellular ATP levels in isolated perfused hearts (48-50). This fact together with our data suggests that besides the potential direct modulation of I_{HERG} by ROS, ATP reduction potentially caused by ROS may also contribute to the I_{HERG} depression under hyperglycemia. This provides an alternative explanation for the depressive effects of the ROS overproduction overcoming the enhancing effects of the expected ATP increase.

In our study, the effects of pyruvate and X/XO were smaller than those of hyperglycemia. This may be because the O_2^- generated by hyperglycemia occurs inside the cell but pyruvate does not readily penetrate cells, the effect of pyruvate observed in the present study may underestimate the true role of oxidative phosphorylation in I_{HERG} modulation. Likewise, the O_2^- generated by X/XO was primarily extracellular with subsequent entry into the cell which could also underestimate the effects of O_2^-.

It was shown that within minutes of exposure to dihydroxyfumaric acid or xanthine plus xanthine oxidase, both of which produce the superoxide anion, action potential duration (APD) was prolonged in canine myocytes, and this effect was followed by the appearance of early after depolarization (EAD) (51). X/XO caused a 30% increase in APD in superfused papillary muscle or small strips of right ventricular walls of guinea pig hearts (52). However, whether the APD prolongation was associated with inhibition of delayed rectifier K^+ current (I_{Kr}) is unknown. Our study provides a potential explanation for these observations.

5.5.3 Impairment of HERG function might contribute to Q-T prolongation caused by hypoglycemia and hyperglycemia

Heart disease is a leading cause of death in diabetic patients. In patients with diabetes a prolongation of the Q-T interval has been associated with an increased risk of sudden cardiac death (2) due to occurrence of lethal ventricular arrhythmias, particularly Torsade de pointes following bradycardia in these patients (1). Several cardiovascular pathological consequences of diabetes such as hypertension and arteriosclerosis affect the heart to varying degrees. Hyperglycemia, as a consequence of diabetes and an independent risk factor, also can directly cause cardiac damages. On the other hand, insulin therapy increases the risk of hypoglycemia in type 2 diabetic patients; according to the United Kingdom Prospective Diabetes Study (UKPDS), approximately one-third of the insulin-treated patients reported one or more hypoglycemic episodes per year during the first 3 years (3). Hypoglycemia is presumed to be the cause of death in about 3% of insulin-treated diabetic patients (11). Intriguingly, it is well recognized that both hyperglycemia and hypoglycemia can cause prolongation of Q-T interval. In type 2 diabetes, the prevalence of Q-T prolongation is as high as 26% and Q-T prolongation during experimentally induced and spontaneously occurring hypoglycemia or diabetic hyperglycemia has also been shown to occur in healthy subjects and in diabetic patients with increased risk of malignant

ventricular arrhythmias (4-11). Yet the potential ionic mechanisms by which hypoglycemia and hyperglycemia cause Q-T prolongation remained poorly understood. Studies on glucose modulation of cardiac ion channels are sparse and have been mostly limited to ATP-sensitive K^+ current (K_{ATP}). On the contrary to I_{HERG}, K_{ATP} is closed with increased intracellular ATP levels (34). One study reported by Xu et al (53) demonstrated that hyperglycemia (18 mM $[Glu]_o$) decreased the density of transient outward K^+ current but did not alter the inward rectifier K^+ current in rat ventricular myocytes which do not express delayed rectifier K^+ current (I_{Kr}), the physiological counterpart of I_{HERG}. In arterial smooth muscles, high glucose diminished *shaker*-type delayed rectifier K^+ current (39). In rat myelinated nerve fibers, 30 mM glucose increased Ca^{2+}-activated K^+ current (54). While none of the data from these studies could fully account for the Q-T prolongation, particularly the Q-T prolongation induced by hypoglycemia, our study provides a plausible, or at least an alternative, explanation; HERG K^+ channel may be a mechanistic link for the Q-T prolongation induced by both hyperglycemia and hypoglycemia. Yet, one should keep it in mind that HERG may be only one of the multiple factors contributing to the Q-T prolongation in hypoglycemia and hyperglycemia.

5.6 Acknowledgements

This work was supported in part by the Canadian Institutes of Health Research (CIHR), the Heart and Stroke Foundation of Quebec (HSFQ), and the Fonds de la Recherche de l'Institut de Cardiologie de Montreal (FRICM). Z. Wang is a research scholar of the Fonds de Recherche en Sante de Quebec (FRSQ). H. Wang is a research fellow of CIHR. The authors thank Mrs. XiaoFan Yang for excellent technical support and Mr. Louis R. Villeneuve for his assistance for confocal microscopic examinations.

5.7 References

(1) Abo, K., Ishida, Y., Yoshida, R., Hozumi, T., Ueno, H., Shiotani, H., Matsunaga, K., and Kazumi, T. (1996) *Diabetes Care* **19,** 1010.

(2) Kahn, J.K., Sisson, J.C., and Vinik, A.I. (1987) *J.Clin.Endocrinol.Metab.* **64,** 751-754

(3) UKPDS. (1995) *Br. Med. J.* **310,** 83-88

(4) Marfella, R., Rossi, F., and Giugliano, D. (2001) *Diabetes Nutr.Metab.* **14,** 63-65

(5) Chelliah,Y.R. (2000) *Anaesth.Intensive Care* **28,** 698-700

(6) Veglio, M., Borra, M., Stevens, L.K.,; Fuller, J.H., and Perin, P.C. (1999) *Diabetologia* **42,** 68-75

(7) Marques, J.L., George, E., Peacey, S.R., Harris, N.D., Macdonald, I.A., Cochrane, T., and Heller, S.R. (1997) *Diabet.Med.* **14,** 648-654

(8) Landstedt-Hallin, L., Englund, A., Adamson, U., and Lins, P-E. (1999) *J. Intern. Med.* **246,** 299-307

(9) Lindstrom, T., Jorfeldt, L., Tegler, L., and Arnqvist, H.J. (1992) *Diabet.Med.* **9,** 536-541

(10) Shimada, R., Nakashima, T., Nunoi, K., Kohno,Y., Takeshita, A., and Omae, T. (1984) *Arch.Intern.Med.* **144,** 1068-1069

(11) Eckert, B., and Agardh, C-D. (1998) *Clin. Physiol.* **18,** 570-575

(12) Sanguinetti, M. C. (1999) *Ann.N.Y.Acad.Sci.* **868,** 406-413

(13) Taglialatela, M., Castaldo, P., Pannaccione, A. (1998) *Biochem. Pharmacol.* **55,** 1741 1746

(14) Zhou, Z., Gong, Q., Ye, B., Fan, Z., Makielski, J. C., Robertson, G. A., and January, C. T. (1998) *Biophys.J.* **74,** 230-241

(15) Wang, J., Wang, H, Han, H., Zhang, Y., Yang, B., Nattel, S., and Wang Z. (2001) *Circulation* **104,** 2645-2648

(16) Wang, H., Yang, B., Zhang, Y., Han, H., Wang, J., Shi, H., and Wang, Z. (2001) *J.Biol.Chem.* **276,** 40811-40816

(17) Splawski, I., Shen, J., Katherine, W., Timothy, G., Vincent, M., Lehmann, M.H., and Keating, M.T. (1998) *Genomics* **51,** 86-97

(18) Ludwig, B., Bender, E., Arnold, S., Huttemann, M., Lee, I., and Kadenbach, B. (2001) *Chembiochem.* **2,** 392-40

(19) Hsieh, T. J., Zhang, S. L., Filep, J. G., Tang, S. S., Ingelfinger, J. R., and Chan, J. S. (2002) *Endocrinology* **143**, 2975-2985s

(20) Wallace, D. C. (2002) *Methods Mol.Biol.* **197**, 3-54

(21) Siraki, A. G., Pourahmad, J., Chan, T. S., Khan, S., and O'Brien, P. J. (2002) *Free Radic.Biol.Med.* **32**, 2-10

(22) Kirkinezos, I.G., and Moraes, C. T. (2001) *Semin.Cell Dev.Biol.* **12**, 449-457

(23) Wallace, D. C. (2001) *Novartis.Found.Symp.* **235**, 247-263

(24) Koo, J. R., Ni, Z., Oviesi, F., and Vaziri, N. D. (2002) *Clin.Exp.Hypertens.* **24**, 333-344

(25) Marfella, R., Quagliaro, L., Nappo, F., Ceriello, A.,; and Giugliano, D. (2001) *J.Clin.Invest.* **108,** 635-636

(26) Srivastava, A. K. (2002) *Int.J.Mol.Med.* **9**, 85-89

(27) Li, P. A., Liu, G. J., He, Q. P., Floyd, R. A., and Siesjo, B. K. (1999) *Free Radic.Biol.Med.* **27**, 1033-1040

(28) van Dam, P. S., van Asbeck, B. S., Bravenboer, B., van Oirschot, J. F., Gispen, W. H., and Marx, J. J. (1998) *Free Radic.Biol.Med.* **24**, 18-26

(29) Giardino, I., Edelstein, D., and Brownlee, M. (1996) *J.Clin.Invest* **97**, 1422-1428

(30) Hsieh, T. J., Zhang, S. L., Filep, J. G., Tang, S. S., Ingelfinger, J. R., and Chan, J. S. (2002) *Endocrinology* **143**, 2975-2985s

(31) Hazen, S.L., Wolf, M.J., Ford, D.A., and Gross, R.W. (1994) *FEBS Lett.* **339,** 213-216

(32) Weiss, J.N., and Hiltbrand, B. (1985) *J. Clin. Invest.* **75,** 436-447

(33) Losito, V.A., Tsushima, R.G., Diaz, R.J., Wilson, G.J., and Backx, P.H. (1998) *J. Physiol.* **511,** 67-78

(34) Weiss, J.N., and Lamo, S.T. (1989) *J. Gen. Physiol.* **94,** 911-935

(35) Yazawa, K., Kameyama, A., Yasui, K., Li, J.M., and Kameyama, M. (1997) *Pflügers Arch.* **433,** 557-562

(36) Zhang, Y,. Wang, H., Wang, J., Han, H., Nattel, S., and Wang, Z. (2002) *FEBS Lett.* (in press).

(37) Nishikawa, T., Edelstein, D., Du, X.L., Yamagishi, S., Matsumura, T., Kaneda, Y., Yorek, M.A., Beebe, D., Oates, P.J., Hammes, H.P., Giardino, I., and Brownlee, M. (2000) *Nature* **404,** 787-790

(38) Du, X.L., Edelstein, D., Rossetti, L., Fantus, I.G., Goldberg, H., Ziyadeh, F., Wu, J., and Brownlee,M. (2000) *Proc.Natl.Acad.Sci.U.S.A* **97,** 12222- 12226

(39) Liu, Y., Terata, K., Rusch, N.J., and Gutterman, D.D. (2001) *Circ.Res.* **89,** 146-152

(40) Graier,W.F.; Posch,K.; Wascher,T.C.; Kostner,G.M. (1997) *Horm.Metab Res.* **29,** 622-629

(41) Graier, W.F., Posch, K., Fleischhacker, E., Wascher, T.C., and Kostner, G.M. (1999) *Diabetes Res.Clin.Pract.* **45,** 153-160

(42) Esposito, K., Marfella, R., and Giugliano, D. (2002) *J.Endocrinol.Invest.* **25,** 485-488

(43) Wolff, S.P., and Dean, R.T. (1987) *Biochem.J.* **245,** 243-250

(44) Oda, A., Bannai, C., Yamaoka, T., Katori, T., Matsushima, T., and Yamashita, K. (1994) *Horm.Metab Res*. **26,** 1-4

(45) Bérubé, J., Caouette, D., and Da;eau, P. (2001) *J. Pharmacol. Exp. Ther.* **297,**96-102

(46) Taglialatela, M., Castaldo, P., Iossa, S., Pannaccione, A., Fresi, A., Ficker, E., and Annunziato, L. (1997) *Proc.Natl.Acad.Sci.U.S.A.* **94,** 11698-11703

(47) Liu, Y., and Gutterman, D.D. (2002). *Clin. Exp. Pharmacol. Physiol.* **29,** 305-311

(48) Ytrehus, K., Myklebust, R., and Mjøs, O.D. (1986) *Cardiovasc. Res*. **20,** 597-603

(49) Miki, S., Ashraf, M., Salka, S., and Sperelakis, N. (1988) *J. Mol. Cell Cardiol.* **20,** 1009-1024

(50) Patane, G., Anello, M., Piro S. Vigneri, R., Purrello, F., and Rabuazzo, A.M. (2002) *Diabetes* **51,** 2749-2756

(51) Barrington, P.L., Meier Jr, C.F., and Weglicki, W.B. (1988) *J. Mol. Cell Cardiol.* **20,** 1163-78

(52) Aiello, E.A., Jabr, R.I., and Cole, W.C. (1995) *Circ.Res*. **77,** 153-162

(53) Xu, Z., Patel, K.P., and Rozanski, G.J. (1998) *Am. J. Physiol.* **271,** H2190-H2196

(54) Takigawa, T., Yasuda, H., Terada, M., Maeda, K., Haneda, M., Kashiwagi, A., Kitasato, H., & Kikkawa, R. (2000) *Neuroreport* **11,** 2547-2551

5.8 Figures and Figure Legends

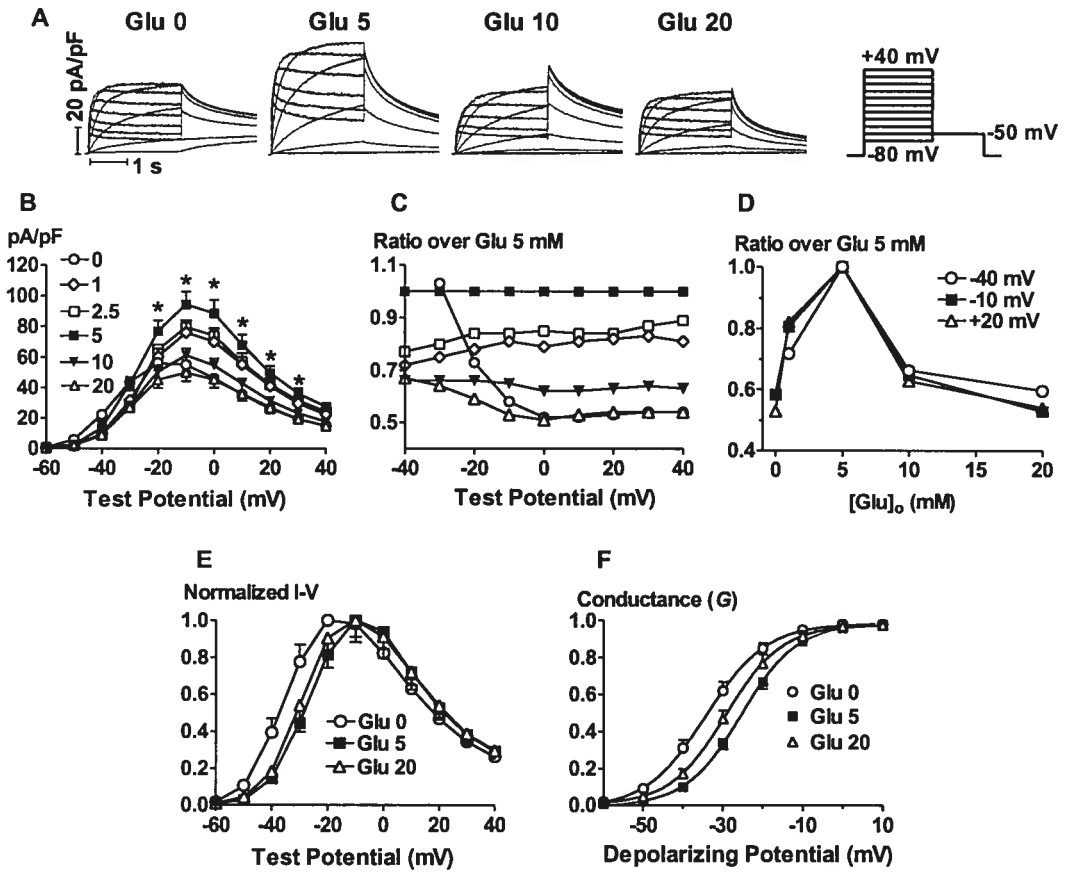

Figure 1. Effects of glucose on HERG K^+ current (I_{HERG}) stably expressed in HEK293 cells. ***A***, Typical examples of I_{HERG} traces recorded in the Tyrode solution containing 0, 5, 10, or 20 mM D-glucose (Glu) with the voltage protocol shown in the inset, and presented as current density (pA/pF) for better group comparisons. The same voltage protocol is applied for the I_{HERG} recordings shown in the subsequent figures, except otherwise indicated. ***B***, Current density-voltage relationships of I_{HERG}. The steady-state step I_{HERG} measured at the end of 2.5-s pulses was normalized to the capacitance of the respective cells and plotted as a function of test potentials. Shown are data averaged from 22, 9, 11, 25, 24 and 15 cells for 0, 1, 2.5, 5, 10, and 20 mM Glu, respectively. *$p< 0.05$ *vs.* 5 mM $[Glu]_o$. ***C***, Ratio of the step I_{HERG} recorded with

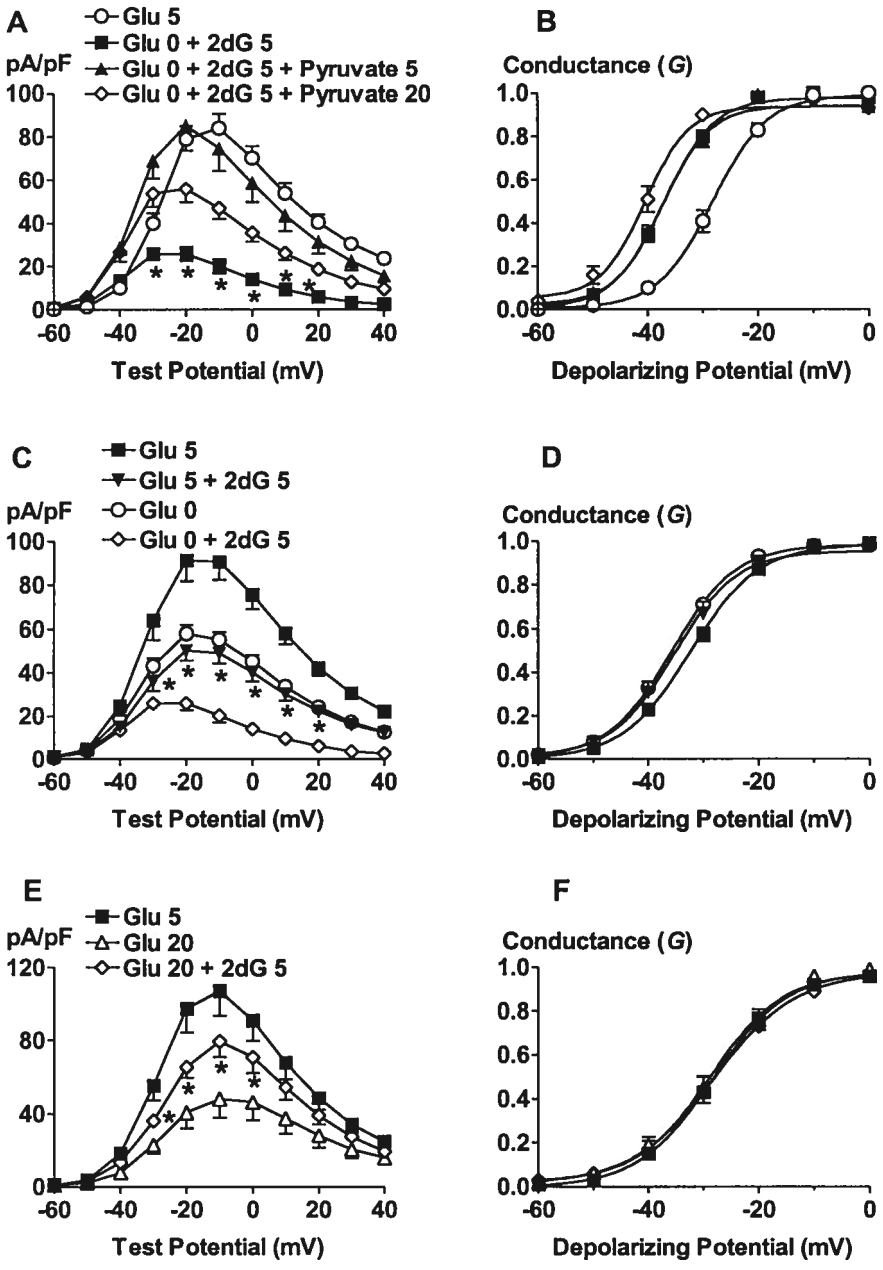
A
Glu 5
Glu 0 + 2dG 5
Glu 0 + 2dG 5 + Pyruvate 5
Glu 0 + 2dG 5 + Pyruvate 20
pA/pF
Test Potential (mV)
B
Conductance (G)
Depolarizing Potential (mV)
C
Glu 5
Glu 5 + 2dG 5
Glu 0
Glu 0 + 2dG 5
pA/pF
Test Potential (mV)
D
Conductance (G)
Depolarizing Potential (mV)
E
Glu 5
Glu 20
Glu 20 + 2dG 5
pA/pF
Test Potential (mV)
F
Conductance (G)
Depolarizing Potential (mV)

Figure 3

Figure 3. Effects of complete inhibition of glucose metabolism or inhibition of glycolysis on I_{HERG}. ***A*** and ***B***, Mean current density (pA/pF)-voltage relationships and activation conductance (*G*) curves of I_{HERG}. Complete inhibition of glucose metabolism was achieved by the addition of 5 mM 2-deoxy-D-glucose (2dG) to the Glu-free solution and inhibition of glycolysis alone was achieved by the addition of pyruvate to the 2dG-containing Glu-free solution. The numbers in the legends represent the concentrations of Glu, 2dG or pyruvate in mM. The number of cells was 8 for "Glu 5 group, 7 for "Glu 0 + 2dG 5 group, 7 for "Glu 0 + 2dG 5 + pyruvate 5 group, and 8 for "Glu 0 + 2dG 5 + pyruvate 20 group. *$p< 0.05$ *vs.* 5 mM $[Glu]_o$. ***C*** and ***D***, Comparison between the effects of 2dG (5 mM) on I_{HERG} under 0 mM $[Glu]_o$ and 5 mM $[Glu]_o$. *$p< 0.05$ *vs.* 5 mM $[Glu]_o$. ***E*** and ***F***, Effects of 2dG (5 mM) on I_{HERG} under 20 mM $[Glu]_o$. The number of cells was 10 for "Glu 5 group, 8 for "Glu 20 group, and 11 for "Glu 20 + 2dG 5 group. *$p< 0.05$ *vs.* 20 mM $[Glu]_o$, unpaired *t*-tests.

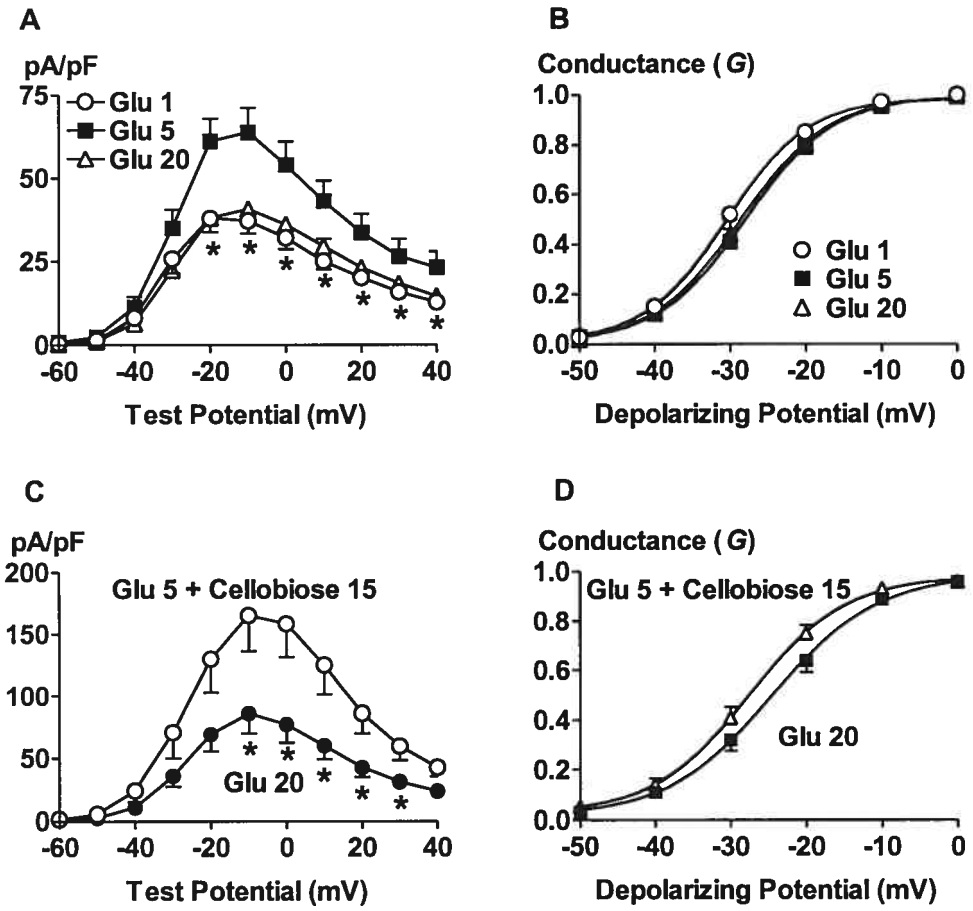

Figure 2. Effects of glucose on I_{HERG} under conditions with corrected osmolarity. ***A*** and ***B***, Mean current density (pA/pF)-voltage relationships and activation conductance (*G*) curves, respectively (n=7, 9 and 7 for 1, 5 and 20 mM $[Glu]_o$, respectively). The cells of different groups were superfused with solutions containing a given concentration of glucose (1, 5 or 20 mM) for >30 min and then switched to the same solution with an identical glucose concentration (10 mM). The I_{HERG} recorded within 3 min at 10 mM $[Glu]_o$ were used for analysis. *$p< 0.05$ *vs.* 5 mM $[Glu]_o$, unpaired *t*-tests. ***C*** and ***D***, Depression of I_{HERG} and negative shift of I_{HERG} activation, respectively, in high glucose (20 mM $[Glu]_o$, n=5), as compared with those in normal glucose (5 mM $[Glu]_o$) + 15 mM cellobiose (n=5) to balance the extracellular osmolarity. *$p< 0.05$ *vs.* Glu 5+cellobiose 15, unpaired *t*-tests.

varying $[Glu]_o$ over the I_{HERG} with 5 mM $[Glu]_o$ as a function of test potentials. ***D***, Ratio of the step I_{HERG} recorded with varying $[Glu]_o$ over the I_{HERG} with 5 mM $[Glu]_o$ as a function of glucose concentrations. Shown are the data obtained at test potentials of –40, -10 and +20 mV. ***E***, Normalized I-V relationships obtained by dividing the current amplitude at various potentials by the maximum current for each concentration of glucose. For clarity, only the data with 0, 5 and 20 mM $[Glu]_o$ are shown. Note the negative shifts of the curves with low and high $[Glu]_o$, relative to 5 mM $[Glu]_o$, along the voltage axis. ***F***, Steady-state voltage-dependent activation of I_{HERG}. The activation curves were constructed by plotting the conductance G as a function of potentials. G was calculated by normalizing the tail currents at -50 mV by dividing the amplitude of the tail currents evoked at various antecedent step potentials by that of the tail current at +40 mV. The symbols are mean of experimental data and the lines represent the Boltzmann fit: $G/G_{max}=1/\{1+\exp[(V_{1/2}-V)/k]\}$, where G_{max} represents the maximal conductance at +40 mV, $V_{1/2}$ is a half-maximal activation voltage, and k is a slope factor. The numbers in the legends represent the extracellular glucose concentrations ($[Glu]_o$) in mM.

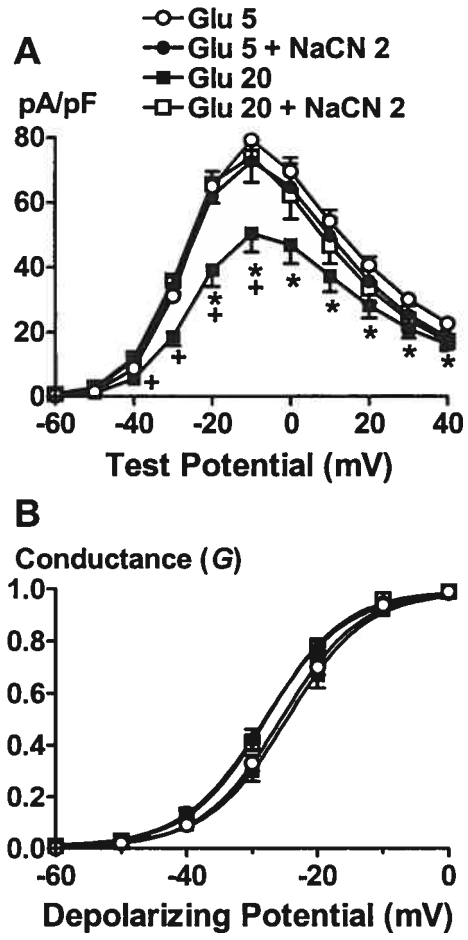

Fig. 4. Effects of inhibition of oxidative phosphorylation on I_{HERG}. Mean current density (pA/pF)-voltage relationships (*A*) and activation conductance (*G*) curves (*B*). Inhibition of oxidative phosphorylation with intact glycolysis was achieved by the addition of NaCN (2 mM) to the Glu (5 or 20 mM)-containing solution. The numbers in the legends represent the concentrations of Glu, or NaCN in mM. n=23 for "Glu 5 group, 15 for "Glu 5 + NaCN 2 group, 14 for "Glu 20 group, and 13 for "Glu 20 + NaCN 2 group. *p<0.05 *vs* Glu 5 mM ; ^{+}p<0.05 *vs* Glu 20 mM, unpaired *t*-tests.

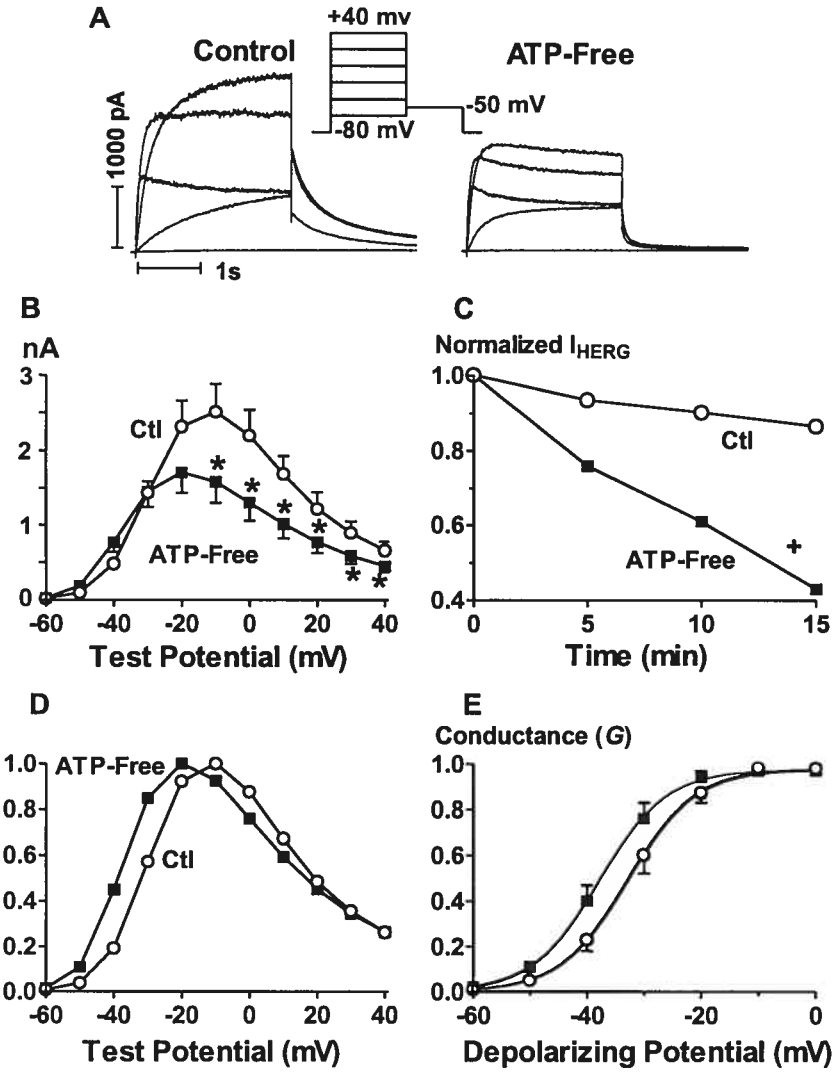

Figure 5. Effects of depletion of intracellular ATP on I_{HERG}. ***A***, Raw I_{HERG} recorded with the ATP-free pipette solution right after membrane rupture as baseline control data (left) and 10 min after membrane rupture with complete dialysis (right). ***B***, Mean I-V relationships (n=5 cells) showing the depression of I_{HERG} caused by depletion of intracellular ATP. ***C***, Time-dependent changes of I_{HERG} at –10 mV showing the current rundown with the ATP-free pipette solution, which is otherwise minimal with the ATP-containing pipette solution. ***D***, Normalized I-V relationships showing the negative shift of voltage-dependence of I_{HERG} caused by the depletion of intracellular ATP. ***E***, Activation conductance (*G*) curves before and after ATP depletion. $^{*}p < 0.05$ *vs* Ctl, paired *t*-tests; $^{+}p<0.05$, *F*-test indicating the statistical significance of the time-dependence.

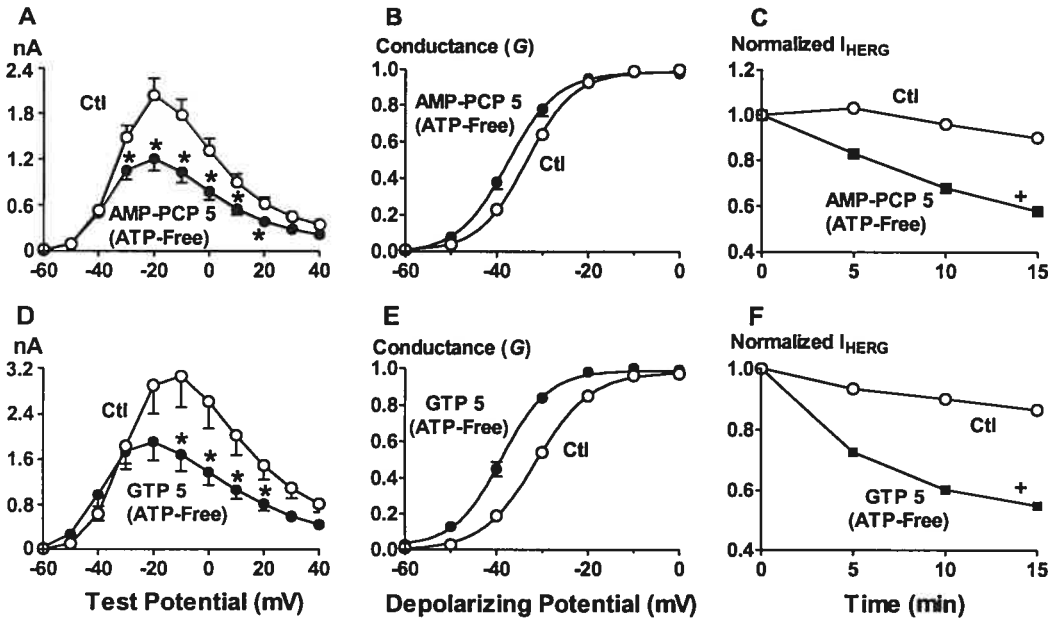

Figure 6. Effects of non-hydrolysable ATP (AMP-PCP) and GTP on I_{HERG}. ***A*** and ***D***, I-V relationships. I_{HERG} was recorded right after membrane rupture and 10 min after dialysis with the ATP-free pipette solution containing AMP-PCP (n=10) (***A***) or GTP (n=7) (***D***). ***B*** and ***E***, Activation conductance (*G*) curves before and after AMP-PCP or GTP in the ATP-free internal solution. The numbers in the legends represent AMP-PCP or GTP concentrations in mM. ***C*** and ***F***, Time-dependent changes of I_{HERG} at −10 mV recorded with the pipette containing ATP (control-Ctl) or AMP-PCP (***C***) or GTP (***F***). $^{*}p < 0.05$ *vs* Ctl, paired *t*-tests; $^{+}p<0.05$, *F*-test indicating the significance of time-dependence.

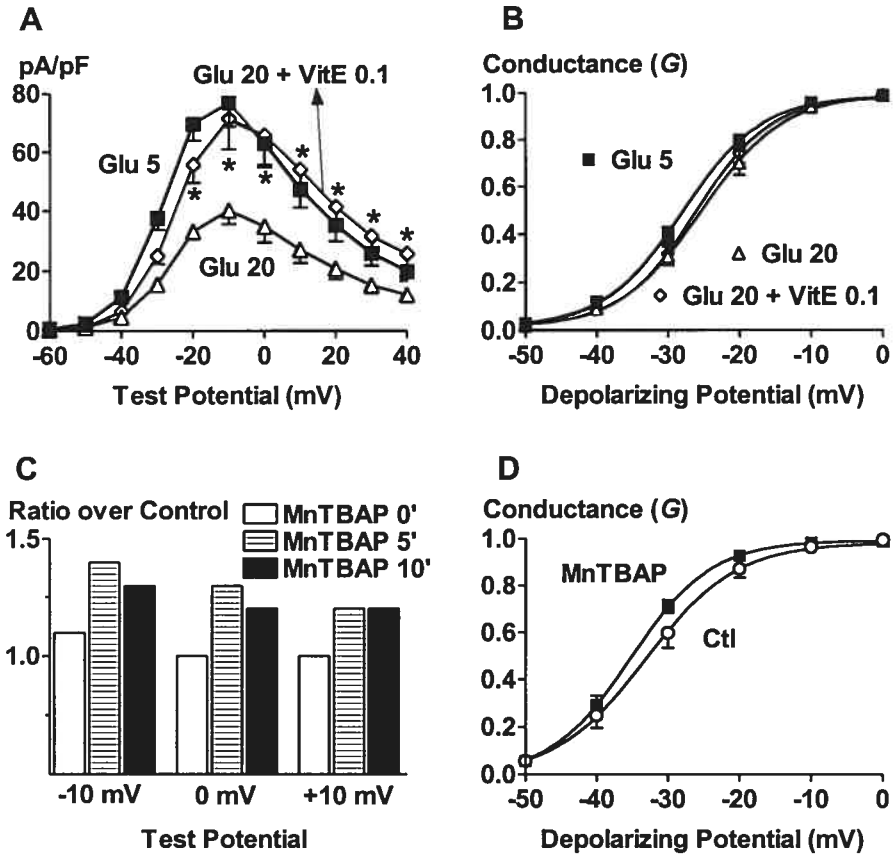

Figure 7. Effects of antioxidants on I_{HERG} depression induced by hyperglycemia (20 mM $[Glu]_o$). ***A*** and ***B***, Mean current density (pA/pF)-voltage relationships and activation conductance (*G*) curves, respectively, showing the effects of vitamin E (VitE, 100 μM) on I_{HERG} under 20 mM $[Glu]_o$. The cells were superfused with VitE for 40 min or with the normal Tyrode solution for control before patch-clamp recordings. Group comparison was made between the untreated control cells (Ctl, n=9) and the VitE-treated (n=8) cells. $*p < 0.05$ *vs* Ctl, unpaired *t*-tests. ***C*** and ***D***, Mean current density (pA/pF)-voltage relationships and activation conductance (*G*) curves, respectively, showing the effects of MnTBAP (5 μM), a superoxide dismutase mimetic, on I_{HERG} under 20 mM $[Glu]_o$. MnTBAP was applied intracellularly through the pipette. I_{HERG} recorded immediately after whole-cell formation and series resistance compensation was taken as baseline control data (Ctl) and that recorded 10 min after dialysis was used for analysis to reflect the effects of MnTBAP. To correct for potential rundown of the current, the I_{HERG} recorded with MnTBAP was normalized to that recorded with the normal internal solution. $*p < 0.05$ *vs* Ctl, paired *t*-tests.

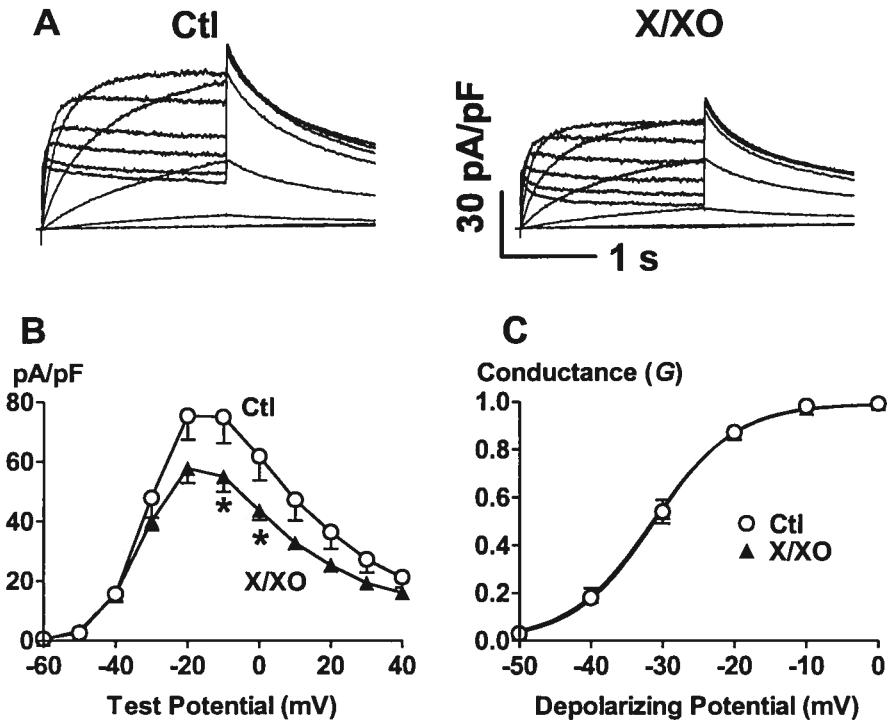

Figure 8. Effects of the oxidant generating system xanthine/xanthine oxidase (X/XO) on I_{HERG} under normoglycemia (5 mM $[Glu]_o$). ***A***, Analog data of I_{HERG} with and without treatment with X/XO. The cells were superfused with X/XO (500 μM/5 mU/ml) for >30 min before patch-clamp recordings. ***B*** and ***C***, Mean current density (pA/pF)-voltage relationships and activation conductance (*G*) curves, respectively. Group comparison was made between the untreated control cells (Ctl) and the X/XO-treated cells. **p*<0.05 *vs* Ctl, unpaired *t*-tests, n=8 for Ctl and n=7 for X/XO.

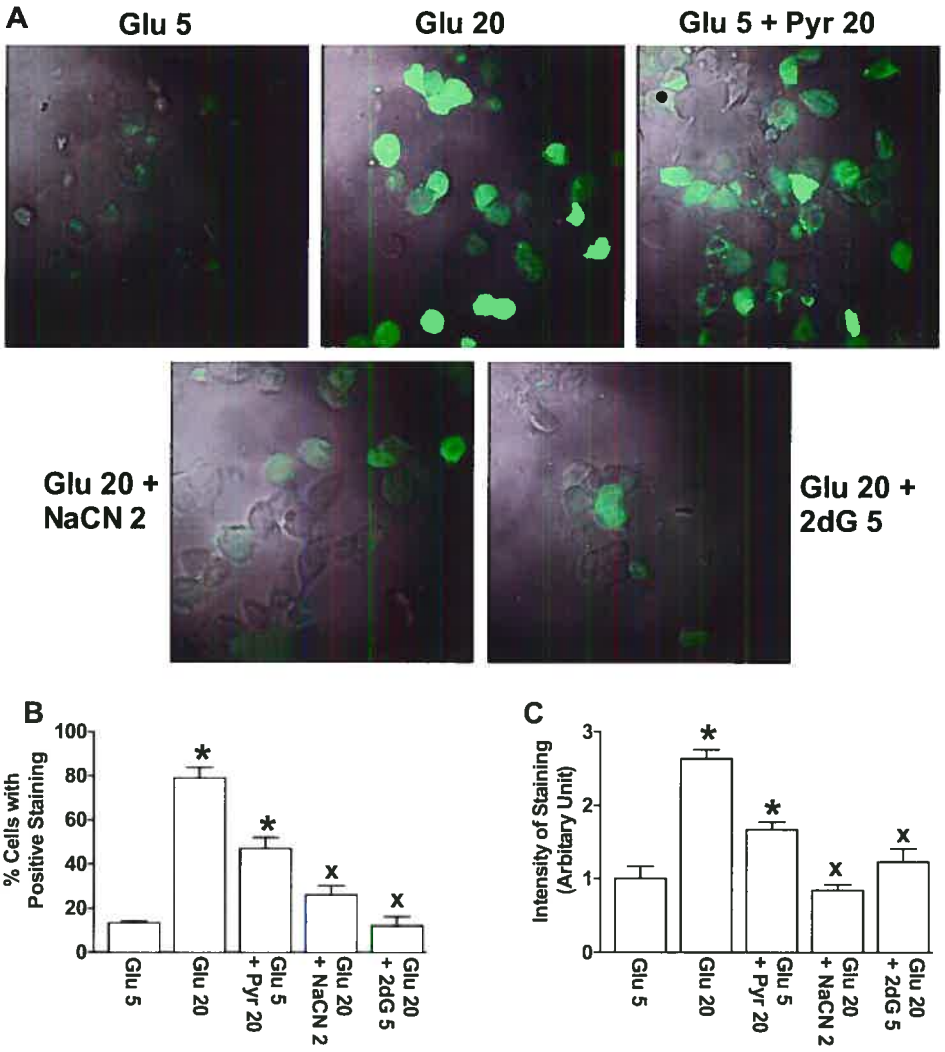

Figure 9. Oxidative phosphorylation and intracellular levels of reactive oxygen species (ROS) measured by CM-H_2DCFDA fluorescence dye. ***A***, Laser scanning confocal microscopic images of CM-H_2DCFDA staining reflecting the intracellular ROS levels. The numbers in the labels indicate the concentrations in mM. Note the focused staining on the rod-shaped structures in the cells under normoglycemia and the diffused staining throughout the cytoplasm in the cells treated with high glucose or pyruvate. ***B***, Percentage of positively stained cells (Mean±S.E.), obtained from 5 fields of 3 experiments by counting the cells with staining intensity ≥ 5 times the background. ***C***, Averaged intensity of CM-H_2DCFDA fluorescence measured from the positively stained cells. Shown are the data normalized to 5 mM $[Glu]_o$. . *$p<0.05$ *vs* Glu 5 mM and $^x p<0.05$ *vs* Glu 20 mM, unpaired *t*-tests.

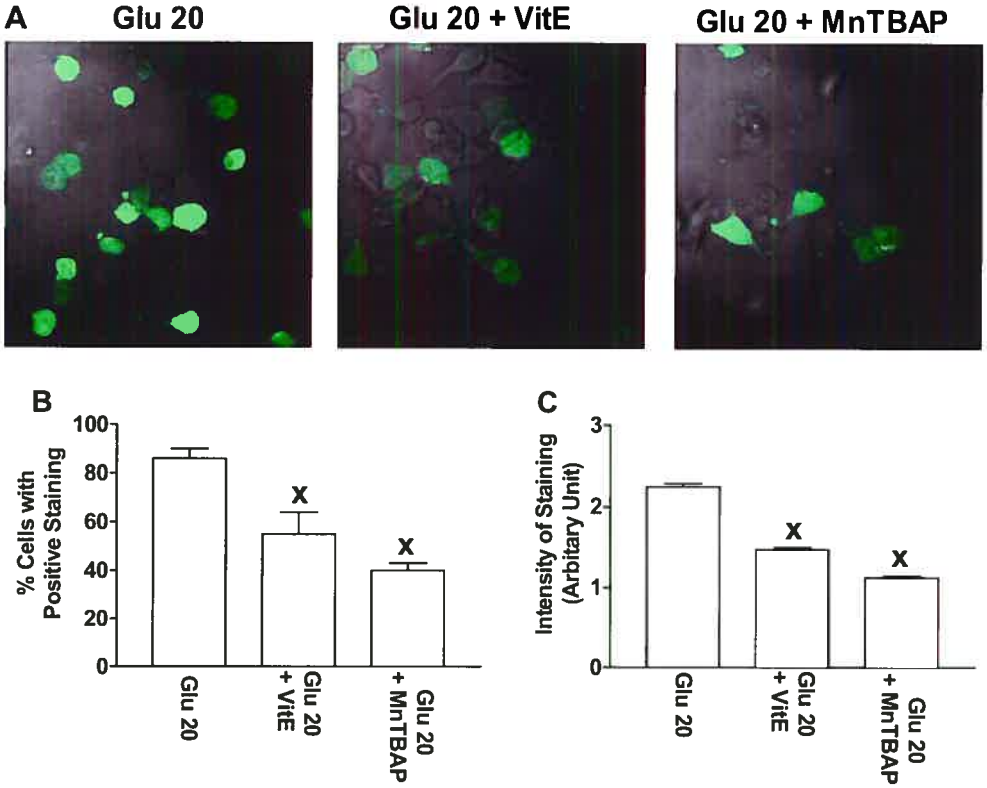

Figure 10. Effects of antioxidants vitamin E (VitE, 100 μM) and superoxide dismutase (SOD) mimetic (MnTBAP, 10 μM) on intracellular ROS levels under hyperglycemia ($[Glu]_o$ **=20 mM).** ***A***, Confocal microscopic images of CM-H_2DCFDA staining showing decreases in the intracellular ROS levels in the cells treated with VitE or MnTBAP. ***B***, Percentage of the positively stained cells (Mean±S.E.), obtained from 5 fields of 3 experiments by counting the cells with staining intensity ≥ 5 times the background. ***C***, Averaged intensity of CM-H_2DCFDA fluorescence measured from the positively stained cells. Shown are the data normalized to the control (Ctl) cells without antioxidant treatment. $^{x}p<0.05$ *vs* Glu 20 mM, unpaired *t*-tests.

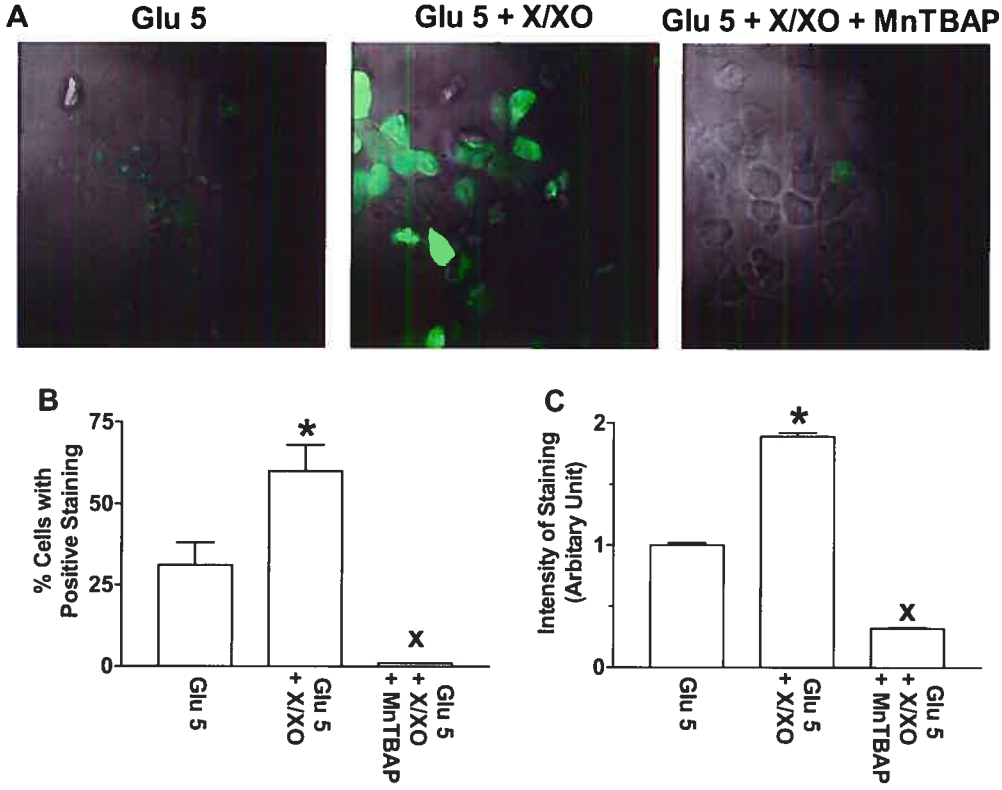

Figure 11. Effects of the superoxide generating system xanthine/xanthine oxidase (X/XO) on the intracellular ROS levels under normoglycemia ($[Glu]_o$ =5 mM). ***A***, Confocal microscopic images of CM-H_2DCFDA staining showing the increases in the intracellular ROS levels by X/XO (0.5 mM/5 mU/ml) and the abrogation of ROS increase by the SOD mimetic MnTBAP (10 μM). ***B***, Percentage of the positively stained cells (Mean±S.E.), obtained from 5 fields of 3 experiments by counting the cells with intensity of staining ≥ 5 times the background. ***C***, Averaged intensity of staining measured from the positively stained cells. Shown are the data normalized to the control (Ctl) cells without X/XO treatment. $^{*}p<0.05$ *vs* Glu 5 mM and $^{x}p<0.05$ *vs* Glu 5 mM + X/XO, unpaired *t*-tests.

6 NORMAL FUNCTION OF HERG K^+ CHANNELS REQUIRES BASAL PROTEIN KINASE B ACTIVITY

Previous chapters have identified the I_{Kr}/HERG impairment as a mechanism for the diabetic APD and QT prolongation, and deciphered the roles of glucose, insulin, ATP and reactive oxygen species on I_{Kr}/HERG K^+ channel. Protein kinase B (PKB) is a downstream molecule in the insulin-signaling cascade which is impaired in DM. Moreover, there are two putative PKB phosphorylation sites on HERG K^+ channels. In this part, I used pharmacological tools together with molecular expression techniques to assess the potential function of PKB on HERG K^+ channel.

This work has been published in the *FEBS Letters* 2003; **534**: 125-132

Normal Function of HERG K^+ Channels Expressed in HEK293 Cells Requires Basal Protein Kinase B Activity

Yiqiang Zhang[a,b], Huizhen Wang[a,b], Jingxiong Wang[a,b], Hong Han[a], Stanley Nattel[a,c,d], and Zhiguo Wang[a,b,*]

[a]Research Center, Montreal Heart Institute, Montreal, Quebec, Canada, H1T 1C8

[b]Department of Medicine, University of Montreal, Montreal, Quebec, Canada, H3C 3J7

[c]Department of Pharmacology, University of Montreal, Montreal, Quebec, Canada, H3C 3J7

[d]Department of Pharmacology and Therapeutics, McGill University, Montreal, Quebec, Canada, H3A 2T5

*Corresponding author: Research Center, Montreal Heart Institute, 5000 Belanger East, Montreal, PQ H1T 1C8, Canada; Tel.: (514) 376-3330. Fax: (514) 376-4452. E-mail: [redacted]

6.1 Abstract

The potential role of protein kinase B (PKB), a serine/threonine protein kinase, in regulating HERG (human *ether-a-go-go* related gene) K^+ channel function was investigated. Wortmannin (a PI3K inhibitor) caused ~30% reduction of HERG current (I_{HERG}) stably-expressed in HEK293 cells. Transient transfection with the constitutively active PI3K in HERG-expressing HEK293 cells slightly increased (~7%) I_{HERG} while a dominant negative PI3K significantly reduced I_{HERG} (~25%) relative to results in vehicle-transfected cells. I_{HERG} was ~35% greater in cells transfected with the constitutively activated PKB (caPKB), whereas it was ~47% smaller in cells transfected with dominant negative PKB (dnPKB). Basal activation of PKB was detected by immunocytochemistry. PKB activity was significantly enhanced in caPKB-transfected cells and nearly abolished in dnPKB-transfected cells. We conclude that normal HERG function in HEK293 cells requires basal activity of PKB. Our data represent the first evidence that PKB phosphorylation regulates K^+ channels.

Key Words: HERG; Protein kinase B; Phosphoinositide 3-kinase; Wortmannin; Patch-clamp, Immunocytochemistry.

Abbreviations: Bis bisindolylmaleimide; *HERG*, human ether-ago-go related gene; HERG, K^+ channel protein encoded by *HERG*; IHERG, current expressed by HERG; PKB, protein kinase B; caPKB, constitutively active PKB; dnPKB, dominant negative PKB; PI3K, phosphoinositide 3-kinase; caPI3K, constitutively active PI3K; dnPI3K, dominant negative PI3K; WMN, wortmaninn.

6.2 Introduction

PKB, a downstream target of phosphatidylinositol 3-kinase (PI3K), is a serine/threonine (Ser/Thr) protein kinase first identified several years ago [1-2]. The cDNA sequence of PKB displays high sequence homology to both the protein kinase C and the protein kinase A family of Ser/Thr kinases. It was therefore termed protein kinase B (PKB) [1-2]. PKB can be activated by a wide variety of stimuli in a PI3K-dependent or -independent manner [3-4]. The fungal metabolite wortmannin is a potent inhibitor of kinase activities of class I PI3K, with an IC_{50} in the range of 1 10 nM [5]. By inhibiting PI3K, wortmannin can prevent PI3K-dependent activation of PKB and it has been widely used to study the physiological role of the PI3K/PKB signaling pathway in various cellular processes.

It is well established that PKA and PKC can both regulate ion channel function by Ser/ Ther phosphorylation of channel proteins, providing an important mechanism for regulation of cell function. In contrast, the potential role of PKB in modulating ion channel function has been largely ignored. Only recently has the PI3K/PKB pathway been found to be involved in the regulation of some ion channels, for example, the potentiation of L-type Ca^{2+} current and M-current in neurons [6-7], enhancement of Cl^- currents in rat hepatoma cell [8], and up-regulation of several *Shaker*-type K^+ channels in human embryonic kidney cell line [9]. It is believed that modulation of these ion channels contributes to regulation by PI3K/PKB of cell survival, cell growth, cell column and other cell functions. Among these studies, however, only the work reported by Blair et al [6] demonstrated that the modulation of the L-channel was PKB-dependent.

HERG encodes the rapid component of delayed rectifier K^+ current in the heart, and HERG dysfunction is known to account for both inherited and acquired long Q-T syndrome [10], a potentially-lethal arrhythmia. Recent studies have revealed widespread distribution of HERG in various tissues and cells outside the heart, including neurons [11-12], pancreatic β-cells [13], and a variety of tumor cells [14-15], where in addition to its cardiac electrophysiological role, HERG may also participate in the regulation of cell growth and death [16]. The HERG protein contains two putative consensus sequence motifs for PKB phosphorylation located at S890 and S331 [4, 17-18). Although HERG has been found to be a target for PKA phosphorylation [19-21] and probably also for PKC [22-23], it is unknown whether it is also a substrate for PKB. The present

study was therefore undertaken to define the potential regulation of HERG channel function by PKB.

6.3 Materials and Methods

6.3.1 Cell culture

HEK293 cells stably expressing HERG (a kind gift from Drs. Z Zhou and C January) [24] were seeded in a 25 cm^2 cell-culture flask and grown in Dulbecco's Modified Eagle's Medium (DMEM, Life Technologies) supplemented with 10% heat-inactivated FBS, 200-μg/mL G418 (Sigma), 100-U/ml penicillin and 100-μg/ml streptomycin (Life Technologies). The cells were subcultured to ~85% confluency, harvested by trypsinization and stored in Tyrode's solution containing 0.5% BSA at 4°C.

6.3.2 Gene transfection

The constructs expressing the constitutively active bovine PI3K (caPI3K), pCMV6-p110α-mycC, and the dominant-negative mouse PI3K (dnPI3K) in pcDNA3, pcDNA3-Δp110α-mycC were kind gifts from Dr. L. Cantley [25]. The constitutively active mouse PKB in pECE (caPKB), and dominant negative bovine PKB in pCMV6 (dnPKB) were kind gifts from Dr. T. Franke and Dr. M. Greenberg [25-26]. The cDNA transfection procedures have been described in detail elsewhere [27]. Cells grown to ~80% confluency in 35 mm culture dishes with DMEM free of antibiotics were washed once with phosphate-buffered saline (PBS). Aliquots containing 2~3 μg of caPI3K, dnPI3K, caPKB, or dnPKB, plus 0.3 μg pπX-CD8 plasmid DNA were diluted into 100 μl DMEM and mixed well with 6 μl Plus reagent from the LipofectAMINE Plus reagent kit (Life Technologies) and incubated at room temperature (RT) for 15 min. The DNA-Plus regent pre-complex was then added to 4 μl LipofectAMINE reagent in 100 μl of DMEM. The mixture was incubated at RT for 15 min and added to the cells in a dish containing fresh serum-free DMEM and swirled to distribute the complex uniformly, and incubated at 37°C under 5% CO_2 for 3 h. The cells were allowed to grow for 48 h before being harvested for analysis. Sham and blank control experiments were conducted in parallel. For electrophysiological experiments, the cells were harvested and incubated with 2 μl anti-CD8 Dynabead (Dynal ASA, Osio, Norway) at RT for 15 min to label the transfected cells [27].

6.3.3 Whole-Cell Patch-Clamp Recording

Patch-clamp techniques have been described in detail elsewhere [27-28]. Currents were recorded with whole-cell voltage-clamp with an Axopatch-200B amplifier (Axon Instruments). Borosilicate glass electrodes had tip resistances of 1-3 MΩ when filled with (mM): 130 KCl, 1 $MgCl_2$, 5 Mg-ATP, 10 EGTA, 10 HEPES (pH 7.3). The extracellular solution contained (mM): 136 NaCl, 5.4 KCl, 1 $CaCl_2$, 1 $MgCl_2$, 10 glucose and 10 HEPES (pH 7.4). Experiments were conducted at 36±1°C. Junction potentials were zeroed before formation of the membrane-pipette seal. Series resistance and capacitance were compensated and leak currents were subtracted.

Wortmannin (WMN; PI3K inhibitor; Sigma Chemicals) and bisindolylmaleimide (Bis; PKC inhibitor; Sigma Chemicals), and N-[2-(p-bromocinnamylamino) ethyl]-5-isoquinoline-sulfonamide-2HCl (H89; PKA inhibitor; Biomol Research Labs, Plymouth Meeting, PA), were dissolved in dimethyl sulfoxide (DMSO) as 1000 x stock solutions and stored at -20°C, and the stock solutions were diluted to the desired concentrations right before the experiments.

6.3.4 Immunocytochemistry

The immunocytochemical procedures used have been previously described in detail [16, 29]. In short, cells grown on coverslips were fixed with freshly prepared 1% paraformaldehyde, followed by permeablization in 0.1% Triton X-100 and blocked in 1% BSA. Cells were then incubated overnight at 4°C with primary antibodies diluted in 1% BSA, followed by incubation with FITC- or TRITC-conjugated secondary antibodies at room temperature for 2 hrs. Rabbit polyclonal antibody against phospho-PKB (S473) was purchased from New England BioLabs (Beverly, MA) and goat polyclonal anti-CD8 antibody was purchased from Santa Cruz (Santa Cruz, CA). The specificity of the anti-phospho-PKB antibody has been tested in our previous studies [30]. Donkey anti-rabbit, FITC-conjugated and donkey anti-goat, TRITC-conjugated antibodies, purchased from Jackson Immuno-Research (Baltimore, USA), were used as secondary antibodies. Nonspecific staining by the secondary antibodies was excluded by the absence of staining in cells treated with the secondary antibodies alone. Coverslips were mounted onto glass slides with anti-fading mounting medium and were immediately examined under confocal laser scanning microscope equipment (model LSM 510; Zeiss). Excitation/ emission wavelengths for FITC and TRITC were 488/512 and 543/576 nm, respectively and FITC (green) and TRITC (red) were excited separately to avoid bleed-through effects. The

settings for laser scanning and image such as laser power, pinhole, amplification factor and gain, were set optimal to avoid false positive or false negative staining and for a given experiment, the settings were identical for all slides under examination. Each image represents an average from four-consecutive slow-speed scannings. Density of staining by anti-phospho-PKB antibody was measured by LSM 510 software suite and only positively stained cells were analyzed except for the cells in control group.

6.3.5 *Data analysis*

Group data are expressed as mean±SEM. Paired or non-paired Student *t*-tests were used for before-and-after or group comparisons as appropriate. A two-tailed $p<0.05$ was taken to indicate a statistically-significant difference. Nonlinear least-square curve-fitting was performed with CLAMPFIT in pCLAMP 8.0 or Graphpad Prism.

6.4 Results

6.4.1 *Effects of wortmannin on HERG currents (I_{HERG})*

Currents were recorded in HEK293 cells stably expressing HERG with a two-step voltage protocol. The cell membrane was held at –80 mV, and stepped from –60 mV to +40 mV in 10 mV increments for 2.5 s to measure the step current and then returned to a constant potential at –50mV for 2.5 s to measure the tail currents (Fig 1A). The effects of the inhibitor of PI3K wortmannin (WMN) were assessed following intracellular application. WMN (50 nM) was included in the pipette solution and dialyzed into the cytosol. Under our experimental conditions, 10 min was sufficient for complete dialysis. I_{HERG} was recorded right after membrane rupture and the same measurements were repeated every 5 min for a total of 20 min. The recordings made 15 min after membrane rupture were used to reflect the effects of WMN. As a control, cells were dialyzed and currents recorded in an identical fashion, but with WMN absent from the pipette solution. As illustrated in Fig. 1, WMN appeared to have 2 effects- a decrease in maximum conductance, along with a voltage shift tending to increase current at negative voltages. To ensure the suppression of I_{HERG} by WMN was not due to rundown of the current, we compared I_{HERG} recorded at various time points after membrane rupture. The data in Fig. 1C show that in absence of WMN rundown of I_{HERG} was minimum (~5%) whilst in presence of WMN I_{HERG}

demonstrated a profound attenuation over a period of 15 min which coincided with the time course of dialysis of internal solution through a pipette under our experimental conditions. WMN did not alter the kinetics (time-dependent activation, inactivation and reactivation) of the current (data not shown).

Additional experiments were performed to ensure that the effects of WMN on I_{HERG} are not due to PKA and/or PKC activation. Cells were first bathed with H89 (1 μM) to inhibit PKA or bisindolylmaleimide (Bis, 100 nM) to inhibit PKC. Inhibitors were added to Tyrode's solution 20 min before patch-clamp recording with WMN (50 nM)-containing pipettes. Under these conditions, WMN produced qualitatively similar effects to those seen in experiments without H89 or Bis treatment. For example, I_{HERG} current density in the presence of H89 was 2.4±0.6 pA/pF before and 3.4±0.9 pA/pF ($p<0.05$, n=6) after WMN at -40 mV, and 51.7±7.9 pA/pF before and 40.8±7.3 pA/pF ($p<0.05$) after WMN at 0 mV. In the presence of Bis, I_{HERG} densities were 2.7±0.6 pA/pF before and 5.4±1.3 pA/pF ($p<0.05$, n=7) after WMN at -40 mV, and 63.9± 10.1 pA/pF before and 55.3±9.8 pA/pF ($p<0.05$) after WMN at 0 mV. To validate the concentrations of H89 and Bis used in our experiments, we conducted additional experiments with Shaw-like voltage-gated K^+ channel Kv4.3 expressed in HEK293 cells and we found that 1 μM H89 and 100 nM Bis completely reversed the effects produced by PKA and PKC stimulation caused by isoproterenol and phenylephrine, respectively (data not shown).

6.4.2 *Effects of constitutively active or dominant negative PI3K on I_{HERG}*

The results of the above experiments suggest that basal PI3K/PKB activation contributes to maintaining I_{HERG}/I_{Kr} function in the absence of external stimuli for PI3K/PKB activation. The data do not indicate whether the effects are due to PI3K activation, PKB activation or both. We began to address this issue by transiently transfecting constitutively active PI3K (caPI3K) into HEK293 cells stably expressing HERG. I_{HERG} recorded in CD8 bead-labeled cells (indicating caPI3K transfection) was compared with I_{HERG} in untransfected cells or sham-treated counterparts. The data are presented in Fig. 2, where greater I_{HERG} density was seen at potentials negative to 0 mV in caPI3K-transfected cells relative to sham cells. For example, I_{HERG} density at -40 mV was 3.3±0.4 pA/pF (n=30) for sham control and 9.6±3.6 pA/pF ($p<0.05$, n=25) for caPI3K (increased by ~2 folds), and at 0 mV was 91.9±9.5 pA/pF for control and 102.4±11.4 pA/pF for caPI3K (increased by ~10%, $p>0.05$, unpaired *t*-test). At potential positive to -10 mV,

no appreciable differences between groups were observed. By contrast, the cells transfected with dnPI3K showed increased I_{HERG} only at potential negative to -20 mV and moderate reduction of I_{HERG} was seen at potentials more positive than -20 mV. For example, I_{HERG} densities in dnPI3K-transfected cells was 7.1±2.6 pA/pF (~2-fold larger than in the sham group, $p>0.05$) at -40 mV, and was 79.1±11.7 pA/pF (~25% smaller than in the sham group, $p>0.05$) at 0 mV. The effects of dnPI3K are qualitatively comparable to those of WMN.

6.4.3 *Effects of constitutively active or dominant negative PKB on I_{HERG}*

To test the potential direct role of PKB, we performed experiments with transient transfection of constitutively active PKB (caPKB) or dominant negative PKB (dnPKB) in HERG-expressing HEK293 cells. Consistent with an important role for PKB, caPKB increased and dnPKB decreased I_{HERG}. Fig. 3 compares I_{HERG} in cells transected with plasmids containing caPKB plus plasmids to cells with cDNAs expressing CD8 alone, as well as untreated control cells. In all cases, there were no significant differences in I_{HERG} between control and CD8-transfected cells. I_{HERG} density measured from caPKB cells was clearly greater than that of control or CD8-transfected cells at all voltages ranging from -40 to +40 mV, and there was a tendency with greater differences at more positive potentials. For example, I_{HERG} density was 36%, 37% and 67% greater at -40 mV, 0 mV and +40 mV, respectively, in caPKB than in control cells (Fig. 3C). On the other hand, I_{HERG} was substantially smaller in dnPKB-transfected than in non-transfected or CD8-transfected cells at potentials positive to -20 mV, but was greater at potentials negative to this voltage (Fig. 3D-3F). For instance, at 0 mV I_{HERG} density values were 90.4±13.4 pA/pF (n=20 cells) and 48.7±3.9 pA/pF ($p<0.05$, n=19) in control and in dnPKB-transfected cells, respectively, whereas at -40 mV, the I_{HERG} density was 11.8±1.6 pA/pF for control and 19.3±5.0 pA/pF ($p<0.05$) for dnPKB cells. These data indicated a 46% decrease at 0 mV and a 53% increase at -40 mV in the presence of dnPKB (Fig. 3F).

6.4.4 *Imuunocytochemical analysis of active PKB*

To confirm that the effects of WMN in our experiments are associated with changes in PKB activity and that the cells transfected with caPKB or dnPKB indeed have increased or reduced PKB activity respectively, we performed immunostaining analyses of PKB activity using anti-phospho-PKB (S473) antibody. For WMN experiments, cells were preincubated with

WMN (100 nM) in the culture medium for 30 min before being collected for immunostaining. As shown in Fig. 4A, the immunoreactivity was obviously weaker in WMN-treated than in control cells.

For caPKB/dnPKB experiments, double staining with anti-PKB antibody and anti-CD8 antibody was performed to distinguish the transfected from the non-transfected cells. The staining for phospho-PKB (green) was evenly distributed throughout the cytoplasm and CD8, a membrane protein co-transfected with caPKB as a marker for successful transfection, was stained red only to the plasma membrane. PKB staining was markedly more intense in cells also stained with CD8 than in cells with negative CD8 staining (non-transfected cells) in the same batch (Fig. 4B). The same was true when compared with the control cells that did not undergo the transfection procedures. In sharp contrast, the staining for phospho-PKB was nearly absent although the staining for CD8 was obvious in dnPKB-transfected cells.

The cells transfected with caPI3K showed a slightly higher intensity, while the cells transfected with dnPI3K showed a slightly lower intensity, of phospho-PKB staining than in their respective non-transfected cells or the control cells (Fig. 4B). The quantitative data are presented in Fig. 4C where the ratios of staining intensity in positively stained cells over non-stained control cells are shown.

6.5 Discussion

We demonstrated here that prevention of PI3K/PKB activation by pharmacological inhibition (WMN) or molecular inactivation (dominant negative PI3K and dominant negative PKB) significantly suppressed HERG function, whereas direct activation of PKB by introducing the constitutively active PKB into the cell markedly enhanced HERG function. Inhibition of PKB activation by WMN or dnPI3K or dnPKB and increased activation of PKB with caPKB transfection were confirmed by immunocytochemistry with the use of the anti-phospho PKB antibody. Our data clearly indicate that HERG K^+ channel function in HEK293 cells is enhanced by PKB activation and also provide the evidence for the first time that PKB phosphorylation participates in K^+ channel modulation.

WMN, used to inhibit PI3K activation thereby the downstream PI3K-dependent PKB activation, produced remarkable depression (~30% reduction) of I_{HERG} stably expressed in

HEK293 cells. The effects were observed under normal conditions in absence of stimuli for PI3K/PKB activation. Coincidentally, dnPI3K caused virtually the same changes of I_{HERG} as WMN did: ~25% decrease in current density and ~5 mV shift of activation towards hyper-polarizing potentials. By comparison, direct inactivation of PKB by dnPKB produced a nearly doubled magnitude of effects on I_{HERG} as produced by WMN; dnPKB diminished I_{HERG} density by ~53% and shifted the $V_{1/2}$ by ~6 mV. In addition, while caPI3K produced only slight enhancement (~18%) of I_{HERG} function, caPKB strikingly increased I_{HERG} density (~52%). Correspondingly, caPI3K caused an only slight increase in the active form of PKB whereas caPKB boosted activation of PKB. Taken together these data allow us to reach the following conclusions: (1) PI3K/PKB signaling pathway has regulatory effects on HERG K^+ channel function because inhibition of the pathway diminishes but activation of the pathway enhances I_{HERG}; (2) PI3K/PKB modulation of HERG is likely mediated by a direct effect of PKB but not PI3K phosphorylation because inhibition/activation of PKB produced far more pronounced effects on I_{HERG} compared with inhibition/activation of PI3K did; (3) HERG is under tonic regulation of basal active PKB, or in the other words, basal PKB activation is required for maintaining the normal physiological function of HERG K^+ channel in HEK293 cells, because the effects of PKB inhibition on I_{HERG}, either by pharmacological blockade (WMN) or molecular inactivation (dnPI3K and dnPKB), were seen in the absence of stimuli for PKB activation; and (4) The basal active PKB in HEK293 cells comes from both PI3K-dependent and PI3K-independent mechanisms. The PI3K-dependent activation PKB is WMN sensitive, which can be prevented by treating the cells with WMN, while the PI3K-indenpendent activation of PKB is WMN insensitive. Introduction of dnPKB is expected to wipe out both PI3K-dependent and PI3K-independent activation of PKB. Indeed, our present study consistently showed that molecular inactivation of PKB by dnPKB produced some doubled magnitudes of I_{HERG} depression in comparison with the effects produced by WMN or dnPI3K. If the effects of WMN or dnPI3K on I_{HERG} arise from the PI3K-dependent activation of PKB, then the excess of effects produced by dnPKB over WMN or dnPI3K should represent PKB activation from PI3K-independent mechanisms.

The major finding of this study is that PKB has a tonic modulatory effect on I_{HERG}. Given the fact that dnPKB renders I_{HERG} density half of its size under normal conditions, it is expected that in the absence of basal PKB activation, I_{HERG} amplitude/density would be only

50% of its normal amplitude/density. It is therefore reasonable to conclude that the basal active PKB is required for maintaining the physiological function of I_{HERG} in HEK293 cells. Moreover, our data from caPKB experiments indicate that any further increase in PKB activation may further increase I_{HERG} beyond the basal conditions. Increased PKB activity has actually been noticed in a variety of physiological (such as growth stimulation, increased adrenergic tone, etc) and diseased conditions (such as metabolic stress, oxidative challenge, ischemia, etc) [3-4].

This finding may have some important pathophysiological implications. For example, it has long been known that the cardiac action potential duration (APD) is initially shortened in the early stage of acute myocardial ischemia and is subsequently prolonged in the late phase of ischemia, which is associated with occurrence of different types of arrhythmias [31]. Coincidentally, PKB activities follow the same pattern of changes: a marked increase in the early phase followed by an also marked drop in the late phase of ischemia [32]. Considering that the HERG-encoded K^+ current (the rapid component of delayed rectifier K^+ current or I_{Kr}) plays a critical role in determining cardiac APD [10, 33], we can speculate that in the early phase of ischemia the increase in PKB activation enhances I_{Kr} which in turn accelerates the rate of cardiac repolarization or shortens APD, whereas in the late phase of ischemia when PKB activities are reduced I_{Kr} is correspondingly diminished which then leads to lengthening of APD. Also, cardiac APD was reported to be prolonged in the myocytes isolated from animals with type I diabetes and slightly shortened in the myocytes from type II diabetic animal model [34-36]. It is unclear whether these are associated with a decrease in PKB activation in type I diabetic subjects and an increased in type II diabetes.

The PI3K signaling pathway is involved in diverse cellular processes and some of these may be mediated by regulating ion channels. A recent work reported by Gamper et al [9] demonstrated that insulin-like growth factor-1 (IGF-1) up-regulates several voltage-gate K^+ channels belonging to the *Shaker* subfamily including Kv1.1, Kv1.2 and Kv1.3 in HEK293 cells, and the effects were mediated by PI3K and its downstream targets 3-phosphoinositide-dependent protein kinase-1 and serum- and glucocorticoid-dependent kinase 1. Their data excluded the contribution of PKB to modulating *Shaker* K^+ channels. Enhancement of Cl^- channel by PI3K that contributes to volume regulation in rat hepatoma cell was reported by Feranchak et al [8]. Using transient expression of wild-type, dominant-negative, and constitutively active forms of PKB in cerebellar granule neurons, Blair et al elegantly showed that IGF-1 partially mediates

granule neuron survival via L-type Ca^{2+} channel activity and that PKB-dependent L channel modulation is a necessary component because PKB mediates the IGF- 1-induced potentiation of L channel currents [6]. There have no other previous studies on ion channel modulation by PKB. Our data represent the first evidence for the direct role of PKB in K^+ channel modulation.

PKA, PKC and PKB are all Ser/Thr protein kinases, which can phosphorylate their downstream effectors and alter the functional status of these downstream components. PKA and PKC both have been shown to modulate K^+ channels including HERG [19-23]. The minimum sequence motif required for optimal phosphorylation of peptide substrates by PKB is RXRXXS/T*, where X is any amino acid, and * is a bulky hydrophobic residue (phenylalanine (F) or leucine (L)) [3-4, 17-18]. The sequence requirement for PKB phosphorylation is quite similar to that for PKC and distinct from that for PKA [18]. There are three putative PKA phosphorylation sites and one PKB-favorite phosphorylation site (S890) in the C-terminal region, as well as one site (S331) in the N-terminal region, of the HERG sequence. Whether these sites are responsible for HERG modulation by PKB merits further studies with site-directed mutagenesis.

6.6 Acknowledgements

This work was supported by the Canadian Institutes of Health Research (CIHR), the Heart and Stroke Foundation of Quebec (HSFQ), and the Fonds de la Recherche de l'Institut de Cardiologie de Montreal. Z. Wang is a research scholar of the Fonds de Recherche en Sante de Quebec. H. Han and H. Wang are research fellows of HSFC and CIHR, respectively. The authors thank XiaoFan Yang for her excellent technical support and Louis Villeneuve for his assistance in confocal microscope examination.

6.7 References

1. Coffer, P. J. and Woodgett, J. R. (1991) Eur.J.Biochem. 201, 475-481.
2. Jones, P. F., Jakubowicz, T., Pitossi, F. J., Maurer, F., and Hemmings, B. A. (1991) Proc.Natl.Acad.Sci.U.S.A 88, 4171-4175.
3. Chan, T. O., Rittenhouse, S. E., and Tsichlis, P. N. (1999) Annu.Rev.Biochem. 68, 965-1014.
4. Vanhaesebroeck, B. and Alessi, D. R. (2000) Biochem.J. 346 Pt 3, 561-576.
5. Wymann, M. P., Bulgarelli-Leva, G., Zvelebil, M. J., Pirola, L., Vanhaesebroeck, B., Waterfield, M. D., and Panayotou, G. (1996) Mol.Cell Biol. 16, 1722-1733.
6. Blair, L. A., Bence-Hanulec, K. K., Mehta, S., Franke, T., Kaplan, D., and Marshall, J. (1999) J.Neurosci. 19, 1940-1951.
7. Tokimasa, T., Ito, M., Simmons, M. A., Schneider, C. R., Tanaka, T., Nakano, T., and Akasu, T. (1995) Br.J.Pharmacol. 114, 489-495.
8. Feranchak, A. P., Roman, R. M., Schwiebert, E. M., and Fitz, J. G. (1998) J.Biol.Chem. 273, 14906-14911.
9. Gamper, N., Fillon, S., Huber, M., Feng, Y., Kobayashi, T., Cohen, P., and Lang, F. (2002) Pflugers Arch. 443, 625-634.
10. Sanguinetti, M. C. (1999) Ann.N.Y.Acad.Sci. 868, 406-413.
11. Chiesa, N., Rosati, B., Arcangeli, A., Olivotto, M., and Wanke, E. (1997) J.Physiol 501 (Pt 2), 313-318.
12. Crociani, O., Cherubini, A., Piccini, E., Polvani, S., Costa, L., Fontana, L., Hofmann, G., Rosati, B., Wanke, E., Olivotto, M., and Arcangeli, A. (2000) Mech.Dev. 95, 239-243.
13. Rosati, B., Marchetti, P., Crociani, O., Lecchi, M., Lupi, R., Arcangeli, A., Olivotto, M., and Wanke, E. (2000) FASEB J. 14, 2601-2610.
14. Arcangeli, A., Rosati, B., Cherubini, A., Crociani, O., Fontana, L., Ziller, C., Wanke, E., and Olivotto, M. (1997) Eur.J.Neurosci. 9, 2596-2604.
15. Bianchi, L., Wible, B., Arcangeli, A., Taglialatela, M., Morra, F., Castaldo, P., Crociani, O., Rosati, B., Faravelli, L., Olivotto, M., and Wanke, E. (1998) Cancer Res. 58, 815-822.

16. Wang, H., Zhang, Y. , Cao, L., Han, H., Wang, J., Yang, B., Nattel, S. and Wang, Z. (2002) Cancer Res. 62, 4843-4848.
17. Alessi, D. R., Caudwell, F. B., Andjelkovic, M., Hemmings, B. A., and Cohen, P. (1996) FEBS Lett. 399, 333-338.
18. Obata, T., Yaffe, M. B., Leparc, G. G., Piro, E. T., Maegawa, H., Kashiwagi, A., Kikkawa, R., and Cantley, L. C. (2000) J.Biol.Chem. 275, 36108-36115.
19. Kiehn, J., Karle, C., Thomas, D., Yao, X., Brachmann, J., and Kubler, W. (1998) J.Biol.Chem. 273, 25285-25291.
20. Thomas, D., Zhang, W., Karle, C. A., Kathofer, S., Schols, W., Kubler, W., and Kiehn, J. (1999) J.Biol.Chem. 274, 27457-27462.
21. Cui, J., Melman, Y., Palma, E., Fishman, G. I., and McDonald, T. V. (2000) Curr.Biol. 10, 671-674.
22. Barros, F., Gomez-Varela, D., Viloria, C. G., Palomero, T., Giraldez, T., and de la, P. P. (1998) J.Physiol 511 (Pt 2), 333-346.
23. Jiang, M., Dun, W., Fan, J. S., and Tseng, G. N. (1999) J.Pharmacol.Exp.Ther. 291, 1324-1336.
24. Zhou, Z., Gong, Q., Ye, B., Fan, Z., Makielski, J. C., Robertson, G. A., and January, C. T. (1998) Biophys.J. 74, 230-241.
25. Franke, T. F., Kaplan, D. R., Cantley, L. C., and Toker, A. (1997) Science 275, 665-668.
26. Dudek, H., Datta, S. R., Franke, T. F., Birnbaum, M. J., Yao, R., Cooper, G. M., Segal, R. A., Kaplan, D. R., and Greenberg, M. E. (1997) Science 275, 661-665.
27. Wang, Z., Feng, J., Shi, H., Pond, A., Nerbonne, J. M., and Nattel, S. (1999) Circ.Res. 84, 551-561.
28. Wang, H., Yang, B., Zhang, Y., Han, H., Wang, J., Shi, H., and Wang, Z. (2001) J.Biol.Chem. 276, 40811-40816.
29. Wang, H., Han, H., Zhang, L., Shi, H., Schram, G., Nattel, S., and Wang, Z. (2001) Mol.Pharmacol. 59, 1029-1036.
30. Han, H., Wang, H., Long, H., Nattel, S., and Wang, Z. (2001) J.Biol.Chem. 276, 26357-26364.
31. Carmeliet, E. (1999) Physiol Rev. 79, 917-1017.

32. Mockridge, J. W., Marber, M. S., and Heads, R. J. (2000) Biochem. Biophys. Res. Commun. 270, 947-952.
33. Wang, Z., Fermini, B., and Nattel, S. (1994) Cardiovasc.Res. 28, 1540-1546.
34. Casis, O., Gallego, M., Iriarte, M., and Sanchez-Chapula, J. A. (2000) Diabetologia 43, 101-109.
35. Nordin, C., Gilat, E., and Aronson, R. S. (1985) Circ.Res. 57, 28-34.
36. Shimoni, Y., Ewart, H. S., and Severson, D. (1998) J.Physiol 507 (Pt 2), 485-496.

6.8 Figures and Figure Legends

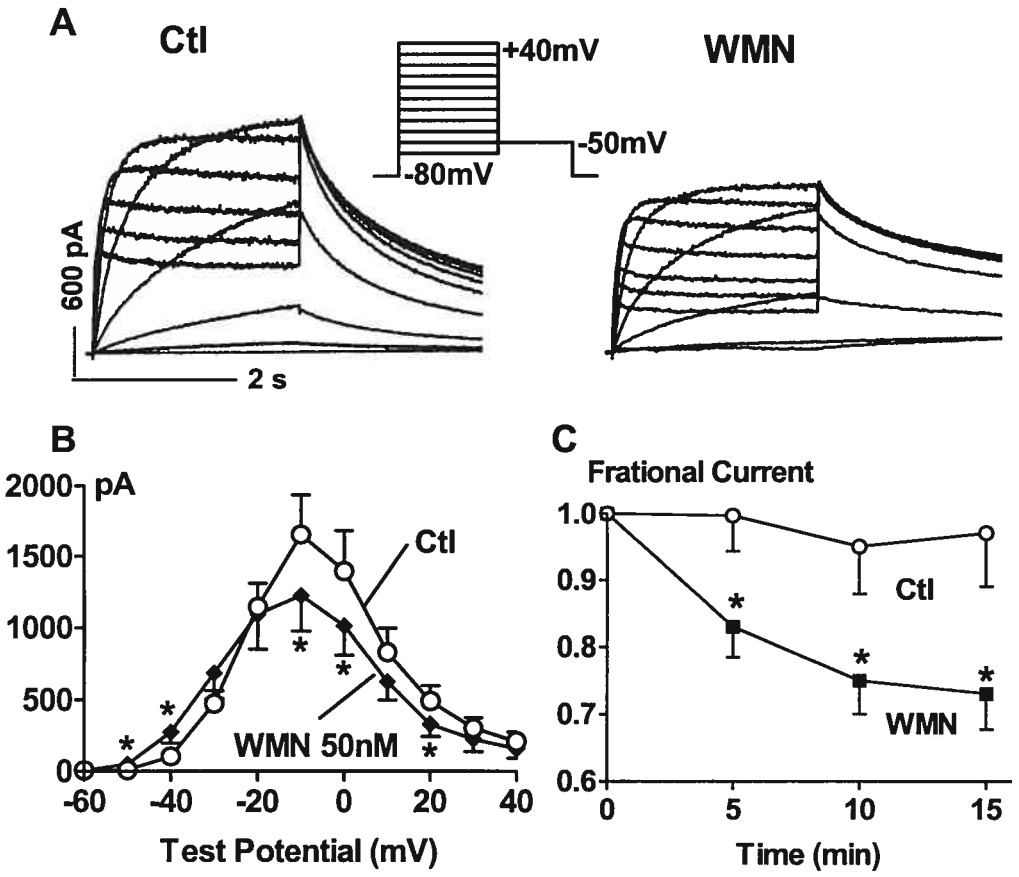

Figure 1. Effects of wortmannin on I_{HERG} stably expressed in HEK293 cells. **A:** I_{HERG} recordings made immediately after membrane rupture with minimal dialysis, taken as baseline control data (Ctl), and 15 min after membrane rupture with complete dialysis through the pipette containing wortmannin (WMN, 50 nM). I_{HERG} was elicited with the voltage protocol shown in the inset. The same voltage protocol is applied to the subsequent figures. **B:** I_{HERG} step current-voltage (I-V) relations (n=25). **C:** Changes of I_{HERG} amplitude at –10 mV with time after formation of whole cell configuration. Shown are data collected from recordings with pipettes without (Ctl, n=10) or with WMN (n=10). *p<0.05 WMN vs. control

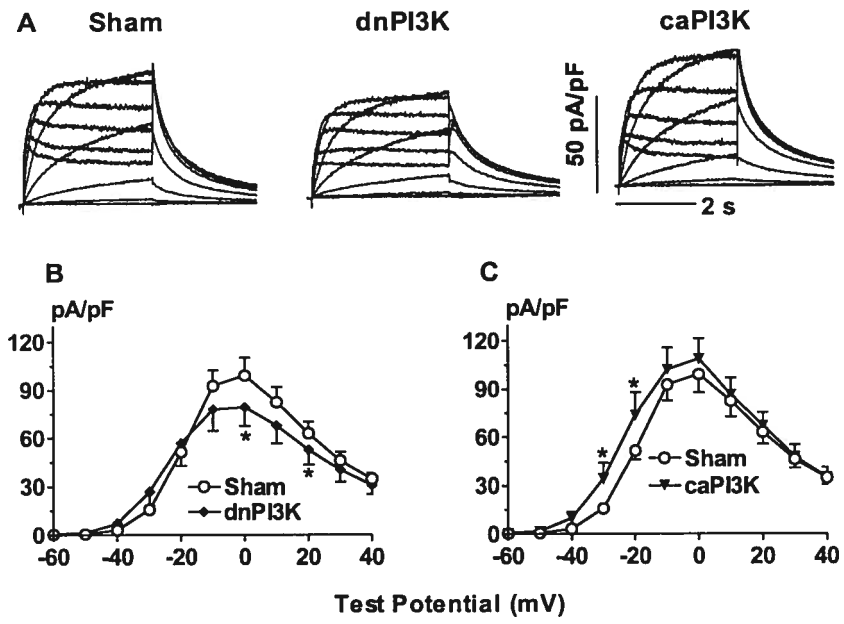

Figure 2. I_{HERG} in cells transfected with constitutively active PI3K (caPI3K) or dominant negative PI3K (dnPI3K). A: Typical examples of I_{HERG} traces presented as current density (pA/pF) for better group comparisons. For the sham group, the cells underwent the same transfection procedures as for dnPI3K and caPI3K groups, except that the plasmids were not included. **B** and **C:** I-V relationships averaged from 30 cell for sham, 25 cells for dnPI3K, and 28 cells for caPI3K group. *$p<0.05$ vs. sham.

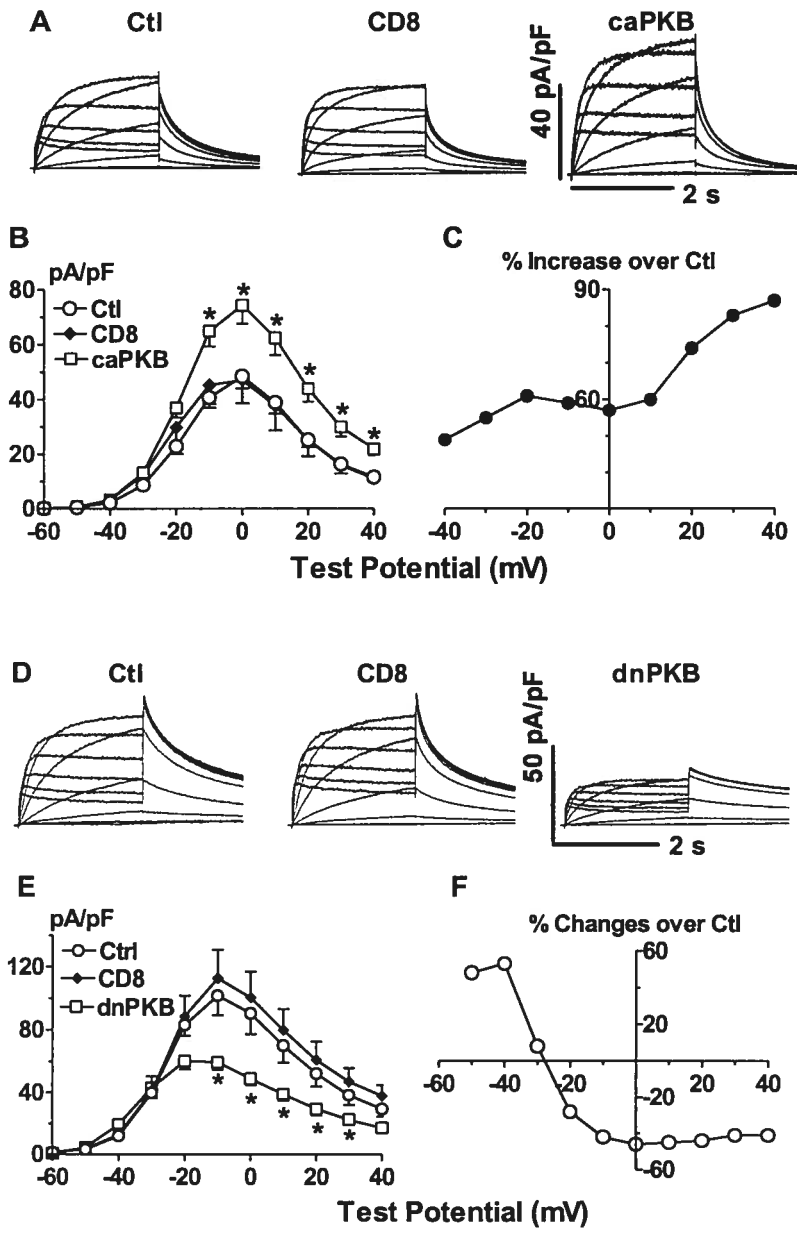

Figure 3. I_{HERG} in HEK293 cells transfected with constitutively active PKB (caPKB) or dominant negative PKB (dnPKB). A and **D:** Capacitance-normalized I_{HERG} traces (pA/pF) for better group comparisons. The HEK293 cells with stable expression of HERG were transiently transfected with plasmids containing cDNAs expressing CD8 alone (CD8 group) or with additional cDNA plasmids encoding caPKB or dnPKB. **B** and **E:** Mean I-V relationships. For caPKB experiments, n=19 cell for Ctl, =16 for CD8 alone, and =23 for caPKB; for dnPKB experiments, n=20 cell for Ctl, n=19 for CD8 alone, and n=19 for dnPKB. **C** and **F:** Percent (%) difference of I_{HERG} density between caPKB or dnPKB and Ctl groups. *$p<0.05$ vs. control (Ctl).

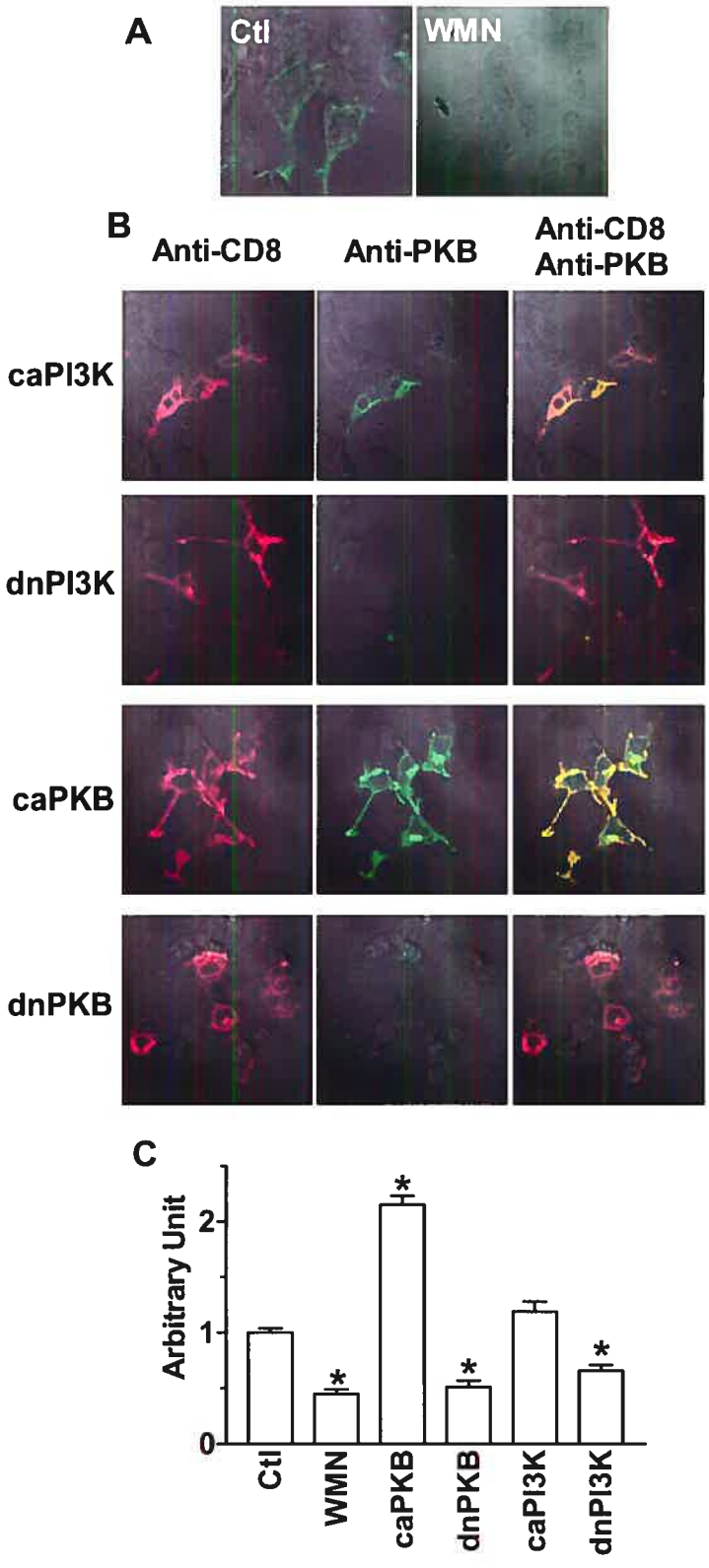
A
Ctl
WMN
B
Anti-CD8
Anti-PKB
Anti-CD8
Anti-PKB
caPI3K
dnPI3K
caPKB
dnPKB
C
Arbitrary Unit
0
1
2
*
*
*
*
Ctl
WMN
caPKB
dnPKB
caPI3K
dnPI3K

Figure 4

Figure 4. Immunocytochemical analysis of active PKB in HEK293 cells with anti-phospho (S473)-PKB antibody. A: Examples of confocal microscope images showing the cytoplasmic staining of the phosphorylated PKB (green) in HEK293 cells without (Control-Ctl, left) or with wortmannin (WMN, 50 nM, right) treatment. **B:** Examples of double stainings showing the membrane staining of CD8 (red) as a marker for successful transfection of varying constructs and the cytoplasmic staining of autophosphorylated (activated) PKB (green) and combination of the two (CD8+PKB, yellow), in HERG-expressing HEK293 cells transfected with caPI3K, dnPI3K, caPKB, or dnPKB. The phase-contract images (Phase C) are superimposed for better views of the cell contour. **C:** Average density of green staining for phospho-PKB (n=5 independent experiments for caPI3K/dnPI3K and n=4 for caPKB/dnPKB) expressed as ratios over control. *$p<0.05$ vs. control (Ctl).

7 IMPAIRMENT OF HERG K^+ CHANNEL FUNCTION BY TUMOR NECROSIS FACTOR-α: ROLES OF REACTIVE OXYGEN SPECIES

Being a consistently elevated product in congestive heart failure (CHF), and contributing to the APD prolongation, TNF-α is also a responsible factor for the development and progress of both type 1 and type 2 diabetes mellitus.

In addition, emerging evidence has demonstrated cellular lipids such as ceramide, diacylglycerol (DAG), phosphatidyl inositol 4,5 bisphosphate (PIP2), lysophosphatidylcholine (LPC), etc, are important second messengers mediating a variety of cellular events including those closely related to the cardiac functions, e.g. ion channel functions. Ceramide is found accumulated in myocardia and partially mediates the effects of TNF-α.

In these situations, TNF-α, and ceramide are involved in triggering cardiomyocyte apoptosis and maybe cardiac arrhythmias, too. In particular, prolongation of APD and QT has been associated with TNF-α and ceramide accumulation.

The studies in Chapters 8 and Chapter 9 aim at identifying the potential effects of TNF-α and ceramide on the HERG K^+ channel, which is critical to set the AP and has been found reduced in diabetic rabbit heart (in our studies), in CHF, and in ischemic myocardium. It will explain, at least partially the molecular mechanisms underlying the I_{Kr}/HERG impairment in diabetic cardiocomplications.

The work in this Chapter has been published in *J. Biol. Chem.* 2004; **279**: 13289- 13292 .

IMPAIRMENT OF HERG K^+ CHANNEL FUNCTION BY TUMOR NECROSIS FACTOR-α: ROLE OF REACTIVE OXYGEN SPECIES AS A MEDIATOR *

Jingxiong Wang[‡§¶‖], Huizhen Wang[‡¶], Yiqiang Zhang[‡§], Huanhuan Gao[‡††], Stanley Nattel[‡§§], and Zhiguo Wang[‡§¶¶]**

From the [‡]Research Center, Montreal Heart Institute, Montreal, Quebec H1T 1C8, the [§]Department of Medicine, University of Montreal, Montreal, Quebec H3C 3J7, and the [§§]Department of Pharmacology and Therapeutics, McGill University, Montreal, Quebec H3A 2T5, Canada

---

* This work was supported in part by the Heart and Stroke Foundation of Canada and Fonds de la Recherche de l'Institut de Cardiologie de Montreal (awarded to Z. W.).

[¶] Both authors contributed equally to this study. [‖] A recipient of Doctoral-Studentship of the Fonds de Recherche en Sante de Quebec. [**] A recipient of Doctoral-Studentship of the Heart and Stroke Foundation of Canada. [††]Current Address: Dept. of Physiology, McGill University, Montreal, Quebec H3A 2T5, Canada. [¶¶] A research scholar of the Fonds de Recherche en Sante de Quebec. To whom correspondence should be addressed: Research Center, Montreal Heart Institute, 5000 Belanger East, Montreal, Quebec H1T 1C8, Canada. Tel.: 514-376-3330; Fax: 514-376-4452; E-mail: [redacted]

7.1 Abstract

Congestive heart failure (CHF)[1] is associated with susceptibility to lethal arrhythmias and typically increased levels of tumor necrosis factor-α (TNF-α) and its receptor, TNFR1. CHF down-regulates rapid delayed-rectifier K^+ current (I_{Kr}) and delays cardiac repolarization. We studied the effects of TNF-α on cloned HERG K^+ channel (human *ether-a-go-go*-related gene) in HEK293 cells and native I_{Kr} in canine cardiomyocytes with whole-cell patch clamp techniques. TNF-α consistently and reversibly decreased HERG current (I_{HERG}). Effects of TNF-α were concentration-dependent, increased with longer incubation period, and occurred at clinically relevant concentrations. TNF-α had similar inhibitory effects on I_{Kr} and markedly prolonged action potential duration (APD) in canine cardiomyocytes. Immunoblotting analysis demonstrated that HERG protein level was slightly higher in canine hearts with tachypacing-induced CHF than in healthy hearts, and TNF-α slightly increased HERG protein level in CHF but not in healthy hearts. In cells pretreated with the inhibitory anti-TNFR1 antibody, TNF-α lost its ability to suppress I_{HERG}, indicating a requirement of TNFR1 activation for HERG suppression. Vitamin E or MnTBAP (Mn(III) tetrakis(4-benzoic acid) porphyrin chloride), a superoxide dismutase mimic) prevented, whereas the superoxide anion generating system xanthine/xanthine oxidase mimicked, TNF-α-induced I_{HERG} depression. TNF-α caused robust increases in intracellular reactive oxygen species, and vitamin E and MnTBAP abolished the increases, in both HEK293 cells and canine ventricular myocytes. We conclude that the TNF-α/TNFR1 system impairs HERG/I_{Kr} function mainly by stimulating reactive oxygen species, particularly superoxide anion, but not by altering HERG expression; the effect may contribute to APD prolongation by TNF-α and may be a novel mechanism for electrophysiological abnormalities and sudden death in CHF.

---

[1]The abbreviations used are: TNF-α, tumor necrosis factor-α; CHF, congestive heart failure; APD, action potential duration; EAD, early afterdepolarization; ROS, reactive oxygen species; CM-H2DFDA, 5-(and-6)-chloromethyl-2',7'-dichlorodihydrofluorescein diacetate; VitE, vitamin E; MnTBAP, Mn(III) tetrakis(4-benzoic acid) porphyrin chloride; X/XO, xanthine/xanthine oxidase.

7.2 Introduction

TNF-α is a potent inducible cytokine with pleiotropic biological effects (1). Up-regulation of TNF-α is a consistent finding in clinical (2) and experimental CHF (3). Circulating concentrations of TNF-α and soluble TNF-α receptors are independent predictors of mortality in CHF (4).

Patients with CHF are at increased risk of sudden death due to cardiac arrhythmias. CHF increases action potential duration (APD) (5), leading to early afterdepolarizations (EADs) and lethal ventricular tachyarrhythmias (6). Polymorphic ventricular tachycardias, likely related to arrhythmogenic afterdepolarizations, are common in CHF (6, 7). The molecular mechanisms underlying APD prolongation in CHF remain incompletely understood.

The rapid delayed rectifier K^+ current (I_{Kr}) is crucial in cardiac repolarization. The human *ether-a-go-go*-related gene (HERG) encodes the pore-forming α-subunit of I_{Kr} and congenital or drug-induced abnormalities in HERG protein function are a common cause of the long QT syndrome. Simulations of cellular electrophysiology predict I_{Kr} inhibition to cause EADs in failing, but not nonfailing, myocytes (8). A recent study demonstrated that transgenic mice overexpressing TNF-α with heart failure had significantly prolonged APD (9). It is unknown whether TNF-α affects cardiac K^+ channels. We therefore examined the hypothesis that TNF-α might affect HERG/I_{Kr}, thereby potentially contributing to CHF-related repolarization abnormalities.

7.3 Experimental Procedures

7.3.1 Cell disposition

HEK293 cells stably expressing HERG were a kind gift from Drs. Zhou and January. Cell culture and handling procedures have been described previously (10). Cardiomyocytes were isolated from healthy adult mongrel dogs as described in detail previously (11, 12). The procedures for animal use were in accordance with institutional guidelines.

7.3.2 Whole-cell patch-clamp recording

Patch clamp techniques have been described in detail elsewhere (13 16). Experiments were conducted at 36 ± 1°C. For current recordings in canine myocyte studies, the following were included in the bath to block contaminating currents: $CdCl_2$ (200-μmol/liter, L-type Ca^{2+} current), 4-aminopyridine (1 mmol/liter, transient outward K^+ currents), glyburide (10 μmol/liter, ATP-sensitive K^+ current), and 293B (10 μmol/liter, slow delayed-rectifier K^+ current). Action potentials were recorded in the current clamp mode with Tyrode solution free of ion channel blockers. TNF-α was either added to the extracellular solution 10 min after formation of whole-cell configuration (acute studies), or cells were incubated with TNF-α in the medium for 10 h before patch clamp recording (long term exposure).

7.3.3 Western Blot

The procedures were similar to those described previously (15). Polyclonal anti-HERG raised in rabbit against highly purified peptide (CY) EEL PAGAPELPQD GPT, corresponding to residues 1118 1133 of human HERG was purchased from Alomone Laboratories (Jerusalem, Israel).

7.3.4 Intracellular Reactive Oxygen Species (ROS) Measurement

5-(and-6)-Chloromethyl-2',7'-dichlorodihydrofluorescein diacetate (CM-H_2DFDA) from Molecular Probes was used to detect oxidative activity in living cells as detailed previously (16).

7.3.5 Data analysis

Group data are mean ± S.E. Paired *t* tests were used for single comparisons. Kinetics was analyzed with CLAMPFIT (pCLAMP 8.0) or Graphpad Prism.

7.4 Results

7.4.1 Impairment of HERG function by TNF-α

I_{HERG} was elicited by 2-s depolarizations followed by 2-s repolarizing steps (Figure 1, *inset*). Currents were recorded immediately after formation of whole-cell configuration and series resistance compensation. Comparisons were made between control cells (without TNF-α) and cells incubated for 10 h with various TNF-α concentrations from 0.01 to 10 ng/ml, which are within the pathophysiological range of TNF-α levels (~0.1 ng/ml) (17 19).

I_{HERG} density was reduced by TNF-α, with effects that were concentration- and voltage-dependent, being larger at more negative potentials (Figure 1*A*). I_{HERG} kinetics was unaltered by TNF-α. Exposure to TNF-α for 15 min concentration-dependently decreased I_{HERG}. I_{HERG} amplitude was decreased by 9, 16, and 35% by TNF-α at 1, 10, and 100 ng/ml, respectively. Results at 100 ng/ml are shown in Figure 1*B*. Depression of I_{Kr} by TNF-α was reproduced in both dog atrial and ventricular myocytes (Figure 1*C*). APD_{50} and APD_{90}, duration at 50 and 90% repolarization, respectively, were both significantly longer in single ventricular cells preincubated with TNF-α at 10 ng/ml in Tyrode solution for 10 h relative to control cells.. (Figure 1*D*).

7.4.2 Mechanisms for HERG depression by TNF-α

Western blot analysis of HERG protein levels in the membrane preparations extracted from HERG-expressing HEK293 cells and from the ventricular myocytes of healthy dogs or dogs with tachypacing induced CHF was performed. A band of around 135 kDa was identified by anti-HERG antibody, and the band was abolished after the antibody had been neutralized by its antigenic peptide. TNF-α treatment neither significantly alter HERG protein level in HEK293 cells nor in healthy dogs. HERG protein level was slightly higher in CHF than in healthy dogs and was slightly increased by TNF-α in CHF dogs (Figure 2*A*).

To clarify whether TNF-α acts on I_{HERG} via activation of TNF receptor I (TNFR1), we incubated HEK293 cells with H389 (an inhibitory anti-TNFR1 antibody) for 1 h before patch clamp recording upon acute exposure to 100 ng/ml TNF-α or beginning 1 h before prolonged (10 h) exposure to 1 ng/ml TNF-α. H389 prevented suppression of I_{HERG} by subsequent acute or

prolonged application of TNF-α. Data from prolonged exposure experiments are shown in Figure 2*B*.

Activation of TNFR1 can stimulate overproduction of intracellular ROS (20). To investigate whether ROS mediates TNF-α-induced HERG depression, we assessed the effects of TNF-α on I_{HERG} in cells pretreated with the antioxidant vitamin E (VitE). Pretreatment with VitE for 2 h prevented I_{HERG} reduction by TNF-α (Figure 2*C*). Another antioxidant MnTBAP (Mn (III) tetrakis (4-benzoic acid) porphyrin chloride), a superoxide dismutase mimetic, produced similar preventive effects on TNF-α-induced HERG impairment (Figure 2*D*). By contrast, preincubation of cells with superoxide anion generating system xanthine/xanthine oxidase (X/XO) mimicked the inhibitory effect of TNF-α on I_{HERG} (Figure 2*E*).

To confirm that intracellular ROS production was indeed stimulated by TNF-α, we detected ROS level using CM-H_2DFDA fluorescence dye to stain the cells. The cells stained with fluorescence intensity ≥5 times the background were defined as positive staining, and the number of cells with positive staining was pooled from five fields. The intensity of staining was analyzed by densitometric scanning using the LSM program, and the data were normalized to the control values without TNF-α (0.01 and 1 ng/ml) treatment (16). Under control conditions, cells stained by CM-H_2DCFDA were sparse, and the staining was weak. Yet with TNF-α treatment, the number of the cells with positive staining was considerably higher and the cells were stained evenly throughout the cytoplasm. Pretreatment with VitE or MnTBAP drastically diminished the number and the intensity of staining (Figure 2*F*). Similar results were obtained with isolated canine ventricular myocytes; TNF-α (0.1 ng/ml) markedly increased ROS level and co-application with VitE (100 μM) or MnTBAP (5 μM) prevented the effects of TNF-α (Figure 2*G*).

7.5 Discussion

Heart failure is associated with APD and QT interval prolongation, believed to contribute to the occurrence of sudden cardiac death (6, 7). We show here that TNF-α suppresses I_{HERG} in HEK293 cells and I_{Kr} in dog cardiomyocytes and prolonged APD. Depression of I_{HERG}/I_{Kr}, as produced by TNF-α in this study, may contribute to delayed repolarization and associated malignant ventricular tachyarrhythmias with increased TNF-α level in patients with CHF.

Ionic remodeling in CHF has been studied (21). L-type Ca^{2+} current density appears to be unaltered (20). The inward-rectifier K^+ current is consistently reduced (5). The transient outward K^+ current (I_{to}) is also reduced, potentially causing APD prolongation (5, 22). However, inhibition of I_{to} reduces APD in human atrial cells (23), canine atrial cells (12), and dog Purkinje fibers (24). The effect of I_{to} on the AP depends largely on the magnitude of I_K (25). Tsuji *et al.* (26) showed I_{Kr}, measured as E-4031-sensitive tail current, to be ~36% smaller in rabbits with ventricular tachypacing-induced CHF than in healthy rabbits. Lodge and Normandin (27) demonstrated earlier that I_{Kr}, measured as dofetilide-sensitive tail current, reduced by ~45% in the BIO TO-2 strain of cardiomyopathic hamster of 10 months old, derived from the BIO 53.58 animals and providing a model of dilated low output heart failure, compared with the 10-month-old control (BIO F1B) hamsters. A recent study by London *et al.* (9) showed significant APD prolongation in transgenic mice which overexpressed TNF-α and developed heart failure. Our study suggests that TNF-α may be an important mediator of CHF-induced I_{Kr} reduction and is the first to demonstrate that TNF-α can modulate cardiac K^+ channels.

We further demonstrated that pretreatment with VitE or MnTBAP prevented, whereas X/XO mimicked, TNF-α-induced I_{HERG} depression. The effects of VitE and MnTBAP are likely due to their antioxidant actions because TNF-α increased the intracellular ROS level in a concentration-dependent manner in both HEK293 cells and canine ventricular myocytes, more specifically $O^{\cdot}_2$ level because VitE or MnTBAP effectively prevented the increase. In line with our finding, a recent study published during the course of this study clearly demonstrated the ability of TNF-α to stimulate mitochondrial production of ROS in cardiomyocytes (20). It has also been shown that ROS is one of the key deleterious factors in failing heart (28, 29). Our data therefore indicate that TNF-α-induced HERG depression occurs at the functional level, but not at

the expression levels (TNF-α did not alter HERG protein content), and the functional impairment of HERG channels by TNF-α is mediated by ROS, particularly $O^{\cdot}_2$.

Circulating TNF-α levels predict mortality in CHF, and therapies directed against TNF-α may limit the pathophysiologic consequences (1). In healthy human subjects, the TNF-α level is below 0.01 ng/ml, but in patients with heart failure, it can increase to over 0.1 ng/ml (17 19). TNF-α significantly inhibited I_{HERG} over this concentration range (*e.g.* by ~35% at plateau voltages from −10 to +10 mV in cells exposed to 0.1 ng/ml TNF-α for 10 h). Our study might have underestimated the effects of TNF-α on APD because the myocytes were incubated with TNF-α at 4 °C to maintain good quality of the cells. Our observations provide new insights into the potential molecular mechanisms underlying electrophysiological abnormalities and sudden arrhythmic death in patients with CHF.

7.6 Acknowledgements

We thank Xiaofan Yang for excellent technical support and Louis R. Villeneuve for his assistance for confocal microscopic examinations.

7.7 References

1. McTiernan, C. F., and Feldman, A. M. (2000) *Curr. Cardiol. Rep.* 2, 189 197
2. Aukrust, P., Ueland, T., Lien, E., Bendtzen, K., Muller, F., Andreassen, A. K., Nordoy, I., Aass, H., Espevik, T., Simonsen, S., Froland, S. S., and Gullestad, L. (1999) *Am. J. Cardiol.* 83, 376 382
3. Irwin, M. W., Mak, S., Mann, D. L., Qu, R., Penninger, J. M., Yan, A., Dawood, F., Wen, W. H., Shou, Z., and Liu, P. (1999) *Circulation* 99, 1492 1498
4. Deswal, A., Petersen, N. J., Feldman, A. M., Young, J. B., White, B. G., and Mann, D. L. (2001) *Circulation* 103, 2055 2059
5. Beuckelmann, D. J., Nabauer, M., and Erdmann, E. (2002) *Circ. Res.* 73, 379 385
6. Marban, E. (2002) *Nature* 415, 213 218
7. Nuss, H. B., Kaab, S., Kass, D. A., Tomaselli, G. F., and Marban, E. (1999) *Am. J. Physiol.* 277, H80 H91
8. Priebe, L., and Beuckelmann, D. J. (1998) *Circ. Res.* 82, 1206 1223
9. London, B., Baker, L. C., Lee, J. S., Shusterman, V., Choi, B-R., Kubota, T., McTiernan, C. F., Feldman, A. M., and Slama, G. (2003) *Am. J. Physiol.* 284, H431 H441
10. Zhou, Z., Gong, Q., Ye, B., Fan, Z., Makielski, J. C., Robertson, G. A., and January, C. T. (1998) *Biophys. J.* 74, 230 241
11. Shi, H., Wang, H., and Wang, Z. (1999) *Mol. Pharmacol.* 55, 497 507
12. Yue, L., Feng, J., Li, G. R., and Nattel, S. (1996) *Am. J. Physiol.* 270, H2157 H2168
13. Wang, J., Wang, H., Han, H., Zhang, Y., Yang, B., Nattel, S., and Wang, Z. (2001) *Circulation* 104, 2645 2648
14. Zhang, Y., Wang, H., Wang, J., Han, H., Nattel, S., and Wang, Z. (2003) *FEBS Lett.* 534, 125 132
15. Wang, H., Zhang, Y., Cao, L., Han, H., Wang, J., Yang, B., Nattel, S., and Wang, Z. (2003) *Cancer Res.* 62, 4843 4848
16. Zhang, Y., Han, H., Wang, J., Wang, H., Yang, B., and Wang, Z. (2003) *J. Biol. Chem.* 278, 10417 10426

17. Anker, S. D., Volterrani, M., Egerer, K. R., Felton, C. V., Kox, W. J., Poole-Wilson, P. A., and Coats, A. J. (1998) *Q. J. Med.* 91, 199 203
18. Ferrari, R., Bachetti, T., Confortini, R., Opasich, C., Febo, O., Corti, A., Cassani, G., and Visioli, O. (1995) *Circulation* 92, 1479 1486
19. Liu, L., and Zhao, S. P. (1999) *Int. J. Cardiol.* 69, 77 82
20. Suematsu, N., Tsutsui, H., Wen, J., Kang, D., Ikeuchi, M., Ide, T., Hayashidani, S., Shiomi, T., Kubota, T., Hamasaki, N., and Takeshita, A. (2003) *Circulation* 107, 1418 1423
21. Tomaselli, G. F., and Marban, E. (1999) *Cardiovasc. Res.* 42, 270 283
22. Nabauer, M., Beuckelmann, D. J., and Erdmann, E. (1993) *Circ. Res.* 73, 386 394
23. Escande, D., Coulombe, A., Faivre, J. F., Deroubaix, E., and Coraboeuf, E. (1987) *Am. J. Physiol.* 252, H142 H148
24. Lee, J. H., and Rosen, M. R. (1994) *J. Cardiovasc. Electrophysiol.* 5, 232 240
25. Nygren, A., Fiset, C., Firek, L., Clark, J. W., Lindblad, D. S., Clark, R. B., and Giles, W. R. (1998) *Circ. Res.* 82, 63 81
26. Tsuji, Y., Opthof, T., Kamiya, K., Yasui, K., Liu, W., Lu, Z., and Kodama, I. (2000) *Cardiovasc. Res.* 48, 300 309
27. Lodge, N. J., and Normandin, D. E. (1997) *J. Mol. Cell. Cardiol.* 29, 3211 3221
28. Choudhary, G., and Dudley, S. C., Jr. (2002) *Congest. Heart Fail.* 8, 148 155
29. Byrne, J. A., Grieve, D. J., Cave, A. C., Shah, A. M. (2003) *Arch. Mal. Coeur. Vaiss.* 96, 214 223

7.8 Figures and Figure Legends

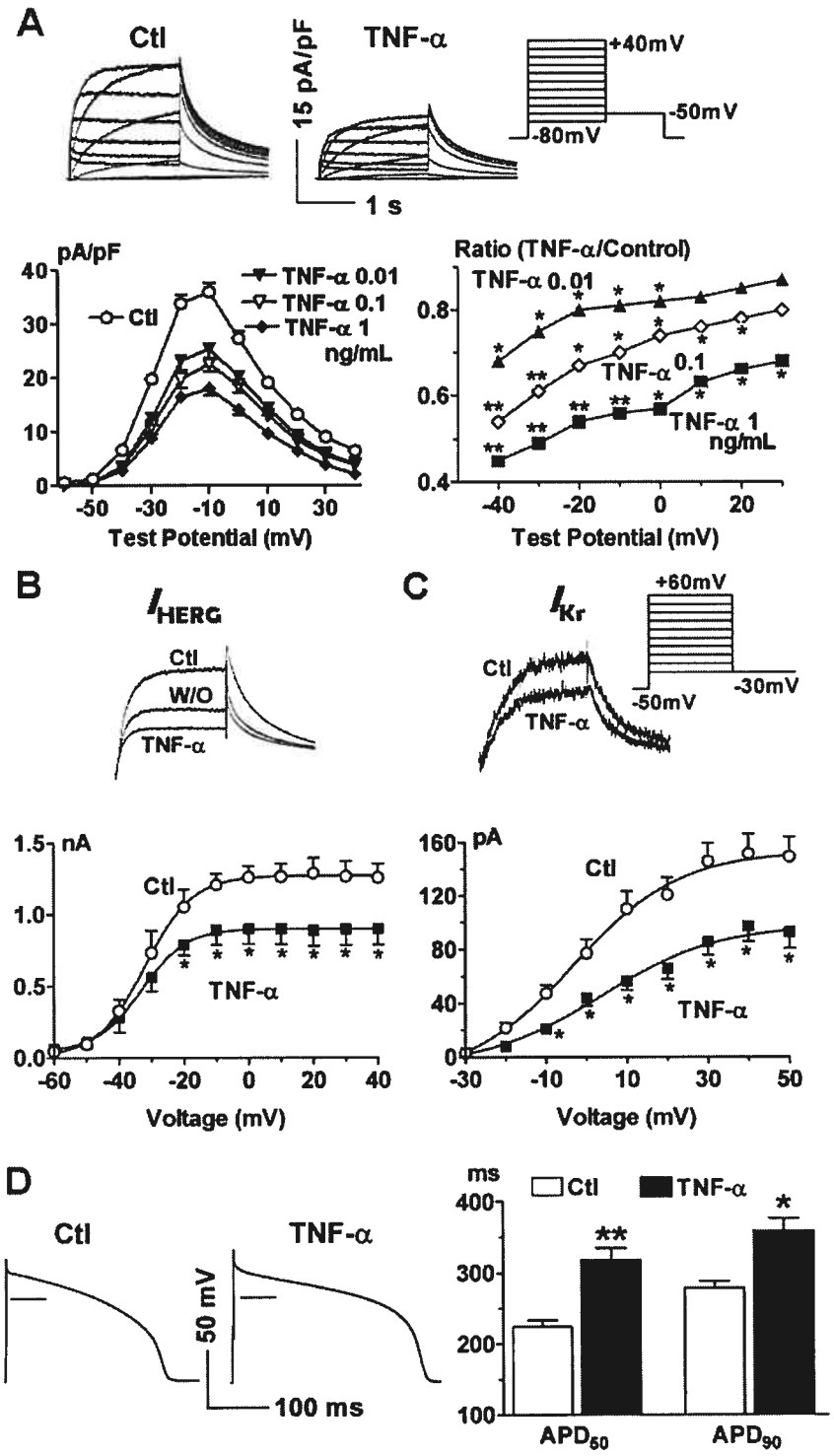

Figure 1. Impairment of HERG function by TNF-α. A, effects of 10-h exposure to various concentrations of TNF-α (in ng/ml) on I_{HERG} stably expressed in HEK293 cells. Original recordings are shown in the *upper panels*, mean current-voltage relations in the *lower left panel* and mean ratios of I_{HERG} in TNF-α-treated to untreated cells in the *lower right panel.* n = 15 for control; n = 13, 17, and 15 for TNF-α 0.01, 0.1, and 1 ng/ml, respectively. For 0.01 ng/ml TNF-α, $p < 0.05$ for voltages from –40 to 0 mV; for 0.1 ng/ml TNF-α, $p < 0.01$ at –40 and –30 mV and $p < 0.05$ from –20 to +20 mV; for 1 ng/ml TNF-α, $p < 0.01$ at –40 and –10 mV and $p < 0.05$ from 0 to +40 mV. **B,** effects of acute exposure to TNF-α (100 ng/ml) on I_{HERG} in HEK293 cells. Shown are mean data (n = 5) from the tail I_{HERG} recorded at –50 mV with original recordings (test pulse: 0 mV) in the *inset.* **C,** effects of bath application of TNF-α (100 ng/ml) on I_{Kr} in dog atrial myocytes, elicited with voltage protocol shown in the *inset*. Shown are mean (n = 4) I_{Kr} tail currents elicited at a repolarizing voltage of –30 mV with original recordings (test pulse: 0 mV) in the *inset.* **D,** effects of TNF-α (10 ng/ml, 6-h incubation at 4 °C) on action potential duration in canine ventricular cells (n = 15 for each group). The *horizontal lines* within the action potential recordings indicate the zero voltage level. *, $p < 0.05$ and **, $p < 0.01$ *versus* control (*Ctl*).

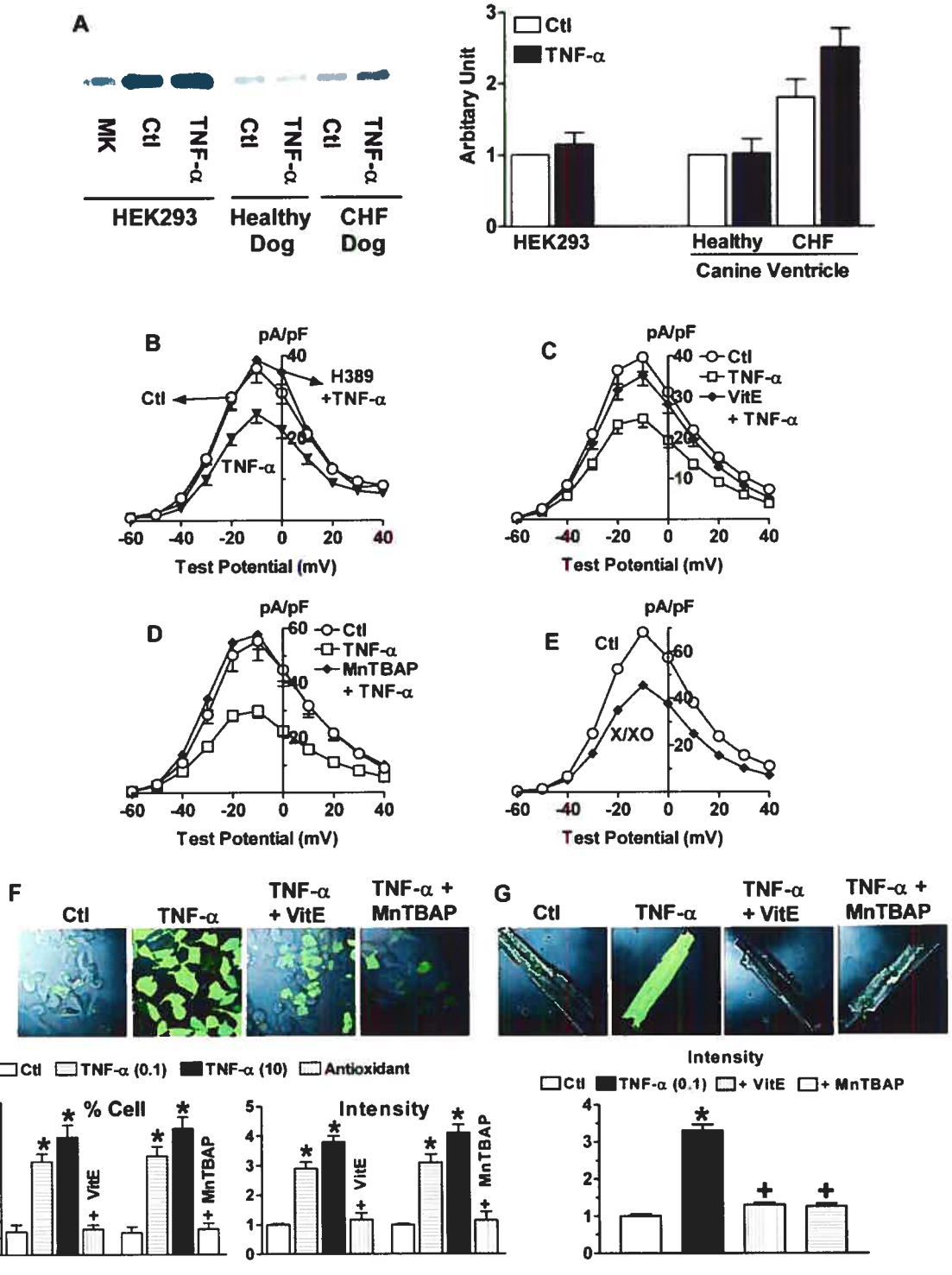
A
MK
Ctl
TNF-α
Ctl
TNF-α
Ctl
TNF-α
HEK293
Healthy Dog
CHF Dog
Ctl
TNF-α
Arbitary Unit
HEK293
Healthy
CHF
Canine Ventricle
B
pA/pF
Ctl
H389 +TNF-α
TNF-α
Test Potential (mV)
C
pA/pF
Ctl
TNF-α
VitE + TNF-α
Test Potential (mV)
D
pA/pF
Ctl
TNF-α
MnTBAP + TNF-α
Test Potential (mV)
E
pA/pF
Ctl
X/XO
Test Potential (mV)
F
Ctl
TNF-α
TNF-α + VitE
TNF-α + MnTBAP
Ctl
TNF-α (0.1)
TNF-α (10)
Antioxidant
% Cell
Intensity
VitE
MnTBAP
G
Ctl
TNF-α
TNF-α + VitE
TNF-α + MnTBAP
Intensity
Ctl
TNF-α (0.1)
+ VitE
+ MnTBAP

Figure 2

Figure 2. Mechanisms for HERG depression by TNF-α. A, Western blot analysis of HERG protein levels. Membrane protein samples were extracted from left ventricular myocytes isolated from healthy dogs and dogs with ventricular tachypacing-induced CHF and from HEK293 cells. HEK293 cells were treated with TNF-α (10 ng/ml) for 10 h in culture medium, and isolated myocytes were treated with TNF-α in Tyrode solution for 10 h. Mean data were calculated from a total of four independent samples for each group. MK, protein marker. *, $p < 0.05$ versus control (Ctl). B, inhibitory anti-TNFR1 antibody H389 prevents HERG depression by TNF-α. Cells were incubated with H389 (10 μg/ml) for 1 h before prolonged (10 h) exposure to TNF-α (10 ng/ml, n = 7). C and D, antioxidants VitE (100 μM, n = 14) or superoxide dismutase mimic MnTBAP (5 μM, n = 12) prevents HERG depression by TNF-α. *, $p < 0.05$ versus TNF-α alone. E, superoxide anion generating system X/XO (400 μM/5 units/ml, n = 16) mimicked the effects of TNF-α on I_{HERG}. F, alterations of the intracellular level of ROS by TNF-α (0.1 or 10 ng/ml) and antioxidants VitE (100 μM) and MnTBAP (5 μM), respectively, determined by CM-H_2DFDA fluorescence dye staining (green) in HERG-expressing HEK293 cells. The upper panels show examples of confocal microscopic images, and the lower panels show the percentage of cells with positive staining (% Cell) and the intensity of positive staining (n = 4 batches of cells for each group). *, $p < 0.05$ versus Ctl; $^{+}$, $p < 0.05$ versus TNF-α alone. G, increase in ROS by TNF-α (0.1 ng/ml) and reversal by VitE (100 μM) or MnTBAP (5 μM) in canine ventricular myocytes. The upper panels show examples of confocal microscopic images, and the lower panels show the intensity of positive staining (n = 3). *, $p < 0.05$ versus Ctl; $^{+}$, $p < 0.05$ versus TNF-α alone.

8 CERAMIDE CAUSES METABOLIC PERTURBATION LEADING TO HERG K^+ CHANNEL DYSFUNCTION AND ABNORMAL SLOWING OF CARDIAC REPOLARIZATION

This article is prepared for publication.

SPHINGOLIPID METABOLITE CERAMIDE CAUSES METABOLIC PERTURBATION LEADING TO HERG K^+ CHANNEL DYSFUNCTION AND ABNORMAL SLOWING OF CARDIAC REPOLARIZATION*

Jingxiong Wang[‡§‖], Yiqiang Zhang[‡§], Huizhen Wang[‡¶], Huixian Lin[‡], Baofeng Yang[¶†], and Zhiguo Wang[‡§†¶¶]**

From the [‡] Research Center, Montreal Heart Institute, Montreal, Quebec H1T 1C8, the [§] Department of Medicine, University of Montreal, Montreal, Quebec H3C 3J7, Canada, the [¶] Department of Pharmacology (Sate-Province Key Laboratory), and the [†] Institute of Cardiovascular Research, Harbin Medical University, Harbin, Heilongjiang 150086, P. R. China

First Author's surname: **Wang**

Running Title: **Cellular mechanisms of HERG depression by ceramide**

---

* This work was supported in part by the Heart and Stroke Foundation of Quebec, and the Fonds de la Recherche de l'Institut de Cardiologie de Montreal, awarded to Dr. Z Wang.

[‖] A recipient of Doctoral-Studentship of the Fonds de Recherche en Sante de Quebec.

[**] A recipient of Doctoral-Studentship of the Heart and Stroke Foundation of Canada.

[¶¶] A research scholar of the Fonds de Recherche en Sante de Quebec. To whom correspondence should be addressed: Research Center, Montreal Heart Institute, 5000 Belanger East, Montreal, PQ H1T 1C8, Canada; Tel.: (514) 376-3330. Fax: (514) 376-4452. E-mail: [redacted]

8.1 Summary

Ceramide, a sphingolipid metabolite, has emerged as a key second messenger molecule that mediates multiple cellular functions. Its *de nova* synthesis and accumulation in ischemic myocardium, and congestive heart failure and diabetic cardiomyopathy have been associated with the pathological processes including the abnormal QT prolongation (QT-↑) and increased risk of arrhythmias. To investigate how ceramide can be involved in modulating cardiac repolarization, we performed whole-cell patch-clamp studies on HERG current (I_{HERG}), a critical determinant of cardiac repolarization, expressed in HEK293 cells. Acute application (bath superfusion for 25 min) of membrane permeable ceramide (C2, 50 μM) did not alter I_{HERG}. Prolonged incubation with C2 for 10 hrs caused pronounced I_{HERG} inhibition in a concentration-dependent and voltage-independent fashion and positive shift of voltage-dependent HERG activation. The IC_{50} for I_{HERG} suppression was 19.5 μM. C2 did not affect the inactivation property and time-dependent kinetics of I_{HERG}. Similar effects were observed with production of endogenous ceramide catalyzed by sphingomyelinase. Tyrosine kinase inhibitors failed to reverse C2-induced suppression of HERG function, and PKA and PKC inhibitors only slightly reversed the I_{HERG} depression. Western blotting and immunocytochemical analyses indicate that C2 does not alter HERG protein expression on the cytoplasmic membrane. The inhibitory effect of C2 on I_{HERG} was reversed by antioxidants vitamin E or MnTBAP. C2 caused considerable production of intracellular reactive oxygen species (ROS), which was prevented by vitamin E or MnTBAP. We conclude that ceramide depresses I_{HERG} mainly via ROS overproduction and ceramide-induced I_{HERG} impairment may contribute to QT-↑ in prolonged myocardial ischemia, heart failure and diabetic cardiomyopathy.

Keywords: ceramide, HERG, reactive oxygen species, vitamin E, MnTBAP, QT prolongation

[1]The abbreviations used are: Bis, bisindolylmaleimide; C2, a membrane permeable ceramide, N-acetyl-D-erythro-sphingosine; CM-H2DCFDA, 5-(and-6)-chloromethyl-2 ,7 -dichlorodihydro-fluorescein diacetate; Dihydro-C2, dihydro-, N-acetyl-D-erythro-sphingosine; Gen, genestein; HA, herbimycin A; MnTBAP, Mn (III) tetrakis (4-benzoic acid) porphyrin chloride; $O_2^{\cdot-}$, superoxide anion; OA, okadiac acid; SMase, sphingomyelinase; VitE, vitamin E.

8.2 Introduction

Ceramide, a long-chain sphingolipid generated intracellularly on hydrolysis of sphingomyelin catalyzed by sphingomyelinase (SMase), has emerged as a key second messenger molecule that is capable of mediating multiple physiological effects including regulation of cellular differentiation, proliferation, and apoptosis by activating a variety of signaling cascades, including those triggered by cytokines, growth factors, and stress (1-3). Ceramide generation can be triggered by diverse stimuli and *de nova* ceramide synthesis and accumulation takes place in the myocardium under various pathological conditions such as myocardial ischemia (MI) or hypoxia, congestive heart failure (CHF), and diabetic cardiomyopathy (DCM) (4-11). In these situations, ceramide is involved in triggering cardiomyocyte apoptosis, cardiac pump failure and cardiac arrhythmias. In particular, prolongation of action potential duration (APD) and QT interval is a common feature with regard to cardiac electrical disturbances in chronic MI (12-13), CHF (14-15) and DCM (16-17).

Upon receiving an incoming impulse, cardiac cells show a rapid membrane depolarization followed by a relatively slow repolarization process. Repolarization disorders, either excessive slowing or accelerating of the rate of repolarization, can cause cardiac electrical perturbations or arrhythmias. The rate of repolarization is determined by several ion currents, of which the rapid delayed rectifier K^+ current (I_{Kr}) has a crucial role, particularly to the plateau phase of action potentials (18-19). The major molecular component of native I_{Kr} has been identified as the human *ether-a-go-go*-related gene (HERG), which generates I_{Kr}-like current when expressed in heterologous systems (20). Impairment of I_{Kr}/HERG can cause excessive prolongation of APD and QT interval, which is commonly believed to be a mechanism for both genetic and drug-induced long QT syndromes. It is important to know whether the sphingolipid metabolite ceramide that is excessively generated in MI, CHF or DCM can interact with HERG K^+ channels, so as to have better understanding of the metabolic and ionic mechanisms for the APD/QT prolongation in these diseased settings. To this end, we performed studies to investigate the effects of ceramide on HERG K^+ channel function and to elucidate the potential signaling mechanisms. Our data identified HERG as a target for ceramide action and intracellular reactive oxygen species (ROS) as a mediator for ceramide-induced impairment of HERG function.

8.3 Experimental Procedures

8.3.1 Cell culture

HEK293 cells stably expressing HERG (a kind gift from Drs. Zhou and January) (21) were grown in Dulbecco's modified Eagle's medium (DMEM) supplemented with 10% heat-inactivated fetal bovine serum, 200 μM G418, 100 units/ml penicillin, and 100 μg/ml streptomycin, as previously described in detail (22-23).

8.3.2 Whole-cell patch-clamp recording

Patch clamp recording of HERG K^+ current (I_{HERG}) has been described in detail elsewhere (22-23). The currents were recorded in the whole-cell voltage-clamp mode with an Axopatch-200B amplifier (Axon Instruments). Borosilicate glass electrodes had tip resistances of 1 3 megohms when filled with the internal solution containing (mM) 130 KCl, 1 $MgCl_2$, 5 Mg-ATP, 10 EGTA, and 10 HEPES (pH 7.2). The extracellular (Tyrode) solution contained (mM) 136 NaCl, 5.4 KCl, 1 $CaCl_2$, 1 $MgCl_2$, 10 glucose, and 10 HEPES (pH 7.4). Experiments were conducted at 36 ±1°C. Junction potentials were zeroed before formation of the membrane-pipette seal. Series resistance and capacitance were compensated, and leak currents were subtracted.

8.3.3 Drugs and treatments

N-acetyl-D-sphingosine, synthetic membrane permeable ceramide (C2), sphingomyelinase (SMase, the neutral form with long-lasting activity), forskolin (FSK; PKA activator), H89 (PKA inhibitor), Phorbol 12, 13-Dl-Decanoate (PDD, PKC activator), bisindolylmaleimide (Bis; PKC inhibitor), okadiac acid (OA), and vitamin E (VitE) were purchased from Sigma (Oakville, ON). Dihydro-, N-acetyl-D-erythro-sphingosine (dihydro-C2, an inactive analogue of C2), herbimycin A (HA, PTK inhibitor) and genistein (Gen, PTK inhibitor) were purchased from Calbiochem (La Jolla, CA). PDD, Bis, C2, dihydro-C2, HA, Gen, and FSK were dissolved in DMSO. OA was dissolved in phosphate-buffered saline (PBS). SMase was prepared in a working solution of 50% glycerol containing 50 mM Tris-HCl. All agents were prepared as 1000 x stock solutions and stored at –20 °C.

For acute exposure, drugs were added to the bathing solution 10 min after baseline recording and the current amplitudes before and after drugs were compared. For prolonged

exposure, cells were incubated in normal culture medium containing agents at the desired final concentrations for 10 hrs prior to patch-clamp recordings and group comparison between treated and untreated cells (treated with the same vehicles as for drug treatment groups) was made. Step I_{HERG} was defined as the current amplitude at the end of the 2.5-sec depolarizing voltage steps and tail I_{HERG} was measured as the peak value of the decaying tail currents upon repolarization to –50 mV. To have more rational comparisons between groups, I_{HERG} density was calculated by dividing the current amplitude by the capacitance of the same cell. For experiments involving protein kinase inhibitors, cells were pre-incubated with the drugs for 2 hrs before exposure to C2.

8.3.4 Western blot

The procedures for measuring HERG protein levels were essentially the same as described previously (24). The primary antibody, polyclonal anti-HERG raised in rabbit against highly purified peptide (CY) EEL PAGAPELPQDGPT, corresponding to residues 1118-1133 of human HERG was purchased from Alomone Labs (Jerusalem, Israel). Bound antibodies were detected using the chemiluminescent substrate (Western Blot Chemiluminescence Reagent Plus, NEN Life Science Products, Boston, USA) and quantified using a Phosphorimager (Bio-Rad). The presence of HERG channel proteins was verified by the presence of a prominent band with expected molecular mass in the range of previous reports and by elimination of the band in preparations preincubated with the antigenic peptide. Coomassie staining was performed to verify equal protein loading for each sample.

8.3.5 Immunocytochemistry

The procedure was the same as previously described in detail (24). The anti-HERG antibody was the same as used for Western blot analysis. The cells were examined under a Laser scanning confocal microscope (Zeiss LSM 510).

8.3.6 Intracellular reactive oxygen species (ROS) measurement

The procedures have been described in detail previously (25). CM-H_2DFDA from Molecular Probes was used to detect oxidative activity in living cells. Cells were divided into 5 groups: control group, C2 10 hrs group, C2 20-min group, C2+VitE, and C2+MnTBAP group. For experiments involving VitE or MnTBAP, the cells were pretreated with VitE (100 μM) or

MnTBAP (5 μM) for 2 hrs and then incubated in the culture medium containing C2 in the continual presence of VitE or MnTBAP. The percentage of positively stained cells and the fluorescence intensity of staining were determined by densitometric scanning with LSM software (Zeiss).

8.3.7 Data analysis

Group data are expressed as mean ± s.e.m. Comparisons among groups were made by analysis of variance (F-test) and Bonferroni-adjusted t-tests were used for multiple group comparisons and paired or unpaired t-test was used, as appropriate, for single comparisons. A two-tailed $p < 0.05$ was taken to indicate a statistically significant difference. Nonlinear least square curve fitting was performed with CLAMPFIT in pCLAMP 8.0 or GraphPad Prism.

8.4 Results

8.4.1 *Effects of membrane permeable ceramide on I_{HERG} expressed in HEK293 Cells*

Depolarizing voltage steps from –60 mV to +40 mV elicited delayed rectifier type of outward currents with characteristic inward rectification that manifests at stronger depolarization. Upon repolarization back to –50 mV, slowly decaying tail currents are recorded. Application of the membrane permeable ceramide (C2) to the superfusate at a concentration of 25 μM for up to 20 min did not significantly alter the HERG currents (Figure 1A), suggesting that ceramide does not directly act on the HERG channels.

In contrast to the acute exposure, preincubation of cells with C2 (1-50 μM) in the culture medium for 10 hrs caused consistent changes of I_{HERG} in two different ways. First, I_{HERG} density was decreased by C2 at a concentration-dependent (Figure 1B and Figure 2) and voltage-independent (Figure 2D) manner. The IC_{50} of C2 for I_{HERG} suppression was calculated by the Hill equation to be 19.5 μM. Second, the steady-state voltage-dependent activation of HERG channels was appreciably shifted by C2 towards depolarizing voltages (Figure 2B). For example, the voltage for half maximum activation ($V_{1/2}$) was changed from –27.0 ± 0.5 mV (n=27) to –4.2 ± 1.0 mV (n=13, $p<0.05$ vs. control) and –22.0 ± 1.1 mV (n=17, $p<0.05$) by 1 and 5 μM C2, respectively, with no changes in the slope factor (k). Intriguingly, the IC_{50} for the $V_{1/2}$ shift was around 1.1 μM, some 20-fold lower than the effect on the current density. Higher concentrations of C2 (10, 25 and 50 μM) did not produce further shift of I_{HERG} activation. Dihydro-C2 (25 μM), the inactive analog of C2, failed to cause any appreciable alterations of I_{HERG} (Figure 2A). No effects of C2 on HERG kinetics and inactivation properties were observed (data not shown).

8.4.2 *Effects of endogenous ceramide generated by sphingomyelinase on I_{HERG}*

To verify the modulation of I_{HERG} by ceramide and the potential pathophysiological implication, we studied the effects of sphingomyelinase (SMase) that catalyzes production of endogenous ceramide, on I_{HERG}. Qualitatively the same effects were observed with SMase as with exogenously applied C2. SMase significantly decreased I_{HERG} in a concentration-dependent but voltage-independent manner (Figure 3). SMase also produced positive shifts of I_{HERG} activation voltage; $V_{1/2}$ was changed from -30.6 ± 0.6 mV (n=25) for control to -27.3 ± 0.8 mV

(n=20, $p< 0.05$) and -24.4 ± 0.6 mV (n=13, $p<0.05$) in the presence of 0.2 U/ml and 0.6 U/ml SMase, respectively. SMase did not affect the activation and deactivation kinetics and inactivation properties of HERG channels (data not shown).

8.4.3 Effects of inhibitors to PTK, PKA or PKC on I_{HERG} modulation by Ceramide

It has been shown that ceramide inhibits T lymphocyte voltage-gated potassium channel via tyrosine phosphorylation of the channel proteins (26). On the contrary, the I_{HERG}-like current has been found to be enhanced by protein tyrosine kinase (PTK) activation in MLS-9 rat microglia cell line (27). To investigate whether this mechanism also applies to HERG modulation by ceramide, we evaluated the effects of two PTK inhibitors herbimycin A (HA) and genistein (Gen). As illustrated in Figure 4A, preincubation of cells with HA (5 μM) alone for 2 hrs remarkably suppressed I_{HERG} (~66% at 0 mV) to a similar extent as the I_{HERG} inhibition caused by 25 μM C2 (~58% at 0 mV). Co-incubation of cells with HA and C2 caused a slightly further decrease in I_{HERG} (by ~77%). Similarly, Gen alone also reduced I_{HERG} albeit to a less extend compared with C2. Pretreatment with Gen (80 μM) did not alter the effects of C2 on I_{HERG} density (Figure 4B).

Ceramide is characterized by its ability to simulate activation of the atypical protein kinase C (PKC_ξ) (28). PKC_ξ can be inhibited by a phospholipase C inhibitor okadiac acid (OA). Our experiments demonstrated that OA (1 μM) alone significantly diminished I_{HERG} and pretreatment of cells with OA failed to prevent I_{HERG} reduction induced by C2; instead, further decreases in I_{HERG} were found in the presence of both OA and C2 (Figure 4C).

PKA phosphorylation of HERG channels was shown to cause reduction of current amplitude due to positive shift of HERG activation voltages (29-30). To investigate the potential involvement of PKA pathway in mediating ceramide-induced I_{HERG} depression, we assessed the effects of a PKA inhibitor H89. As illustrated in Figure 5A, incubation of cells with H89 (1 μM) alone for 10 hrs produced a marked shift of the HERG I-V relationship and activation curve towards more negative potentials. The maximum step I_{HERG} was unaltered despite that because of the negative shift; I_{HERG} was increased at potentials negative to –10 mV and decreased thereafter. The maximum tail I_{HERG}, however, was reduced by approximately 11%. Pretreatment with H89 only slightly reduced the degree of C2-induced I_{HERG} diminishment (Figure 5A).

PKC is another target of ceramide action. To investigate the possible involvement of PKC in mediating I_{HERG} modulation by ceramide, we evaluated the effects of a PKC inhibitor bisindolylmaleimide (Bis, 0.1 μM) on C2-induced I_{HERG} depression. Cells treated with Bis alone for 10 hrs had significantly smaller I_{HERG} density (30.5 ± 2.2 pA/pF, n=22, $p<0.05$) compared with control untreated cells (39.8 ± 2.8 pA/pF, n=22) (Figure 5B). The I_{HERG} activation property was not different between Bis and control groups. Bis pretreatment partially reduced C2-induced I_{HERG} depression (Figure 6A). Similarly, pretreatment with another PKC inhibitor cherylethrine (1 μM) partly restored C2-induced I_{HERG} reduction and cherylethrine alone also significantly decreased I_{HERG} (data not shown).

8.4.4 Lack of effects of ceramide on HERG protein expression level

There is a possibility that the decrease of I_{HERG} in presence of ceramide was due to down-regulation of HERG channel protein expression. To test this notion, we carried out Western blot analysis with membrane protein samples extracted from HERG-expressing HEK293 cells to compare the HERG protein levels between control cells and C2-treated cells. As shown in Figure 6A, anti-HERG antibody recognized a band of ~135 kDa, consistent with the molecular mass of HERG protein (21, 24), and the band disappeared if the antibody had been pretreated with its antigenic peptide. HERG protein levels were comparable between the C2-treated cells and control untreated cells.

This result was further reinforced by our immunocytochemical analysis demonstrating similar pattern and intensity of HERG staining on the surface membrane between C2-treated cells and control untreated cells (Figure 6B).

8.4.5 Role of reactive oxygen species (ROS) in I_{HERG} modulation by ceramide

It has been well established by numerous studies that ceramide can act on mitochondria and stimulate production of ROS, particularly superoxide anion ($O_2^{-\bullet}$) (2, 31-32). We have previously demonstrated that $O_2^{-\bullet}$ causes impairment of HERG K^+ channel function (25). It is quite plausible that C2-induced depression of I_{HERG} is related to increased ROS generation. We tested this notion by preincubating the cells with vitamin E (VitE, 100 μM) alone for 2 hrs and then incubating the cells with C2 (25 μM) in the continual presence of VitE for another 10 hrs. As shown in Figure 7A, VitE substantially weakened the depressing effects of C2, but VitE

alone did not produce any appreciable effects, on I_{HERG}. For example, I_{HERG} density was ~50% smaller in the cells treated with C2 alone than in control, but it was only ~24% smaller in the cells treated with both VitE and C2. In other words, I_{HERG} density in the VitE+C2 group was approximately 52% greater than in the group with C2 alone (48.2 ± 3.2 pA/pF, n=19, vs. 31.7 ± 2.0 pA/pF, n=16, $p<0.05$), at 0 mV (Figure 7A). Furthermore, Mn (III) tetrakis (4-benzoic acid) porphyrin chloride (MnTBAP), a superoxide dismutase (SOD) mimic, resembled the effects of VitE; it reversed C2-induced I_{HERG} reduction (Figure 7B).

To confirm that ROS production was indeed increased by C2, and the induced ROS was mainly of $O_2^{-\bullet}$, we proceeded to measure the intracellular ROS levels using CM-H_2DCFDA fluorescence dye. The ROS level was measured in cells incubated with the culture medium containing 25 μM C2 for 10 hrs. The cells showing fluorescence intensity ≥5 times the background were defined as positive staining, and the number of cells with positive staining was pooled from 5 fields for each batch of cells (a total of 4 independent batches of cells for each group were studied). The intensity of staining by the fluorescent probe for ROS was analyzed by densitometric scanning using the LSM program, and cells with positive staining were taken for analysis, and the data were normalized to the control values. Under control conditions, cells with positive staining were sparse. Yet in the cells treated with C2, the number of the cells with positive staining, as well as the intensity of staining, was consistently higher. If pretreated with VitE or MnTBAP prior to exposure to C2, the cells had significantly lower ROS levels, as indicated by the smaller number of positively stained cells and the weaker intensity of staining (Figure 8A and 8B). Since 20 min superfusion of cells with C2 failed to affect I_{HERG}, we also conducted CM-H_2DCFDA experiments with cells treated with C2 for only 20 min. In sharp contrast with 10 hrs exposure, 20 min treatment did not alter the level of intracellular ROS.

8.5 Discussion

The present study identifies HERG K^+ channel as a new target for ceramide action. The major findings of the study are: (1) prolonged exposure (chronic incubation), but not brief exposure (acute superfusion), of cells to C2 significantly impairs HERG K^+ channel function and (2) stimulation of intracellular reactive oxygen species (ROS) by C2 mediates the depressing effects of C2 on HERG K^+ channel function. In view of the critical role of HERG K^+ channel in regulating cardiac repolarization and the fact that ceramide is overproduced in MI, CHF or DCM, it is possible that HERG impairment by ceramide contributes to the electrical disturbances in these pathological conditions.

It has been reported that the HERG-equivalent K^+ current in rat microglia MLS-9 cell (27) is significantly reduced by inhibitors of PTK, indicating the role of PTK in maintaining HERG function. Consistent with these findings, our data demonstrated that PTK inhibitors herbimycin A and genestein alone both markedly depressed I_{HERG} amplitude, indicating a role of basal PTK activity in maintaining HERG function. Co-application of these inhibitors with ceramide did not alter ceramide-induced I_{HERG} depression, or if anything, caused further reduction of I_{HERG}. The latter suggests that ceramide has the ability to enhance HERG function and partially offsetting its inhibitory effect by stimulating PTK activities, but failed to do so in the presence of PTK inhibitors. Thus, PTKs do not account for ceramide-induced I_{HERG} depression. Involvement of PKA or PKC in ceramide-induced I_{HERG} depression appears to be minimal, if any. This conclusion was drawn on the basis that neither PKA inhibitor H89 nor PKC inhibitor Bis significantly reversed the effects of C2, despite that these compounds themselves when applied in the absence of C2 produced direct effects on I_{HERG}. Obviously, these direct effects of H89 and Bis are unlikely related to ceramide action on I_{HERG}, but the positive shift of HERG activation may be caused by PKA because H89 completely abolished ceramide-induced shift.

A growing body of evidence is emerging indicating that oxidative stress and ceramide generation are intimately connected in cell death signaling. The major source for ROS in most cell types is probably the electron leakage from the mitochondrial electron transport chain, which results in the formation of superoxide anion ($O_2^{\cdot-}$). Experimental evidence indicates that cell-permeable ceramide analogs elicit a direct effect on mitochondria, ranging from the inhibition of the respiratory chain and ROS overproduction to the induction of mitochondrial permeability

transition in intact cells and cytoplasts (33-34). Several studies have identified the mitochondrial ubiquinone pool of complex III (a protein complex that links proton translocation to electron transfer from ubiquinone to cytochrome c) as a ceramide target to produce ROS. Indeed, it has been reported that MnTBAP, an SOD mimic, inhibits ceramide-induced apoptosis in neuronal cells (35). The present study confirmed that C2 stimulates intracellular production of ROS as indicated by the increased ROS level and the increase was attenuated by VitE. Furthermore, our data suggest that C2-induced generation of ROS was mainly of $O_2^{\cdot-}$ because MnTBAP nearly abolished the ROS increases. These data are consistent with the electrophysiological results that VitE or MnTBAP reversed the C2-induced reduction of I_{HERG} amplitude. The fact that 20 min superfusion of the cells with C2 failed to affect I_{HERG} in our experiments (Figure 1A) may well be due to failure of C2 to increase ROS within such a short time frame and this notion is indeed supported by the data shown in Figure 8A. In other words, the reason why prolonged exposure (>2.5 hrs) was required for C2 to produce effects on I_{HERG} is that sufficient level of ROS needs to be raised with time in the presence of C2 to affect I_{HERG}. The ability of ceramide to induce ROS production in cultured neonatal rat ventricular myocytes has indeed been recently confirmed by Suematsu *et al* (36). Noticeably, neither VitE nor MnTBAP altered C2-induced positive shift of HERG activation, indicating that ROS is not responsible for ceramide-induced shift.

The present study has several important pathophysiological implications. First, it is known that ischemic myocardium demonstrates characteristic bi-phasic changes of electrophysiology with APD shortening during early phase of acute ischemia and subsequent APD lengthening after prolonged ischemic period, which are associated with different types of arrhythmias (12-13). However, the ionic mechanisms underlying these sequential alterations of APD remained unresolved. This study together with our previous work seems to provide an explanation. It is well recognized that altered lipid metabolism is an important deleterious factor in ischemic myocardial injury; some lipid metabolites such as lysophosphatidylcholines (LPCs) are overproduced rapidly within the first 10 min of acute myocardial ischemia, while others like ceramide accumulate progressively in the late phase (30 min after) of ischemia (1-3, 7). We have recently reported that LPCs produce pronounced enhancement of HERG function (22-23). This finding may explain in part the APD shortening and the associated arrhythmias occurring in the early phase of ischemia. On the other hand, *in vitro* ischemia leads to a progressive accumulation of ceramide in cardiomyocytes. The content of ceramide in ischemic area was found to be

elevated to 155% baseline levels after 30 min, and to 330% after 210 min, of ischemia; Ischemia (30 min) followed by reperfusion (180 min) increased the ceramide level to 250% in the ischemic area (4). In another study, the total basal ceramide concentration in the myocardium was 135 nmol/g tissue, and it was increased by 14.1% and 48.4% in 30 min global ischemia and 30 min ischemia/30 min reperfusion groups, respectively (5). Cordis *et al* (6) showed a 50% decrease of sphingomylein both during ischemia and subsequent reperfusion with a corresponding increase in ceramide. Another study suggests that a longer time period (>30 min) may be needed to alter ceramide mass in tissues in response to ischemic insult (7). Intriguingly, the cardiac AP is abnormally lengthened after prolonged ischemia (12-13). In lieu of the critical role of HERG K^+ channel in cardiac repolarization and the ability of ceramide to inhibit I_{HERG}, it is tempting to speculate that I_{HERG} depression produced by ceramide that accumulates during the late phase of myocardial ischemia might contribute to the observed prolongation of APD and the associated arrhythmias.

The second implication of our study is related to arrhythmias in CHF. One characteristic electrophysiological alteration in CHF is abnormally prolonged APD at the cellular level and QT interval as reflected in electrocardiogram (15, 37). This prolongation provides an electro-physiological substrate for early afterdepolarizations (EADs) to occur, which can result in ventricular tachycardias that often predispose to ventricular fibrillation leading to sudden cardiac death (14). Polymorphic ventricular tachycardias, likely related to arrhythmogenic EADs, are common in CHF (14). The ionic mechanisms underlying APD prolongation in CHF have not been precisely defined. Intriguingly, *de novo* ceramide synthesis has been found to be increased in heart failure (8). Increased ceramide level in cardiomyopathy can cause impairment of HERG function and result in excessive APD prolongation. More importantly, our data demonstrate that ROS mediates the inhibitory effect of ceramide on I_{HERG} and antioxidants can prevent the I_{HERG} depression. This explains at least partly the benefits of antioxidants in preventing and suppressing arrhythmias in ischemic myocardium and failing hearts (38-39). Indeed, Tsuji *et al.* (40) showed I_{Kr}, measured as E-4031-sensitive tail current, to be ~36% smaller in rabbits with ventricular tachypacing-induced CHF than in healthy rabbits. Lodge and Normandin (41) demonstrated earlier that I_{Kr}, measured as dofetilide-sensitive tail current, reduced by ~45% in the BIO TO-2 strain of cardiomyopathic hamster of 10 months old, derived from the BIO 53.58 animals and providing a model of dilated low output heart failure, compared with the 10-month-

old control (BIO F1B) hamsters. Moreover, simulations of cellular electrophysiology predict I_{Kr} inhibition to cause EADs in failing, but not nonfailing, myocytes (42).

Finally, the results of this study also have implications in diabetic cardiomyopathy (DCM). DCM is characterized by electrical remodeling with aberrant electrophysiology, metabolic remodeling with malignant biochemical processes and anatomical remodeling with progressive loss of cardiomyocytes, which result in impaired cardiac contractile and increased risk of lethal arrhythmias. QT prolongation and QT dispersion have been suggested as the predictor of mortality in both type I and type II diabetes (16-17, 43). It has been documented that *de nova* synthesis and accumulation of ceramide in diabetic myocardium contributes to the development of DCM (8, 10-11). In addition, oxidative stress is also known to be a critical deleterious factor for DCM (44-45). Moreover, we have recently found that I_{Kr}/HERG function is impaired in the rabbit model of DCM (46). Taken together, it seems plausible that ceramide-induced HERG depression may be one of the multiple determinants for diabetic QT prolongation.

8.6 Acknowledgements

This work was supported in part by the Heart and Stroke Foundation of Quebec awarded to Dr. Z Wang. The authors wish to thank XiaoFan Yang for excellent technical support and Louis R. Villeneuve for assistance with the confocal microscopic examinations.

8.7 References

1. Kolesnick, R. (2002) J. Clin. Invest. 110, 3-8
2. Mathias, S., Pena, L.A., and Kolesnick, R.N. (1998) Biochem. J. 335, 465-480
3. Ohanian, J., and Ohanian, V. (2001) Cell. Mol. Life Sci. 58, 2053-2068
4. Bielawska, A.E., Shapiro, J.P., Jiang, L., Melkonyan, H.S., Piot, C., Wolfe, C.L., Tomei, L.D., Hannun, Y.A., and Umansky, S.R. (1997) Am. J. Pathol. 151, 1257-1263
5. Beresewicz, A., Dobrzyn, A., and Gorski, J. (2002) J. Physiol. Pharmacol. 53, 371-382
6. Cordis, G.A,, Yoshida, T., and Das, D.K. (1998) J. Pharmaceutical. Biomedical. Analysis 16, 1189 1193

7. Murase, K., Okumura, K., Hayashi, K., Matsui, H., Toki, Y., Ito, T., and Hayakawa, T. (2000) Life Sci. 66, 1491-1500
8. Listenberger, L. L., and Schaffer, J. E. (2002) Trends Cardiovasc. Med., 12, 134-138
9. McTiernan,C.F., and Feldman, A.M. (2000) Curr. Cardiol. Rep. 2, 189-197
10. Kremer, G.J., Atzpodien, W., and Schnellbacher, E. (1975) Klin. Wochenschr. 53, 637-638
11. Hayat, S.A., Patel, B., Khattar, R.S., and Malik, R.A. (2005) Clin. Sci.(Lond) 107, 539-557
12. Boyden, P.A., and Jeck, C.D. (1995) Cardiovasc. Res. 29, 312-318
13. Carmeliet, E. (1999) Physiol. Rev. 79, 917-1017
14. Marban, E. (2002) Nature 415, 213-218
15. Nuss, H.B., Kaab, S., Kass, D.A., Tomaselli, G.F., and Marban, E. (1999) Am. J. Physiol. 277, H80-H91
16. Abo, K., Ishida, Y., Yoshida, R., Hozumi, T., Ueno, H., Shiotani, H., Matsunaga, K., and Kazumi, T. (1996) Diabetes Care 19, 1010
17. Veglio, M., Chinaglia, A., and Cavallo-Perin, P. (2004) J. Endocrinol. Invest. 27, 175-181
18. Wang, Z., Fermini, B., and Nattel, S. (1993) Circ. Res. 73, 276-285
19. Wang, Z., Fermini, B., and Nattel, S. (1994) Cardiovasc. Res. 28, 1540-1547
20. Sanguinetti, M. C., Jiang, C., Curran, M. E., and Keating, M. T. (1995) Cell 81, 299-307
21. Zhou, Z., Gong, Q., Ye, B., Fan, Z., Makielski, J.C., Robertson, G.A., and January, C.T. (1998) Biophys. J. 74, 230-241
22. Wang, J., Wang, H., Han, H., Zhang, Y., Yang, B., and Wang, Z. (2001) Circulation, 104, 2645-2648
23. Wang, J., Zhang, Y., Wang, H., Han, H., Nattel, S., Yang, B., and Wang, Z. (2004) Br. J. Pharmacol. 141, 586-599
24. Wang, H., Zhang, Y., Han, H., Cao, L., Wang, J., Long, H., Nattel, S., and Wang, Z. (2002) Cancer Res., 62, 4843-4848
25. Zhang, Y., Wang, J., Wang, H., Yang, B., and Wang, Z. (2003) J. Biol. Chem. 278, 10417-10426
26. Gulbins, E., Szabo, I., Baltzer, K., and Lang, F. (1997) Proc. Natl. Acad. Sci. U. S. A., 94, 7661-7666
27. Cayabyab, F.S., and Schlichter, L.C. (2002) J. Biol. Chem. 277, 13673-13681
28. Ruvolo, P.P. (2003) Pharmacol. Res. 47, 383-392

29. Thomas, D., Zhang, W., Karle, C.A., Kathofer, S., Schols, W., Kubler, W., and Kiehn, J. (1999) J. Biol. Chem. 274, 27457-27462
30. Cui, J., Melman, Y., Palma, E., Fishman, G.I., and Mcdonald, T.V. (2000) Curr. Biol. 10, 671-674
31. Cadenas, E., and Davies, K.J. (2000) Free Radic. Biol. Med. 29, 222-230
32. Raha, S., Myint, A.T., Johnstone, L., and Robinson, B.H. (2002) Free Radic. Biol. Med. 32, 421-430
33. Arora, A.S., Jones, B.J., Patel, T.C., Bronk, S.F., and Gores, G.J. (1997) Hepatology 25, 958 963
34. Garcia-Ruiz, C., Colell, A., Mari, M., Morales, A., and Fernandez-Checa, J.C. (1997) J. Biol. Chem. 272, 11369-11377
35. Patel, M. (1998) J. Neurochem. 71, 1068 1074
36. Suematsu, N., Tsutsui, H., Wen, J., Kang, D., Ikeuchi, M., Ide, T., Hayashidani, S., Shiomi, T., Kubota, T., Hamasaki, N., and Takeshita, A. (2003) Circulation 107, 1418-1423
37. Beuckelmann, D.J., Nabauer, M., and Erdmann, E. (1993) Circ. Res. 73, 379-385
38. Frolkis, V.V., Frolkis, R.A., Dubur, G.Y., Khmelevsky, Y.V., Shevchuk, V.G., Golovchenko, S.F., Mkhitarjan, L.S., Voronkov, G.S., Tsyomik, V.A., and Lysenko, I.V. (1987) Cardiology 74, 124-132
39. Walker, M. K., Vergely, C., Lecour, S., Abadie, C., Maupoil, V., and Rochette, L. (1998) Fundam. Clin. Pharmacol. 12, 164-172
40. Tsuji, Y., Opthof, T., Kamiya, K., Yasui, K., Liu, W., Lu, Z., and Kodama, I. (2000) Cardiovasc. Res. 48, 300 309
41. Lodge, N. J., and Normandin, D. E. (1997) J. Mol. Cell. Cardiol. 29, 3211 3221
42. Priebe, L., and Beuckelmann, D. J. (1998) Circ. Res. 82, 1206 1223
43. Christensen, P.K., Gall, M.A., Major-Pedersen, A., Sato, A., Rossing, P., Breum, L., Pietersen, A., Kastrup, J., and Parving, H.H. (2000) Scand. J. Clin. Lab. Invest. 60, 323-332
44. Maritim, A.C., Sanders, R.A., and Watkins, J.B. (2003) J. Biochem. Mol. Toxicol. 17, 24 38
45. Johansen, J.S., Harris, A.K., Rychly, D.J., and Ergul, A. (2005) Cardiovasc. Diabetol. 4, 5
46. Zhang, Y., Wang, J., and Wang, Z. (2004) Circulation 110, III-193

8.8 Figures and Figure Legends

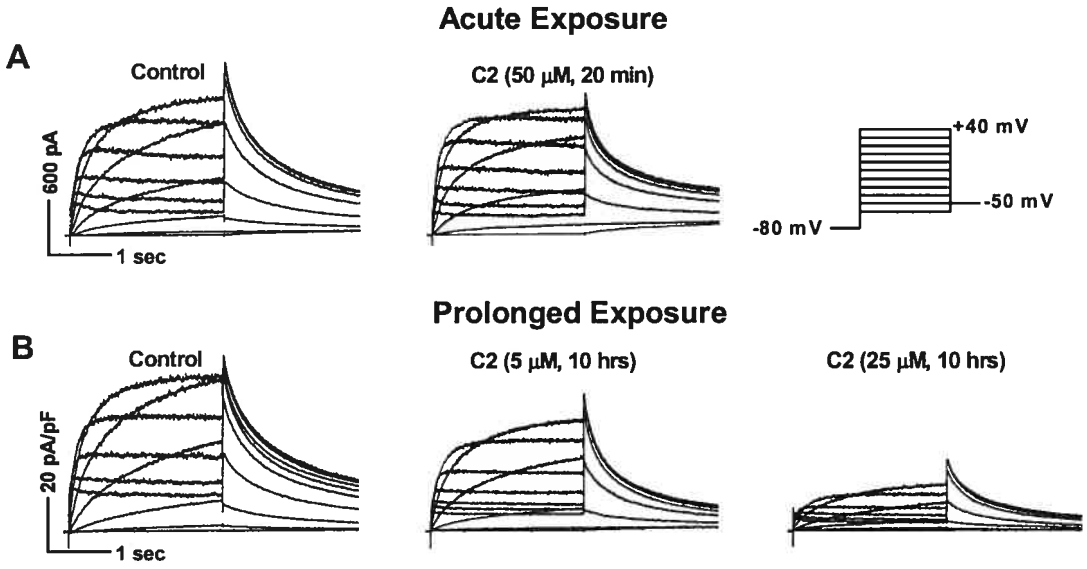

Figure 1. Analog data showing the effects of membrane permeable ceramide (C2) on HERG current (I_{HERG}) expressed in HEK293 cells. For acute exposure (**A**), C2 was applied to the Tyrode solution for patch-clamp recordings and currents recorded up to 20 min superfusion with C2 were taken to measure the drug effect as compared with the before-drug values. For prolonged exposure (**B**), HEK293 cells were preincubated with C2 in the normal culture medium for 10 hrs before patch-clamp studies and the current amplitude was normalized to cell capacitance to minimize the inter-cell variations of cell size for group comparison with untreated cells. I_{HERG} was elicited by 2.5-s depolarizing pulses to voltages ranging from –60 to +40 mV to record the step current, followed by 2.5-s repolarization step to –50 mV to record the tail current, as shown with the voltage protocol shown in the inset.

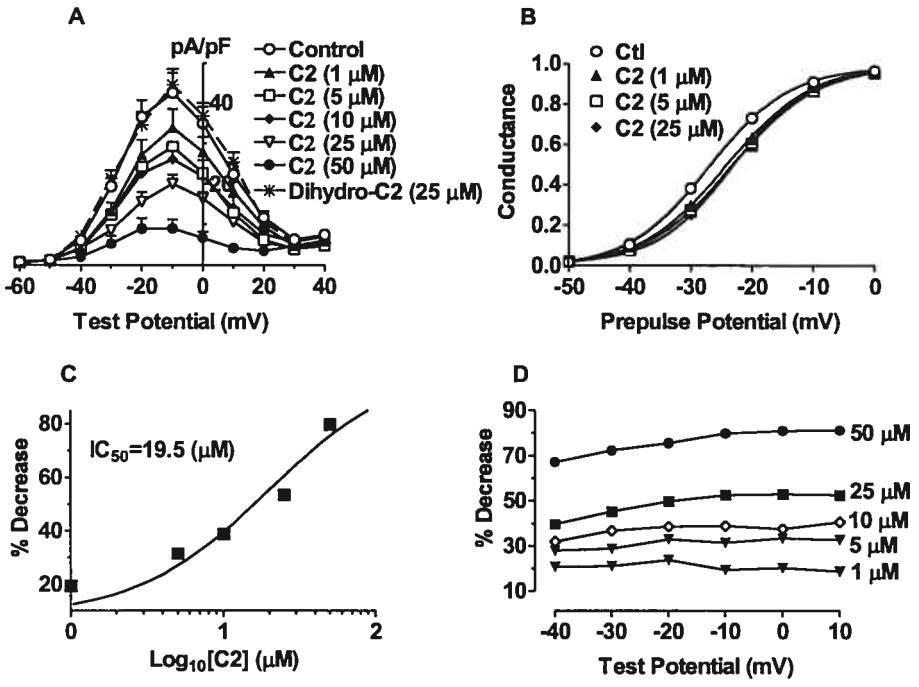

Figure 2. Characterization of I_{HERG} with prolonged exposure to ceramide (C2). (**A**) current density-voltage relationships. Shown are mean values from n=13 cells for control (Ctl), n=12 for 1 μM C2, n=14 for 5 μM, 10 μM, 50 μM C2, and 25 μM for dihydro-C2 (the inactive analogue of C2), respectively. (**B**) Steady-state voltage-dependent activation curves. The activation curves were constructed by plotting the conductance *G* as a function of depolarizing potentials. *G* was calculated by normalizing the tail currents at -50 mV by dividing the amplitude of the tail currents measured at various antecedent depolarizing potentials by that of the tail current at +40 mV. Symbols are mean of experimental data and lines represent the Boltzmann fit: $G/G_{max}=1/\{1+\exp[(V_{1/2}-V)/k]\}$, where G_{max} represents the maximal conductance at +40 mV, $V_{1/2}$ is a half-maximal activation voltage, and *k* is a slope factor. Note that C2 produces positive shift of HERG activation. (**C**) Concentration-dependent block of I_{HERG} by C2. Symbols are experimental data and the curve represents the fit to the Hill equation: $Y=B+(T-B)/(1+10\text{^}((\text{LogIC}_{50}-[\text{C2}]_o)*n))$, where *Y* is the percentage of I_{HERG} inhibition, *B* is the minimum inhibition and *T* the maximum inhibition observed, IC_{50} represents the concentration of C2 $[C2]_o$ for half-maximal inhibition of I_{HERG}, and *n* represents the Hill coefficient. (**D**) Percent decrease in I_{HERG} produced by various concentrations of C2. *$p<0.05$ *vs.* Ctl.

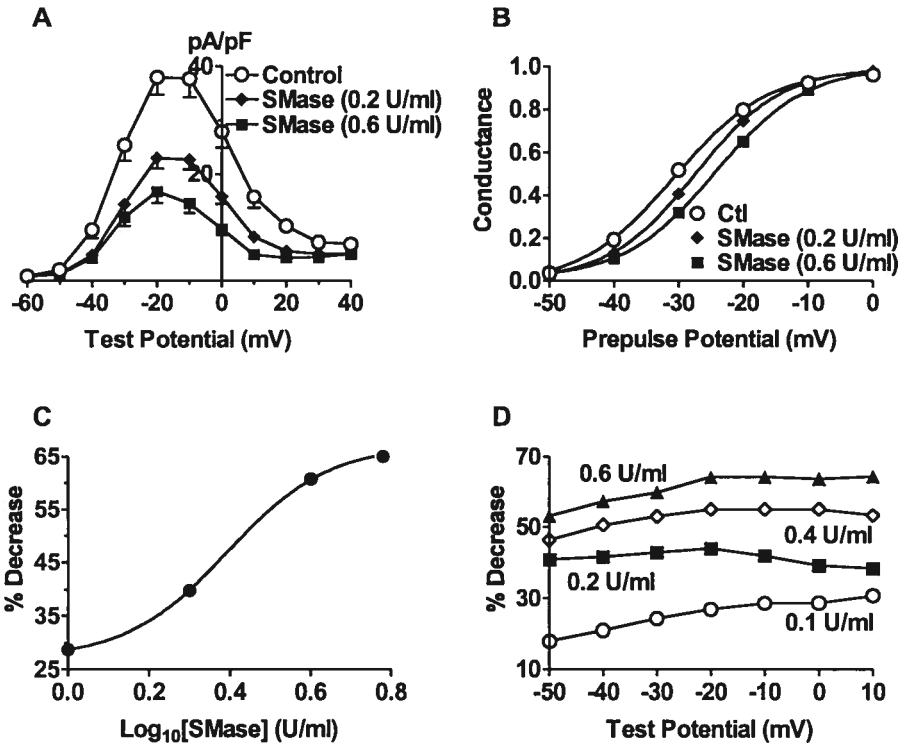

Figure 3. Characterization of I_{HERG} depression caused by sphingomyelinase (SMase). (**A**) Current density-voltage relationships. Shown are mean values from n=19 cells for control (Ctl), n=9 cells for 0.1 U/ml SMase, n=17 cells for 0.2 U/ml SMase, n=8 cells for 0.4 U/ml SMase and n=13 cells for 0.6 U/ml SMase. (**B**) Steady-state voltage-dependent activation curves. Note that similar to C2, SMase also produces positive shifts of HERG activation. (**C**) Concentration-dependent block of I_{HERG} by SMase. Symbols are experimental data and the curve represents the fit to the Hill equation. (**D**) Percent decrease in I_{HERG} produced by various concentrations of SMase. *p<0.05 *vs.* Ctl.

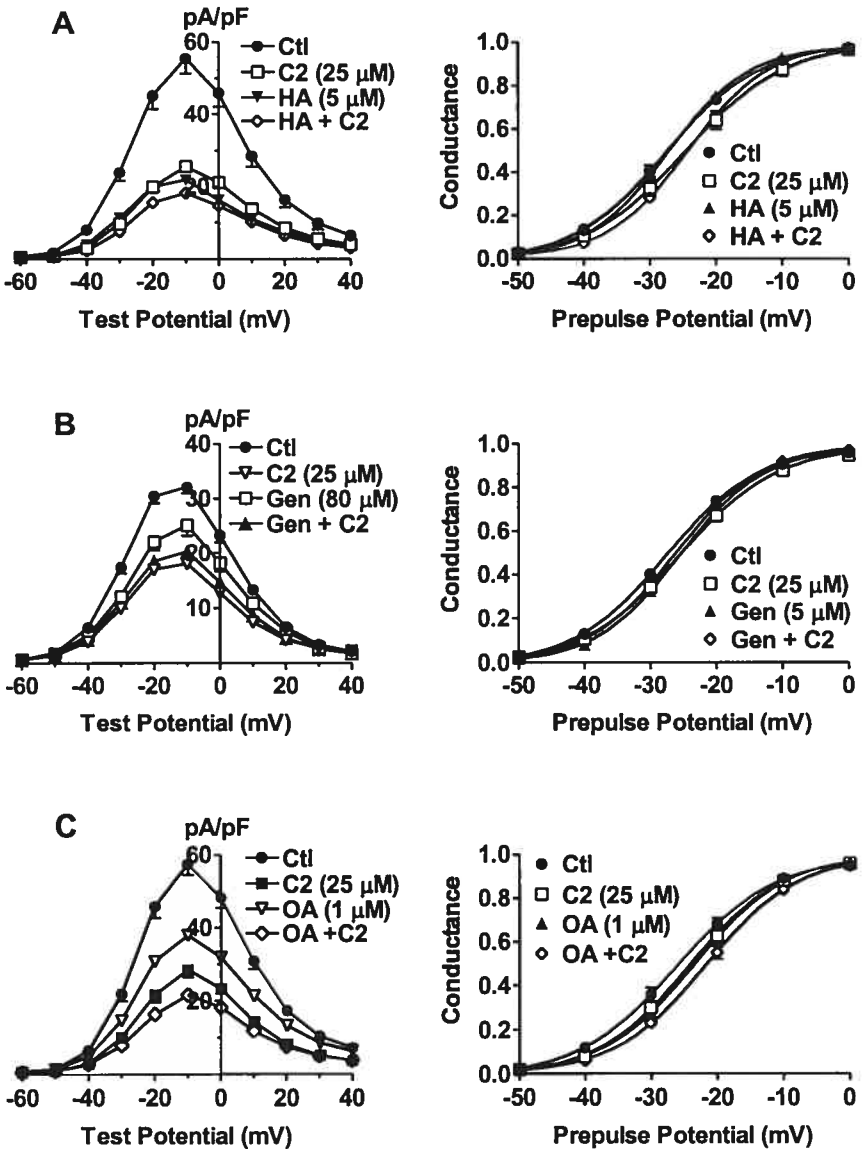

Figure 4. Effects of inhibitors of tyrosine protein kinases (TPKs) and atypical protein kinase C (PKC_ξ) on I_{HERG} modulation by ceramide (C2). Left panels: current density-voltage relationships; right panels: steady-state voltage-dependent activation curves. PTK inhibitors herbimycin A (HA, 5 μM) and genestein (Gen, 80 μM); PKC_ξ inhibitor okadiac acid (OA, 1 μM). Comparisons were made among 4 groups: Ctl-control untreated cells (Ctl), C2-cells treated with C2 alone, cells treated with an inhibitor alone, and cells co-incubated with an inhibitor and C2 for 10 hrs after 2-hrs preincubation with the inhibitor alone. *$p<0.05$ *vs.* Ctl.

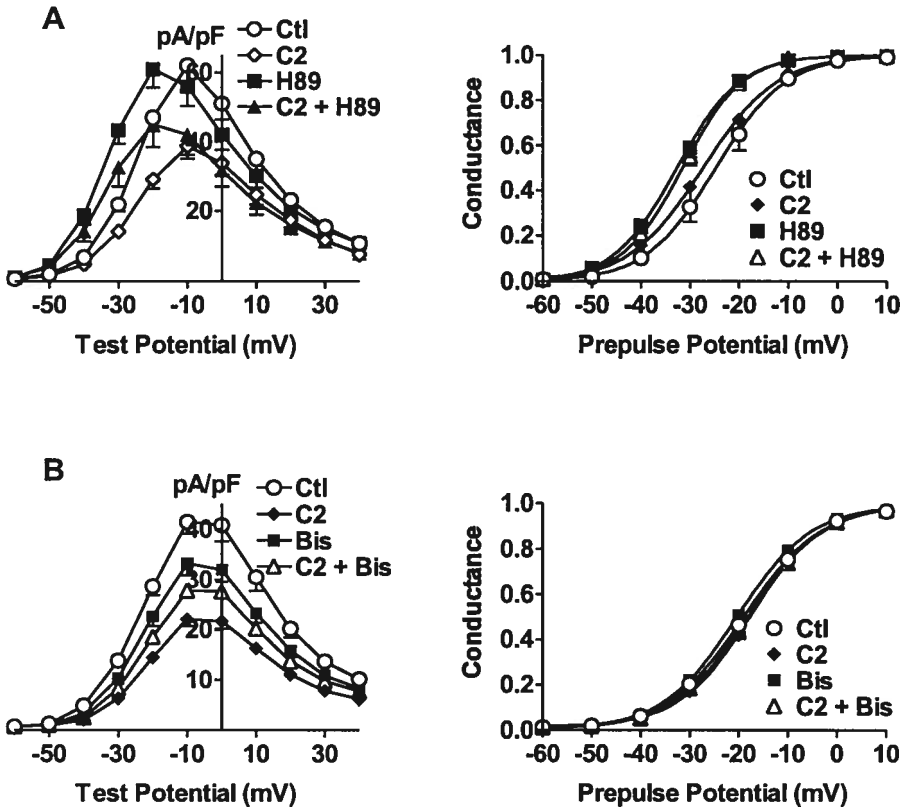

Figure 5. Effects of inhibitors of protein kinase A (PKA) or protein kinase C (PKC) on I_{HERG} modulation by ceramide (C2). (**A**) Effects of PKA inhibitor H89 (1 μM) on C2-induced I_{HERG} depression. Left panels: current density-voltage relationships; right panels: steady-state voltage-dependent activation curves. For experiments involving co-application of H89 and C2, the cells were preincubated with H89 for 2 hrs and then incubated with C2 (5 μM) in the presence of H89 for 10 hrs before patch-clamp recordings. *p<0.05 *vs.* Ctl. (**B**) Effects of PKC inhibitor bisindolylmaleimide (Bis) on C2-induced I_{HERG} depression. Left panels: current density-voltage relationships; right panels: steady-state voltage-dependent activation curves. For experiments involving co-application of Bis and C2, the cells were preincubated with Bis for 2 hrs and then incubated with C2 (5 μM) in the presence of Bis for 10 hrs before patch-clamp recordings. *p<0.05 *vs.* Ctl.

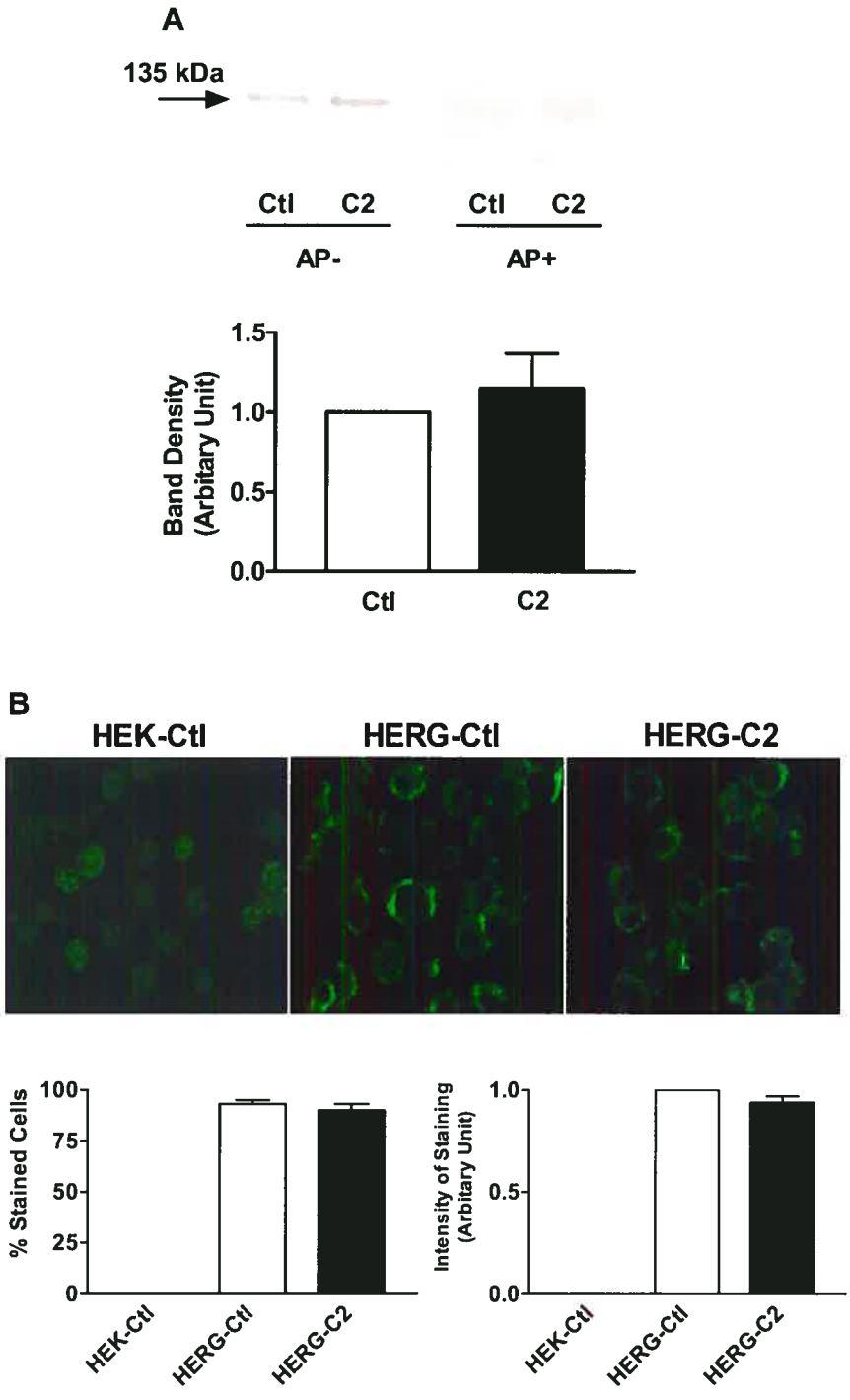
A
135 kDa
Ctl
C2
Ctl
C2
AP-
AP+
Band Density (Arbitary Unit)
1.5
1.0
0.5
0.0
Ctl
C2
B
HEK-Ctl
HERG-Ctl
HERG-C2
% Stained Cells
100
75
50
25
0
HEK-Ctl
HERG-Ctl
HERG-C2
Intensity of Staining (Arbitary Unit)
1.0
0.5
0.0
HEK-Ctl
HERG-Ctl
HERG-C2

Figure 6

Figure 6. Expression level of HERG protein determined by immunoblotting with membrane protein preparations extracted from HERG-expressing HEK293 cells. (**A**) Upper panel: examples of immunoblotting bands of ~135 kDa, corresponding to the molecular mass of HERG protein, from C2 treated (C2) and untreated cells (Ctl). Cells were incubated with C2 (25 μM) for 10 hrs in the culture medium prior to the procedures for membrane protein extraction. Lower panel: mean band density from 3 independent protein samples. AP- and AP+, without or with antigenic peptide pretreatment for anti-HERG antibody, respectively. (**B**) Upper panel: examples of immunocytochemical staining of HERG proteins on the cytoplasmic membrane. Lower panel: averaged data from four independent experiments, showing % cells with positive staining with anti-HERG antibody and intensity of staining.

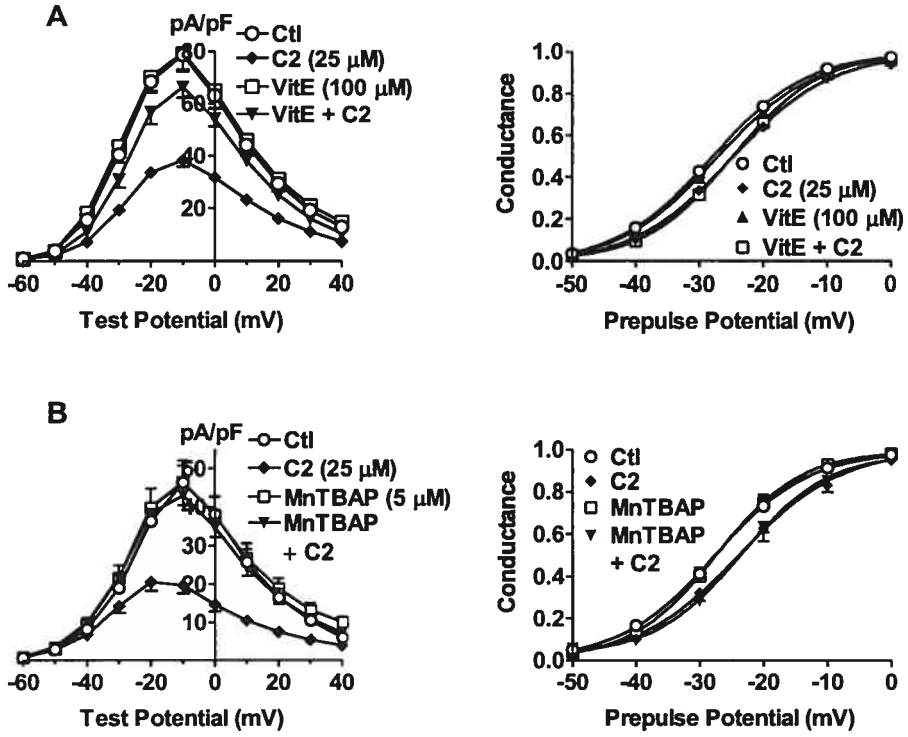

Figure 7. Role of reactive oxygen species (ROS) on I_{HERG} modulation by ceramide (C2).
(**A**) Effects of vitamin E (VitE) on C2-induced I_{HERG} depression. (**B**) Effects of MnTBAP, a superoxide dismutase mimic, on C2-induced I_{HERG} depression. Left panels: current density-voltage relationships; right panels: steady-state voltage-dependent activation curves. The cells were preincubated with VitE (100 μM) or MnTBAP (5 μM) for 2 hrs and then incubated with C2 (25 μM, n=16 cells) in the presence of VitE (n=16 cells) or MnTBAP (n=16 cells) for 10 hrs before patch-clamp recordings. *p<0.05 *vs.* Ctl (n=14 cells).

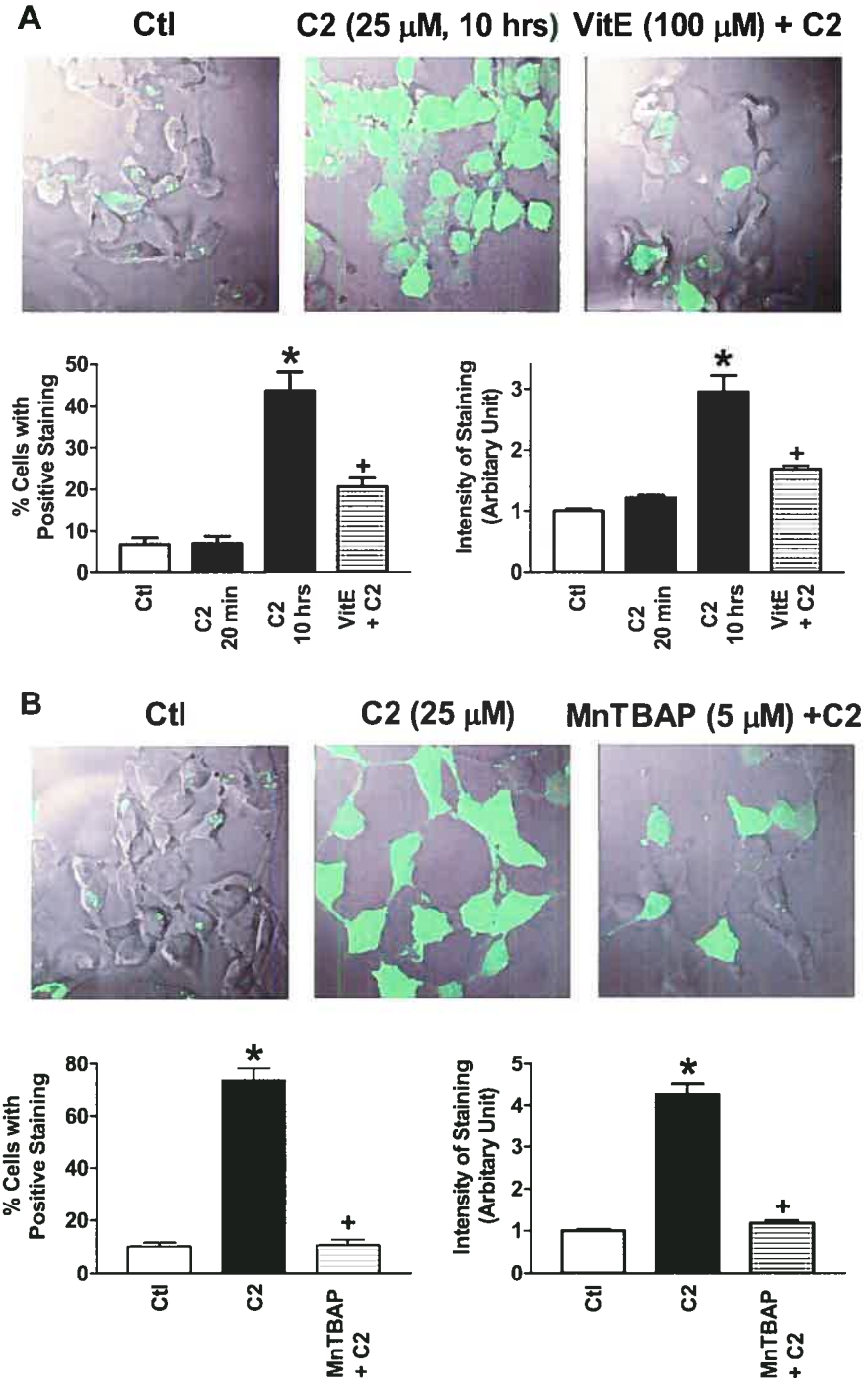
A
Ctl
C2 (25 μM, 10 hrs)
VitE (100 μM) + C2
% Cells with Positive Staining
Intensity of Staining (Arbitary Unit)
Ctl
C2 20 min
C2 10 hrs
VitE + C2
B
Ctl
C2 (25 μM)
MnTBAP (5 μM) +C2
% Cells with Positive Staining
Intensity of Staining (Arbitary Unit)
Ctl
C2
MnTBAP + C2

Figure 8

Figure 8. Effects of vitamin E (VitE) or MnTBAP (an SOD mimic) on intracellular levels of ROS measured by CM-H2DCFDA fluorescence dye. (**A**) and (**B**) Upper panels: laser scanning confocal microscopic images of CM-H_2DCFDA staining reflecting the intracellular ROS levels. Lower panels: percentage of positively stained cells (mean ± S.E.), obtained from 5 fields of 4 experiments by counting the cells with staining intensity ≥ 5 times the background and averaged intensity of CM-H_2DCFDA fluorescence measured from the positively stained cells. Data were obtained from control untreated cells (Ctl), cells treated with C2 (25 μM for 20 min or 10 hrs), and cells pretreated with VitE (100 μM) or MnTBAP (5 μM). *p<0.05 *vs.* Ctl; +p<0.05 vs. C2.

9 GENERAL DISCUSSION AND CONCLUSIONS

This chapter summarizes the major findings in the thesis project, their significance and implications, the potential limitations of the work, and the prospects for future research related to this project. Conclusive remarks are made in the final section to complete the thesis.

9.1 Summary of Novel Findings and Their Significances

The diabetic cardiocomplictions are characterized by electrical remodeling with aberrant cardiac electrical and contractile functions and arrhythmias,[1-4] metabolic remodeling with dysregulated biochemical processes,[5;6] and anatomical remodeling with progressive loss of cardiomyocytes.[7] QT prolongation as well as dispersion is a predictor for the prognosis of diabetics in clinic, while the underlying mechanisms were not well understood despite that the works on diabetic mice and rats have pointed to several candidates, such as reduced I_{to} and I_{ss}, are responsible for the APD and QT prolongation.

In this thesis, we have established a type 1 diabetic model in rabbits, which have been shown to have typical cardiomyopathy as that in diabetic patients by previous works of other groups, and possess many similarities of electrophysiology as in humans. We have systemically studied the alterations of both inward and outward currents and identified the significantly reduced I_{Kr} as a principal contributor to the APD and QT prolongation and the arrhythmia in diabetic hearts. Moreover, insulin corrects the QT prolongation in diabetic rabbits, via several mechanisms, e.g. by reducing oxidative stress and enhancing PKB activity which is essential for proper function of I_{Kr}/HERG channel as demonstrated in our work. Since elevated oxidative stress, i.e. reactive oxygen species (ROS), has impairing effects on I_{Kr}/HERG channel, evidenced in hyperglycemic cells and in diabetic rabbits in our studies, vitamin E alone showed great potential to overcome the oxidative stress in myocardium, in isolated cardiomyocytes, and in HERG-expressing HEK293 cells, thus correct the deficiency of I_{Kr}/HERG function and prevent QT prolongation in diabetic rabbits.

Besides glucose and insulin-PKB signaling transduction pathway, we have also put effort in delineating mechanisms underlying the depressing effects on I_{Kr}/HERG channels by another

two metabolic stress factor, TNF-α and ceramide which accumulate remarkably in diabetes and stimulate the production of intracellular ROS that diminishes the function of I_{Kr}/HERG K^+ channel.

9.1.1 I_{Kr} as a major contributor to the APD/QT prolongation in diabetic hearts

Consistent with studies of ionic remodeling in diabetic models of rats and mice,[8-17] we found significant reduction (60% smaller) of I_{to} in diabetic rabbits. However, it has no significance in the APD lengthening in diabetic cardiomyocytes, as demonstrated by the simulation using a program LabHEART which reproduces faithfully the electrophysiological and Ca^{2+} transport characteristics of rabbit ventricular myocytes.[18]

Rather than I_{to}, we identified I_{Kr}, encoded by *HERG* in men, as the major player among the inward and outward currents we have studied, although another repolarization current I_{Ks} in myocytes from diabetic rabbits is also much smaller than in the healthy ones. Prediction using LabHEART program shows that ~70% reduction of I_{Kr} as found in diabetic rabbit hearts prolongs APD_{50} in 27% and APD_{90} in 30%, which is close to the actual APD prolongation in myocytes from diabetic rabbits (24% longer). Since rabbit resembles human in most of the ion channel functions, it is suggested that I_{Kr} impairment is a critical factor contributing to the APD and QT prolongation in humans, thus being a potential target to prevent and treat the QT prolongation and arrhythmias, and the sudden cardiac death in diabetics.

9.1.2 Metabolic perturbations cause I_{Kr}/HERG channelopathy thereby the APD/QT prolongation in diabetic hearts.

Diabetes mellitus is characterized by metabolic remodeling with malignant biochemical processes, which are results of significantly changed metabolic basis, e.g. elevated plasma sugar level, insufficient insulin source, and so on. Chronic and even acuate disturbance of these cellular milieu lead to significant augmentation in ROS, defects in insulin-PI3K-PKB signaling that is required for glucose transport, and marked generation and accumulation of deleterious cellular metabolites such as TNF-α and ceramide.

The ionic channelopathy is responsible for the diabetic APD and QT prolongation, which was previously evidenced by the studies on the diminishment of I_{to} in rat and mouse models. Our works in diabetic rabbit model demonstrated that diabetic metabolic perturbations cause I_{Kr}

impairment (Figure 1). Impairment of I_{Kr}/HERG function in DM animals and in hyperglycemic cells was primarily ascribed to the enhanced oxidative damages to the myocardium as indicated by the increased intracellular level of ROS and simultaneously decreased endogenous antioxidant reserve and by the increased myocardial lipid and protein oxidations. Moreover, DM or hyperglycemia resulted in downregulation of HERG protein level and loss of HERG protein stability. The I_{Kr}/HERG impairment can be corrected by insulin treatment, even though when the blood glucose level is still higher than normal, for which we consider that a certain level of glucose is necessary to let the deleterious pathways occupy the major outcomes. Insulin treatment dramatically reduces ROS in diabetic hearts, restores the impaired function of I_{Kr}/HERG K^+ channels and shortens the prolonged APD in diabetic cardiomyocytes and in HEK293 cells in mimicked hyperglycemia. Consistently, diabetic rabbits administrated with insulin did not show arrhythmic signs. Despite of the uncontrolled hyperglycemia, vitamin E partially restores the depressed I_{Kr}/HERG and prevents APD and QTc prolongation and the associated arrhythmias, with similar mechanism as by insulin, with antioxidant ability as a primary function. Our study represents the first documentation of oxidative stress caused by hyperglycemia or insulin insufficiency as the major metabolic mechanism for diabetic I_{Kr}/HERG channelopathy. Correcting either insulin insufficiency or reducing oxidative stress (e.g. by antioxidants) would rescue I_{Kr}/HERG functions thus being a promising therapy for the diabetic QT prolongation and arrhythmias.

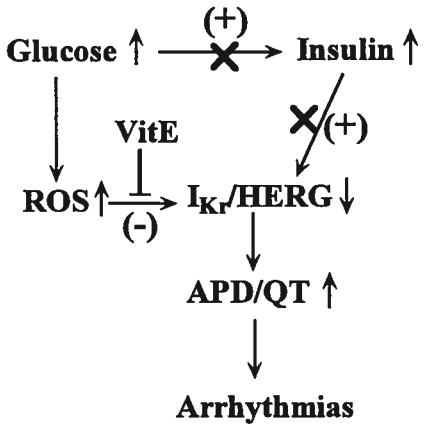

Figure 1. Schematic diagram of pathophysiology of diabetic arrhythmias. Physiologically, increased glucose results in insulin release from pancreatic-ß cells. Under this condition, the negative (-) effects of hyperglycemia on I_{Kr}/HERG will be counteracted by the positive (+) effects of insulin, therefore there is not significant changed in I_{Kr}/HERG. In IDDM, due to the deficiency of insulin secretion and remarkable elevated ROS level, I_{Kr}/HERG will be reduced and APD and QT prolonged, leading to arrhythmias.

9.1.3 Hypoglycemia and hyperglycemia impair HERG K^+ channel function with different mechanisms

As both hyperglycemia and hypoglycemia can cause prolongation of Q-T interval and ventricular arrhythmias, we designed a study to elucidate the detail mechanisms by which they modulate I_{Kr}/HERG function which has been shown in IDDM rabbit model to be drastically impaired. I_{HERG} current in HEK293 cells in mimicked hypoglycemia (extracellular glucose concentration $[Glu]_o$=5 mM) or hyperglycemia ($[Glu]_o$=10, 20 mM) was significantly smaller than that in normoglycemia ($[Glu]_o$=5 mM). The effects of hypoglycemia was mimicked by inhibiting glucose metabolism (by 2-deoxy-D-glucose, blocker of both the glycolysis and the oxidative phosphorylation), and by depleting intracellular ATP content, or replacing ATP by GTP or non-hydrolysable ATP.

The effects of hyperglycemia on HERG were abolished by inhibition of oxidative phosphorylation or by application of antioxidants vitamin E or superoxide dismutase mimetic (MnTBAP); and incubation with xanthine/xanthine oxidase (X/XO) mimicked the effects of

hyperglycemia. Hyperglycemia or X/XO markedly increased intracellular level of ROS, as measured by a ROS sensitive fluorescence dye, and this increase was prevented by oxidative phosphrylation inhibitor NaCN, or antioxidants vitamin E and MnTBAP.

Thus our work demonstrated the first time ATP as critical regulator for proper HERG function and deciphered a common phenotype of HERG impairment by hypoglycemia and hyperglycemia, via different mechanisms: depression of I_{HERG} in hypoglycemia results from underproduction of ATP and in hyperglycemia from overproduction of ROS.

9.1.4 Basal activity of protein kinase B is essential for proper I_{Kr}/HERG functions

Using pharmacological and molecular tools, we demonstrated that basal activity of PKB is essential for proper I_{Kr}/HERG function. The PI3K inhibitor wortmannin caused ~30% (p<0.05) reduction of I_{HERG} stably-expressed in HEK293 cells; similar effect was found by transient expression (by transfection) of dominant negative PI3K (dnPI3K) which reduced I_{HERG} in 25%, and a stronger effect by transfection of dominant negative PKB (dnPKB, 47%). Overexpression of the constitutively active PI3K (caPI3K) slightly increased (~7%) I_{HERG} while a constitutively activated PKB (caPKB) boosted I_{HERG} for ~35%. The smaller effect of PI3K is likely due to the possible PI3K-independent modulation of PKB,[19] while directly enhancing or reducing PKB activity results in pronounced modulation of I_{HERG}. We confirmed the basal activation of PKB using immuno-cytochemical detection that PKB activity was significantly enhanced in caPKB-transfected cells and nearly completely abolished in dnPKB-transfected cells, but less changed when transfected with dnPI3K or caPI3K. These results suggest that the effects of PI3K inhibitor wortmannin on I_{HERG} are mediated by PI3K's downstream target PKB, to which HERG has two putative consensus phosphorylation sites (S331 and S890). Our data represent the first evidence that PKB phosphorylation regulates K^+ channels.

Since the activation of PI3K-PKB signaling pathway requires insulin and other stimuli, while in IDDM both the decreased insulin level and the increased metabolic stress (e.g. glycotoxic, ROS, TNF-α, ceramide) can reduce PKB activity, it is an outcome of the balance between beneficial and deleterious factors of I_{Kr}/HERG K^+ channels. By either correcting the insulin insufficiency or metabolic disturbance, or directly restore PKB activity may provide a novel and rational therapy for the I_{Kr}/HERG channelopathy thereby the APD/QT prolongation and very likely arrhythmias, too.

9.1.5 TNF-α and ceramide depress I_{Kr}/HERG function by generating ROS

TNF-α is known to have deleterious effects on a diversity of cellular functions, for example, inducing apoptosis,[20] inhibiting K^+ current in ligodendrocytes[21] and I_{CaL} and Ca^{2+} transients in cardiomyocytes,[22] but it is inadequately understood what effects it has and how it will work to alter other ionic channels. In addition, the potential roles of ceramide, although emerging as a new second messenger of different cellular processes, was not well defined in the area of heart diseases, either.

We found that when treated acutely or chronically (10 hr) with TNF-α, I_{Kr} in isolated cardiomyocytes or I_{HERG} in HEK293 cells is significantly reduced in a concentration-dependent manner. Consistently, this treatment prolongs the APDs in ventricular myocytes. In stead of changing the expression of HERG K^+ channel protein, TNF-α generates enormous amount of ROS in both HEK293 cells and cardiomyocytes, which is resembled to the effects of superoxide anion produced by an artificial system (xanthine/xanthine oxidase), and can be eliminated by either vitamin E or by MnTBAP which is a SOD mimetic. These antioxidants also prevent the diminishing effects of TNF-α on I_{Kr}/I_{HERG}. Moreover, pretreating the cells with inhibitory anti-TNFR1 antibody (to block the TNF receptor) removes TNF-α action on I_{Kr}/I_{HERG}.

Ceramide has not significantly influence on I_{HERG} when exposed to HEK293 cells with a short period, while markedly depresses I_{HERG} by chronic exposure with concentration-dependence, or by treatment of the cells with sphingomyelinase (SMase) that catalyzes the production of endogenous ceramide. Our data showed that neither tyrosine kinase, nor PKA, nor PKC contributed significantly to the ceramide effects on I_{HERG}. Prolonged exposure does not affect the expression of HERG, either, but causes considerable production of ROS, with similar mechanisms as induced by TNF-α..

Thus, our data demonstrate a common mechanism – overproduction of ROS, by which TNF-α and ceramide, two different classes of metabolic products, modulate the I_{Kr}/HERG K^+ channel function. Figure 2 summarizes current knowledge and our novel findings in diabetic signaling factors contributing to APD/QT prolongation and arrhythmias.

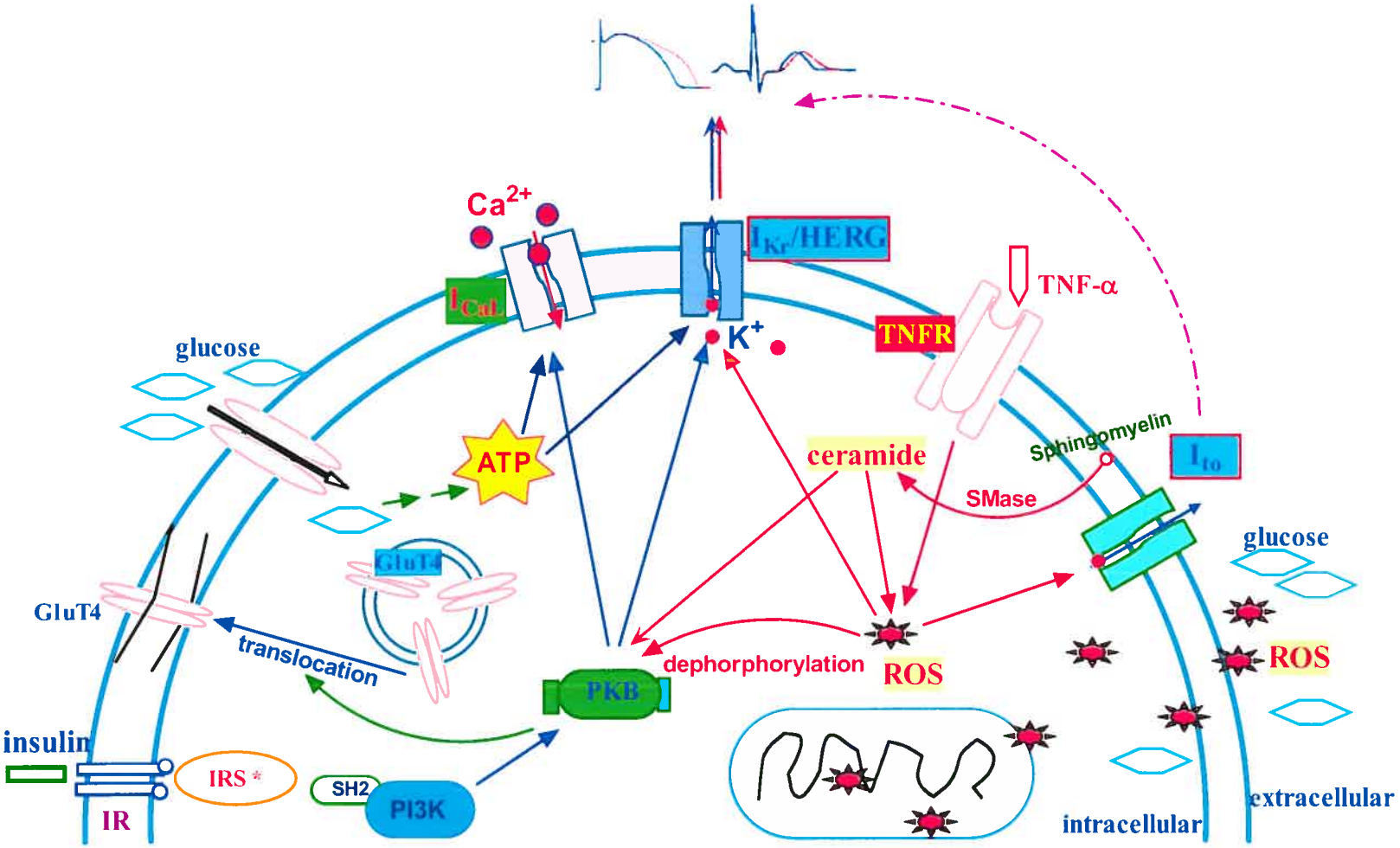

Figure 2. Signaling factors in diabetic QT prolongation and arrhythmias.

Figure 2. Signaling factors in diabetic QT prolongation and arrhythmias. Besides the down-regulation of HERG channel protein, signaling factors also participate to modulate ion channels functions thus the QT interval as well as arrhythmias. Insulin binds to insulin receptor (IR) and leads to the autophosphorylation of IR substrate (IRS). Active IRS phosphorylates the SH2 group of phosphoinositide 3-kinase (PI3K) that activates the downstream protein kinase B (PKB). PKB promotes the translocation of glucose transporterase (GLUT4) to the cell membrane so that the glucose level is regulated. The generated ATP product and PKB activity are necessarily for proper function of calcium channel (I_{CaL}) and I_{Kr}/HERG K^+ channel. Under hyperglycemia, the elevated level of reactive oxygen species (ROS) impairs the functions of PKB and ion channels: I_{Kr}/HERG and transient outward K^+ channel (I_{to}). When bound to the tumor necrosis factor receptor (TNFR), TNF-α induces the production of ROS thus diminishes the I_{Kr}/HERG function. Ceramide also mediates the ROS production. Impairment of I_{Kr}/HERG function leads to the APD/QT prolongation and the resultant arrhythmias. I_{to} dysfunction is a contributory factor for the QT prolongation in diabetic rodents but not in species possessing I_{Kr}. For arrows pointing to ion channel, the red ones indicate negative effects and the blue ones indicate positive effects.

9.2 Potential Limitations

9.2.1 Animal model used in this study

In this thesis, we employed rabbit to establish the IDDM model, which showed significant cardiomyopathy after around 4 weeks of disease, demonstrated in previous studies.[23-25] Rabbit was preferred because it possesses similar ionic channels as in man, especially in the aspects of channel functions, thus pertain to our goals to study the ionic mechanisms underlying the APD and QT prolongations in diabetics.

We chose male animals in our experiment, as in Canada, the diabetes prevalence is 3.5% among males while 2.9% in females ($p<0.001$).[26] However, the diabetic females are more prevalence to diabetic heart diseases. Young diabetic patients which is a population in whom comorbidity such as ischemic heart disease or hypertension can be considered as absent or minimal, have significant changes in left ventricular dimensions and myocardial relaxation in their early disease stage, with girls clearly being more affected.[27;28] In the EURODIAB IDDM Complications Study (3250 insulin-dependent diabetic patients attending 31 centers in 16 European countries), QTc in diabetic female patients is longer than in male patients, even in the absence of diabetic complications known to increase the risk of corrected QT prolongation.[29]

Thus our study may underestimate the contribution of I_{Kr}/HERG to the APD/QT prolongation, and the QT prolongation itself in female diabetics, due to the gender difference which is commonly believed to be a result of the hormone tone and the ion channels profiles: the smaller currents of I_{Kr},[30;31] I_{to} and I_{ss} (albeit it is likely absent in humans)[32;33] ultrarapid delayed rectifier K^+ current,[34;35] and stronger I_{CaL} current,[36;37] therefore the resultant longer QT-induced arrhythmic risk in females.[26;30;31;34;35;38-40]

Studies by Shimoni et al[32] did demonstrate the sex-differential remodelings of I_{to} and I_{ss} in diabetic rats: they are significantly attenuated in diabetic male rats but at a less extent in females; and inhibitors angiotensin-converting enzyme (ACE) and endothelin-converting enzyme (ECE) for angiotensin II (ATII) and endothelin-1 (ET-1) respectively, significantly enhanced K^+ currents in myocytes from male diabetic rats, but had no effect on cells from female diabetic rats. Their study indicates that autocrine modulation of K^+ currents by renin-angiotensin and endothelin systems is attenuated or absent in female diabetic rats and oestradiol plays a key role in reducing this modulation. Moreover, ATII is increased in male diabetic rats but not

altered in diabetic females, thus results in enhancing PKC activity but reducing PKA activity in male, and downregulates K^+ currents.[33]

Due to the time limit of a PhD project, our studies do not address the gender difference in I_{Kr} alteration in diabetes. More study is needed to advance our understanding in the potential difference and the implications in gender-based intervention on diabetic cardiocomplications, e.g. QT prolongation as well as arrhythmias.

9.2.2 *Ion current and AP recordings in diabetic cardiomyocytes*

Because the experiments to study the ionic currents and APs were done with patch-clamp in isolated cardiomyocytes, the washable effects such as those from the undefined diabetic signaling molecules, maybe are not observed; most of those washable diabetic signaling factors (e.g. ROS, TNF-α, ceramide) have depressing effects on I_{Kr} (Chapter 6~9) and other ion channels, [21;41-44] thus we may underestimate the potential impairment of I_{Kr}/HERG K^+ channels and the resultant APD prolongation in the *in vivo* diabetic conditions.

Moreover, the significantly altered biochemical processes in diabetes result in various metabolic stresses besides the conditions we have tested in the thesis project. For instance, ketoacidosis, a serious condition in DM where the body has dangerously high levels of ketones, or acids that build up in the blood, can lead to diabetic coma (passing out for a long time) or even death. This acidification can reduce I_{Kr} and I_{to} K^+ currents,[45;46] and alter gap junctional conductance between cardiac ventricular myocyte.[47] While potassium loss due to the shift of potassium from the intracellular to the extracellular space in an exchange with hydrogen ions that accumulate extracellularly in acidosis, can also impair cardiac functions. Hypernatremia or elevated blood sodium in uncontrolled DM can block I_{Kr}/HERG channel,[48] increase I_{Na} conduction, and may lead to serious arrhythmias such as tachycardia. Moreover, reduced adrenergic level as in diabetic neuropathy can affect numerous cellular functions, e.g. those of ion channels.[49-51] In our studies, we have not addressed these aspects, which may underestimate the potential roles of these factors in diabetic QT prolongation and arrhythmias.

9.2.3 *Links between insulin, TNF-α / ceramide and intracellular ROS*

Our studies have demonstrated that ROS is a critical mediator for the I_{Kr}/HERG dysfunction induced by TNF-α and ceramide in HEK293 cells and cardiomyocytes. It should be

noted that our studies have not addressed the mechanistic link between TNF-α and ceramide and the intracellular ROS production: how do insulin insufficiency, hyperglycemia, TNF-α and ceramide change the redox system and bring about the overproduction of ROS in diabetic animal and cell models; is the source of ROS from mitochondrial or cytosolic and how do TNF-α and ceramide increase intracellular ROS; how do the ROS from either TNF-α/ ceramide or xanthine/ xanthine oxidase system affect I_{Kr}/HERG channel, directly or via other bridges? In addition, our experiments demonstrated the capability of insulin to reduce ROS, while the mechanism is not defined yet, although it is possible being the same as its functions in regulating I_{to} in diabetic rats and mice.

9.3 Future Directions

Given the crucial role of I_{Kr}/HERG in regulating the cardiac repolarization thus the lengths of action potential duration and QT interval, and the tonic regulation of I_{Kr}/HERG by insulin-PI3K-PKB signaling but down-regulation by elevated ROS, future studies will be preferred to test the possible therapeutic effects of I_{Kr} enhancer which has recently been discovered,[52] or the outcome of rescuing I_{Kr} directly by gene expression of *ERG* or indirectly by PKB that is downregulated in diabetes. Such goal can be achieved by using *in vivo* transferring the genes carried by lentivirus or adenovirus vector.[53;54] Moreover, our studies have demonstrated that ROS serves as a major deleterious factor to the I_{Kr}/HERG channelopathy, testing other antioxidants would provide clearer prospect about the clinical application of antioxidants in preventing or treating diabetic arrhythmias. In addition, the PKB modulation on HERG can be confirmed by further study, e.g. mutating the putative of PKB phosphorylation sites on HERG gene (S331, S890) and comparing their currents modulated by PKB phosphorylation.

Dysfunctions of both diminished repolarization (e.g. reduced I_{Kr} and I_{to} in diabetic hearts) and/or increased depolarization result in APD/QT prolongation, providing substrates for arrhythmias. Change in cardiac conduction may also be crucial for the generation of arrhythmias. We found around10% widening of QRS complex in some diabetic rabbit ECGs and a little slower heart rate which is agreed with clinical evidence.[55] Since the important I_{Na} is not affected in IDDM rabbits in our studies, it is possible other factors such as gap junction channels are changed. Studies have shown connexin-43 (Cx-43), a gap junction channel expressed in both atrium and ventricles,[56] is a keeper for the integrity of cardiac rhythm. In deed, our preliminary data in immunohistochemical and immunocytochemical study show significantly reduction of Cx-43 in ventricle tissue and isolated cardiomyocytes from diabetic rabbit hearts, particularly, on intercalated disk and along longitude membrane of the myocytes (Figure 3). Thus it may contribute to the arrhythmias and the QRS widening in some of the diabetic animals in an undefined mechanism and requires more detail studies. Other factors such as diabetic neuropathy may also participate in remodeling the cardiac functions.

In addition, as discussed in the section *9.2 Potential Limitations*, comparing the gender difference in the ionic remodeling of diabetic hearts may be important to understand the clinical

difference in both the morbidity and the mortality in diabetic men and women. Specific studies may include the hormone modulation on ion channels in diabetics, and the susceptibility of drug induced arrhythmias, etc.

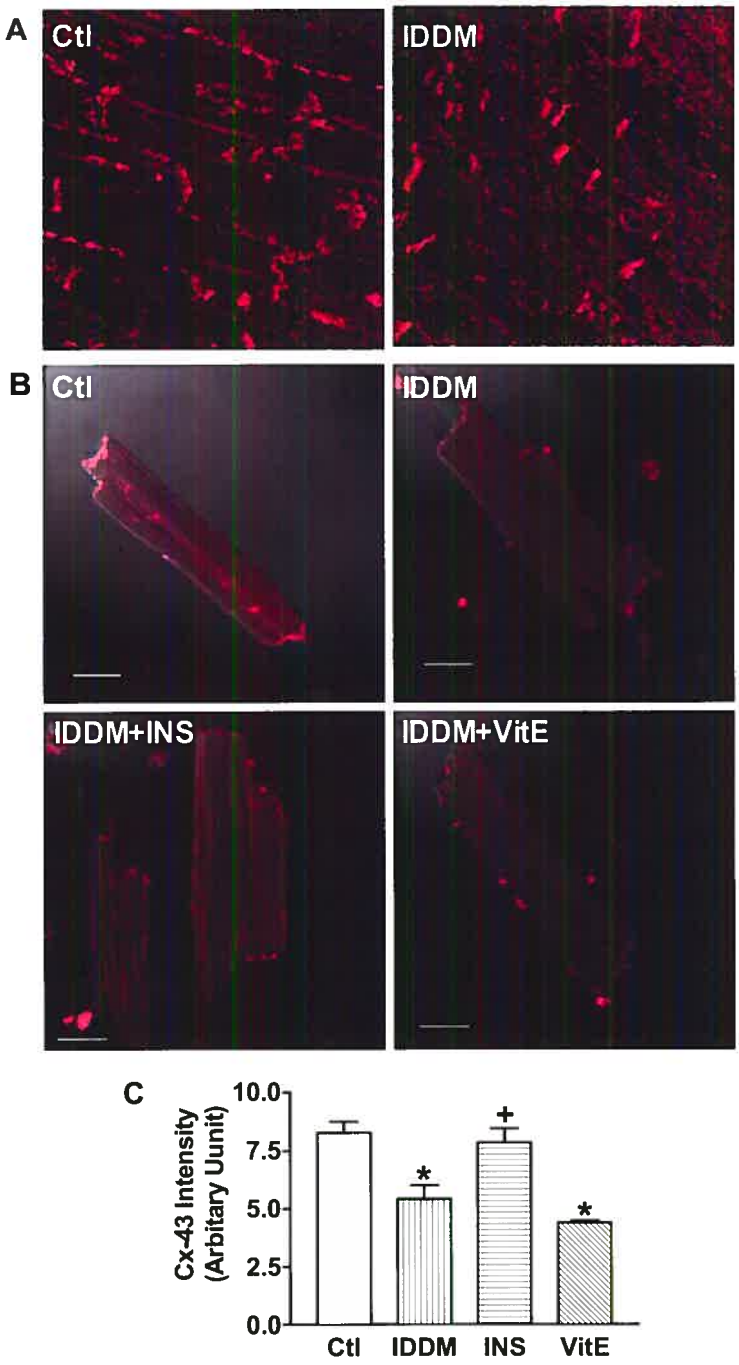

Figure 3. Expression of connexin-43 in rabbit hearts.

Figure 3. Expression of connexin-43 in rabbit hearts. Immunol histo- and cyto-chemical (***A, B***) staining against connexin-43 (Cx-43) in ventricular section (14 μm) or isolated myocytes from diabetic heart (IDDM) is less than in healthy heart (Ctl). Insulin (IDDM+INS) recovered the expression and distribution of Cx-43 in cardiomyocytes while vitamin E (IDDM+VitE) treatment has not significant effect (***B***). ***C.*** Mean data of Cx-43 staining intensity from immunocytochemical studies. *$p<0.05$ *vs* Ctl, +$p<0.05$ *vs* IDDM. (8~10 cells from each of 3 rabbits in each group).

9.4 Conclusions

According to our data in the present studies and above discussions, we can draw the following conclusions:

1) Instead of I_{to}, the critical contributor to the APD/QT prolongation in diabetic rodents, I_{Kr} is a major factor in diabetic rabbits who has similar ionic components as in humans. Besides being a target of inherited and drug induced long QT syndrome (LQTS), I_{Kr}/HERG is also a brittle target in "pathological LQTS", prompt to be defected in many diseases such as diabetic cardiomyopathy. I_{Kr}/HERG dysfunction is an important or even the major ionic mechanism underlying diabetic APD/QT prolongation, which forms the electrophysiologic substrate for increased disposition of arrhythmias and sudden cardiac death in diabetic hearts.

2) I_{Kr}/HERG channelopathy includes down-regulation of the ion channel protein, and functional impairment by metabolic alterations. Cellular metabolic perturbations are the direct mechanism underlying the dysfunction of I_{Kr}/HERG channels. Correcting the metabolic disturbance by either increasing insulin/PKB activity, or lowering glucose, or reducing ROS, can restored I_{Kr}/HERG from dysfunction, thus prevent APD/QT prolongation and arrhythmias in diabetics.

3) The metabolic perturbations in diabetic hearts are triggered mainly by hyperglycemia and the resultant deficiency of energy metabolism and over-production of ROS. ROS appears the common pathway linking metabolic perturbations to I_{Kr}/HERG dysfunction.

4) Finally, the modulation of I_{Kr}/HERG is a net outcome between enhancing factors (e.g. insulin, PKB) and suppressing factors (e.g. hyperglycemia, elevated ROS, TNF-α and ceramide). Thus, I_{Kr}/HERG serves as a target for therapies of diabetic QT prolongation and arrhythmias; enhancing I_{Kr}/I_{HERG} by manipulating HERG expression and functional modulation using cellular signaling molecules can retard and even reverse, at least partially, the electrical disorders in IDDM hearts.

9.5 References

1. Fang ZY, Prins JB, Marwick TH. Diabetic cardiomyopathy: evidence, mechanisms, and therapeutic implications. *Endocr Rev*. 2004;25:543-567.
2. Hayat S, Patel B, Khattar RS, Malik RA. Diabetic cardiomyopathy: mechanisms, diagnosis and treatment. *Clin Sci (Lond)*. 2004;107:539-557.
3. Mahgoub MA, Abd-Elfattah AS. Diabetes mellitus and cardiac function. *Mol Cell Biochem*. 1998;180:59-64.
4. Casis O, Echevarria E. Diabetic cardiomyopathy: electromechanical cellular alterations. *Curr Vasc Pharmacol*. 2004;2:237-248.
5. Lopaschuk GD. Metabolic abnormalities in the diabetic heart. *Heart Fail Rev*. 2002;7:149-159.
6. Rodrigues B, Cam MC, McNeill JH. Myocardial substrate metabolism: implications for diabetic cardiomyopathy. *J Mol Cell Cardiol*. 1995;27:169-179.
7. Frustaci A, Kajstura J, Chimenti C, Jakoniuk I, Leri A, Maseri A, Nadal-Ginard B, Anversa P. Myocardial cell death in human diabetes. *Circ Res*. 2000;87:1123-1132.
8. Shimoni Y, Ewart HS, Severson D. Type I and II models of diabetes produce different modifications of K^+ currents in rat heart: role of insulin. *J Physiol*. 1998;507 (Pt 2):485-496.
9. Shimoni Y, Severson D, Giles W. Thyroid status and diabetes modulate regional differences in potassium currents in rat ventricle. *J Physiol*. 1995;488 (Pt 3):673-688.
10. Shimoni Y. Inhibition of the formation or action of angiotensin II reverses attenuated K^+ currents in type 1 and type 2 diabetes. *J Physiol*. 2001;537:83-92.
11. Shimoni Y, Light PE, French RJ. Altered ATP sensitivity of ATP-dependent K^+ channels in diabetic rat hearts. *Am J Physiol*. 1998;275:E568-E576.
12. Shimoni Y, Rattner JB. Type 1 diabetes leads to cytoskeleton changes that are reflected in insulin action on rat cardiac K^+ currents. *Am J Physiol Endocrinol Metab*. 2001;281:E575-E585.
13. Shimoni Y. Protein kinase C regulation of K^+ currents in rat ventricular myocytes and its modification by hormonal status. *J Physiol*. 1999;520 Pt 2:439-449.

14. Shimoni Y, Ewart HS, Severson D. Insulin stimulation of rat ventricular K^+ currents depends on the integrity of the cytoskeleton. *J Physiol.* 1999;514 (Pt 3):735-745.
15. Shimoni Y, Firek L, Severson D, Giles W. Short-term diabetes alters K^+ currents in rat ventricular myocytes. *Circ Res.* 1994;74:620-628.
16. Magyar J, Cseresnyes Z, Rusznak Z, Sipos I, Szucs G, Kovacs L. Effects of insulin on potassium currents of rat ventricular myocytes in streptozotocin diabetes. *Gen Physiol Biophys.* 1995;14:191-201.
17. Wang DW, Kiyosue T, Shigematsu S, Arita M. Abnormalities of K^+ and Ca^{2+} currents in ventricular myocytes from rats with chronic diabetes. *Am J Physiol.* 1995;269:H1288-H1296.
18. Puglisi JL, Bers DM. LabHEART: an interactive computer model of rabbit ventricular myocyte ion channels and Ca transport. *Am J Physiol Cell Physiol.* 2001;281:C2049-C2060.
19. Vanhaesebroeck B, Alessi DR. The PI3K-PDK1 connection: more than just a road to PKB. *Biochem J.* 2000;346 Pt 3:561-576.
20. Feuerstein GZ. Apoptosis in cardiac diseases--new opportunities for novel therapeutics for heart diseases. *Cardiovasc Drugs Ther.* 1999;13:289-294.
21. Soliven B, Szuchet S, Nelson DJ. Tumor necrosis factor inhibits K^+ current expression in cultured oligodendrocytes. *J Membr Biol.* 1991;124:127-137.
22. Krown KA, Yasui K, Brooker MJ, Dubin AE, Nguyen C, Harris GL, McDonough PM, Glembotski CC, Palade PT, Sabbadini RA. TNF alpha receptor expression in rat cardiac myocytes: TNF alpha inhibition of L-type Ca^{2+} current and Ca^{2+} transients. *FEBS Lett.* 1995;376:24-30.
23. Fein FS, Miller-Green B, Sonnenblick EH. Altered myocardial mechanics in diabetic rabbits. *Am J Physiol.* 1985;248:H729-H736.
24. Fein FS. Diabetic cardiomyopathy. *Diabetes Care.* 1990;13:1169-1179.
25. Pollack PS, Malhotra A, Fein FS, Scheuer J. Effects of diabetes on cardiac contractile proteins in rabbits and reversal with insulin. *Am J Physiol.* 1986;251:H448-H454.
26. Public Health Agency of Canada / Agence de santé publique du Canada. Diabetes in Canada: National Statistics and Opportunities for Improved Surveillance, Prevention and Control/Le diabète au Canada: Statistiques nationales et possibilites d'accroitre la

surveillance, la prevention et la lutte (Cat. No. H49-121/1999). 1999. Minister of Public Works and Government Services Canada.

27. Suys BE, Huybrechts SJ, De Wolf D, Op DB, Matthys D, Van Overmeire B, Du Caju MV, Rooman RP. QTc interval prolongation and QTc dispersion in children and adolescents with type 1 diabetes. *J Pediatr*. 2002;141:59-63.
28. Suys BE, Katier N, Rooman RP, Matthys D, Op DB, Du Caju MV, De Wolf D. Female children and adolescents with type 1 diabetes have more pronounced early echocardiographic signs of diabetic cardiomyopathy. *Diabetes Care*. 2004;27:1947-1953.
29. Veglio M, Borra M, Stevens LK, Fuller JH, Perin PC. The relation between QTc interval prolongation and diabetic complications. The EURODIAB IDDM Complication Study Group. *Diabetologia*. 1999;42:68-75.
30. Liu XK, Katchman A, Drici MD, Ebert SN, Ducic I, Morad M, Woosley RL. Gender difference in the cycle length-dependent QT and potassium currents in rabbits. *J Pharmacol Exp Ther*. 1998;285:672-679.
31. Liu XK, Wang W, Ebert SN, Franz MR, Katchman A, Woosley RL. Female gender is a risk factor for torsades de pointes in an in vitro animal model. *J Cardiovasc Pharmacol*. 1999;34:287-294.
32. Shimoni Y, Liu XF. Sex differences in the modulation of K^+ currents in diabetic rat cardiac myocytes. *J Physiol*. 2003;550:401-412.
33. Shimoni Y, Liu XF. Gender differences in ANG II levels and action on multiple K^+ current modulation pathways in diabetic rats. *Am J Physiol Heart Circ Physiol*. 2004;287:H311-H319.
34. Brouillette J, Rivard K, Lizotte E, Fiset C. Sex and strain differences in adult mouse cardiac repolarization: importance of androgens. *Cardiovasc Res*. 2005;65:148-157.
35. Trepanier-Boulay V, St Michel C, Tremblay A, Fiset C. Gender-based differences in cardiac repolarization in mouse ventricle. *Circ Res*. 2001;89:437-444.
36. Chu SH, Sutherland K, Beck J, Kowalski J, Goldspink P, Schwertz D. Sex differences in expression of calcium-handling proteins and beta-adrenergic receptors in rat heart ventricle. *Life Sci*. 2005;76:2735-2749.

37. Pham TV, Robinson RB, Danilo P, Jr., Rosen MR. Effects of gonadal steroids on gender-related differences in transmural dispersion of L-type calcium current. *Cardiovasc Res.* 2002;53:752-762.

38. Lu HR, Remeysen P, Somers K, Saels A, De Clerck F. Female gender is a risk factor for drug-induced long QT and cardiac arrhythmias in an in vivo rabbit model. *J Cardiovasc Electrophysiol.* 2001;12:538-545.

39. Ebert SN, Liu XK, Woosley RL. Female gender as a risk factor for drug-induced cardiac arrhythmias: evaluation of clinical and experimental evidence. *J Womens Health.* 1998;7:547-557.

40. Peters RW, Gold MR. The influence of gender on arrhythmias. *Cardiol Rev.* 2004;12:97-105.

41. Vicente R, Coma M, Busquets S, Moore-Carrasco R, Lopez-Soriano FJ, Argiles JM, Felipe A. The systemic inflammatory response is involved in the regulation of K^+ channel expression in brain via TNF-alpha-dependent and -independent pathways. *FEBS Lett.* 2004;572:189-194.

42. McDonough PM, Yasui K, Betto R, Salviati G, Glembotski CC, Palade PT, Sabbadini RA. Control of cardiac Ca^{2+} levels. Inhibitory actions of sphingosine on Ca^{2+} transients and L-type Ca^{2+} channel conductance. *Circ Res.* 1994;75:981-989.

43. Schreur KD, Liu S. Involvement of ceramide in inhibitory effect of IL-1 beta on L-type Ca^{2+} current in adult rat ventricular myocytes. *Am J Physiol.* 1997;272:H2591-H2598.

44. Sugishita K, Kinugawa K, Shimizu T, Harada K, Matsui H, Takahashi T, Serizawa T, Kohmoto O. Cellular basis for the acute inhibitory effects of IL-6 and TNF- alpha on excitation-contraction coupling. *J Mol Cell Cardiol.* 1999;31:1457-1467.

45. Vereecke J, Carmeliet E. The effect of external pH on the delayed rectifying K^+ current in cardiac ventricular myocytes. *Pflugers Arch.* 2000;439:739-751.

46. Xu Z, Patel KP, Rozanski GJ. Intracellular protons inhibit transient outward K^+ current in ventricular myocytes from diabetic rats. *Am J Physiol.* 1996;271:H2154-H2161.

47. White RL, Doeller JE, Verselis VK, Wittenberg BA. Gap junctional conductance between pairs of ventricular myocytes is modulated synergistically by H^+ and Ca^{2+}. *J Gen Physiol.* 1990;95:1061-1075.

48. Mullins FM, Stepanovic SZ, Desai RR, George AL, Jr., Balser JR. Extracellular sodium interacts with the HERG channel at an outer pore site. *J Gen Physiol*. 2002;120:517-537.
49. Reuter H. Calcium channel modulation by beta-adrenergic neurotransmitters in the heart. *Experientia*. 1987;43:1173-1175.
50. Tessari F, Travagli RA, Zanoni R, Prosdocimi M. Effects of long-term diabetes and treatment with gangliosides on cardiac sympathetic innervation: a biochemical and functional study in mice. *J Diabet Complications*. 1988;2:34-37.
51. Thomas D, Kiehn J, Katus HA, Karle CA. Adrenergic regulation of the rapid component of the cardiac delayed rectifier potassium current, I_{Kr}, and the underlying hERG ion channel. *Basic Res Cardiol*. 2004;99:279-287.
52. Kang J, Chen XL, Wang H, Ji J, Cheng H, Incardona J, Reynolds W, Viviani F, Tabart M, Rampe D. Discovery of a small molecule activator of the human ether-a-go-go-related gene (HERG) cardiac K^+ channel. *Mol Pharmacol*. 2005;67:827-836.
53. Dedieu JF, Mahfoudi A, Le Roux A, Branellec D. Vectors for gene therapy of cardiovascular disease. *Curr Cardiol Rep*. 2000;2:39-47.
54. Hua F, Johns DC, Gilmour RF, Jr. Suppression of electrical alternans by overexpression of HERG in canine ventricular myocytes. *Am J Physiol Heart Circ Physiol*. 2004;286:H2342-H2351.
55. Lancellotti P, Kulbertus HE, Pierard LA. Predictors of rapid QRS widening in patients with coronary artery disease and left ventricular dysfunction. *Am J Cardiol*. 2004;93:1410-2, A9.
56. Severs NJ, Rothery S, Dupont E, Coppen SR, Yeh HI, Ko YS, Matsushita T, Kaba R, Halliday D. Immunocytochemical analysis of connexin expression in the healthy and diseased cardiovascular system. *Microsc Res Tech*. 2001;52:301-322.

10 APPENDIX

Appendix 1. Additional Publications

Here is a list of additional articles from the studies during my PhD training period (2001-2005). The works constitute parts of the trainings in a PhD program.

Peer-Reviewed Articles:

1.* Wang J, **Zhang Y**, Wang H, Han H, Nattel S, Yang B, Wang Z. Potential mechanisms for the enhancement of HERG K^+ channel function by phospholipid metabolites. *Br. J. Pharmacol.* 2004; **141**:586-599

2. Wang J, Wang H, **Zhang Y**, Gao H, Nattel S, Wang Z. Impairment of HERG K^+ channel function by tumor necrosis factor-alpha: role of reactive oxygen species as a mediator. *J Biol Chem.* 2004;**279**:13289-92

3. Han H, Wang J, **Zhang Y,** Long H, Wang H, Xu D, Wang Z. HERG K^+ channel conductance promotes H_2O_2-induced apoptosis in HEK293 cells: cellular mechanisms. *Cell Physiol Biochem.* 2004; **14**: 121-134

4. Han H, Long H, Wang H, Wang J, **Zhang Y**, Wang Z. Progressive apoptotic cell death triggered by transient oxidative insult in H9c2 rat ventricular cells: a novel pattern of apoptosis and the mechanisms. *Am.J.Physiol Heart Circ.Physiol.* 2004; **286**:H2169-82

5.* Wang H, **Zhang Y**, Cao L, Han H, Wang J, Yang B, Nattel S, Wang Z. HERG K^+ channel, a regulator of tumor cell apoptosis and proliferation. *Cancer Res.* 2002; **62**: 4843-4848

6.* **Zhang Y**, Zhang H, Zhong C, Zhao X, Chen S. Behaviors of ^{14}C-butachlor, ^{14}C-chlorpyrifos and ^{14}C-DDT in *Rana japonica japonica* Guenther. *Acta Agriculturae Nucleatae Sinca.* 2002; **16:** 174-178

7.* Wang H, Yang B, **Zhang Y**, Han H, Wang J, Shi H, Wang Z. Different subtypes of alpha 1- adrenoceptor modulate different K^+ currents via different signaling pathways in canine ventricular myocytes. *J. Biol. Chem.* 2001; **276**: 40811-40816

8. Wang J, Wang H, Han H, **Zhang Y**, Yang B, Nattel S, Wang Z. Phospholipid metabolite 1-palmitoyl-lysophosphatidylcholine enhances human *ether-a-go-go*-related gene (HERG) K^+ channel function. *Circulation* 2001; **104**: 2645-2648
9. Chen S, Zhong C, Zhao X, **Zhang Y**. Biological characteristics of concentration factors and distribution of ^{90}Sr in two kinds of fresh water gastropods. *Acta Agriculturae Nucleatae Sinica*. 2001; **15**: 45-50

In-reviewed:

10. Yang B, **Zhang Y,** Luo X, Jiao J, Dong D, Xu C, Lin H, Wang Z. Physiological function of HERG K^+ channels in cardiac repolarization as reported by action potential-clamp techniques: Regional heterogeneity and biophysical mechanisms. *Cell Physiol Biochem* (2005-8, in review)

Published Abstracts and Conference Proceedings

1.* **Zhang Y**, Wang H, Wang J, Xiao J, Zhang H, Lin H, Wang Z. Metabolic stress on I_{Kr}/ HERG K^+ channel, a potential mechanisms underlying the abnormal QT prolongation and the associated arrhythmias in diabetic rabbits. *Circulation* 2005;(in press) (AHA 2005 Scientific Sections)
2.* **Zhang Y**, Wang J, Wang Z. Ionic mechanisms underlying the QT prolongation in type I diabetic rabbit hearts. *Biophysical Journal* 2005; **88** (suppl. 2): p472a
3.* Wang J, **Zhang Y**, Wang Z. Different reactive oxygen species differentially modulate HERG K^+ channel function. *Biophysical Journal* 2005; **88** (suppl. 2): p608a
4. Wang J, Lin H, **Zhang Y**, Wang Z. Modulation of HERG K^+ channel function by PKA and PKC activators and inhibitors: direct actions and indirect mediation by reactive oxygen species. *Biophysical Journal* 2005;
5.* **Zhang Y**, Wang J, Wang Z. I_{Kr}/HERG K^+ channel, a potential molecular contributor to the QT prolongation in type I diabetic hearts. *Circulation* 2004;**110**(suppl. III): III 193. (AHA 2004 Scientific Sections)
6.* **Zhang Y,** Wang J, Wang Z. I_{Kr}/HERG K^+ channel, a potential molecular contributor to the QT prolongation in type I diabetes hearts. *In* 7th Research Day of Montreal Heart Institute, Montreal, Canada, June 16, 2004. p4. (awarded presentation)

7. Wang J, Gillis M-A, **Zhang Y**, Nattel S, Wang Z. The mechanism underlying arrhythmogenesis of lysophosphatidylcholine during early phase of acute global ischemia in isolated perfused rabbit hearts. *Intern J Cardio* 2004; **97**(suppl.2): S44

8. Wang J, **Zhang Y**, Yu F, Wang Z. Sphingolipid ceramide impairs HERG K^+ channel function: involvement of multiple protein kinases and role of reactive oxygen species as a mediator. *Intern J Cardio* 2004; **97**(suppl.2): S57

9.* **Zhang Y**, Han H, Wang J, Wang H, Yang B; Wang Z. Impairment of HERG (Human *ether-a-go-go* Related Gene) K^+ channel Function by hypoglycemia and hyperglycemia: similar phenotypes but different mechanisms. American Heart and Stroke Foundation Second Asia Pacific Scientific Forum, Honolulu, HI, Jun 8-10, 2003. p35

10. Wang J, **Zhang Y**, Wang H, Han H, Nattel S, Wang Z. Mechanisms for the enhancement of HERG K^+ channel Function by phospholipid metabolites. *Circulation* 2003; supplement May; p35; American Heart and Stroke Foundation Second Asia Pacific Scientific Forum, Honolulu, HI, Jun 8-10, 2003. p35

11.* Wang H, Wang J, **Zhang Y**, Han H, Nattel S, Wang Z. TNF-α depresses HERG K^+ function: A potential molecular contributor to sudden cardiac death in heart failure? American Heart and Stroke Foundation Second Asia Pacific Scientific Forum, Honolulu, HI, Jun 8-10, 2003. p36

12.* **Zhang Y**, Wang J, Wang H, Han H, Nattel S, Wang Z. Protein kinase B enhances HERG K^+ channel function. In: 46th Annual Meting of Biophysical Society. February 23-27, 2002, San Francisco, California. *Biophysical Journal* **82**(1): 583a

13.* **Zhang Y**, Wang J, Han H, Wang H, Long H, Wang Z. Glucose produces dual effects on HERG K^+ channel function. In: 46th Annual Meting of Biophysical Society. February 23-27, 2002, San Francisco, California. *Biophysical Journal* **82**(1): 583a

14. Wang J, Wang H, Han H, **Zhang Y**, Nattel S, Wang Z. The phospholipid metabolite 1-palmitoyl-lysophosphatidylcholine enhances HERG K^+ channel function.. In: 46th Annual Meting of Biophysical Society. February 23-27, 2002, San Francisco, California. *Biophysical Journal* **82**(1): 583a

15.* **Zhang Y**, Wang H, Han H, Long H, Nattel S, Wang Z. Occurrence of DNA fragmentation in apoptosis cells depends on different apoptotic stimuli and signalling pathways. In: *11th International Conference of Second Messengers & Phopsphoproteins*, p7-8, April 22-26, 2001, Melbourne, Australia

Note:

(1) For publications in which I am the first author, I generated the idea, designed and performed the experiments, analyzed the data and wrote the manuscripts;

(2) For publications in which I am a 2nd ~3rd co-author, I participated in about 30~40% work of the projects, including idea generation, experiments design and carry-out, data analysis, manuscript correction and discussion, etc.;

(3) * denotes that I was involved in major parts of the project.